Coordination Chemistry Reviews, 106 (1990) 25–170
Elsevier Science Publishers B.V., Amsterdam

THE ACTIVATION OF SMALL MOLECULES BY DINUCLEAR COMPLEXES OF COPPER AND OTHER METALS

PIETRO A. VIGATO and SERGIO TAMBURINI

Istituto di Chimica e Tecnologia dei Radioelementi, C.N.R. Corso Stati Uniti 4, 35100-Padova (Italy)

DAVID E. FENTON

Department of Chemistry, University of Sheffield, Sheffield (U.K.)

(Received 23 October 1989)

CONTENTS

A. INTRODUCTION

Dinuclear complexes containing metal centres in close proximity have been the subject of recent extensive investigations since these structural units are thought to be involved in a variety of important biochemical processes, especially oxygen transport and oxygen activation by metal-containing proteins and enzymes [1–17].

Reactions involving the catalytic insertion of one or both atoms of dioxygen into an organic substrate are of importance in the synthesis of metabolic products and intermediates. Dioxygen also serves as an electron sink in the oxidation of a variety of small molecules including those of biological importance such as ascorbic acid, catechols and amino acids [18,19].

A number of dinuclear complexes (especially those of copper(I), copper (II), cobalt(II) and iron(II)) have therefore been reported and studied as

0010-8545/90/$51.10

models of metal–metal interaction and redox catalysis. The metal centres of these complexes are often incorporated into cavities presented by macrocyclic or macroacyclic polydentate ligands.

The rapidly growing interest in dinuclear and polynuclear complexes arises also from the awareness that pairs or clusters of metal ions have the potential to mediate certain chemical reactions of industrial relevance either more efficiently than, or in a different manner to, isolated metal centres. For instance, dipalladium complexes have been successfully tested in the hydration of acetonitrile or similar organic substrates and epoxidation processes may be improved by the use of dinuclear catalysts.

Both synthetic and natural complexes which reversibly bind dioxygen have been termed oxygen carriers. In addition to their significance as models for natural oxygen carriers, synthetic dioxygen complexes have potential applications in dioxygen separation and storage, industrial processes and catalysis [19]. They act in some cases in a catalytic fashion and in other cases in a stoichiometric fashion. Concepts derived from such studies may also be expected to contribute to the development of practical synthetic systems for the reversible binding of oxygen and/or oxidation of organic compounds.

The chemical reaction of dioxygen which is of major importance for biological systems and for oxygenation reactions is reduction. The free energy change for four-electron reduction of dioxygen (to two water molecules) is negative by 316 $\mathrm{kJ/mol^{-1}}$ at pH 7 according to the reaction

$$O_2 + 4H^+ + 4e^- = 2H_2O \qquad E^\circ = +0.815\ \mathrm{V}\ \text{(vs. the normal hydrogen electrode)}$$

The potential is quite attractive for energy storage. Such a reduction process does not occur in one step but rather through a series of steps involving successive one-electron transfers. Mechanistic limitations severely restrict the usefulness of the reduction. The most common pathway for dioxygen reduction is one-electron transfer followed by disproportionation to form OH^- under basic conditions or H_2O_2 under acidic conditions. The effective potential is pH independent and the one-electron reduction is endothermic by 128 $\mathrm{kJ/mol^{-1}}$. The reverse of the above equation is also of major importance since it represents the overall oxidation process which occurs in photosynthesis. As before, however, the reaction proceeds by one- and two-electron steps rather than by a single four-electron oxidation.

One-electron reductants react with dioxygen to form complexes having molar dioxygen-to-metal ratios 1:1 or 1:2, with binding for these two binding stoichiometries of type **A**, **B** or **C** respectively (Scheme 1). Complexes of type **A** are considered to be superoxide complexes of one-electron-oxidized metal ions while those of type **B** are μ-peroxo complexes. Two-

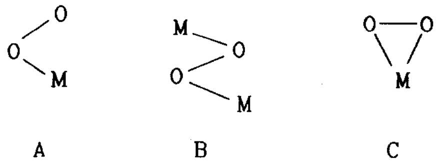

Scheme 1. Coordination of O_2 to a metal ion.

electron donors form complexes of type **C**, which can be considered as a peroxo bound to a metal ion which has undergone a two-electron oxidation.

The direct participation of dioxygen in the oxidation of organic compounds effected by metal complexes has been proved to be more efficient when dinuclear compounds are used.

In the oxidation reactions the formation of metal hydroperoxides is considered of fundamental importance; consequently the formation of such species has been investigated, and in some cases hydroperoxide intermediates have been isolated, characterized and their reactivity tested.

The most widely studied reactions with dinuclear complexes are the oxidation of phenols, the epoxidation of olefins, and the formation of sulphoxides or phosphine oxides from the reduced analogues.

As mentioned above, the formation of hydrogen peroxide occurs in oxygen reduction; therefore the use of hydrogen peroxide in oxidation processes by dinuclear metal systems was also studied.

A comparison of the ability of dinuclear complexes to act as catalysts in oxidation processes with the analogous mononuclear analogues was carried out using the oxidation of the two well-known two-electron reducing agents, ascorbic acid and 3,5-di-*t*-butylcatechol (DTBC), and *N*,*N*,*N*′,*N*′-tetramethyl-*p*-phenylenediamine (TMPD) which is a one-electron reducing agent (Scheme 2), as model reactions.

Recently, fundamental studies have been devoted to the development of electrocatalysts [20–28]. An electrocatalyst can be effective only in the vicinity of an electrode surface, and many present or proposed catalysts are

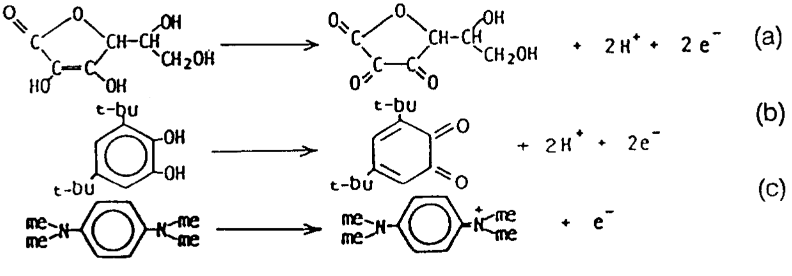

Scheme 2. Oxidation reaction of (a) ascorbic acid, (b) DTBC and (c) TMPD.

expensive. Incorporating them into microstructures on electrodes, therefore, has been very attractive as a way of confining them to the effective spatial region and minimizing the amount of catalyst required in a system.

A goal worthy of the sophisticated attention being given to it is the electrocatalysis of the reduction of oxygen to water. This seemingly simple process is actually quite complex. It proceeds through high energy intermediates that cause sluggish kinetics, and it tends to stop after two electrons and two protons have been added, producing hydrogen peroxide: this fault robs the system of much of its ability to deliver energy.

The economic incentive for finding an effective, inexpensive means for reducing oxygen to water is truly enormous. Methanol/oxygen and hydrogen/oxygen fuel cells would then become immediately attractive as large-volume energy converters for electric vehicles and possibly for load levelling in power systems. Since fuel cells are not heat engines, they are not limited to the efficiency of a Carnot cycle. They are capable of extraordinarily efficient conversion of the energy in a fuel to electricity. Unfortunately, the only really effective oxygen electrodes currently available use dispersions of platinum on carbon and are too expensive for widespread application. In specialized use, for example in the space programme, they have served extremely well.

Inexpensive oxygen electrodes also would facilitate the development of a new generation of air-breathing batteries, such as zinc/air and aluminium/air systems, which achieve high energy per unit of mass and volume by not not requiring storage of the oxidant. The wide use of such batteries in automobiles could greatly reduce fuel costs, and effective use in load levelling would significantly reduce the generating capacity needed to meet peak demands of electricity.

This present review is concerned with the activation of small molecules by dinuclear coordination complexes derived from synthetic macrocycles and macroacycles.

B. NATURALLY OCCURRING DINUCLEAR ACTIVE SITES

The active sites of many metalloproteins comprise pairs of metal ions in close proximity.

Superoxide dismutase, an enzyme (E) containing copper with zinc, iron, or manganese, which protects organisms from the toxic effects of superoxide produced from dioxygen in the presence of free radicals, reacts with $O_2{}^-$ forming dioxygen and peroxide [29–34] by the cyclic process

$$\mathrm{ECu(II)} + \mathrm{O_2}^- \rightarrow \mathrm{ECu(I)} + \mathrm{O_2} \xrightarrow{\mathrm{H^+}} \mathrm{ECu(II)} + \mathrm{H_2O_2}$$

The reaction is driven by protonation of the peroxide ion O_2^{2-}.

The Cu–Zn protein obtained from bovine tissue is the most thoroughly studied [1,19]. The complete sequence of 150 residues in the polypeptide chain is known and the three-dimensional X-ray structure has been determined to a resolution of 3 Å. The protein consists of two identical, non-covalently associated subunits in each of which the metal binding sites are near the ends of the cylindrical arrangements. The essential features of the bimetal binding region shows (Fig. 1) each copper(II) to be coordinated to a water molecule and four histidines, one of which acts as a bridge to the zinc and is deprotonated; thus each copper(II) is five coordinate. The zinc atom is coordinated to a further two histidines and one aspartic acid residue in an approximately tetrahedral geometry. The Cu–Zn distance is 5.4 Å. The zinc atom plays a structural role in that it helps the protein to perform the coordination environment around the copper, and the copper is the active catalytic centre.

Hemocyanin (Hc) and tyrosinase (Tyr) contain dinuclear copper active sites in which copper(II) centres are electronically coupled. Hemocyanins function as dioxygen carriers in the hemolymph of arthropods and molluscs whereas tyrosinase is a mono-oxygenase utilizing O_2 in the hydroxylation of monophenols and further acts as a two-electron oxidase (i.e. *o*-catechol to quinone). Spectroscopic and chemical evidence suggests that, in the deoxy form of Hc, two or three imidazole ligands from histidine coordinate to each cuprous ion [35–41]. A recent X-ray structural investigation (3.2 Å resolution) of *Panulirus interruptus* deoxy-hemocyanin strongly suggests that three imidazoles are coordinated to each copper centre with a Cu(I)···Cu(I) distance of 3.8 Å [32]. Upon reaction of deoxy-Hc with O_2, significant coordination changes take place, giving rise to tetragonally coordinated copper(II) ions separated by 3.6 Å and bridged by the O_2^{2-} ligand that is derived from O_2, and an endogenous oxygen-containing group [42]. There are parallels between the structures and reactivities of the Hc and Tyr active sites: for instance, Tyr forms an O_2-containing species (oxy-Tyr) which has spectral features similar to those of oxy-Hc. Thus the binding of dioxygen by Hc and O_2 activation (leading to facile and selective oxygen incorporation into a substrate) by Tyr appear to be related processes [43] (Fig. 2).

Cytochrome *c* oxidase [44–53] is a complex enzyme which contains two heme units, low spin heme and high spin heme, and two copper(II) atoms. It

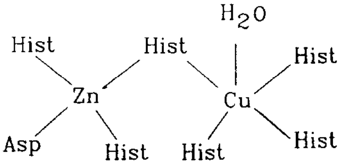

Fig. 1. Schematic representation of the bimetal site in Zn–Cu superoxide dismutase.

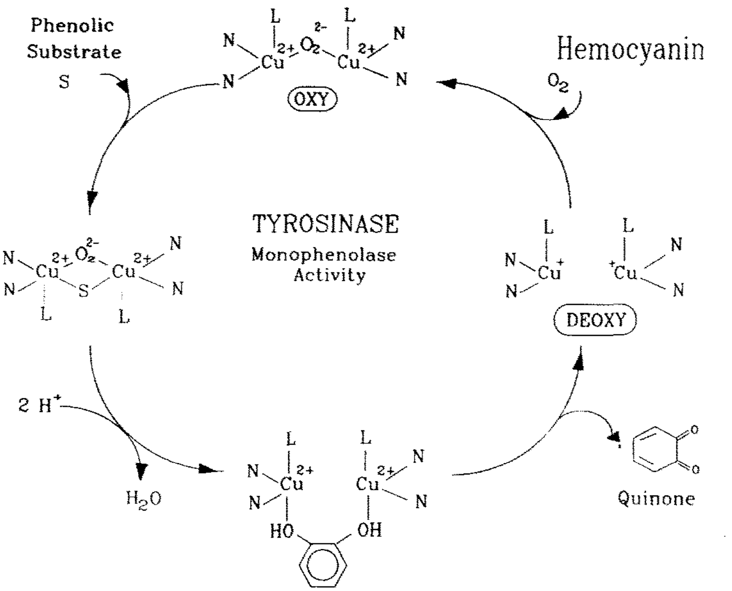

Fig. 2. Proposed working mechanism of tyrosinase and relationship between hemocyanin and tyrosinase (from ref. 43).

is located as the terminal component of the mitochrondrial respiratory chain and has the important role of catalysing the rapid, four-electron reduction of molecular oxygen to water. The mechanism of this reduction is not clear but it is likely that dioxygen interacts with one pair of heme and copper(II) only — heme$_{a3}$ and Cu$_{a3}$.

In the oxidized form, heme$_{a3}$ and Cu$_{a3}$ exhibit properties which indicate that the two metal centres are strongly antiferromagnetically coupled ($-J > 200$ cm^{-1}), making the two metals EPR silent and reducing their magnetic susceptibilities. The heme$_{a3}$ and Cu$_{a3}$ were therefore assumed to be in close proximity and linked by a ligand which could mediate any magnetic exchange. Several potential links have been proposed, namely, imidazolate, carboxylate, oxo and mercapto bridges, and criticized at length. An oxo bridge was preferred as a working hypothesis for the site. No X-ray crystal structure is available for the bimetallic site of cytochrome *c* oxidase but extended X-ray absorption fine structure (EXAFS) data have been interpreted as showing that the copper(II)$_{a3}$ is surrounded by a combination of sulphur and nitrogen (or oxygen) donors. The Cu–S distance was 2.27 Å, comparable with that found for the Cu(II)–cysteine distance in the blue copper proteins, and the Cu–N (or Cu–O) distance was 1.97 ± 0.2 Å. A more detailed investigation for the fully oxidized heterobimetallic site (Fig. 3) suggests the copper atom to be surrounded by two nitrogen atoms, and a bridging sulphur, with a further donor atom at 2.82 Å. The iron atom has

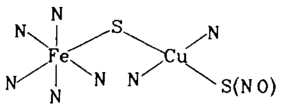

Fig. 3. Proposed active site in cytochrome oxidase (from EXAFS).

four heme nitrogen atoms at 2.01 Å, a proximal nitrogen at 2.14 Å and the octahedral coordination is completed by the bridging sulphur, shared with the copper atom, at 2.60 Å. This sulphur is believed to be sp^3. The Cu–Fe distance is 3.75 Å.

Hemerythrin [54–72], an alternative dioxygen carrier, which contains no heme unit, is present in the red blood cells of some marine invertebrate phyla, notably *Siphunculid* worms [54]. The active centre is a pair of iron atoms about 3.5 Å apart and contained within a single polypeptide chain. Most hemerythrins are oligomeric; dimeric, trimeric, tetrameric and octameric forms are known, and although the dioxygen binding affinity for each iron is comparable with that for hemoglobin there is little cooperative action in hemerythrin. Myohemerythrin occurs as a monomeric unit and has a molecular weight comparable with that of a subunit of the octamer.

Deoxyhemerythrin is colourless and contains two high spin iron(II) centres which can each add dioxygen to give oxyhemerythrin which is violet pink and involves two iron(III) centres and a hydroperoxo ligand [73]. Both forms may be oxidized to methemerythrin which has iron(III) pairs. The low magnetic moment indicates strong antiferromagnetic coupling.

X-Ray crystal structure studies of the met-azido and the met form with the dioxygen-bonding site vacant show that the two iron atoms are bridged by an oxygen atom and two carboxylate groups [74,75]. From EXAFS studies [76–80] it has been concluded that the active site is very similar in the oxy and met forms, but distinctly different in deoxyhemerythrin; the dinuclear iron centre in the oxy and met forms contains a μ-oxo bridge (Figs. 4(a) and 4(b)). Deoxyhemerythrin shows distinct changes and the Fe–Fe peak has disappeared, indicating loss of the μ-oxo bridge upon reduction.

An iron-containing enzyme believed to be related to hemerythrin is ribonucleotide reductase. This enzyme catalyses the reduction of ribonucleotides to the corresponding deoxyribonucleotides and one subunit participates in the reaction via a tyrosyl-free radical formed in conjunction with a dinuclear antiferromagnetically coupled, high spin iron(III) centre with a μ-oxo bridge as in hemerythrin.

The active site in methane mono-oxygenase, a non-heme mono-oxygenase from *Methyllococcus capsulatus* [81], has been suggested to consist of a diiron site similar to that found in hemerythrin. Attempts to mimic the

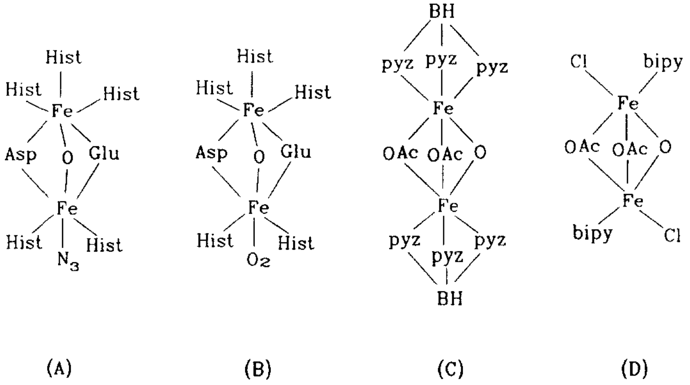

Fig. 4. (A) Dinuclear iron site in metazidohemerythrin from *T. dyscritum*. (B) Proposed iron site in oxyhemerythrin. (C) Dinuclear μ-oxo iron hemerythrin analogue. (D) Dinuclear μ-oxo iron met-chloromerythrin analogue.

dioxygen oxidation of alkanes have been made using dinuclear μ-oxo iron models first described as hemerythrin analogues.

The compound in Fig. 4(c), first prepared as a model for hemerythrin [82], has been found to catalyse the oxidation of adamantane to adamantan-1-ol, adamantan-2-ol and adamantan-2-one in the presence of acetic acid (proton source) and zinc powder (electron donor), and using CH_2Cl_2 as the solvent [83]. The ion ratio of tertiary position oxidation to secondary position oxidation implies that the reaction is different from a Fenton-type free radical oxidation. Cyclohexane and cyclohexene may be oxidized to cyclohexanol and cyclohex-2-en-1-ol respectively using the same technique. The reaction conditions are quite sensitive; for example, if excess acetic acid is added then the oxidation does not occur owing to the formation of the mononuclear species $[Fe(HBpyz_3)_2]^+$.

Biomimetic catalysis studies have also been made using the complex in Fig. 4(d); this may be viewed as a model for the substrate-analogue bound form of hemerythrin (met-chlorohemerythrin) [84].

Using *t*-BuOOH as a mono-oxygen transfer agent, in MeCN at room temperature, catalytic oxidation of ethane to ethanol, propane to *n*-propanol and isopropanol, and cyclohexane to cyclohexanol was achieved. The reactivity sequence followed the ease of C–H bond dissociation: $C_6 > C_3 > C_2$. Evaluation of the activity of the complex in Fig. 4(d) with dioxygen as the mono-oxygen transfer agent in the presence of zinc powder and glacial acetic acid gave cyclohexanone from cyclohexane, but not cyclohexanol. The activity of the complex in Fig. 4(d) was found to be greater in the presence of *t*-BuOOH; this may arise via a more favourable formation of the active Fe–oxo species in the former species, and because the two systems generate different Fe–oxo intermediates.

There are several proteins exhibiting oxidase activity which contain four or more copper atoms [85–92]. Laccases, which catalyse the oxidation of *p*-diphenols to *p*-diquinones, with the accompanying four-electron reduction of dioxygen to water, contain four copper atoms. Ceruloplasmin, the major copper-containing protein from mammalian blood contains eight copper atoms; its precise role is conjectural although it catalyses the reduction of dioxygen to water and may act as a copper-carrying protein. Ascorbate oxidase also contains eight copper atoms. In each of these systems there are at least three coordination environments available to the metal and these have been designated as types 1, 2 and 3 [93].

Type 1 copper is characterized by an intense absorption band near 600 nm and an EPR spectrum with an unusually small hyperfine coupling constant. Structural data are available for this site from X-ray crystallographic studies on plastocyanin and azurin, both of which have their single copper atom in a distorted tetrahedral geometry. The presence of this site gives the oxidase an intense blue colour and leads to their name blue oxidases.

Type 2 copper is present in all the blue multi-copper oxidases and is characterized by lacking sufficient optical absorption to be observed above the other copper chromophores. The EPR signal is similar to those exhibited by most small copper(II) complexes.

Type 3 copper is a strongly antiferromagnetically coupled copper(II) dimer which can act as a two-electron donating system and is essential to the reduction of dioxygen. The site has an absorption band at about 300 nm, a lack of EPR signal and is non-paramagnetic over a wide temperature range.

Laccase contains one each of type 1 and type 2, and type 3 copper atoms, and both ceruloplasmin and ascorbate oxidase contain two type 1, two type 2 and four type 3 copper atoms.

Recently the crystal structure of the blue oxidase, ascorbate oxidase from zucchini, has revealed the presence of four copper atoms in each subunit of the protein bound as mononuclear and trinuclear species. The novel trinuclear cluster has eight histidine ligands and may be subdivided into a pair of copper atoms with six histidine ligands arranged trigonally prismatic and a single copper atom. There is possibly an OH^- associated with this copper. The two copper atoms of the pair are 3.4 Å apart and probably type 3, with the third copper of the triangle 3.9 Å distant [94].

C. DINUCLEATING LIGANDS

The preparation of complexes which contain two transition metal ions separated by distances of 3.5–6 Å is of considerable interest; at these distances no direct interaction between the metal ions is expected, yet a substrate could interact simultaneously with both ions. Such involvement in multisite interactions has an analogy also in surface and cluster chemistry.

In 1970 the term dinucleating ligands was introduced for a series of polydentate ligands capable of simultaneously securing two metal ions [95,96]. Since 1970 there has been a continuous increase in the synthesis of dinucleating ligands and related complexes, and several reviews have been published on this subject [4–8,97].

The complexes obtained by these ligands have recently been divided into two general classes [1].

(a) Complexes with metals sharing at least one donor atom of ligands containing adjacent sites in which the central donor atom provides a bridge. Ligands providing these complexes have collectively been termed compartmental ligands [4–8].

(b) Complexes in which the donor atoms are not shared. These complexes thus derive from ligands having isolated donor sets.

Ligands suitable for giving the most appropriate structural arrangement of the metal ions for such activation and/or oxidation reactions are reported in Scheme 3.

As can be seen in Scheme 3, the simultaneous presence of two metal ions at a suitable distance from each other provides a requisite for the formation of the "activation space" necessary for the coordination of oxygen and/or organic substrates and for their subsequent oxidation or transformation. A problem encountered with these complexes in the reaction with oxygen is the poor reversibility. Most copper(I) complexes, for instance, that are reported to form dioxygen adducts in solution quickly react further at room temperature to give irreversibly oxidized products. In some cases copper(II) complexes can be isolated, usually containing the thermodynamically favoured $[Cu_2(OR)_2]^{2+}$ core. Such oxidation reactions are interesting in themselves, but are also important if the complexes are to be useful as potential reagents and/or catalysts, since the reactivity of the ligands may present competing reactions and destruction of the reagents or catalyst. Understanding ligand reactivity is thus important in the design of molecules for specific reactive purposes so that synthetic strategies may be planned to either block it or enhance it.

As mentioned above, there are several examples of dioxygen adducts which have given rise to complexes containing oxidized ligands in high enough yield to allow isolation and characterization. Recent examples include aromatic hydroxylation, oxidative dehydrogenation of amines and also aliphatic hydroxylation [98]. An example can be the isolation and the structural characterization of copper-promoted oxidative degradation products of the dinucleating ligand **I** [98].

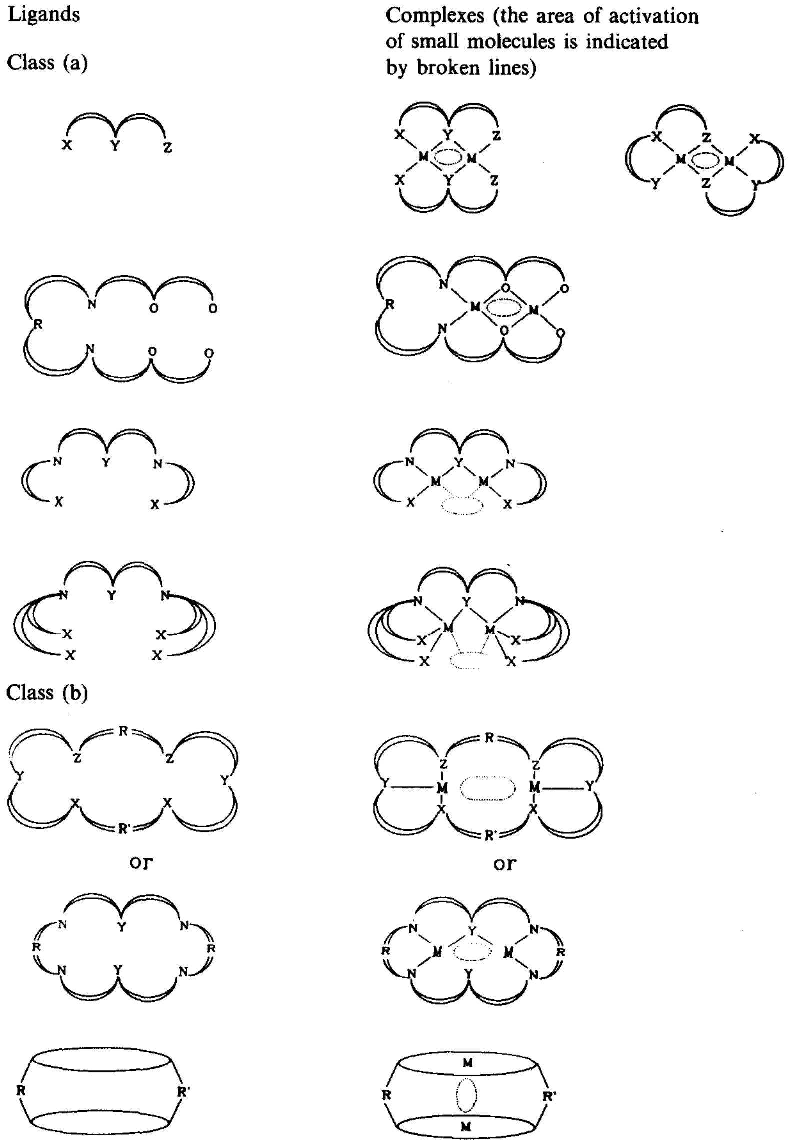

Scheme 3. Schematic representation of dinucleating ligands, related complexes and the "area of activation" of small molecules.

It was found that the benzylic-like methylene groups are susceptible to oxidative cleavage under a variety of conditions. The isolated product is the copper(II) bis complex of 2-carboxylate *N*-ethylbenzimidazole. The structure of this complex is planar, excluding the ethyl groups, with no significant axial interactions (Fig. 5).

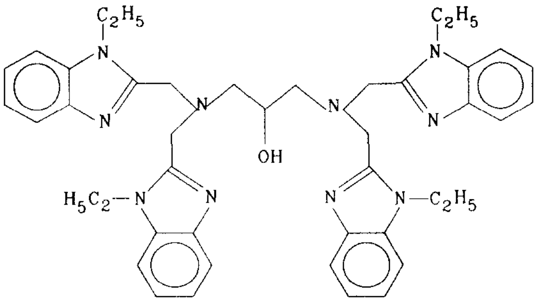

I

Further examples of ligand oxidation have been observed with the trinuclear nickel(II) complex of 2,2-dimethyl-3,5,7-octanetrione (H_3PAA), $Ni_3(PAA)_2(OH)(CH_3OH)_4$ [99], and with bis(1,7-diphenyl-1,3,5,7-heptane tetraonato)dicobalt(II) [100].

Crystallization of the trinuclear nickel(II) complex from pyridine in air results in ligand oxidation and migration of the *t*-butyl group from the 3- to the 4-carbon in a benzylic acid type rearrangement. The dinuclear nickel(II) complex recovered contains the new ligand 2-*t*-butyl-2-hydroxy-3,5-dioxo-hexanoate, obtained according to a proposed mechanism of the type reported in Scheme 4. The dicobalt(II) complex is oxidized at the 4-carbon of the ligand upon crystallization from 10%pyridine–90%benzene in air. The oxidation of the 4-carbon atom to carbonyl, according to Scheme 5, does not destroy the dianionic character of the ligand and therefore the complex. For both nickel(II)- and cobalt(II)-oxidized complexes, the X-ray structure has been reported [99,100].

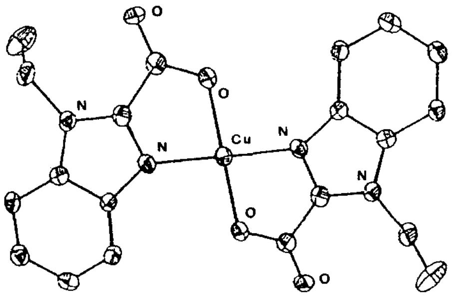

Fig. 5. Structure of the bis(2-carboxylate *N*-ethylbenzimidazole) copper(II) complex (from ref. 98).

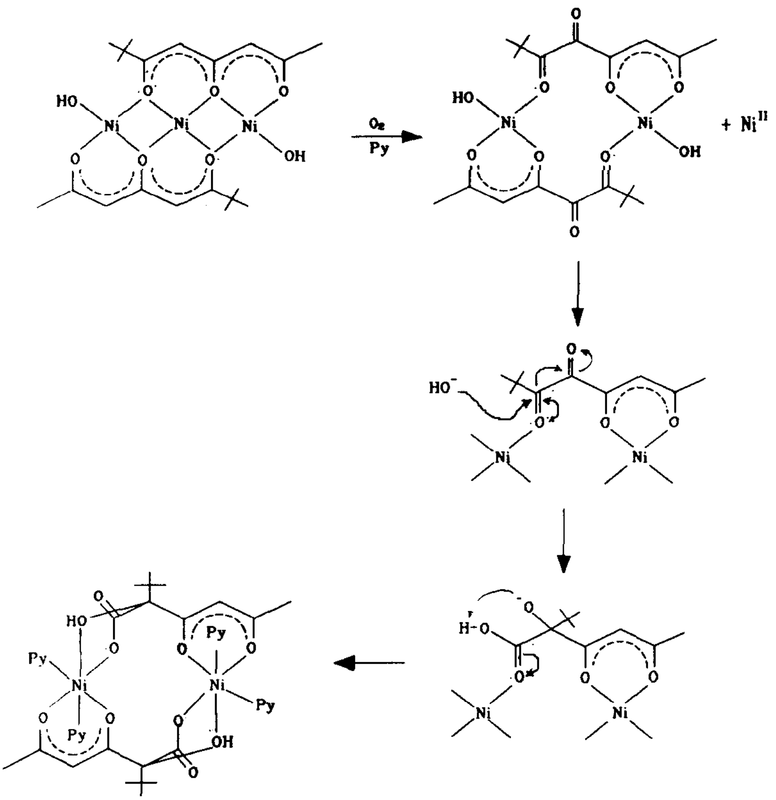

Scheme 4. Oxidation of a trinuclear nickel(II)triketonato complex.

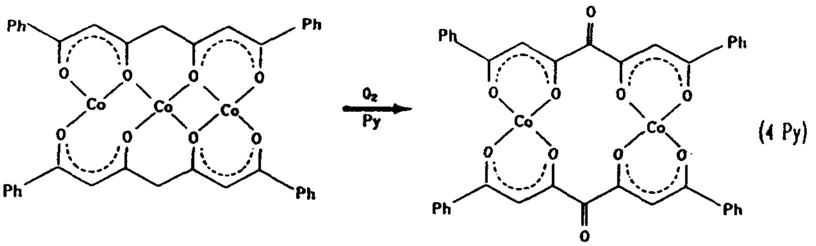

Scheme 5. Ligand oxidation by O_2 for bis(1,7-diphenyl-1,3,5,7-heptane tetraionate)dicobalt(II).

D. COMPLEXES DERIVED FROM KETO PRECURSORS AND RELATED LIGANDS

Potentially tridentate ligands have been used for the synthesis of dinuclear complexes of the type reported in Scheme 6.

Some complexes, particularly copper(II) complexes, have been used in the oxidation of catechols under anaerobic and aerobic conditions. It was reported that 4-*t*-butylcatechol (TBC) or 3,5-di-*t*-butylcatechol (DTBC) can

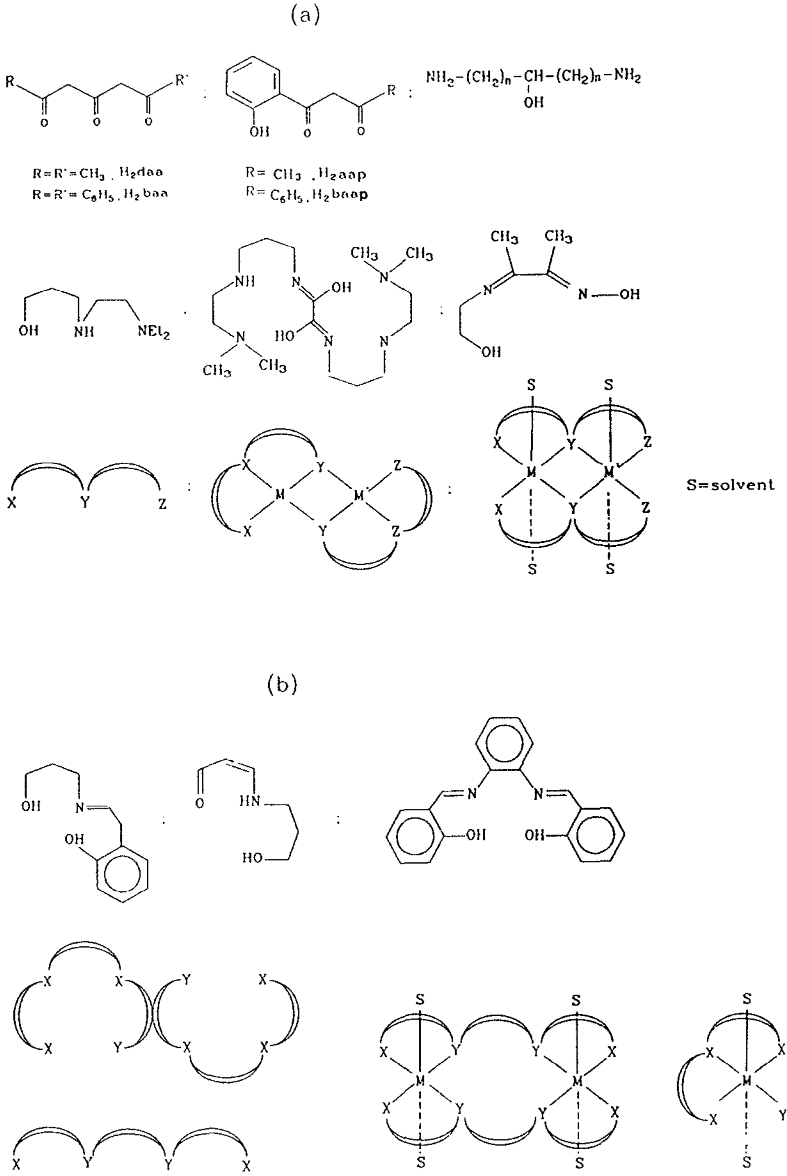

Scheme 6. (a) Potentially tridentate ligands and related dinuclear complexes with a short metal–metal distance. (b) Potentially tetradentate ligands and related dinuclear complexes with a long metal–metal distance.

be recovered unchanged when treated under anaerobic conditions with an excess of bis(1-phenyl-1,3,5-hexanetrionato)dicopper(II) [Cu_2(DBA)] in pyridine or in CH_2Cl_2 for a long period of time [101,102]. Similar results were obtained in the presence of triethylamine. It was found, however, that 10% of 3,5-di-*t*-butylquinone (DTBQ) was produced from the corresponding catechol when the oxidation reaction was carried out with $Cu_2(DBA)_2$ in the presence of $CuCl_2$ [102]. $Cu_2(DBA)_2$ in the presence of one equivalent of triethylamine catalyses the above oxidation reaction with molecular oxygen, giving DTBQ quantitatively [101].

A comparison of the activity for the above DTBC → DTBQ aerobic oxidation in a group of mononuclear and homodinuclear complexes has been carried out. For the dinuclear complexes the activity is $Cu_2(aap) > Cu_2(baap) > Cu_2(daa)_2 > Cu_2(baa)_2$. In addition, the dinuclear complexes show an enhanced activity over the analogous mononuclear complexes. It must be noted that Cu(β-acetylacetonate)$_2$ shows practically no activity [101–103]. The oxidation rate of DTBC, using dinuclear copper(II) complexes as catalysts, is lowered by the presence of DTBQ. As an explanation it was suggested that the electron transfer from catechol to the copper(II) complex begins after the formation of an intermediate of the type Cu_2(L)(DTBC) (L = triketones or β-ketophenols) which could be prevented by the competitive formation of the complex $Cu_2(L)_2$(DTBQ).

The dinuclear cobalt(II) complexes, with the above triketones and β-ketophenols show a catalytic oxidation of 3,5-DTBC; however, in contrast with the corresponding mononuclear copper(II) complexes, the cobalt(II) complexes, such as $Co(Haap)_2 \cdot 2H_2O$, $Co(Hbaap)_2 \cdot 2H_2O$ have little or no catalytic activity [103].

The reactions of ascorbic acid, DTBC, TMPD and H_2O_2 with a series of dinuclear copper(II) complexes were investigated and the results have been compared with those obtained with similar mononuclear copper(II) complexes [104–106] (Scheme 6).

The catalytic activity largely depends on the structure of the complex, and the general trend is the same for ascorbic acid, DTBC and TMPD. The planar mononuclear complexes and the dinuclear complexes with a large Cu–Cu distance (greater than 5 Å) show practically no catalytic activity, whereas non-planar mononuclear complexes and dinuclear complexes with an equivalent coordination site at an appropriate distance (3–4 Å) catalyse the reaction. It was also suggested, on the basis of electrochemical data, that the reduction potential is not the determining factor for the catalytic activity of these complexes, but rather the structural configuration of the compounds.

Dinuclear complexes of the type reported in Fig. 6 have been suggested as intermediate complexes for the oxidation of ascorbic acid or DTBC (a) and also for the oxidation of TMPD (b) by O_2.

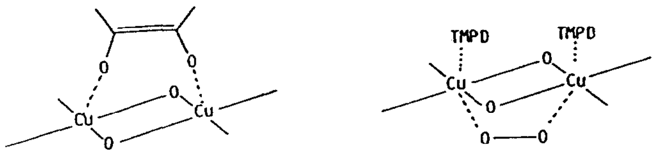

(a) (b)

Fig. 6. Intermediate complexes assumed (a) for the oxidation of ascorbic acid or DTBC, and (b) for the oxidation of TMPD by O_2.

For the catalytic decomposition of H_2O_2 the reaction was run in a solution containing H_2O_2 and a copper complex in 10:1 mole ratio. The reaction was first order with respect to H_2O_2. The general trend is the same as that observed for the reactions with ascorbic acid, DTBC and TMPD; therefore a similar reaction mechanism has been proposed [107]. Thus the high catalytic activity of dinuclear complexes with an appropriate Cu–Cu distance has been explained on the assumption of the two-electron transfer between two H_2O_2 molecules through a dinuclear complex to which both molecules are bonded bidentately, analogously to the case of the O_2 oxidation of DTBC and/or ascorbic acid.

E. COMPLEXES WITH SIDE-OFF LIGANDS

Copper(II) complexes (**II–IV**) of the potentially hexadentate compartmental ligands [108–110] derived from condensation of ethylenediamine with

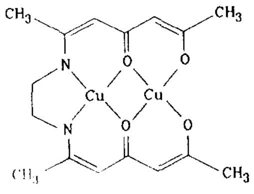

II

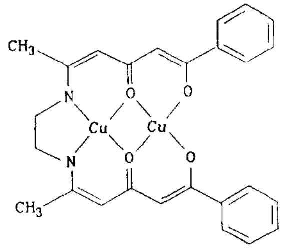

III

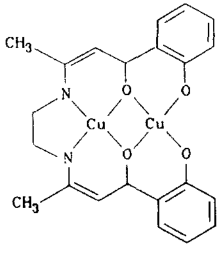

IV

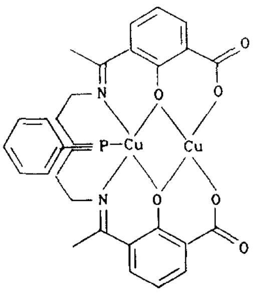

V

diacetylacetone, 1-phenyl-1,3,5-hexanetrione and *o*-acetoacetylphenol have shown little or no catalytic activity [104,107].

In contrast, complex **V** derived from a potentially heptadentate ligand has been found to oxidize 3,5-DTBC to 3,5-DTBQ. This may be due to the presence of an additional donor atom in the aliphatic chain [111].

F. COMPLEXES WITH END-OFF LIGANDS

The catalytic air oxidation of substituted diphenols [112,113] by copper (II) complexes derived from condensation of 2,6-diformyl-4-methylphenol and the amino acids glycine (**VI**), histidine (**VII**), lysine (**VIII**), glutamic acid (**IX**) and arginine (**X**) in the presence of the appropriate copper(II) salt [114,115], gives several products (Scheme 7).

The acidic products were supposed to be *cis,cis*-muconic acid and other open ring-acidic products; the formation of dimers or oligomers, followed by the precipitation of a black polymer from solution, was also observed [113].

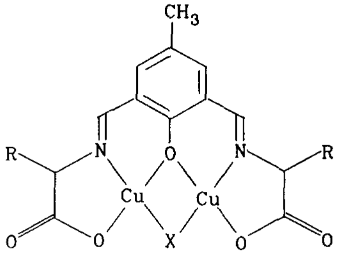

(VI -X)

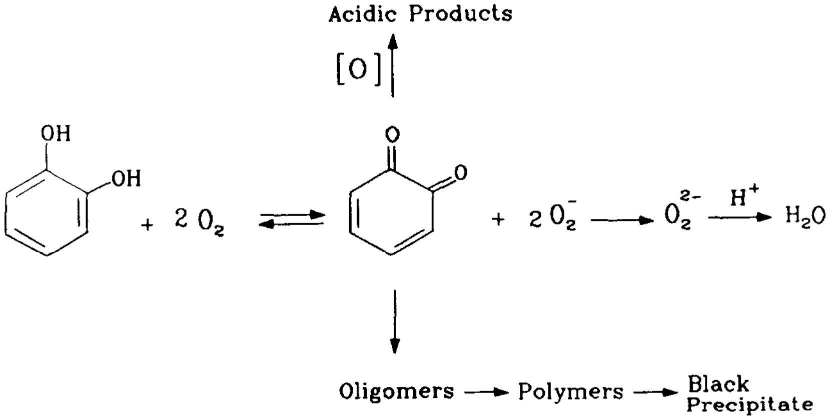

Scheme 7. Oxidation of *o*-diphenol by O_2 in the presence of the complexes VI–X.

The oxygen uptake and *o*-quinone production from the oxidation of 4-methylcatechol by the complexes derived from glycine and histidine (**VI** and **VII**) [113] follow in a rate ratio of approximately two; a one-electron transfer reaction which produces the superoxide ion was suggested [113]. After 8–10 min the O_2 uptake to *o*-quinone ratio becomes even larger than 2.5, making the reaction too complex for kinetic studies. The increased oxygen uptake to *o*-quinone ratio may be due to the use of O_2 in the ring-opening oxidation of the substrate [113].

The glycine complex shows a higher activity than the histidine one.

The oxidase activity, extended over a series of substituted *o*-phenols, decreases in the order catechol > 4-methylcatechol > dopamine > 3,4-dihydroxybenzonitrile > 3,4-dihydroxybenzoic acid; the *o*-diphenol, whose substituent is the best electron-donating group, gives the highest activity. The oxidase activity decreases with decrease in pH [113].

The ability of the copper(II) complexes derived from lysine (**VIII**), glutamic acid (**IX**) and arginine (**X**) to catalyse the dioxygen oxidation of 4-*t*-butylcatechol, 3-methoxycatechol, 4-methylcatechol, pyrocatechol and dopamine in aqueous solution generally parallels the inductive effect of the substituents on the benzene ring; steric effects also influence the reactivity [89]. For the first 8–10 min, 4 mol oxygen are used for every mole of catechol oxidized [112]. The large amount of oxygen used causes oligomerization and ring opening of *o*-quinones, all these reactions making the reaction mechanism impossible to be determined completely without a full characterization of all the oxidation products.

Similar dicopper(II) complexes (**XI** and **XII**) have been prepared by attaching 2,6-diformyl-4-methylphenol to polyethyleneimine (PEI) or to the copolymer poly(vinylamine–vinylsulphonate) sodium salt (PVA) to enhance the catecholase activity of the system and at the same time to immobilize the simple complex [116].

PEI complexes are soluble in water; thus they can be considered as homogeneous catalysts while the PVA complexes, owing to their insolubility in H_2O, have been studied as heterogeneous catalysts [116]. It was found that the activity of PEI copper complexes increases with increase in PEI polymer in the complex. The oxygen uptake rate for PEI complexes is greater than the number of moles of *o*-quinone produced, as reported above for related simple complexes [112–115].

The PVA copper complexes showed little or no activity, most probably due to their being a tightly coiled polymer which prevents catechol access to the dicopper sites. The slight activities observed for two of the PVA copper complexes resulted from surface effects [116]. The reversed activity on going from PEI to PVA complexes is, however, not easily explained on the basis of the published data.

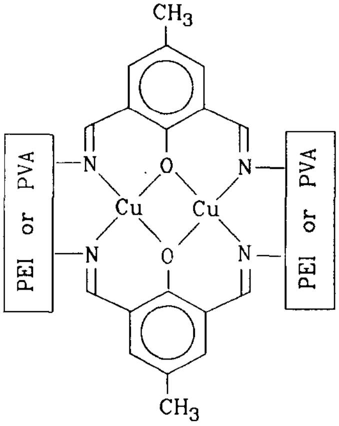

XI

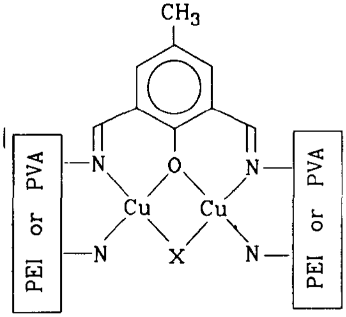

XII

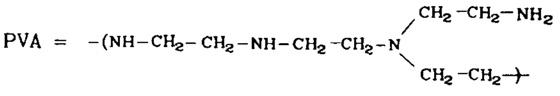

$$\mathrm{PVA} = -(\mathrm{NH{-}CH_2{-}CH_2{-}NH{-}CH_2{-}CH_2{-}N}\begin{array}{l}\diagup \mathrm{CH_2{-}CH_2{-}NH_2}\\ \diagdown \mathrm{CH_2{-}CH_2{-})\!-}\end{array}$$

polyethyleneimine

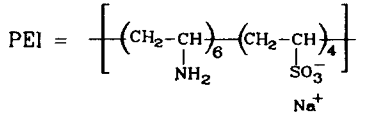

$$\mathrm{PEI} = \left[(\underset{\mathrm{NH_2}}{\mathrm{CH_2{-}CH}})_6 {-} (\underset{\underset{\mathrm{Na^+}}{\mathrm{SO_3^-}}}{\mathrm{CH_2{-}CH}})_4 \right]$$

copolymer of poly(vinylamine–vinylsulphonate)
60% amine–40% sulphonate

The copper(II) complexes derived from 2,6-diformyl-4-methylphenol and lysine or glutamic acid were also anchored to polystyrene or polyacrylic beads [117] through either the primary amine or the carboxylic acid not involved in the coordination to the copper ions, respectively (Scheme 8).

The complexes are reasonably stable and soluble in water. The glutamic acid complexes contain a high percentage of copper and were presumed to react better than the lysine complexes. The complex **XIII** gave the highest activity both in the *o*-quinone produced and in the oxygen uptake for the oxidation reaction in Scheme 7. It contained the largest amount of copper and its high activity is thus attributed to the high copper content. The complex **XV**, which was also found to be high in copper, exhibited high activities in *o*-quinone production and oxygen uptake. The complexes **XIV** and **XVI** were found to be low in copper content and exhibit low oxygen

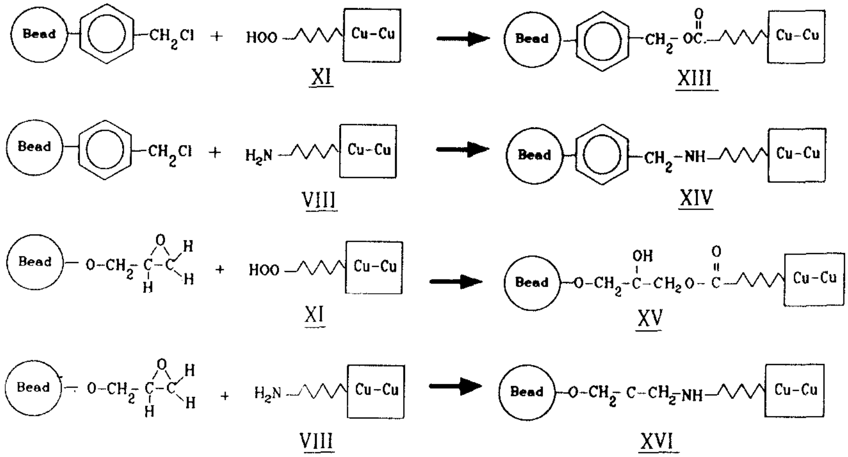

Scheme 8. Preparation of the polymeric dinuclear complexes **XIII–XVI**.

uptake. The *o*-quinone production activities of the **XIV** and **XVI** complexes were too low to be accurately measured.

The mole ratio of oxygen to *o*-quinone found (about 5:1), in line with the oxygen uptake observed for the simple complex (4:1), indicates that oxidation (Scheme 7) is also operating with these polymeric complexes.

A somewhat larger value of the activity of the simple complex **IX** over that of complexes **XIII** or **XV** at the same copper content was observed.

It was verified that end-off ligands, containing a central phenoxide bridging group, fail to impose a dinuclear structure with soft metals such as palladium(II) and platinum(II), unless the exogenous bridging group (Z) is a good donor for these metals and capable of giving the dinucleating ligand substantial assistance in maintaining the dinuclear structure (i.e. $Z=S^-$, pyrazolate anion) [118–121].

The synthesis of ligands H_3-**XVII** and H_3-**XVIII**, containing a bridging sulphur donor, was carried out and the corresponding palladium(II) complexes Pd_2(**XVII**)(Z) and Pd_2(**XVIII**)(Z) have been reported [118–121]. With H_3-**XVIII**, complexes readily soluble and crystallizable in $CHCl_3$ have been obtained. The ligand (H_3-**XVIII**) was synthesized by condensation of cyclohexane carboxylic acid hydrazide and 2-(*N*,*N*-dimethyl-thiocarbamato)-5-methylisophthalaldehyde.

Reaction of this dinucleating ligand with $Pd(CH_3COO)_2$ in $CHCl_3$ produces Pd_2(**XVIII**)(CH_3COO). The crystal structures of this dinuclear complex and its chloroform solvate [122] (Fig. 7) are quite similar to that of the complex in which an acetate group bridges palladium centres; both display similar distorted square-planar geometries. The long Pd–Pd distance (about 3.68 Å) is attributed to the presence of the bulky thiophenoxide bridge.

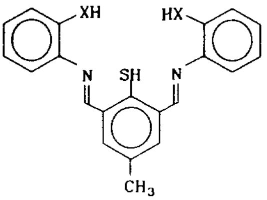

H_3-XVII

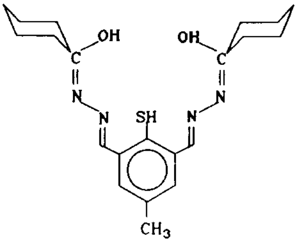

H_3-XVIII

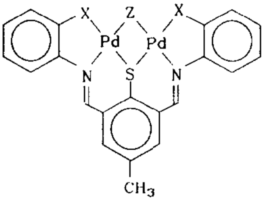

Pd_2(XVII)(Z)

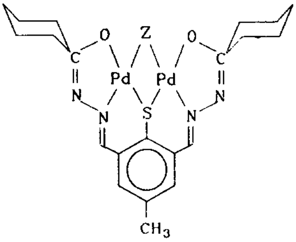

Pd_2(XVIII)(Z)

The acetato complex Pd_2(XVIII)(CH_3COO) readily undergoes a number of bridge substitution reactions [166,167]. Reactions with heterocycles [122,123] generate unusual organometallic complexes in which nitrogen and carbon centres of the bridging species serve as donors to palladium(II). The outgoing acetate often serves as a base to deprotonate the incoming bridge (Scheme 9).

The structure of Pd_2(XVIII)(1-propylimidazolate) obtained by boiling 1-*n*-propylimidazole with Pd_2(XVIII)(CH_3COO) in benzene containing some methanol, confirms the above scheme [123] (Fig. 8).

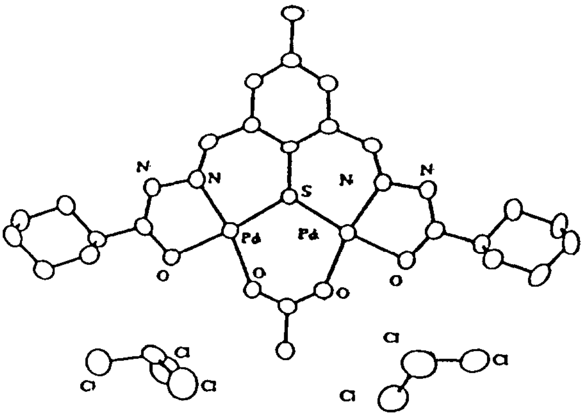

Fig. 7. Structure of [Pd_2(XVIII) (CH_3COO)]·$CHCl_3$ (from ref. 122).

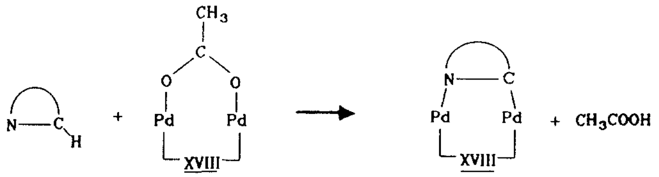

Scheme 9. Formation of dipalladium(II) organometallic complexes by heterocycles.

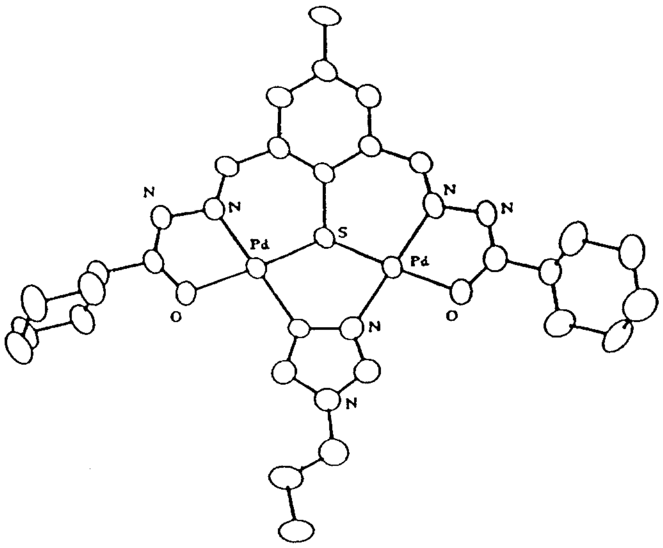

Fig. 8. Structure of [Pd_2(XVIII)(1-propylimidazolate) (from ref. 123).

The ligand side-arms are essentially equivalent, with both palladium centres displaying similar distorted square-planar geometries, the separation being 3.605 Å.

The bridging group of the imidazolate ligand coordinates to the metal centres through adjacent carbon and nitrogen atoms, as suggested on the basis of NMR data [119–121].

Pd_2(XVIII)(CH_3COO) reacts with 2-vinylpyridine in the presence of methanol or ethanol to generate the complexes Pd_2(XVIII)(C_5H_5NCH-CH_2OR):

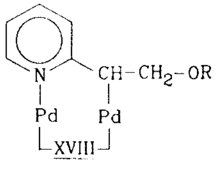

$R = CH_3, C_2H_5$,

^1H and ^{13}C NMR spectra indicate the presence in solution of two slowly interconverting forms at room temperature [119–121].

The acetato bridge in Pd_2(**XVIII**)(CH_3COO) can also be replaced by two separate ligands to give the compounds Pd_2(**XVIII**)(X)(Y) which are termed non-bridged complexes:

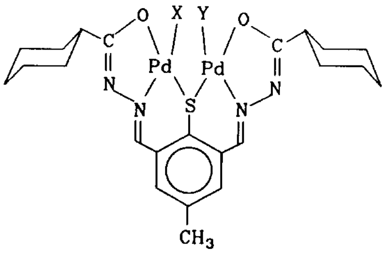

The treatment of Pd_2(**XVIII**)(CH_3COO) in $CHCl_3$ with an aqueous solution of glycine ethyl ester hydrochloride, to which one equivalent of hydroxide has been added, produces Pd_2(**XVIII**)(Cl)($NH_2CH_2COOC_2H_5$) [124] (Fig. 9), where the $[Pd_2(\mathbf{XVIII})]^+$ core has incorporated two independent donor groups, the chloride and ethyl glycinate groups, bonded to separate palladium centres.

Other similar complexes Pd_2(**XVIII**)(Cl)(NH_2R) (R = H, $CH_2C_6H_5$, $CH_2C_6H_4$-$p$$NO_2$) have been obtained by similar procedures; their spectroscopic properties support structures analogous to that of the glycine ester derivative. The chloride ion has been exchanged with N_3^- for R = H, while Pd_2(**XVIII**)(CH_3COO), when heated for a short time with 1-*n*-propylimidazole, produces [Pd_2(**XVIII**)(CH_3COO)(1-*n*-propylimidazole)], where the acetate ion is monodentate; in this complex the acetate and the imidazole

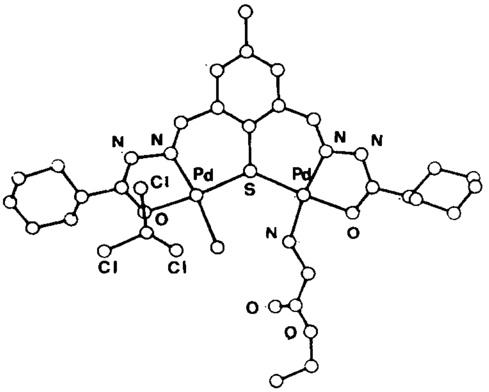

Fig. 9. Structure of [Pd_2(XVIII)(Cl)$NH_2CH_2COOC_2H_5$) (from ref. 124).

units exchange coordination positions at the palladium(II) site at a significant rate at room temperature. The other above similar complexes, on the contrary, do not show such exchange.

These results show that there is the possibility to bond a potentially nucleophilic centre to one metal ion while a substrate molecule is attached (through a π or σ bond to the metal) to an adjacent metal, being thereby activated towards nucleophilic attack. Electronically and sterically the intermediate **A** is predisposed to the formation of a Z–Y bond as in **B** in Scheme 10.

The formation of Pd_2(**XVIII**)(X)(Y) complexes containing two separate ligands and the ready incorporation of a wide range of three-atom bridges into the [Pd_2(**XVIII**)]$^+$ moiety strongly suggest that processes of the type **A**→**B** of the scheme may be possible. The first example of such a process is represented by the facile hydration of nitrile at a dipalladium(II) site under mild conditions [125]. Pd_2(**XVIII**)(CH_3COO) reacts with hydroxide ion to generate a Pd_2(**XVIII**) hydroxo compound, whose exact nature is uncertain although it exists as [Pd_2(**XVIII**)(OH)]$_n$ in $CHCl_3$.

Generally in the preparation of the hydroxo species a two-phase reaction mixture has been employed consisting of Pd_2(**XVIII**)(CH_3COO) in an organic phase ($CHCl_3$, CH_2Cl_2, tetrahydrofuran (THF), dioxane or benzene) and a basic aqueous phase (hydroxide, or carbonate or bicarbonate) both with and without a phase transfer agent [$M(C_4H_9)_4$]$^+$.

When the Pd_2(**XVIII**) hydroxo compound is dissolved in a 1:1 mixture of benzene and benzonitrile at room temperature a pale yellow crystalline solid separates. This product is identical with LPd_2(**XVIII**)(C_6H_5CONH) obtained by the bridge substitution reaction, under much more forcing conditions, between Pd_2(**XVIII**)(CH_3COO) and benzamide. A similar rapid reaction at room temperature occurs between acetonitrile and the Pd_2(**XVIII**) hydroxo complex. Again the same Pd_2(**XVIII**)(CH_3CONH) complex can be prepared by the bridge substitution reaction between Pd_2(**XVIII**)(CH_3COO) and acetamide in refluxing benzene–methanol.

Using the acetate-bridged complex as the promoter, acetonitrile could be hydrated to acetamide (bound as its conjugate base) under exceedingly mild

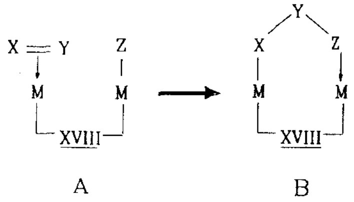

Scheme 10. Formation of a new species at a dipalladium(II) centre.

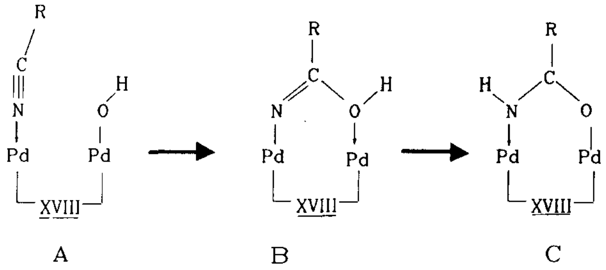

Scheme 11. Formation of Pd_2(**XVIII**)(R_3CONH).

basic conditions at room temperature: thus, when a two-phase mixture consisting of Pd_2(**XVIII**)(CH_3COO) in chloroform and an aqueous phase containing HCO_3^-, CO_3^{2-} and $[N(C_4H_9)_4]^+$ together with acetonitrile was stirred at room temperature for 30 min, Pd_2(**XVIII**)(CH_3CONH) was isolated essentially quantitatively from the organic phase (Scheme 11). In view of the ability of the $[Pd_2(\mathbf{XVIII})]^+$ unit to accommodate two separate ligands, it seems highly likely that the above nitrile hydration reactions proceed via the "non-bridged" intermediate of Scheme 10, formed either by displacement of the water ligand by the nitrile, if the Pd_2 hydroxo compound has the formulation Pd_2(**XVIII**)(OH,H_2O), or by breaking hydroxy bridges if the formulation is $[Pd_2(\mathbf{XVIII})(OH)]_n$.

2-(Acetylthio)-*N*,*N*′-bis(pyridin-2-ylmethyl)butanediamine (H_2-**XIX**(S–$COCH_3$)), synthesized according to Scheme 12, by reaction with $M(CH_3COO)_2$ (M = Pd(II), Ni(II), Cu(II)) leads to a rapid metal-promoted S-deprotection and yields M_2(**XIX**)(CH_3COO) [126]. The S-deprotected H_3-**XIX** can readily be obtained by hydrolysis of the S-acetyl derivative with aqueous ammonia at room temperature.

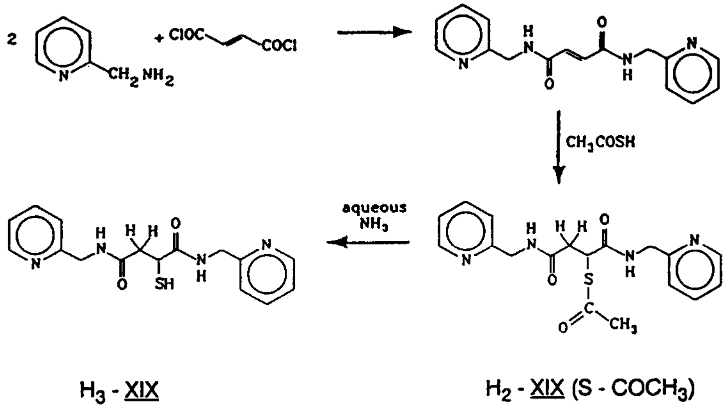

Scheme 12. The synthesis of H_3-**XIX**.

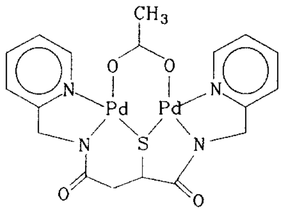

$Pd_2(XIX)(CH_3COO)$

Again the bridging acetate in Pd_2(**XIX**)(CH_3COO) can be substituted by other carboxylates, pyrazolates, I^-, N_3^-, SCN^-, $RCONH^-$ (the conjugate base of a carboxamide), and $(CH_3)_2NO^-$ (the conjugate base of *N*,*N*-dimethylhydroxylamine) and the resulting complexes have been studied by ^1H and ^{13}C NMR spectroscopy. Reaction of Pd_2(**XIX**)(CH_3COO) with NaI gives Na[Pd_2(**XIX**)I_2] and with NaN_3 gives Na[Pd_2(**XIX**)$(N_3)_2$], but reaction with NaSCN gives Pd_2 (**XIX**)(SCN).

The acetato-bridging substitution reaction in Pd_2(**XIX**)(CH_3COO) by $RCONH_2$ is only partial; a considerable amount of the initial carboxylate complex remains unchanged. The relative reluctance of the $[Pd_2$(**XIX**)$]^+$ system, compared with $[Pd_2$(**XVIII**)$]^+$, to accept the conjugate base of the amide at the bridging site has important implications with regard to the dinuclear catalysis of nitrile hydration. This reluctance probably stems from the unfavourable steric clash between the NH of the bridging group and the closely adjacent H or H′ as in the two possible geometrical isomers **A** and **B** in Scheme 11. For preparative purposes, the equilibrium above could readily be displaced to provide the amido-bridged complex free of carboxylate complex simply by adding 1,8-diazabicyclo[5.4.0]-7-undecene. In this way the complexes [Pd_2(**XIX**)(RCONH)] ($R = CH_3$, C_6H_{11}, CH_2CH) have been prepared [126,127]. NMR spectra of the three amido-bridged complexes are consistent with the presence in solution of a mixture of the geometrical isomers **a** and **b** (Scheme 13).

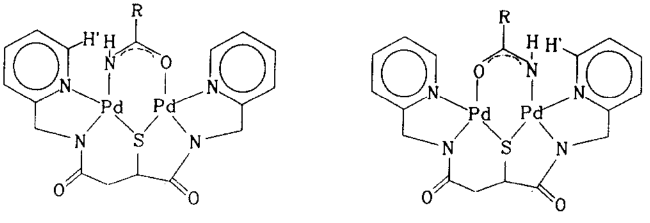

a b

Scheme 13. The hydrogen hindrances in the two isomers of Pd_2(**XIX**)(RCONH).

Reaction of Pd_2(**XIX**)(CH_3COO) with *N*,*N*-dimethylhydroxylamine and base gives Pd_2(**XIX**) ($(CH_3)_2NO$), which exists in only one of the two possible geometrical isomeric forms and which shows non-equivalent *N*-methyl groups.

Homogeneous catalytic hydration of acetonitrile by Pd(**XVIII**)(MeCONH) and Pd(**XIX**)(MeCONH) was conducted in a refluxing H_2O–MeCN mixture (2:5) with THF or cyclopentanone co-solvent for the complexes. The reactions were co-catalysed by acid.

The catalytic cycle shown in Scheme 12 was obtained [127], in which the process **A**→**C** reported in Scheme 11 constitutes step (a) of Scheme 14.

The ^1H NMR spectrum of Pd_2(**XVIII**)(OH) with $MeCONH_2$ in $CDCl_3$ at 25°C shows essentially complete conversion to Pd_2 (**XVIII**)(MeCONH) within 50 min. This indicates that step (b) is a reversible equilibrium lying in favour of Pd_2(**XVIII**)(MeCONH) in the absence of acid. ^1H NMR spectroscopy also shows that in the presence of HBF_4, free acetamide is released quantitatively from the bridging site within the time required to make the measurement.

Parallel reactions without dinuclear palladium(II) catalysts produced a negligible amount of acetamide. Negligible secondary hydrolysis of acetamide was observed. The rate of hydration catalysed by Pd_2(**XVIII**)(MeCONH) (THF co-solvent) was reduced by about 80% in the presence of added OH^- (1 equivalent). Degradation of **XIX** by OH^- precluded similar studies with Pd_2(**XIX**)(MeCONH).

Rates of acetamide production, with and without acid, decreased with time, very much more so with Pd_2 (**XVIII**)(MeCONH). This fall-off did not arise from catalyst decomposition (catalysts could be recovered), but rather from inhibition by the acetamide produced, as a consequence of the reversibility of step (b).

Nitrile hydration is known to be catalysed by mononuclear hydroxoplatinum(II) complexes in strongly basic solution, the C–O bond-forming step involving nucleophilic attack by free, uncoordinated hydroxide upon the coordinated nitrile. The above evidence for the dinuclear palladium(II) catalysts, in particular the co-catalysis by acid and the inhibition by hydroxide, excludes a similar mechanism in which free OH^- attacks a nitrile

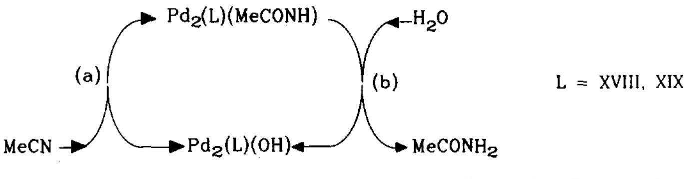

Scheme 14. Catalytic formation of acetamide by dipalladium(II) complexes (from ref. 127).

coordinated to one palladium atom with no participation by its neighbour. The evidence is, however, entirely consistent with the bimetallic mechanism in which the nucleophile is coordinated OH^- as in steps **A**→**C** in Scheme 11; step (a) in Scheme 14 is expected to be very slow at high acid concentration when the concentration of the hydroxo intermediate is negligible and step (b) to be very slow at low acid concentration because protonation of the bridging $MeCONH^-$ is required for its release; only at intermediate acid concentrations do both steps proceed at significant rates, leading to a maximum in the rate vs. $[H^+]$ plots. Coordination of OH^- greatly reduces its basicity, allowing it to exist in sufficient concentration for the overall cycle to proceed, even in a solution acidic enough to accelerate the amide-releasing step (b).

Hydration of acrylonitrile catalysed by Pt–OH complexes is generally very indiscriminate, giving a mixture of acrylamide, often as a minor product, and products of attack at the alkene such as $HOCH_2CH_2CN$, $O(CH_2CH_2CN)_2$ and $CH_2{=}C(CN)CH_2CH_2CN$. By contrast, acrylonitrile hydration catalysed by $Pd_2(\mathbf{XIX})(CH_2CHCONH)$ yields acrylamide very cleanly with no detectable amounts of the above products. This reaction also is co-catalysed by acid. The specificity of this reaction provides further support for the bimetallic pathway via a highly organized intermediate (**A** of Scheme 11).

G. COMPLEXES DERIVED FROM POLYPODAL LIGANDS

Several polypodal ligands have been prepared and used for dinuclear complexation. These complexes, owing to their flexibility, appear to be very promising agents in oxygen activation and in oxidation reactions. The ligands (Scheme 3) contain ionizable (i.e. COOH) or neutral (i.e. pyridine) groups in the pendent arms X while the central bridging group Y is a phenolic or an alcoholic OH. *N*,*N′*-(2-Hydroxy-5-methyl-1,3-xylene)bis(*N*-(carboxymethyl) glycine) (H_5-**XX**) [128] has been synthesized by the reaction of *p*-methylphenol, formaldehyde and iminodiacetic acid water. It reacts with iron(III) ions to form mononuclear, dinuclear and tetranuclear complexes and it is possible to follow the subsequent formation of these species step by step [129]. The addition of two equivalents of base and one of iron(III) to an aqueous solution of the ligand results in the formation of a purple complex assigned as the mononuclear species. Addition of a second aliquot of base and iron(III) to the purple solution then yields a red solution from which crystals of $Fe_2(\mathbf{XX})(OH)(H_2O)_2$ can be obtained. Further addition of an equivalent of base per iron(III) then affords an orange solution from which $M_4[Fe_4(\mathbf{XX})(O)_2(OH)_2]$ is obtained.

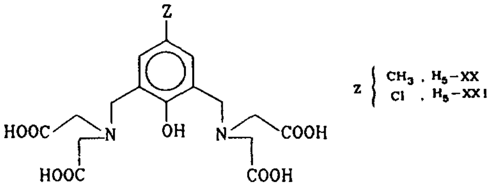

In the dinuclear complex the iron ions are coordinated in distorted octahedra and bridged by the phenolate and hydroxide oxygen atoms, which are somewhat asymmetrically disposed between the iron ions. Two water oxygen atoms complete the coordination polyhedra (Fig. 10). NMR spectra and the solid state magnetic moment ($\mu_{\text{eff}} = 5.1$ BM) indicate that a weak antiferro-magnetic interaction operates in this complex ($-J = 15\ \text{cm}^{-1}$).

By addition of acetate at pH 5 to $Fe_2(XX)(OH)(H_2O)_2$ and metathesis with $[N(CH_3)_4]Cl$, $[(CH_3)_4N][Fe_2(XX)(OAc)_2]$ has been obtained [130], and X-ray crystallography shows that the phenolate and two acetate groups bridge the iron ions to give a confacial octahedral structure (Fig. 11).

The same structure has been proposed for the chloro analogue $[N(CH_3)_4][Fe_2(XXI)(OAc)_2]$ (H_5-**XXI** is [1-oxy-2,6-di(*N*,*N*-biscarboxymethyl)aminomethyl]4-chlorobenzol) [130].

Addition of H_2O_2 to $[Fe_2(XXI)(OAc)_2]^-$ results in the probable formation of a peroxo–Fe(III) complex; only one acetate remains coordinated in this complex, suggesting that the peroxide has replaced the other acetate group, giving rise to $[Fe_2(XXI)(O_2)(OAc)]^-$ [130].

This peroxide complex can catalyse the disproportionation of H_2O_2 to O_2 and water. In the absence of an oxidizable substrate the complex slowly

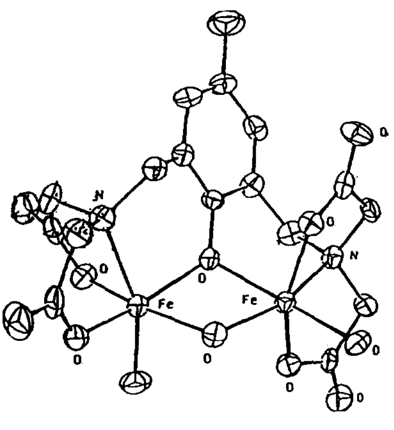

Fig. 10. Structure of $Fe_2(XX)(OH)(H_2O)_2$ (from ref. 129).

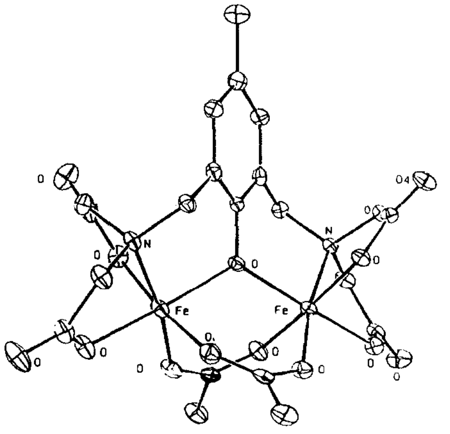

Fig. 11. Structure of $[Fe_2(XX)(OAc)_2]^-$ (from ref. 130).

destroys itself. In the presence of alkenes, epoxides along with byproducts of autoxidation have been obtained [130]. The epoxide constitutes 10% of the H_2O_2 consumed in the reaction; the epoxidation of *cis*-stilbene results in 95% trans epoxide and 5% cis epoxide.

The mononuclear iron(III) complex $Fe(Cl_2HDA)(H_2O)$, obtained by crystallization of aqueous solutions of $Fe(ClO_4)_3$ and $Na_3[Cl_2HDA]$, the trisodium salt of *N*-(4,6-dichloro-2-hydroxybenzyl)-*N*-(carboxymethyl)glycine, binds neither acetate nor peroxide, suggesting a requirement for a dinuclear unit for forming such complexes. The $Fe(Cl_2HDA)(H_2O)_2$–H_2O_2 mixture does not epoxidize alkenes but does catalyse peroxide disproportionation and one-electron oxidations such as the conversion of *o*-dianisidine and 2,4,6-tri-*t*-butylphenol to their corresponding cation radicals. This comparison seems to suggest that a dinuclear iron unit is required for the epoxidation chemistry [130].

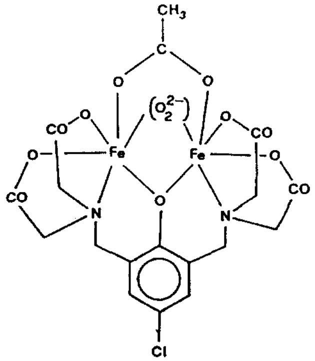

$[Fe_2(XXI)(O_2)(OAc)]^-$

The catalytic activiy of the similar dinuclear iron(III) complex [128], $Fe_2(XXI)(OH)(H_2O)_2$, in the oxidation of 3,5-di-*t*=butylcatechol (DTBC) has been tested [131]. DTBC in methanol was added to a borate buffer solution (pH 8.5) of the complex at 20°C and maintained under an oxygen atmosphere for several days; *N*,*N*-dimethylformamide (DMF) was also used in these oxidation reactions.

$Fe_2(XXI)(OH)(H_2O)_2$ is not selective and the catechol is preferentially oxidized to quinone (82–87%) and the lactone **XXII** (13–18%) instead of undergoing a catechol cleavage. For comparison, the catalytic activities of the analogous copper(II), manganese(II) and cobalt(II) complexes have been tested [131] and only DTBQ has been isolated from the reaction mixture.

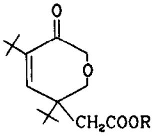

XXII

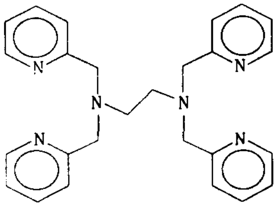

XXIII

Reaction of *N*,*N*,*N*′,*N*′-tetrakis(2-pyridylmethyl)ethylenediamine (**XXIII**) with $[Cu(CH_3CN)_4]BF_4$ produces $[Cu_2(\mathbf{XXIII})](BF_4)_2$, which is only slightly soluble in methanol, but saturation of a methanol suspension with CO results in complete dissolution. Upon purging this colourless solution with nitrogen, $[Cu_2(XXIII)](BF_4)_2$ is re-obtained. This process is totally reversible and may be repeated at will [156]. Evaporation of the methanol with a stream of CO gives off-white crystals of the dicarbonyl complex $[Cu_2(XXIII)(CO)_2](BF_4)_2$. The crystal structures of both complexes have been reported [132]. In $[Cu_2(XXIII)](BF_4)_2$ (Fig. 12) the ligand acts as a dinucleating chelate, securing the two copper(I) ions in close proximity. This causes a metal–metal separation of 2.78 Å.

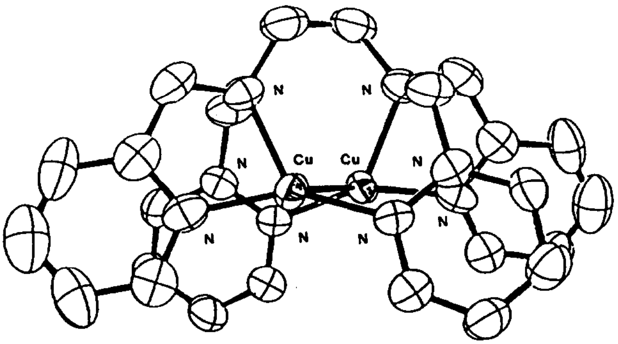

Fig. 12. Structure of $[Cu_2(XXIII)]^{2+}$ (from ref. 132).

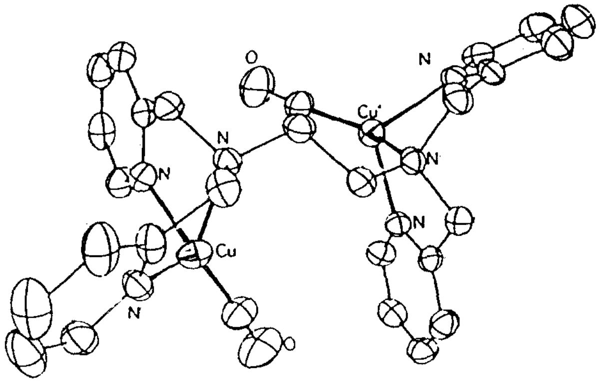

Fig. 13. Structure of $[Cu_2(\mathbf{XXIII})(CO)_2]^{2+}$ (from ref. 132).

In $[Cu_2(\mathbf{XXIII})(CO)_2](BF_4)_2$ (Fig. 13) an additional CO molecule has coordinated to each copper ion which assumes a pseudotetrahedral geometry, with the other three bound groups consisting of an amine nitrogen and the two pyridylmethyl groups attached to it.

Although the dicarbonyl compound is insoluble in most organic solvents, it is very soluble in acetonitrile, where it forms a deep yellow solution indicative of coordination of CH_3CN to copper to give a structure similar to that observed for the carbonyl adduct. $[Cu_2(\mathbf{XXIII})(CO)_2](BF_4)_2$ disproportionates in DMF: a single carbonyl stretching band at 2110 cm^{-1} was observed in the IR in this solvent, while its Nujol mull IR spectrum shows two CO bands at 2097 and 2107 cm^{-1}, consistent with the observation of two non-equivalent carbonyl groups in the crystal structure of the compound. Neither $[Cu_2(\mathbf{XXIII})](BF_4)_2$ nor its carbonyl adduct shows reactivity towards oxygen in the solid state, but solutions of the dicarbonyl complex in CH_2Cl_2, CH_3OH or DMF change from colourless to blue. This reaction cannot be reversed by purging the solutions with argon.

The oxidation of TMPD and substituted catechols by O_2 or H_2O_2, promoted by dinuclear iron(III) complexes with the ligands **XXIV** has been investigated [133]. For the complexes $Fe(\mathbf{XXIV})(NO_3)_5 \cdot n$S (S = EtOH, $n = 2$; S = MeOH, $n = 4$) and $Fe_2(\mathbf{XXIV})Cl_5$, which derive from a potentially

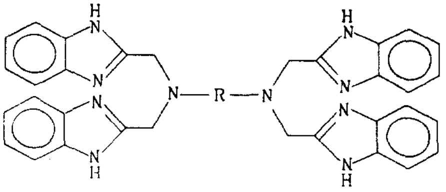

R

$-(CH_2)_4-$; $-(CH_2)_6-$;

$-CH_2C_6H_4CH_2-$; $-CH_2CH(OH)CH_2-$

XXIV

compartmental ligand containing an ionizable alcoholic OH group inside the aliphatic chain (R = $-CH_2-CH(OH)-CH_2-$), the compartmental structure **XXV** was supposed to be responsible for the enhanced catalytic activity of the above oxidation reactions in comparison with the other dinuclear complexes where the coordinating moieties of the ligands are linked by aliphatic or aromatic chains, not containing coordinating donor groups.

The alkoxo-bridged complexes (**XXV**) form a 1:1 adduct with catechol or H_2O_2 and for these complexes a dinuclear structure, similar to that proposed for the oxygen adduct was suggested [133].

The other iron(III) complexes do not form similar species when reacted with catechol. Orange methanolic solutions of Fe_2(**XXIV**)$(NO_3)_5$ (R = $-CH_2CH(OH)CH_2-$) were turned blue by addition of H_2O_2; similar behaviour was found in DMF, dimethyl sulphoxide (DMSO) or dimethylacetamide solutions. In water the colour changed from orange to violet. The blue species, attributed to the formation of **XXV**, gradually changes to orange. By addition of H_2O the orange solution turns blue again; 2,4-di-*t*-butylphenol accelerates the decomposition of the blue species. Methanolic solutions of these dinuclear complexes produce after standing for 4 days with an excess of H_2O_2 and 2,4-di-*t*-butylphenol, the corresponding quinone.

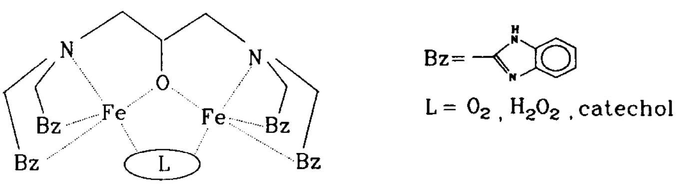

XXV

Copper(I) with the ligand 1,3-bis[*N*,*N*-bis(2-benzoimidazolylmethyl)aminomethyl]cyclohexane (**XXVI**) undergoes a reversible colour change when O_2 and N_2 are bubbled through alternatively [98]. Under an atmosphere of N_2, a CH_3OH-CH_3CN (1:14) solution of **XXVI** and $[Cu(CH_3CN)_4]BF_4$ is pale yellow; it gradually turns to deep violet when exposed to air at 5°C, while it immediately changes to violet on bubbling O_2 through it. This violet solution does not noticeably change at 0°C for at least 30 min. Bubbling N_2 into this solution changes its colour to yellowish green in about 10 min. Bubbling O_2 again into the yellowish green solution at 5°C resulted in a brownish blue solution. This solution turns green when N_2 is bubbled through at 20°C. The green solution no longer shows any remarkable colour change on bubbling with O_2.

XXVI

The absorption spectrum of a solution of the copper(II) complex, prepared by dissolving copper(II) tetrafluoroborate and **XXVI** in CH_3OH–CH_3CN in the ratio 2:1 is entirely different from that of the violet species mentioned above. It was accordingly suggested that the violet colour obtained from the reaction of $[Cu_2(\mathbf{XXVI})]^{2+}$ and O_2 is due to the formation of $[Cu_2(\mathbf{XXVI})(O_2)]^{2+}$, and the fading of the violet colour corresponds to the deoxygenation of the $[Cu_2(\mathbf{XXVI})O_2]^{2+}$ complex.

Copper(I) and copper(II) complexes with the similar, benzimidazole-containing ligands *N*,*N*,*N*′,*N*′-tetrakis(2-benzimidazolylmethyl)-1,2-ethanediamine (**XXVII**), *N*,*N*,*N*′,*N*′-tetrakis[(1-methyl-2-benzimidazolyl)methyl]-1,2-ethanediamine (**XXVIII**), *N*,*N*,*N*′,*N*′-tetrakis[(1-benzyl-2-benzimidazolyl)methyl]1,2-ethanediamine (**XXIX**), *N*,*N*,*N*′,*N*′-tetrakis[(5-methyl-2-benzimidazolyl)methyl-1,2-ethanediamine (**XXX**), or *N*,*N*,*N*′,*N*′-tetrakis[(5,6-dimethyl-2-benzimidazolyl)methyl]-1,2-ethanediamine (**XXXI**) have been reported [99]. They can be formulated at $Cu^{II}_2(L)(anion)_4$ and $Cu^{I}_2(L)(anion)_2$ and the structures of $[Cu^{I}_2(\mathbf{XXVII})](ClO_4)_2$ and $[Cu^{II}_2(\mathbf{XXIX})(NO_3)_3]NO_3 \cdot 4H_2O$ have been determined [135].

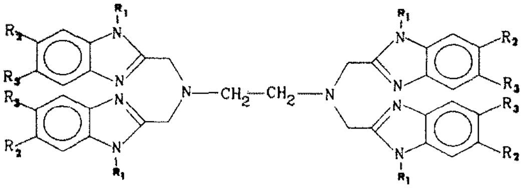

XXVII–XXXI

$[Cu_2(\mathbf{XXIX})(NO_3)_3]NO_3 \cdot 4H_2O$ consists of a dinuclear $[Cu_2(\mathbf{XXIX})(NO_3)_3]^+$ cation and a separate NO_3^- anion with C_2 symmetry. Each copper atom is coordinated by two imidazole nitrogen atoms of an asymmetric bidentate nitrate which lies on the twofold axis forming a bridge between the two symmetry-related copper atoms. The coordination geometry around copper(II) can be described as distorted octahedral, or owing to a weakly coordinated oxygen, as square pyramidal [135] (Fig. 14).

In the structure of $[Cu_2(\mathbf{XXVII})](ClO_4)_2$ the $[Cu_2(\mathbf{XXVII})]^{2+}$ cation has C_2 symmetry (Fig. 15). The coordination geometry around each copper(I)

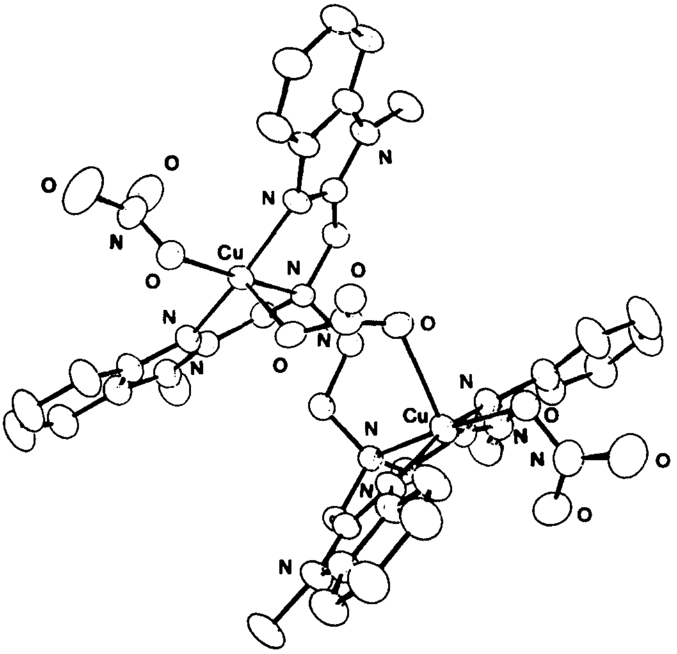

Fig. 14. Structure of $[Cu_2(XXIX)(NO_3)_3]^+$ (from ref. 135).

atom is nearly linear with a Cu···Cu distance of 3.043 Å Each copper(I) atom is coordinated by two imidazole groups, which are bonded via methylene groups to different amine nitrogen atoms.

Oxygenation reactions of these copper(I) compounds were carried out in DMSO solution at 25°C. The colourless solution of $[Cu_2(XXVII)](ClO_4)_2$ in

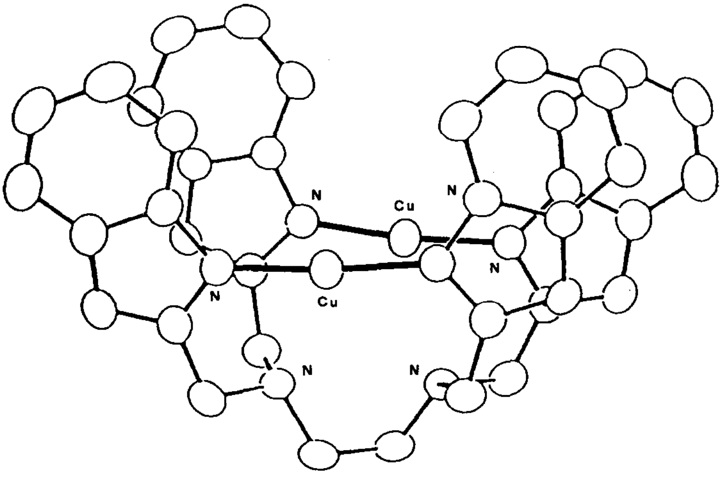

Fig. 15. Structure of $[Cu_2(XXVII)]^{2+}$ (from ref. 135).

DMSO shows an uptake of dioxygen of 0.96±0.05 mmol per Cu^I_2 (with $[Cu_2(\mathbf{XXVIII})](ClO_4)_2$ the uptake is 0.97±0.05 mmol per Cu^I_2), this suggesting the formation of a $Cu{-}O_2{-}Cu$ species. The resulting solution is green with an electronic spectrum characteristic for copper(II). Flushing the solution with dinitrogen, however, does not decolourize the solution; only a decrease in the intensity of colour occurs, indicating that the reaction with oxygen is not completely reversible. Addition of ascorbic acid or hydrazine results in complete decolourization of the solution. When small amounts of the reducing agent are used, this cycle can be repeated 3–5 times. Methylation of **XXVII** has no effect on the reaction with oxygen, showing that acid hydrogen atoms, which are present in **XXVII**, are not responsible for the reaction with oxygen. Also variations in the counter-ion have no effect upon the reaction with oxygen.

No Raman bands have been found in DMSO solutions of the oxygenated product which can be assigned to coordinated O_2. Frozen solution EPR spectra (DMSO–MeOH) of an oxygenated solution of $[Cu_2(\mathbf{XXVIII})]^{2+}$ are very similar to those of $[Cu(\mathbf{XXVIII})](NO_3)_2$. Apparently the dimeric unit decomposes after the reaction with oxygen. No EPR signal due to the other copper ion can be detected; reaction with the solvent might have resulted in an EPR-inactive species. Oxygenation reactions, carried out in other solvents such as MeOH, CH_3CN and DMF, do not give reproducible results as obtained in DMSO. In a subsequent investigation it was seen that when $[Cu_2(\mathbf{XXVII})](ClO_4)_2$ is suspended in a small amount of absolute ethanol, and oxygen is bubbled through, the colour changes to green, giving an oxygenated complex of formula $Cu_2(\mathbf{XXVII})(ClO_4)_2 \cdot O_2 \cdot 2H_2O$ [136]. This compound gives a Raman peak for dioxygen at 1007 cm^{-1}. Cyclic voltammetry studies suggest that the oxygenated product of $[Cu_2(\mathbf{XXVII})](ClO_4)_2$ is a $Cu(II){-}O_2{-}Cu(II)$ complex in the initial stages of oxygenation. The voltammogram obtained for $[Cu_2(\mathbf{XXVII})](ClO_4)_2$ under CO indicates CO binding to the dicopper(I) compound, with the formation of $[Cu_2(\mathbf{XXVII})(CO)](ClO_4)_2$ where CO is bound to only one of the two copper ions. EPR and absorbance studies have shown that the two copper ions are not equivalent in the oxygenated compound, which is paramagnetic, because the distance between the two metal ions is too large for coupling [136].

The ligand 1,8-bis[bis(1′-methylbenzimidazol-2′-ylmethyl)amino]-3,6-dioxaoctane (**XXXII**) has been synthesized by the ring-closure reaction of 1,2-diaminobenzene and 3,6-dioxaoctane-1,8-diamine-*N*,*N*,*N*′,*N*′-tetraacetic acid, followed by a methylation procedure [137]. Its reaction with $[Cu(CH_3CN)_4]ClO_4$ in refluxing $CH_3CN{-}CH_2Cl_2$, followed by CO bubbling for 30–60 minutes, forms $[Cu_2(\mathbf{XXXII})(CO)_2](ClO_4)_2$ [137] which is stable in a nitrogen atmosphere but in moist air slowly turns green. The CO can be removed from the solid sample at 150°C in high vacuum with decomposi-

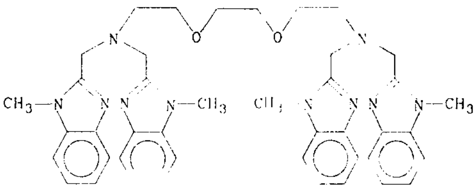

XXXII

tion. The IR spectrum shows a pair of CO bands at 2097 and 2107 cm^{-1}. A tetrahedral chromophore Cu^IN_3CO was suggested for this complex.

2,6-Bis[bis(2-pyridylmethyl)-aminomethyl]-4-methylphenol (H-**XXXIII**), obtained by condensation of 2,6-bis(chloromethyl)-4-methylphenol with bis(2-pyridylmethyl)amine [138,139], reacts under N_2 with $Co(CH_3COO)_2 \cdot 4H_2O$ in the presence of the equivalent amount of $NaClO_4$ to form the pink complex $[Co_2($**XXXIII**$)(CH_3COO)_2]ClO_4$ which is air stable when dried but turns brown in methanol on bubbling O_2 through the solution, giving rise after addition of $NaClO_4$ to the brown complex $[Co_2($**XXXIII**$)(CH_3COO)(O_2)](ClO_4)_2 \cdot 2H_2O$ [138].

Deoxygenation of the O_2 adduct by boiling the methanol solution under N_2 for a few minutes produces $[Co_2($**XXXIII**$)(CH_3COO)](ClO_4)_2$ as pink crystals which are air sensitive and change gradually in colour to brown; heating the brown solid at 150°C in vacuo regenerates the pink powder.

Electronic (bands at 9430 and 21100 cm^{-1}) and room temperature magnetic data ($\mu_{eff} = 4.5$ BM) indicate a high spin octahedral structure for $[Co_2($**XXXIII**$)(CH_3COO)_2]ClO_4$, the two acetate ions acting as chelate or bridging bidentate ligands towards the cobalt(II) ions.

No oxygenation was observed in acetonitrile and dichloromethane; in addition, oxygenation in methanol solution was suppressed by the addition of sodium acetate. The oxygenation was proposed to proceed via the five-coordinate complex, $[Co_2($**XXXIII**$)(CH_3COO)]^{2+}$.

Freshly prepared $[Co_2($**XXXIII**$)(CH_3COO)](ClO_4)_2$, which has a high spin pentacoordinate geometry ($\mu_{eff} = 4.32$ BM) with the acetate ion presumably acting as a bridging bidentate ligand also exhibits reversible oxygenation. Its electronic spectrum in CH_3CN in an air atmosphere is in agreement with full oxygenation to produce $[Co_2($**XXXIII**$)(CH_3COO)(O_2)](ClO_4)_2$.

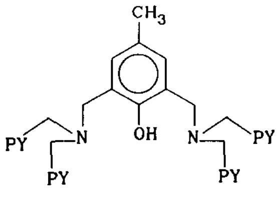

H-XXXIII

Bubbling N_2 through the acetonitrile solution of $[Co_2(\mathbf{XXXIII})(CH_3COO)(O_2)]^{2+}$ results in an extremely slow deoxygenation reaction at room temperature. However, heating at about 80°C causes a fast deoxygenation reaction, and no decomposition is observed after ten cycles of the oxygenation–deoxygenation process. The oxygenation–deoxygenation reactions may be represented by the reactions

$$[Co_2(\mathbf{XXXIII})(CH_3COO)_2]^+ \; + O_2 \rightarrow [Co(\mathbf{XXXIII})(CH_3COO)(O_2)]^{2+} \underset{+O_2}{\overset{-O_2}{\rightleftarrows}}$$

$$[Co_2(\mathbf{XXXIII})(CH_3COO)]^{2+}$$

$[Co_2(\mathbf{XXXIII})(CH_3COO)(O_2)](ClO_4)_2 \cdot 2H_2O$ is diamagnetic ($\mu_{eff}=0.48$ BM) at room temperature; its Raman spectrum shows an intense band at $820\ cm^{-1}$, assigned to the stretching vibration of oxygen coordinated to the metal in a μ-peroxo fashion, while its **IR** spectrum shows the $\nu_{asymm}(COO)$ and $\mu_{symm}(COO)$ at $1530\ cm^{-1}$ and $1410\ cm^{-1}$ respectively in agreement with bidentate coordination. The proposed structure is similar to that determined by X-ray analysis for the diamagnetic complex $[Co_2(\mathbf{XXXIII})(C_6H_5COO)(O_2)](BF_4)_2 \cdot 2H_2O$ [140]. This complex has been prepared by addition of $Co(BF_4)_2 \cdot 6H_2O$ and sodium benzoate to a methanolic solution of H-**XXXIII** in a 2:1:1 molar ratio followed by bubbling O_2 into the solution obtained and subsequent standing overnight at room temperature.

The molecular structure of the cation (Fig. 16) shows that the two cobalt ions are linked by bridging dioxygen, phenolate and benzoate in an approxi-

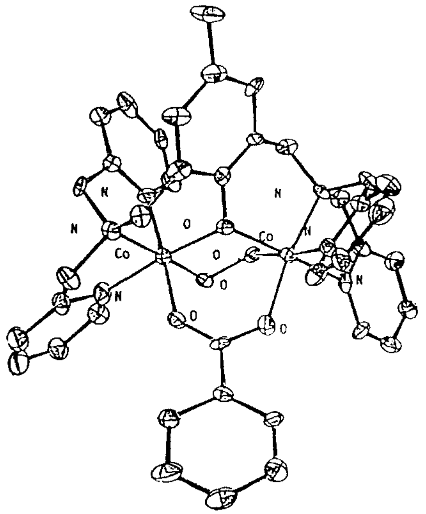

Fig. 16. Structure of $[Co_2(\mathbf{XXXIII})(C_6H_5COO)(O_2)]^{2+}$ (from ref. 140).

mately octahedral environment and in a *cis,cis*-N_3O_3 structure. The coordination geometries of Co(1) and Co(2), however, are different from each other. The Co···Co distance is 3.151 Å, while the O_2 bond distance is 1.43 Å.

[Co_2(**XXXIII**)(benzoate)(O_2)](BF_4)$_2$]·$2H_2O$, which is thermally much more stable than other complexes containing oxygen [141], binds reversibly to O_2 in the solid state. Upon heating at 180°C under N_2 it changes from brown to pink and the absorption spectrum of the pink complex is the same as that of [Co_2(**XXXIII**)(benzoate)](BF_4)$_2$. In the presence of O_2 the pink compound absorbs O_2 at room temperature, giving rise to the O_2 adduct.

These studies have been subsequently extended [142] to the dinuclear cobalt(II) complexes, [$Co_2L(CH_3COO)_2$]ClO_4, [$Co_2L(CH_3COO)$](ClO_4)$_2$, [$Co_2L(OH)$](ClO_4)$_2$, [$Co_2L(C_3H_3N_2)$](ClO_4)$_2$ ($C_3H_3N_2{}^-$ = pyrazolate), and [Co_2LX_2](ClO_4)$_n$, where HL represents H-**XXXIII**, 2,6-bis[*N*-(2-pyridylmethyl)-2-(2-pyridyl)ethylaminomethyl]-4-methylphenol (H-**XXXIV**), 2,6-bis-[bis[2-(2-pyridyl)ethyl]aminomethyl]-4-methylphenol (H-**XXXV**), and 2,6-bis[bis(2-benzimidazolylmethyl)aminomethyl]-4-methylphenol (H-**XXXVI**), and X is N_3^-, NCS^-, Cl^-, Br^-, H_2O or pyridine.

The electronic spectra and magnetic moments of the complexes reveal that [$Co_2L(CH_3COO)_2$]ClO_4 (L = **XXXIII**–**XXXV**) are high spin octahedral complexes, whereas the other complexes are high spin five-coordinate.

In the six-coordinate complexes the two acetate groups act as bridging bidentate ligands in [Co_2(**XXXVI**)(CH_3COO)$_2$]$^+$; the acetates are monodentate. Steric interaction between bulky benzimidazolyl groups and methyl groups of the acetate ions was suggested to be responsible for the five-cordinate structure.

[Co_2(**XXXIV**)(CH_3COO)$_2$]$^+$ also reacts reversibly with molecular oxygen in methanol; however, the oxygen affinity is low and no oxygenation was observed in methanol even at −40°C.

The dioxygen complex, [Co_2(**XXXIV**)(CH_3COO)(O_2)](ClO_4)$_2$·$2H_2O$, also undergoes reversible deoxygenation–oxygenation in acetonitrile. In contrast with the above complexes, [Co_2(**XXXV**)(CH_3COO)]$^{2+}$ did not react with molecular oxygen even at −40°C in acetonitrile.

The pyrazolato-bridged complexes with **XXXIII** and **XXXIV** are also air sensitive in the solid state. The reddish brown compounds turn brown upon exposure to air; by heating the brown compound derived from **XXXIV** at 140°C the reddish brown compound is regenerated whereas the complex derived from **XXXIII** decomposed without the colour change to reddish brown. However, reversible O_2 binding was observed for the **XXXIII** complex in acetonitrile. For the pyrazolate complex derived from **XXXIV**, oxygenation was not completely reversible in acetonitrile at 20°C.

[Co_2(**XXXIII**)(OH)](ClO_4)$_2$·$0.5H_2O$ is stable on exposure to air in the solid state. The complex reacts with molecular oxygen in acetonitrile to give a brown solution, and heating the brown solution at about 70°C under argon regenerates a green solution. The addition of sodium tetraphenylborate to an acetonitrile solution in air affords brown crystals of $[Co_2(\mathbf{XXXIII})(OH)(O_2)](BPh_4)_2 \cdot CH_3CN \cdot H_2O$ for which a structure with bridging $OH^-$and $O_2{}^{2-}$ groups essentially identical with those of the corresponding acetato and pyrazolato complexes has been proposed.

$[Co_2(\mathbf{XXXIII})(OH)]^{2+}$ does not react with molecular oxygen in the solid state and the oxygenation is extremely slow when compared with that of the acetato and pyrazolato complexes in acetonitrile.

The complexes $[Co_2(\mathbf{XXXIII})X_2]^+$ ($X = N_3^-$ or NCS^-) react reversibly with molecular oxygen in acetonitrile; however, the oxygenated complexes could be isolated. Conductivity measurements on the azido complex show that the oxygenated complex is a 1:1 electrolyte in acetonitrile, formulated as $[Co_2(\mathbf{XXXIII})(N_3)_2(O_2)]^+$. The chloro and bromo complexes $[Co_2(\mathbf{XXXIII})X_2]^+$ do not react with molecular oxygen even at −40°C.

In a series of complexes, $[Co_2(\mathbf{XXXIII})X_2]^+$, the order of the oxygen affinity is $N_3^- > NCS^- > Cl^-, Br^-$. The stronger the electron donor ability of the ligand, the greater the amount of the electron density on the cobalt centres, and the greater the oxygen affinity.

The oxygen affinities of the complexes derived from the ligands **XXXIII**–**XXXVI** are highly dependent on the nature of the dinucleating ligand. The order of the oxygen affinities for changes in the dinucleating ligands is **XXXIII** > **XXXIV** > **XXXV** and has been explained by considering the effect of the chelate ring size of the dinucleating ligand. The nitrogen donor atoms in the six-membered chelate rings are weaker electron donors than those in the corresponding five-membered chelate rings. In addition, the observed differences in the oxygen affinities of these complexes have also been attributed to the steric requirement of the dinucleating ligand. The oxygen binding sites of the two cobalt ions must be held in suitable positions for the O_2 binding in μ-peroxo fashion and such a steric requirement which is governed by the nature of the dinucleating ligand would also be responsible for the stability of the dioxygen complex. The lack of reactivity of the

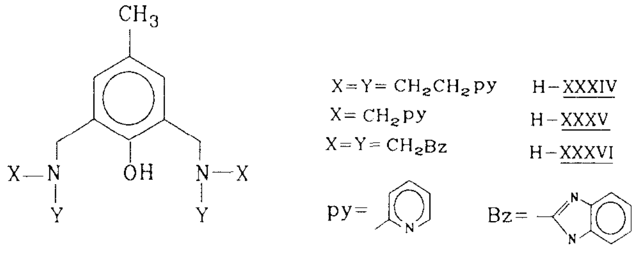

XXXVI complexes with molecular oxygen is also due to such a steric effect of benzimidazolyl groups. The oxygen affinities of $[Co_2L(C_3H_3N_2)]^{2+}$ are comparable with or smaller than those of $[Co_2L(CH_3COO)]^{2+}$(L = **XXXIII** or **XXXIV**).

It is well known that the nitrogen donors tend to promote oxygenation, whereas the oxygen donors such as carboxylates tend to retard dioxygen adduct formation. Pyrazolate must be a more effective σ-donor than acetate; thus the observed oxygen affinities of the pyrazolato complexes seem to be much weaker than those expected from the above general concept and the basicity argument. It was suggested that pyrazolate plays a role as a strong π-acceptor and/or that a pyrazolate bridge prevents optimum binding of O_2 in the μ-peroxo fashion.

The binding and activation of molecular oxygen has been studied in depth and recently reviewed by Karlin and Gultneh [143].

The interesting reaction, which can be viewed as a model system of the action of copper(II) monoxygenates, involves the copper-mediated hydroxylation of an arene [144]. A further review concerning the synthetic aspect of models for dinuclear copper proteins has recently appeared [97].

The *m*-xylyl ligand **XXXVII** (Scheme 15), derived by the reaction of bis-2-(2-pyridyl)ethylamine with α,α'-dibromo-*m*-xylene in ethyl acetate in the presence of diisopropylethylamine, reacts with $[Cu(CH_3CN)_4]PF_6$ in MeOH–CH_2Cl_2 to yield an extremely air-sensitive dinuclear copper(I) complex, which reacts with O_2 and gives rise to the phenoxy and methoxy copper(II) bridged complex shown in Fig. 17; this was confirmed by X-ray studies [145]. The cation has a planar Cu_2O_2 bridging unit and the ligand arranged around each copper atom is almost square pyramidal with an axial pyridyl nitrogen atom and a basal N_2O_2 donor set which includes the tertiary amines and pyridyl atoms. Two PF_6^- groups form the counter-anions.

Subsequent studies including manometric measurements of O_2 uptake, mass spectrometric analyses and structural determinations [144,146,147] have demonstrated that the reaction of the *m*-xylyl ligand **XXXVII** with copper(I) salts leads to the formation of the complex $[Cu_2(\mathbf{XXXVII})]^{2+}$ which reacts with oxygen to give $[Cu_2(\mathbf{XXXVIII})(OH)]^{2+}$. The copper ions can be removed from $[Cu_2(\mathbf{XXXVIII})(OH)]^{2+}$ to produce the ligand H-**XXXVIII** which by reaction with copper(I) gives $[Cu_2(\mathbf{XXXVIII})]^{+}$.

The structure of $[Cu_2(\mathbf{XXXVII})](PF_6)_2$ [144,146] consists of one discrete complex dication and two well-separated anions per asymmetric unit. The cation consists of two crystallographically independent cuprous ion coordination environments; each copper(I) is three coordinate, in a distorted trigonal planar coordination, with ligation from two pyridine molecules and one tertiary amino donor group (Fig. 18).

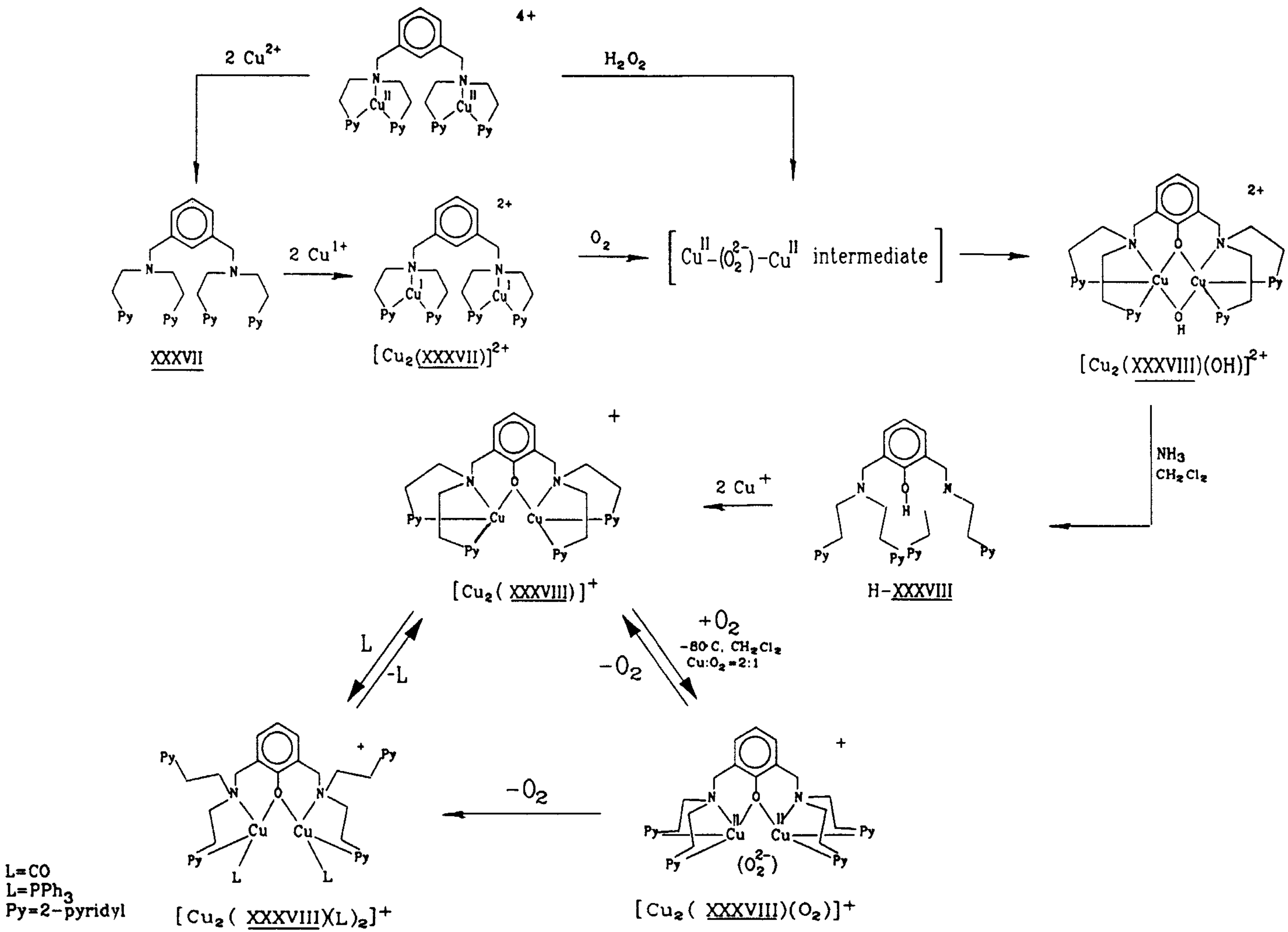

Scheme 15. Synthesis and reactivity of copper(I) and copper(II) complexes derived from **XXXVII**.

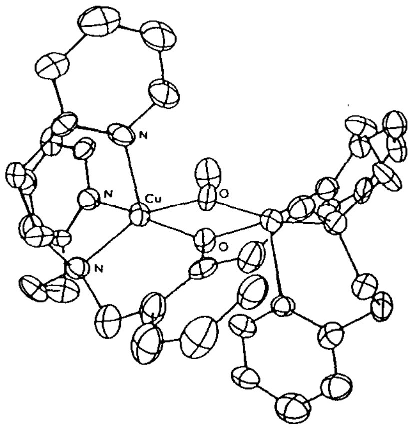

Fig. 17. Structure of $[Cu_2(XXXVIII)(OCH_3)]^{2+}$ (from ref. 145).

The structure of $[Cu_2(XXXVIII)(OH)](PF_6)_2$ [144] (Fig. 19) is composed of one discrete dication and two well-separated PF_6^- anions per asymmetric unit. The cation consists of two crystallographically independent but very similar copper(II) coordination environments in each dinuclear unit. Each copper ion is coordinated by the tertiary amine and two pyridine nitrogen atoms; the bridging-phenolate and hydroxide oxygen atoms complete the pentacoordination. The geometry around each copper is a tetragonal pyramid with two pyridine nitrogen atoms occupying axial positions on opposite sides of the Cu_2O_2 plane which is essentially planar.

For a better understanding of the reaction $[Cu_2(XXXVII)]^{2+} + O_2 \rightarrow [Cu_2(XXXVIII)(OH)]^{2+}$ in Scheme 15 and in particular to see if peroxo-bridged dicopper intermediates are required for hydroxylation of this system, the complex $[Cu_2(XXXVII)]^{4+}$ was prepared by reaction of $Cu(BF_4)_2 \cdot 6H_2O$ or $Cu(NO_3)_2 \cdot 3H_2O$ with **XXXVII** [110] (Scheme 15). $[Cu_2(XXXVII)]^{4+}$ reacts with H_2O_2 to give $[Cu_2(XXXVIII)(OH)]^{2+}$. No

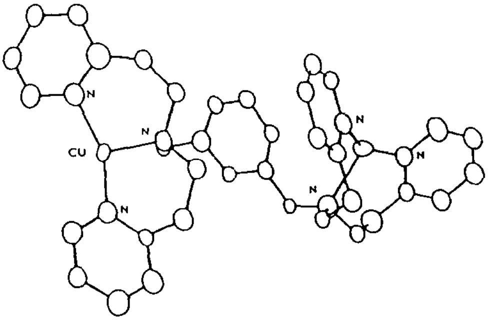

Fig. 18. Structure of $[Cu_2(XXXVII)]^{2+}$ (from ref. 146).

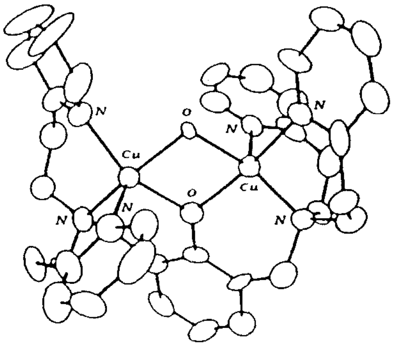

Fig. 19. Structure of $[Cu_2(\mathbf{XXXVIII})(OH)]^{2+}$ (from ref. 144).

hydroxylation was observed in the reaction of a free *m*-xylyl ligand with H_2O_2 or when $[Cu_2(\mathbf{XXXVIII})(OH)]^{2+}$ was first treated with ethylenediaminetetraacetic acid in aqueous DMF. This result suggests that a peroxo–Cu^{II} species is a common intermediate in pathways developing either from Cu^{I}–O_2 or Cu^{II}–H_2O_2.

To confirm that two copper ions are required for efficient hydroxylation the copper(I) complex $[Cu(\mathbf{XXXIX})]PF_6$ has been prepared [148] by treating **XXXIX** in THF with $[Cu(CH_3CN)_4]PF_6$ and crystallizing the resulting product from CH_2Cl_2–Et_2O. The cation displays a planar coordination (Fig. 20).

In solution, $[Cu(\mathbf{XXXIX})]^+$ reacts rapidly with oxygen, forming oxo– and hydroxo–Cu^{2+} species, without hydroxylation of the ligand, confirming that a second copper(I) ion is required for dioxygen activation and insertion into an organic substrate in the two-electron transformation $[Cu_2(\mathbf{XXXVII})^{2+}] + O_2 \rightarrow [Cu_2(\mathbf{XXXVIII})(OH)]^{2+}$ (Scheme 15). Also for the monomeric copper(II) complex, prepared from **XXXIX** and $Cu(BF_4)_2$, no hydroxylation of the ligand occurs upon mixing this complex with H_2O_2 in DMF–H_2O. The reaction of O_2 with $[Cu(\mathbf{XXXIX})]^+$, instead of hydroxylation of the phenyl group, forms a dinuclear oxo-bridged copper(II) complex [Cu(**XXXIX**)–O–

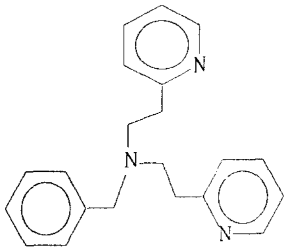

XXXIX

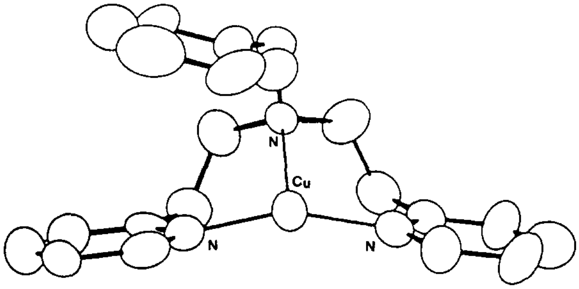

Fig. 20. Structure of [Cu(XXXIX)]$^+$ (from ref. 148).

Cu(XXXIX)]$^{2+}$, which with H_2O gives the dinuclear hydroxo-bridged complex [Cu(XXXIX)(OH)$_2$]$^{2+}$ [149] whose cation (Fig. 21) is a centrosymmetric dimer possessing a parallel-planar structure. This consists of square-based pyramidal copper(II) coordination spheres which are joined by axial-and basal-edged (equatorial) hydroxy groups. Basal coordination to copper (II) occurs from the two pyridyl nitrogen atoms and the tertiary amino nitrogen atom of **XXXIX** along with the equatorial hydroxy group. The Cu···Cu distance is 3.271 Å.

The formulation of the oxo-bridged complex [Cu(XXXIX)–O–Cu(XXXIX)]$^{2+}$ was supported by oxygen uptake (consistent with the four-electron reduction of O_2) and reactivity. [Cu(XXXIX)]$^+$ produces the oxo complex by reaction with iodosylbenzene, used as the source of O_2, in a 2:1 molar ratio.

The oxo- and hydroxo-bridged complexes are related by a water molecule. The dinuclear hydroxo-complex, which exhibits a sharp υ(OH) IR band at 3620 cm^{-1} when heated under vacuum, transforms into the green oxo-complex which does not show such a band in its IR spectrum. In a

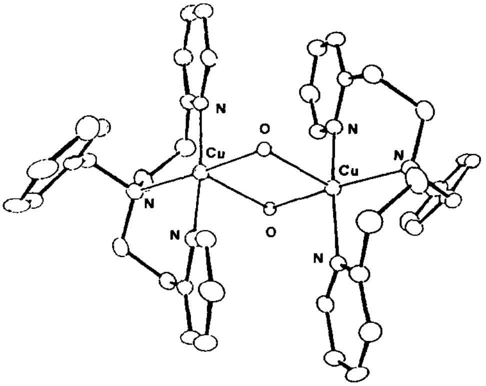

Fig. 21. Structure of [Cu$_2$(XXXIX)$_2$(OH)$_2$]$^{2+}$ (from ref. 149).

polar solvent such as methanol, both oxo- and hydroxo-species dissolve to give identical normal tetragonal EPR spectra, suggesting that weak bridging interactions are broken to give monomers. In CH_2Cl_2, however, dimeric structures for both oxo and hydroxo complexes are retained. Both complexes have a room-temperature μ_{eff} in agreement with a structure with bridging interactions.

Reaction of the dinuclear oxo-complex with triphenylphosphine in CH_2Cl_2 results in the stoichiometric production of triphenylphosphine oxide and regeneration of copper(I).

The similar series of ligands **XL-*n***, where two bis[2-(2-pyridyl)ethyl]amine molecules are connected by alkyl chains of varying length ($n = 3$–5), has been synthesized by the reaction of excess 2-vinylpyridine with the appropriate alkyldiamine and purified by column chromatography [112] with the aim of verifying the coordination requirements in Cu(I)–O_2 activation.

The reaction of $[Cu(CH_3CN)_4]ClO_4$ with **XL-3** in THF–acetone under argon produces $[Cu_2(\mathbf{XL\text{-}3})](ClO_4)_2$ which with O_2 in methanol at room temperature gives the dimethoxo-bridged copper(II) complex $[Cu_2(\mathbf{XL\text{-}3})(OMe)_2](ClO_4)_2$ [150,151]. In the cation $[Cu_2(\mathbf{XL\text{-}3})](OMe)_2]^{2+}$, two tetragonally coordinated copper(II) ions are bridged in the equatorial position by the methoxy ligands. The Cu_2O_2 bridging unit is planar; the two copper atoms are related by a crystallographic mirror plane containing the oxygen and the carbon atoms of the methoxy groups and the central carbon atoms of the connecting aliphatic chain in the ligand. The other two basal planes of the copper ions are taken by pyridine nitrogen ligands; the Cu···Cu distance is 3.070 Å [151] (Fig. 22).

The formation of this complex may also result from methanol attack on oxygen intermediates formed by the reaction of $[Cu_2(\mathbf{XL\text{-}3})]^{2+}$ with O_2. It was also observed that, if the reaction with dioxygen is carried out in CH_2Cl_2, the corresponding dihydroxy-bridged complex $[Cu_2(\mathbf{XL\text{-}3})(OH)_2]^{2+}$ is formed. No oxygenation of the dinucleating ligand occurs in these reactions.

Mixing $[Cu(CH_3CN)_4]Y(Y = ClO_4^- \text{ or } PF_6^-)$ with CO-saturated solutions of **XL-*n*** in methanol gives yellow-brown solutions of $[Cu_2(\mathbf{XL\text{-}}\boldsymbol{n})$

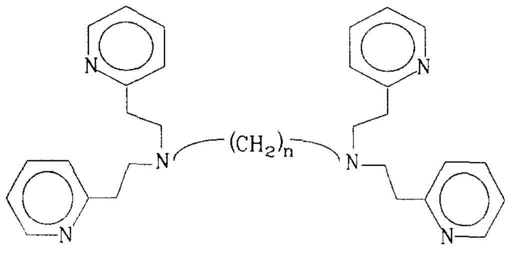

XL−*n* ($n = 3$–5)

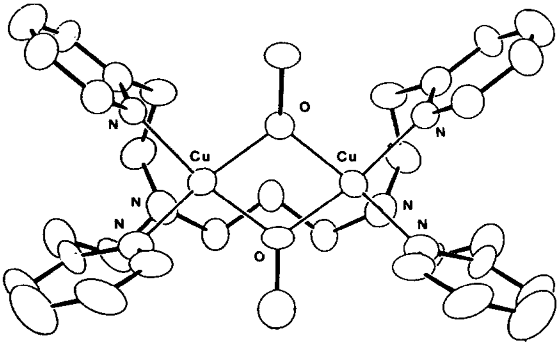

Fig. 22. Structure of $[Cu_2(XL\text{-}3)(OCH_3)]^{2+}$ (from ref. 151).

$(CO)_2]Y_2$ which are precipitated with diethyl ether and recrystallized from $CH_2Cl_2^-Et_2O$. X-ray crystallographic studies on the complexes with $n = 3$ and 5 show that they consist of well-separated copper ion moieties, each possessing Cu–N_3(CO) tetracoordination.

The complexes $[Cu_2(\mathbf{XL\text{-}4})(CH_3CN)_2]^{2+}$, formed in acetonitrile, are good starting materials for the reactions with dioxygen or other ligands since they are quite soluble, and the coordinated CH_3CN ligands are readily displaced [160].

The structure of $[Cu_2(\mathbf{XL\text{-}4})(CH_3CN)_2](ClO_4)_2$ consists of the discrete $[Cu_2(\mathbf{XL\text{-}4})(CH_3CN)_2]^{2+}$ dication and well-separated ClO_4^- anions; in the dication each identical copper(I) moiety possesses ligation to two pyridyl atoms and one amino nitrogen atom of the pyridyl unit and one N-bonded CH_3CN molecule in a pseudotetrahedral geometry (Fig. 23).

Decarbonylation of $[Cu_2(\mathbf{XL\text{-}n})(CO)_2]^{2+}$ in CH_2Cl_2 by vacuum-purge cycles under argon presumably gives $[Cu_2(\mathbf{XL\text{-}n})]^{2+}$. The tricoordinate compounds $[Cu_2(\mathbf{XL\text{-}4})](Y)_2$ ($Y = ClO_4^-$, PF_6^-) serve as useful precursors for reactions of the type

$$[Cu_2(\mathbf{XL\text{-}4})]^{2+} + 2D \rightarrow [Cu_2(\mathbf{XL\text{-}4})(D)_2]^{2+} \text{ where } D = CH_3CN, CO, PPh_3.$$

The order of binding strength of copper(I) in these complexes appears to

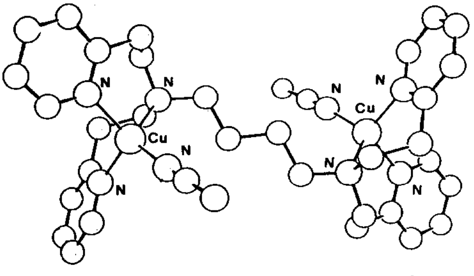

Fig. 23. Structure of $[Cu_2(XL\text{-}4)(CH_3CN)_2]^{2+}$ (from ref. 152).

be $CH_3CN < CO < PPh_3$ on the basis of the observation that CO displaces CH_3CN and PPh_3 displaces CO in the appropriate complexes, and these displacement reactions can be utilized to generate nearly quantitative yields of the substituted products.

$[Cu_2(\mathbf{XL\text{-}4})](ClO_4)_2$ possesses a crystallographic centre of symmetry midway along the tetramethylene backbone of the **XL-4** ligand; the cuprous ion polyhedra extend away from each other, with a Cu···Cu distance of 6.181 Å (Fig. 24). Each copper(I) ion is tetracoordinate in the solid state, with ligation to the three nitrogen atoms of the ligand and weak coordination to a single oxygen atom of the ClO_4^- anion. However, since the reactivity and solution behaviour of $[Cu_2(\mathbf{XL\text{-}4})]^{2+}$ complexes are predominantly independent of the anion, the binding of copper(I) in $[Cu_2(\mathbf{XL\text{-}4})](ClO_4)_2$ can be considered essentially that of a tricoordinate species [152].

Oxygenation of the pale yellow solutions of $[Cu_2(\mathbf{XL\text{-}n})]^{2+}$ at −80°C results in the rapid formation of intensely coloured solutions varying from deep purple to brown, depending on the value of *n*. Manometric measurements (−80°C) confirm that the stoichiometry of the reaction is $Cu{:}O_2 = 2{:}1$, thus giving complexes in solution formulated as $[Cu_2(\mathbf{XL\text{-}n})(O_2)]^{2+}$. The electronic spectra in the visible region of these dioxygen complexes show strong absorptions, characteristic of LMCT and/or *d–d* transitions for copper(II) ions.

$[Cu_2(\mathbf{XL\text{-}4})(CO)_2]^{2+}$ can be decarbonylated to give $[Cu_2(\mathbf{XL\text{-}4})]^{2+}$, which at low temperature is oxygenated to give the dioxygen complex $[Cu_2(\mathbf{XL\text{-}4})(O)_2]^{2+}$. Saturation of this solution with CO at low temperature and allowing the solution to warm up to room temperature converts the dioxygen adduct back to $[Cu_2(\mathbf{XL\text{-}4})(CO)_2]^{2+}$. The process can be repeated; it has been shown that less than 10% decomposition occurs over five cycles.

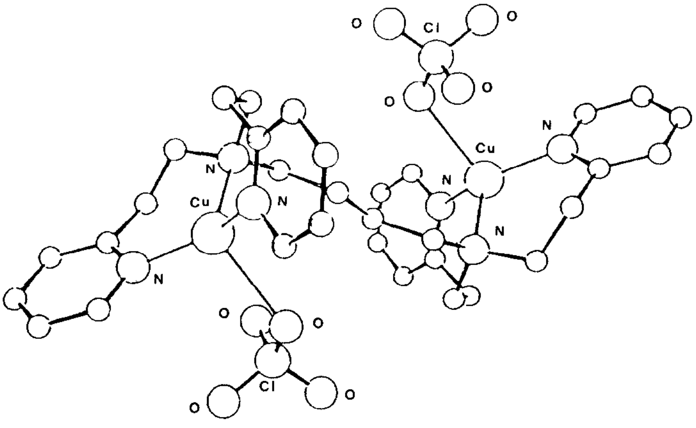

Fig. 24. Structure of $[Cu_2(\mathbf{XL\text{-}4})]^{2+}$ (from ref. 152).

$[Cu_2(\mathbf{XL\text{-}4})]^{2+}$ and $[Cu_2(\mathbf{XL\text{-}4})(O_2)]^{2+}$ can also be directly interconverted without appreciable decomposition through several cycles by alternate oxygenation and deoxygenation by warming under vacuum. The reversible binding of CO and O_2 by copper(I) complexes of **XL-3** and **XL-5** has also been confirmed by similar cycling experiments.

$[Cu_2(\mathbf{XL\text{-}4})(OH)_2](PF_6)_2$, a bis($\mu$-hydroxy)-bridged dicopper(II) complex, with a structure very similar to that known for $[Cu_2(\mathbf{XL\text{-}3})(OMe)_2](ClO_4)_2$, has been obtained by oxidation of $[Cu_2(\mathbf{XL\text{-}4})(CH_3CN)_2]^{2+}$ when allowed to react with O_2 in MeOH or CH_2Cl_2 at temperatures greater than 0°C or when the dioxygen adduct $[Cu_2(\mathbf{XL\text{-}4})(O_2)]^{2+}$ is allowed to decompose by warming to room temperature.

Using 1,2-diphenylhydrazine as a two-electron reductant, $[Cu_2(\mathbf{XL\text{-}4})(OH)_2](PF_6)_2$ is reduced to $[Cu_2(\mathbf{XL\text{-}4})](PF_6)_2$ in CH_2Cl_2, while heating in acetonitrile under argon results in its reduction to $[Cu(\mathbf{XL\text{-}4})(CH_3CN)_2](PF_6)_2$; however, the yield is low (30%).

No O_2 gas is evolved at any temperature when $[Cu_2(\mathbf{XL\text{-}4})(O_2)]^{2+}$ is reacted with PPh_3. $[Cu_2(\mathbf{XL\text{-}4})(O_2)]^{2+}$, by reaction with 2 equivalents of PPh_3, produces a less than stoichiometric amount of $O{=}PPh_3$, and even when an excess of triphenylphosphine is added the reaction is sluggish and the yield of $O{=}PPh_3$ is low. Thus $[Cu_2(\mathbf{XL\text{-}4})(O_2)]^{2+}$ does not efficiently oxygenate a substrate as easily oxidizable as PPh_3. On the other hand, O_2 is not displaced from $[Cu(\mathbf{XL\text{-}4})(O_2)]^{2+}$ by PPh_3 in spite of the fact that $[Cu_2(\mathbf{XL\text{-}4})(PPh_3)_2]^{2+}$ is a stable complex (Scheme 16).

The occurrence of a strong charge-transfer transition (suggestive of copper(II)) in the spectra of $[Cu_2(\mathbf{XL}\text{-}\boldsymbol{n})(O_2)]^{2+}$, the observed Cu:$O_2$ stoichiometry of 2:1, and the reversibility of O_2 and CO binding all suggest that these dioxygen complexes are probably best described as peroxo-dicopper(II) compounds.

The results obtained with the ligands (**XL-*n***), which have no potential Cu···Cu bridging group, indicate that a Cu···Cu bridging ligand is not a prerequisite for systems capable of binding CO and O_2 reversibly.

Further evidence for the intermediacy of the peroxo–dicopper(II) complex derives from the reactivity of O_2 with the dicopper(I) complex, $[Cu_2(\mathbf{XLI})](PF_6)_2$ [153].

The ligand **XLI** was prepared by synthesizing 2,6-bis(bromomethyl)fluorobenzene via the diazotization of 2,6-dimethylaniline using standard procedures and fluorination with HF–pyridine followed by bromination which was effected by using *N*-bromosuccinamide in CCl_4. Addition of $(C_5H_5N{-}CH_2)_2NH$ in the presence of base afforded the desired dinucleating ligand after column chromatography. The dicopper(I) complex, $[Cu_2(\mathbf{XLI})](PF_6)_2$, prepared by the anaerobic addition of two equivalents of $[Cu(CH_3CN)_4]PF_6$ to the ligand in methanol, followed by evaporation and

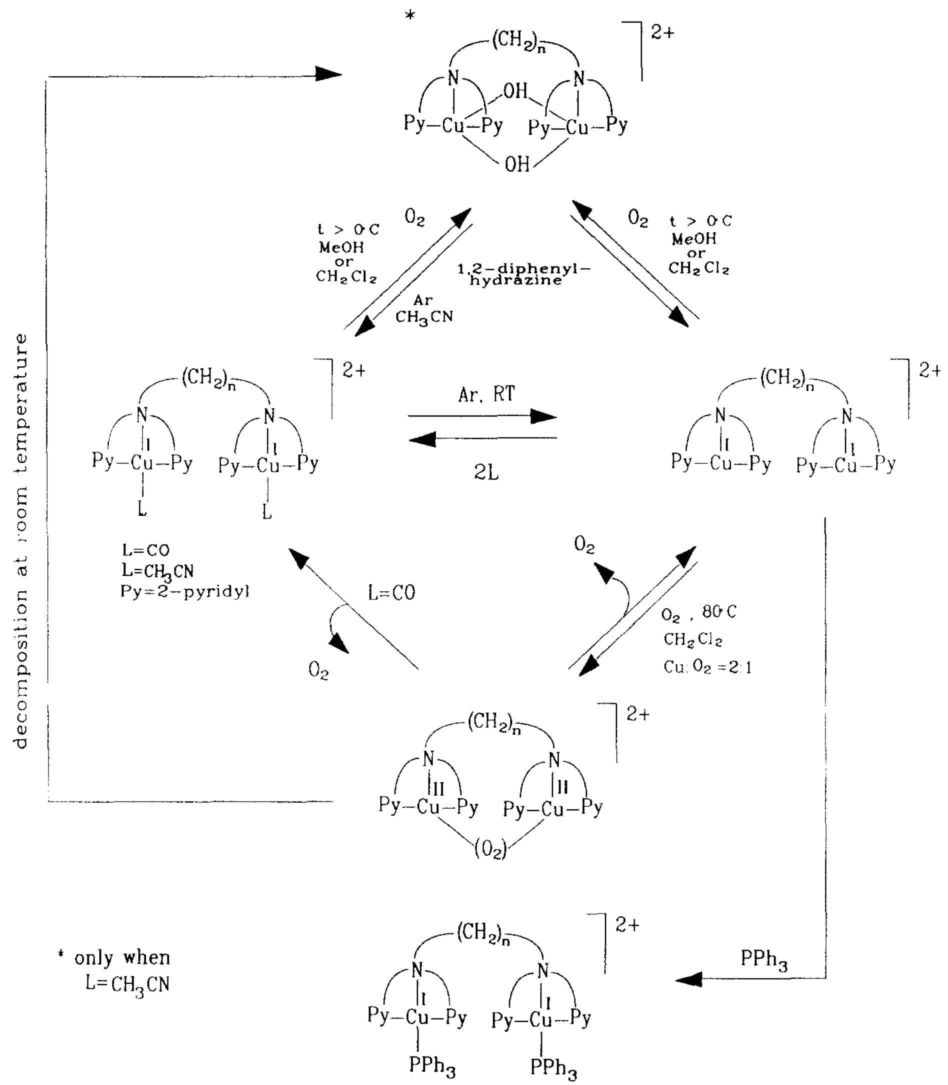

Scheme 16. Synthesis and reactivity of copper(I) and copper(II) complexes derived from **XL-*n***.

crystallization at 0°C, and by reaction with O_2 at $-80°C$ in CH_2Cl_2 produces the peroxo species $[Cu_2(\mathbf{XLI})(O_2)]^{2+}$ which shows a close similarity to the analogous complex $[Cu_2(\mathbf{XL\text{-}5})(O_2)]^{2+}$.

As an extension of this study, a CH_3 group was placed in the 2-position of the *m*-xylyl dinucleating ligand (**XLII**) [154]. This ligand, prepared by reaction of 2,6-bis(chloromethyl)mesitylene with bis[2-(2-pyridyl)ethyl]amine in the presence of a base, followed by column chromatography, when reacted with $[Cu(CH_3CN)_4]PF_6$ under argon produces the dicopper(I)

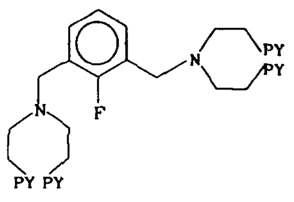

XLI

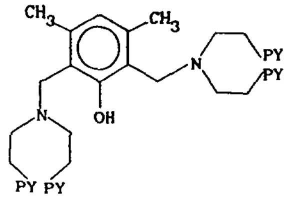

XLII

complex $[Cu_2(\mathbf{XLII})](PF_6)_2 \cdot 1.25CH_2Cl_2$. This complex, where dicopper(I) centres are presumed to be three-coordinate [154], reacts with O_2 in CH_2Cl_2 in a Cu:O_2 ratio of 2:1 to give a purple-brown solution. When the copper ions are stripped from the complexed organic product, by extraction with aqueous ammonia, the hydroxylated product (H-**XLIII**) and $(C_5H_4N\text{-}C_2H_4)_2NH$ are obtained (Scheme 17).

The phenol oxygen atom in H-**XLIII** was shown to be derived from dioxygen by carrying out the experiment using $^{18}O_2$ (greater than 70% ^{18}O

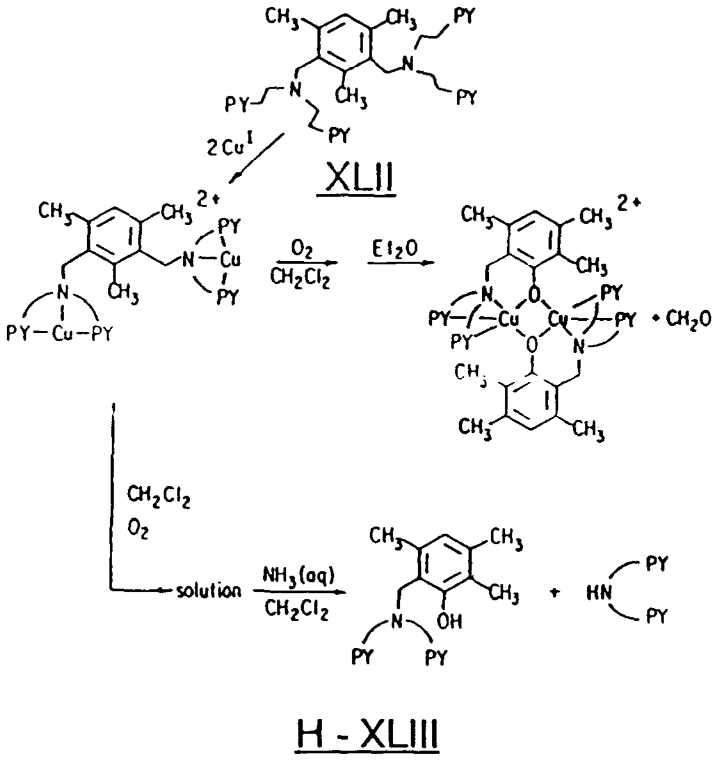

Scheme 17. Synthesis and reactivity of $[Cu_2(\mathbf{XLII})]^{2+}$.

incorporation). The detection of CH_2O was made difficult by using this base extraction procedure. However, when diethyl ether was added to the reaction product mixture of $[Cu_2(\mathbf{XLII})]^{2+}$ plus O_2, a dimeric copper complex, $[Cu_2(\mathbf{XLIII})_2]^{2+}$, was precipitated, and formaldehyde was detected.

The structure of $[Cu_2(\mathbf{XLIII})_2]^{2+}$ confirms the formation of H-**XLIII** and the regiochemistry of the methyl and hydroxyl groups in this compound. The dication $[Cu_2(\mathbf{XLIII})_2]^{2+}$ (Fig. 25) is a non-centrosymmetric dimer composed of distorted square-based pyramidal copper(II) coordination spheres, which are joined by basal-edged μ-phenoxo ligands. Pentacoordination is completed by an amino and one pyridyl nitrogen atom in the remaining basal positions; the other pyridine nitrogen atoms occupy the axial sites at significantly longer Cu–N bond lengths. The $Cu\cdots Cu$ distance is 3.091 Å.

The observed methyl migration provides support for the notion that in the reaction of $[Cu_2(\mathbf{XXXVII})]^{2+}$ or $[Cu_2(\mathbf{XLIII})_2]^{2+}$ with O_2 an electrophilic copper–oxy species (derived from the dicopper(I) complex plus O_2) attacks the arene, which then collapses to the observed products. Thus, in the reaction of $[Cu_2(\mathbf{XXXVII})]^{2+}$ with O_2, it is suggested that the 2-H atom undergoes a 1,2-migration and is then lost as H^+ (probably to the resulting μ-hydroxy group) during the re-aromatization of an oxygenated intermediate (e.g. arene oxide, or carbenium ion intermediate). Rather than lose CH_3^+ in the case of $[Cu_2(\mathbf{XLII})]^{2+} + O_2$, the lone pair on one amine nitrogen atom can be seen to "assist" with resulting loss of the iminium ion, $[(C_5H_4N{-}CH_2CH_2)_2N{=}CH_2]^+$, and formation of $[Cu_2(\mathbf{XLIII})_2]^{2+}$. The former product could readily undergo hydrolysis to give $(C_5H_4N{-}CH_2)_2NH$ and CH_2O under the reaction conditions employed.

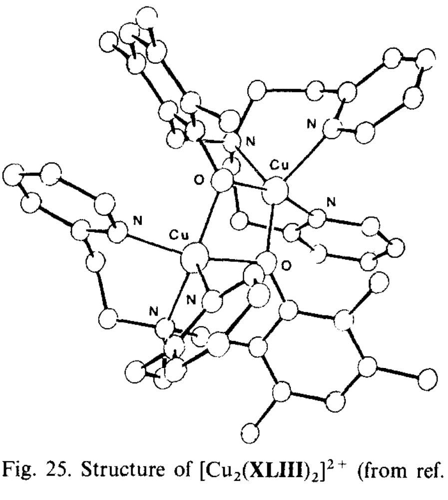

Fig. 25. Structure of $[Cu_2(\mathbf{XLIII})_2]^{2+}$ (from ref. 154).

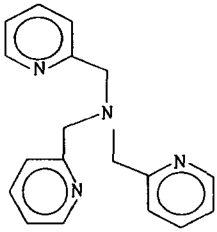

XLIV

A Cu–dioxygen complex has been recently fully characterized with the ligand tris [2-pyridyl]amine **XLIV**, which, although not dinucleating, resembles the above ligands [159]. This ligand with $[Cu(RCN)_4]PF_6$ forms $[Cu(\mathbf{XLIV})(RCN)](PF_6)$ which reacts with O_2, CO and PPh_3 according to Scheme 18.

The binding of O_2 and CO is reversible. When a vacuum is applied to $[Cu_2(\mathbf{XLIV})_2(O_2)]^{2+}$ in EtCN while heating briefly, the purple solution decolourizes, and $[Cu(\mathbf{XLIV})(EtCN)]^+$ is produced. Rechilling (below −80°C) followed by introduction of O_2 regenerates $[Cu_2(\mathbf{XLIV})_2(O_2)]^{2+}$. Via the reaction of $[Cu_2(\mathbf{XLIV})_2(O_2)]^{2+}$ with either PPh_3 or CO (in EtCN) the adducts $[Cu(\mathbf{XLIV})(D)]^+$ ($D = CO, PPh_3$) are obtained. CO can be used to effect repetitive carbonyl cycling where, in EtCN, O_2 is displaced from $[Cu_2(\mathbf{XLIV})_2(O_2)]^{2+}$ to give $[Cu(\mathbf{XLIV})(CO)]^+$. The CO is removed from the carbonyl complex via vacuum argon purge cycles (room temperature) providing $[Cu(\mathbf{XLIV})(RCN)]^+$, which by rechilling followed by oxygenation regenerates $[Cu_2(\mathbf{XLIV})_2(O_2)]^{2+}$.

If the reaction of PPh_3 with $[Cu_2(\mathbf{XLIV})_2(O_2)](PF_6)_2$ is carried out in the presence of acid ($2HPF_6 \cdot Et_2O$), $O{=}PPh_3$ (97%) is produced instead, along with the dicationic complex, $[Cu(\mathbf{XLIV})(MeCN)](PF_6)_2$. This occurs via PPh_3 oxidation by H_2O_2 since direct protonation of $[Cu_2(\mathbf{XLIV})_2(O_2)](PF_6)_2$ provides $[Cu(\mathbf{XLIV})(MeCN)](PF_6)_2$ and H_2O_2.

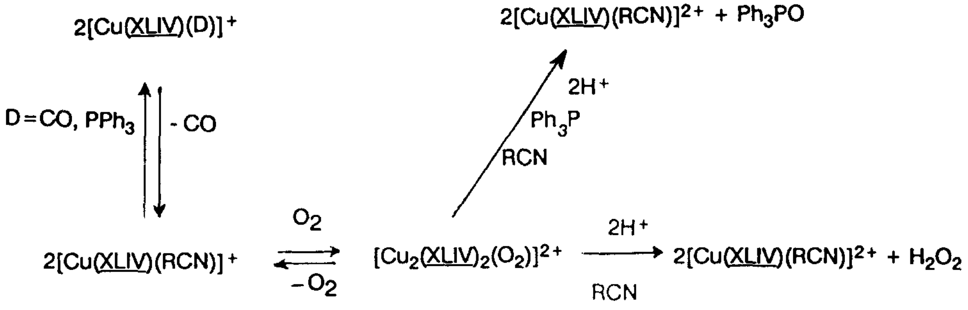

Scheme 18. Reactivity of $[Cu_2(\mathbf{XLIV})(RCN)]^+$ towards O_2, CO and PPh_3.

The complexes [Cu(**XLIV**)(D)]PF_6 (D = RCN, CO, PPh_3) are reported to contain D coordinated while **XLIV** acts as a tridentate ligand, one pyridine nitrogen not being involved in coordination to the copper(I) ion [147,159]. The dioxygen complex $[Cu_2(\mathbf{XLIV})(O_2)](PF_6)_2 \cdot 5Et_2O$ has been described as a peroxo–dicopper species containing a trans μ-1,2-O_2^{2-} group derived from O_2 bridging the two copper(II) ions. There is one dinuclear copper(II) complex per unit cell with a crystallographic inversion centre between the two oxygen atoms of the O_2^{2-} group. The copper atom is pentacoordinate with a distorted trigonal bipyramidal geometry. The equatorial ligands are the three pyridyl nitrogen donors, with an aliphatic amine nitrogen and one peroxo oxygen atom occupying axial sites. The Cu···Cu separation is 4.359 Å, and the O–O bond length is 1.432 Å [155] (Fig. 26).

The mode of binding of dioxygen to copper in the complexes derived from the reversible reaction of the dicopper(I) complexes $[Cu_2(\mathbf{XL}\text{-}\boldsymbol{n})]^{2+}$ with O_2 in CH_2Cl_2 at −80°C (Scheme 19) has been investigated by X-ray absorption studies [156] which confirm that the dioxygen adducts $[Cu_2(\mathbf{XL}\text{-}\boldsymbol{n})(O_2)]^{2+}$ are copper(II)-containing species. Along with electronic, EPR and NMR spectroscopic evidence, the Cu···Cu distances observed (3.2–3.4 Å) by EXAFS spectroscopy suggest that a peroxo (O_2^{2-}) ligand bridges and magnetically couples the two copper(II) ions in $[Cu_2(\mathbf{XL}\text{-}\boldsymbol{n})(O_2)]^{2+}$.

EXAFS analysis and model-building studies [156] suggest two possible structures (**A** and **B** in Scheme 19) for these peroxo–copper(II) complexes. The best data have been obtained with the complex derived from **XL-4**.

In structure **A**, a 3.37 Å Cu···Cu distance predicts reasonable hybridization at the coordinated oxygen atoms, and a model of the structure shows that a stacked configuration for the pyridine rings of adjacent tridentate units of the **XL-4** ligand would ensue. In structure **A**, the inner coordination

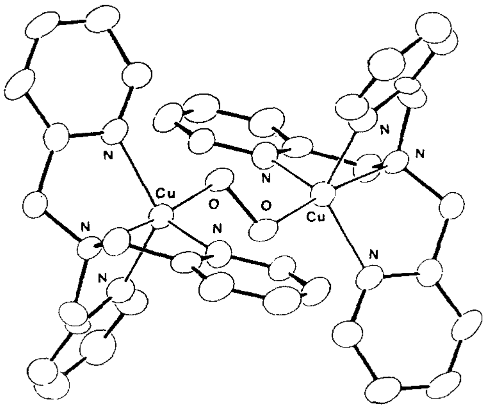

Fig. 26. Structure of $[Cu_2(\mathbf{XLIV})_2(O_2)]^{2+}$ (from ref. 155).

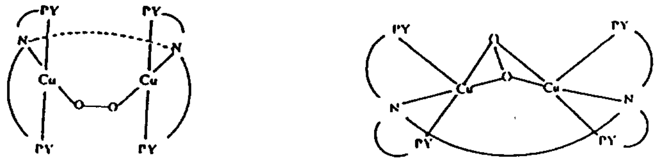

A B

Scheme 19. The two possible structures for the peroxo(II) complexes [Cu_2(XL-**n**)(O_2)]$^{2+}$ according to EXAFS studies (from ref. 156).

sphere would consist of the three nitrogen donors of the tridentate ligand plus one oxygen donor from the coordinated peroxo group. However, neither the 2.5 Å Cu–N distance nor the evidence for one axially coordinated pyridine group per copper(II) can be accommodated within this structure. Structure **B** may be thought of as a symmetrically bridged η^2:η^2 species, where the inner coordination shell would consist of two nitrogen donors and two peroxo oxygen atoms. A third nitrogen donor at a longer distance (2.56 Å) is consistent with both the EXAFS data and the tendency of planar four-coordinate copper(II) to achieve pentacoordination. The observed Cu···Cu distance of 3.37 Å in **XL-4** would require a non-planar $Cu_2(O_2)$ unit. For compounds derived from **XL-3** and **XL-5**, although the Cu···Cu distance has been determined with less confidence, the details of the EXAFS analysis, similar to that for the compound derived from **XL-4**, suggest similar structures.

Very recently the μ-η^2:η^2-peroxo bridge has been shown, through an X-ray crystal structure, to be present in the dinuclear complex {Cu_2[HB(3,5-$iPr_2pz)_3]_2(O_2)$} where the terminal ligands are tripodal tris(3,5-isopropylpyrazolyl)borate anions [157]. The spectroscopic properties of this complex are closely similar to those of oxyhaemocyanin. The Cu···Cu separation is 3.56 Å and so is significantly shorter than that found in the *trans*-μ-1,2-peroxo bridge (Fig. 26) but consistent with the proposed distances for oxyhaemocyanin (3.58–3.66 Å). A *cis*-μ-1,2-peroxo bridge has been the favoured proposition as a consequence of cumulative magnetic and spectroscopic studies on both natural and model complexes. However, there is as yet no direct evidence for such a bridge. Consequently with the structure of deoxyhaemocyanin indicating that there is no bridging atom proximal to the dinuclear site it is possible to advance the proposition that, in the absence of an additional bridge at the copper site, the μ-η^2:η^2-coordination mode of peroxide occurs.

All these data provide evidence that the hydroxylation reaction [Cu_2(**XXXVII**)]$^{2+}$ + O_2 → [Cu_2(**XXXVIII**)(OH)]$^{2+}$ in Scheme 15 initially proceeds via the formation of a peroxo–copper(II) species. The complex $[Cu_2(\textbf{XXXVIII})](PF_6)_2$ [159] has been obtained by addition of H-**XXXVIII**, containing NaOH, to $[Cu(CH_3CN)_4]PF_6$. Each of the two crystallographically independent molecules of the cation in the asymmetric unit consists of two four-coordinate copper(I) ions bonded to the amino nitrogen, to two pyridine nitrogen atoms, and to a bridging phenoxo oxygen. The geometry about each copper(I) has been described as pyramidal, the basal plane being formed by the two pyridine donors and the oxygen atoms; the longer axial position is occupied by the tertiary amino nitrogen. The Cu···Cu distances in the molecules are 3.619 and 3.715 Å (Fig. 27).

When $[Cu_2(\textbf{XXXVIII})]^{2+}$ in CH_2Cl_2 is exposed to O_2 below −50°C the purple peroxo–copper(II) complex $[Cu_2(\textbf{XXXVIII})(O_2)]^{2+}$ is formed [159]. Manometric measurements at −78°C indicated that 1 mol dioxygen is taken up per mole of complex, and Raman and electronic spectra confirmed the formation of a copper peroxide complex.

The reversibility of dioxygen binding to $[Cu_2(\textbf{XXXVIII})]^{+}$ is indicated by its oxygenation ability and by the deoxygenation of $[Cu_2(\textbf{XXXVIII})(O_2)]$ through several cycles in a quasi-reversible manner without severe decomposition. This is accomplished by the application of a vacuum to a CH_2Cl_2 solution of $[Cu_2(\textbf{XXXVIII})(O_2)]^{+}$ to remove the bound dioxygen ligand. Spectrometric data show that beginning with the pure dicopper(I) complex $[Cu_2(\textbf{XXXVIII})]^{+}$, oxygenation at −80°C gives the spectrum of the complex $[Cu_2(\textbf{XXXVIII})(O_2)]^{+}$. Rapid warming to room temperature under vacuum removes O_2, regenerating the deoxy complex $[Cu_2(\textbf{XXXVIII})]^{+}$.

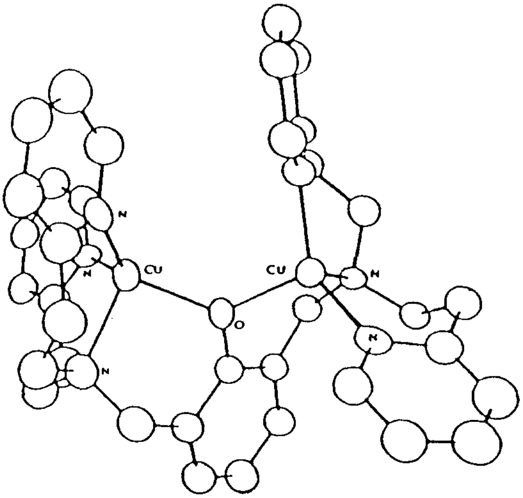

Fig. 27. Structure of $[Cu_2(\textbf{XXXVIII})]^{+}$ (from ref. 159).

Lowering the temperature again to −80°C and bubbling the solution with O_2 regenerates the oxy compound with a small amount of decomposition (about 10%). The cycle can be repeated, although with a greater degree of decomposition. Dioxygen is also removed when a vacuum is applied to solutions of $[Cu_2(XXXVIII)(O_2)]$.

Solutions of $[Cu_2(XXXVIII)]^+$, allowed to warm up to room temperature, have the same electronic spectrum as $[Cu_2(XXXVIII)(OH)]^{2+}$. It was suggested [117] that the primary decomposition pathway of $[Cu_2(XXXVIII)]^+$ would be that giving $[Cu_2(XXXVIII)(OH)]^{2+}$ which, however, was not isolated by this route.

Both CO and PPh_3 react with $[Cu_2(XXXVIII)(O_2)]^+$ to form the complexes $[Cu_2(XXXVIII)(L)_2]^+$ (L=CO, PPh_3) which have also been prepared by reaction of $[Cu_2(XXXVIII)]^+$ with the appropriate ligand (Scheme 14). The complex $[Cu_2(XXXVIII)(PPh_3)_2]^+$ have been crystallized, and the structure of the cation (Fig. 28) shows that each copper(I) ion is tetracoordinated, in a pseudotetrahedral geometry, by the amino nitrogen and one pyridine arm of the $(C_5H_4N{-}C_2H_4)_2NH$ tridentate unit, the phenoxo oxygen atom and the phosphorus atom of the triphenylphosphine ligand. The Cu···Cu distance is quite long (3.992 Å) which is probably due to the steric crowding of the PPh_3 ligands at the dinuclear coordination centre.

Bubbling CO through a dichloromethane solution of $[Cu_2(XXXVIII)]^+$ results in a colour change from orange to pale yellow. The IR spectrum of the carbonyl adduct so formed in solution exhibits υ(CO) at 200 cm^{-1} which is in the range accepted for coordinated CO. However, the compound $[Cu_2(XXXVIII)(CO)_2]^+$ cannot be isolated as a solid even under 1 atm of

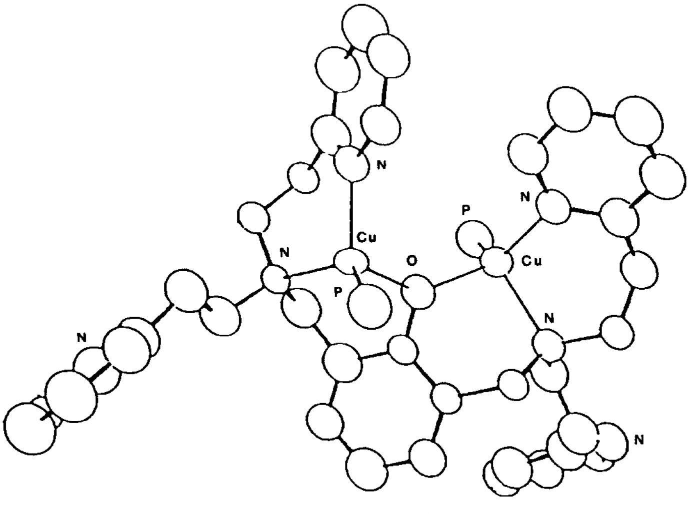

Fig. 28. Structure of $[Cu_2(XXXVIII)(PPh_3)_2]^+$ (from ref. 159).

CO; attempts to do this result only in the recovery of $[Cu_2(\mathbf{XXXVIII})]^+$. The stoichiometry of adduct formation is confirmed by manometric measurements at −80°C which indicate that 2 mol CO are taken up per mole of $[Cu_2(\mathbf{XXXVIII})]^+$ in dichloromethane.

Decarbonylation occurs on the application of reduced pressure to a CH_2Cl_2 solution of $[Cu_2(\mathbf{XXXVIII})(CO)_2]^+$ at room temperature. The carbonylation–decarbonylation process can be repeated indefinitely [159].

$[Cu_2(\mathbf{XXXVIII})(O_2)]^+$ is obtained only from $[Cu_2(\mathbf{XXXVIII})]^+$ because at −50°C O_2 will not react with the dicarbonyl complex.

The reaction of O_2 with $[Cu_2(\mathbf{XXXVIII})(CO)_2]^+$ at room temperature results in the loss of CO with rapid irreversible oxidation to form $[Cu_2(\mathbf{XXXVIII})(OH)]^{2+}$. The binding of CO to $[Cu_2(\mathbf{XXXVIII})]^+$ appears stronger than that of O_2 at −80 °C, and CO can be used to displace the bound dioxygen ligand, thereby allowing carbonyl cycling to take place.

The solution of complex $[Cu_2(\mathbf{XXXVIII})_2]^+$ is chilled to −80°C and bubbled with O_2 to produce $[Cu_2(\mathbf{XXXVIII})(O_2)]^+$. This solution, saturated with CO and allowed to warm slightly above −80°C in the air, on recooling and equilibration at −80°C gives the bis(carbonyl) adduct $[Cu_2(\mathbf{XXXVIII})(CO)_2]^+$ along with some of the decomposition product $[Cu_2(\mathbf{XXXVIII})(OH)]^{2+}$. This cycle can be repeated many times and an estimated 5–15% decomposition to $[Cu_2(\mathbf{XXXVIII})(OH)]^{2+}$ occurs per cycle.

Spectroscopic studies have been performed on the complex $[Cu_2(\mathbf{XXXVIII})(O_2)]^{2+}$ to determine the geometric and electronic structure of peroxide binding in this complex [160]. The two Raman peaks at 488 and 803 cm^{-1} have been observed to shift to 464 cm^{-1} and 750 cm^{-1} respectively for the complex prepared with isotopically labelled dioxygen (99% $^{18}O_2$).

The feature at 803 cm^{-1} in the $^{16}O_2$ complex is composed of two peaks, a main peak at 803 cm^{-1} and a smaller feature at 776 cm^{-1}. However, samples prepared with $^{18}O_2$ do not show a similar lower energy shoulder on the 750 cm^{-1} band. The Raman spectrum of the oxygenated complex, obtained with dioxygen containing an isotopic mixture of $^{18}O_2$, $^{16,18}O_2$ and $^{16}O_2$ approximately in a ratio of 1.17:2.14:1.00, consists of a broad unresolved feature centred at about 780 cm^{-1} and a resolved two-component feature (465 and 486 cm^{-1}) in the metal ligand region. The presence of a vibrational peak at 803 cm^{-1} which shifts to 750 cm^{-1} upon isotopic substitution is indicative of dioxygen bound as peroxide. The mixed-isotope vibrational data have been analysed to determine the mode of peroxide binding in $[Cu_2(\mathbf{XXXVIII})(O_2)]^{2+}$. The two-peaked appearance of the copper peroxide vibrational feature thus demonstrates an asymmetric peroxide geometry, either terminal or μ-1,1.

In the case of $[Cu_2(\mathbf{XXXVIII})(OH)]^{2+}$, the bandwidths are too broad to lead to a resolved isotopic splitting even if the $^{16,18}O_2$ components are split by as much as 6–10 cm^{-1}. The copper peroxide peak, however, exhibits a pronounced difference in the predicted isotopic band shape for the two geometries.

The two-peak appearance of the copper peroxide stretch requires that the peroxide is bound in an asymmetric geometry. EXAFS results [161] indicate a Cu–Cu distance of 3.31 Å for $[Cu_2(XXXVIII)(O_2)]^{2+}$ which rules out the μ-1,1-bridging geometry, since structural data for phenoxide and OH^- or OMe^- doubly bridged complexes with similar ligands show that a μ-1,1 geometry is only compatible with a Cu–Cu distance of less than 3.15 Å.

This result, however, cannot distinguish between μ-1,2-bridging or terminal peroxo coordination at the dinuclear copper site. However, a terminal geometry would require that the peroxide is coordinatively unsaturated. Steric considerations do suggest that the free end of the peroxide could be stabilized by a weaker axial interaction with the second copper, and molecular models indicate that the 3.31 Å Cu–Cu distance would be compatible with μ-1,2 equatorial to axial peroxide geometry. However, even if an axial interaction is present, the mixed-isotope results indicate a peroxide geometry that is essentially terminal in character.

The resonance Raman enhancement profiles indicate that two absorption bands can be assigned as peroxide to copper(II) charge-transfer transitions: an intense peak at 503 nm and a weaker band at 625 nm as observed in visible spectra (a band at 505 nm and a shoulder at 610 nm).

The kinetics and mechanism of hydroxylation with H_2O_2 of the dicopper(II) complex $[Cu_2(XXXVII)]^{4+}$ to $[Cu_2(XXXVIII)(OH)]^{2+}$ have been studied [162]. In 50%H_2O–50% DMF the reaction is second order in the complex, first order in H_2O_2, and inversely first order in $[H^+]$.

The complete rate law is given by

$$v = k\{[Cu_2(XXXVII)]^{4+}\}^2[H_2O_2]/\{[H^+](1 + K[Cu_2(XXXVII)]^{4+})\}$$

where $k = 0.4\ M^{-1}\ s^{-1}$ and $K = 4500\ M^{-1}$. The absence of a deuterium effect with $[Cu_2(XXXVII\text{-}D)]^{4+}$ in the place of $[Cu_2\ (XXXVII\text{–}H)]^{4+}$ eliminates hydrogen as the rate-limiting step and points to an attack by a reactive and probably electrophilic hydroxylating agent. The second-order dependence on $[Cu_2(XXXVII)]^{4+}$ and the pH dependence have been explained by the formation of the hydroperoxide intermediate $[Cu_2(XXXVII)(OOH)]^{3+}$, which is subsequently transformed into $[Cu_2(XXXVIII)(OH)]^{2+}$ under the influence of a second molecule of $[Cu_2(XXXVII)]^{4+}$ which acts as a Lewis acid and promotes O–O bond rupture in the hydroperoxide complex (Scheme 20).

The peroxo tetracopper species is an unstable intermediate of unknown structure. A 1,1-binding mode of HO_2 with a terminal OH group was proposed.

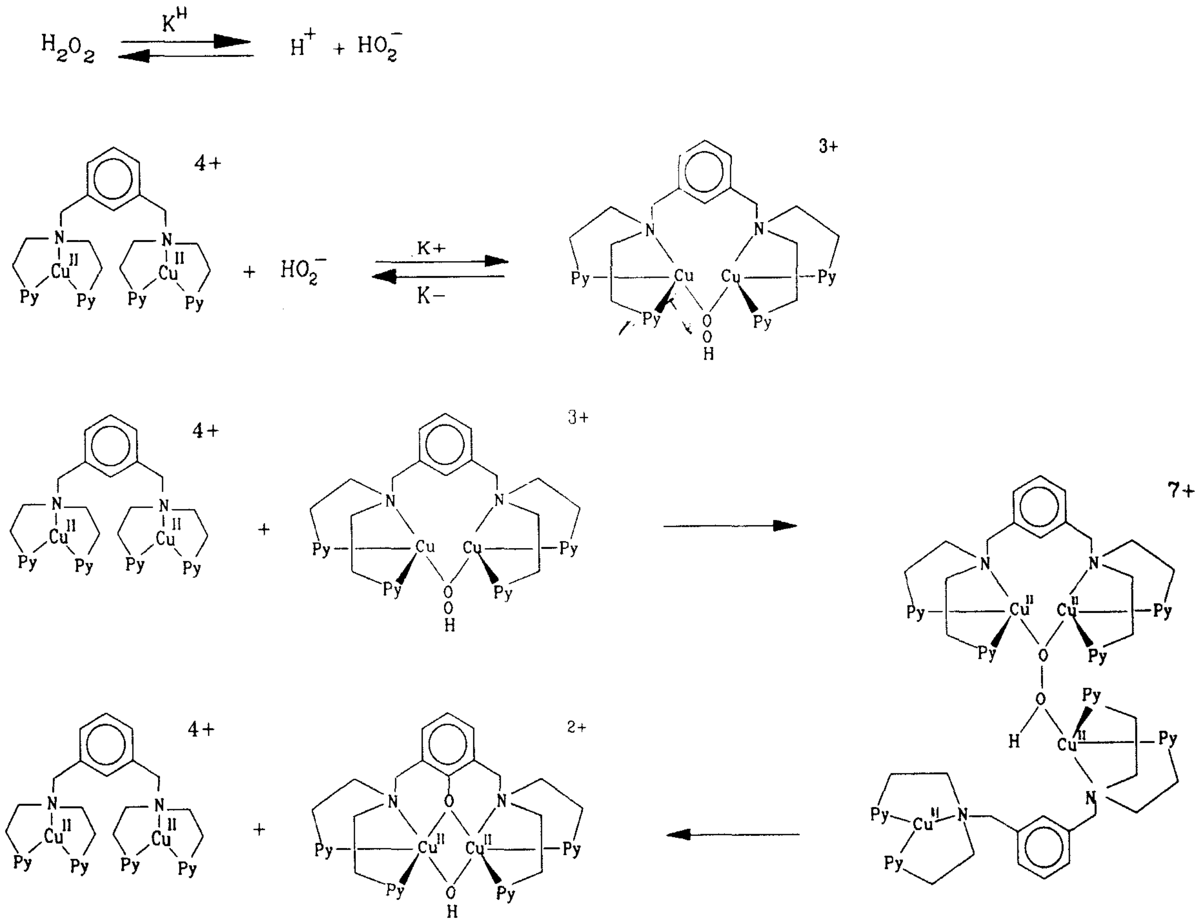

Scheme 20. Proposed mechanism of hydroxylation by H_2O_2 of $[Cu_2(\textbf{XXXVII})]^{4+}$ (from ref. 162).

Kinetics data indicate that $[Cu_2(XXXVII)]^{2+}$ reacts with O_2 reversibly to form the dioxygen adduct $[Cu_2(XXXVII)(O_2)]^{2+}$ which irreversibly decomposes in a first-order process, giving the hydroxylated product $[Cu_2(XXXVIII)(OH)]^{2+}$ (Scheme 21(a)) [163].

The O_2 binding is a one-step process; no evidence for other intermediates (e.g. mononuclear $Cu-O_2$) was found. The rapid reaction of O_2 with $[Cu_2(XXXVII)]^{2+}$ is characterized by a low activation enthalpy and a large negative activation entropy. The spectroscopic observation of the intermediate $[Cu_2(XXXVII)O_2)]^{2+}$ is facilitated by the favourable relative rates of formation of $[Cu_2(XXXVII)(O_2)]^{2+}$ and its decomposition to $[Cu_2(XXXVII)(OH)]^{2+}$, i.e. $k_1[O_2] > k_2$ at low temperatures ($[O_2] = 2 \times 10^{-3}$M).

The thermodynamic stability of the dioxygen intermediate $[Cu_2(XXXVII)(O_2)]^{2+}$ is clearly derived from the strong binding ($\Delta H° = -62 \pm 1$ kJ mol^{-1}). The disappearance of the Cu_2-O_2 adduct at room temperature is not due to unfavourable kinetics but rather to the thermodynamics, with a negative entropy of $\Delta S° = -200 \pm 6$ J mol^{-1} K^{-1}.

For the reversibile system in Scheme 21(b), the analysis also provides for the existence of a simple reversible system, and the values of $\Delta H°$ and $\Delta S°$ determined are very close to those obtained for the system $1 \rightarrow 2$ in Scheme 21(a).

However, the rate of reaction with dioxygen was too fast to be measured even at -100°C, indicating that $k_+ > 10^6$ M^{-1} s^{-1}. Forcing the two copper(I) ions into close proximity by the presence of a bridging phenoxo ligand apparently causes a dramatic enhancement of the rate of reaction with O_2.

In Scheme 14, the preparation of $[Cu_2(XXXVIII)]PF_6$ from $[Cu(CH_3CN)_4](PF_6)$ and H-XXXVIII has been reported. An elegant and superior method for obtaining the same complex is to reduce directly $[Cu_2(XXXVIII)(OH)]^{2+}$ with diphenylhydrazine, a two-electron reductant, in the presence of a base. The same reduction reaction, carried out in the absence of base, produces the three-coordinated dicopper(I) complex $[Cu_2(H\text{-}XXXVIII)]^{2+}$ or the bis adducts $[Cu_2(H\text{-}XXXVIII)(L)_2]^{2+}$ (L = CO, PPh_3, $(CH_2)_4S$, CH_2CN) where the phenol group is not deprotonated. $[Cu_2(XXXVIII)]^+$ and $[Cu_2(H\text{-}XXXVIII)]^{2+}$ can be readily interconverted in an acid-base reaction: HPF_6 decolourizes the orange methanolic solution of $[Cu_2(XXXVIII)]^+$ to form $[Cu_2(H\text{-}XXXVIII)]^{2+}$ which is deprotonated by triethylamine to give again $[Cu_2(XXXVIII)]^+$ [164,165]. An X-ray investigation on crystals of a bis(triphenylphosphine) adduct, $[Cu_2(H\text{-}XXXVIII)((PPh_3)_2](ClO_4)_2$, confirms the structure proposed above; particularly it shows that the phenol oxygen atom is too far from the two copper(I) ions for any sort of interaction. The structure consists of discrete $[Cu_2(H\text{-}XXXVIII)(PPh_3)_2]^{2+}$ cations and separated ClO_4^- anions (Fig. 29).

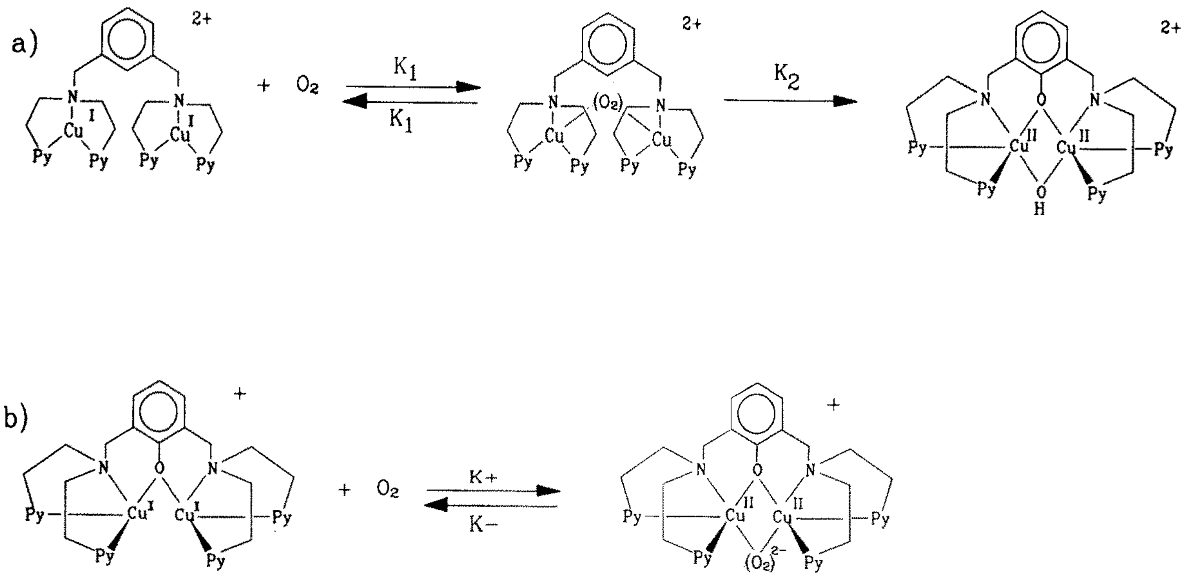

Scheme 21. Proposed mechanism of hydroxylation of (a) [Cu_2(**XXXVII**)]$^{2+}$ and (b) [Cu_2(**XXXVIII**)]$^{+}$ by O_2 (from ref. 163).

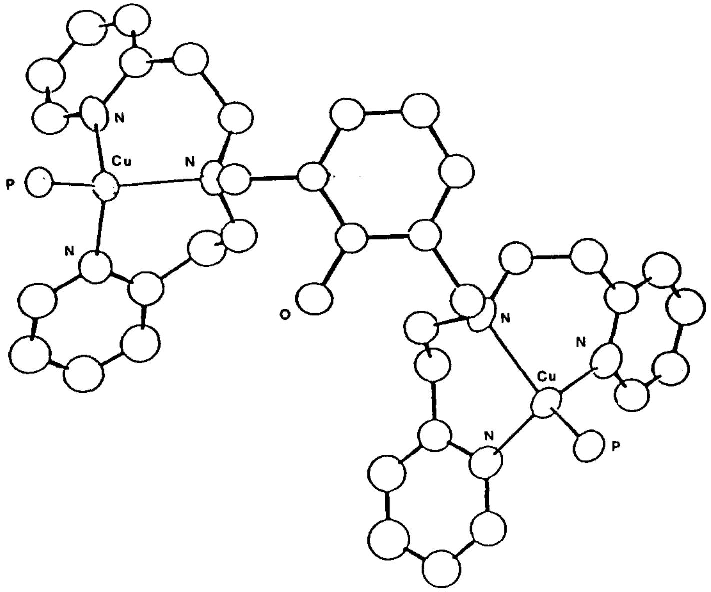

Fig. 29. Structure of $[Cu_2(H\text{-}XXXVIII)(PPh_3)_2]^{2+}$ (from ref. 164).

The dicopper complex contains two crystallographically independent and well-separated copper(I) moieties, each possessing nearly identical pseudo-tetrahedral coordination to two pyridyl and one amino nitrogen atom of the xylyl ligand and a phosphorus atom of the triphenylphosphine ligand.

The dicopper(I) complexes $[Cu_2(XXXVIII)]^+$, $[Cu_2(H\text{-}XXXVIII)]^{2+}$ and $[Cu_2(H\text{-}XXXVIII)(L)_2]^{2+}$ and the dicopper(II) complexes $[Cu_2(XXXVIII)(OH)]^{2+}$ and $[Cu_2(XXXVIII)(O_2)]^+$ are precursors in the generation of the hydroperoxo–dicopper(II) complex $[Cu_2(XXXVIII)(OOH)]^{2+}$ by one of the following synthetic procedures (Scheme 22):

(i) protonation of $[Cu_2(XXXVIII)(O_2)]^{2+}$;
(ii) reaction of H_2O_2 with $[Cu_2(XXXVIII)(OH)]^{2+}$;
(iii) oxygenation of $[Cu_2(H\text{-}XXXVIII)]^{2+}$ or its bis adducts $[Cu_2(H\text{-}XXXVIII)(L)_2]^{2+}$.

The peroxo complex $[Cu_2(XXXVIII)(O_2)]^+$ can be protonated directly using HBF_4–Et_2O in CH_2Cl_2 at −80°C to produce the green ESR-silent complex $[Cu_2(XXXVIII)(OOH)]^{2+}$ [164]. A spectrophotometric titration in which the acid is added to the purple solution of $[Cu_2(XXXVIII)(O_2)]^+$ indicates that only two species are involved in this protonation reaction and thus the peroxo complex $[Cu_2(XXXVIII)(O_2)]^+$ is directly converted into the hydroperoxo complex $[Cu_2(XXXVIII)(OOH)]^{2+}$.

The second approach involves the addition of dioxygen to the dicopper(I) complexes, $[Cu_2(H\text{-}XXXVIII)]^{2+}$ and $[Cu_2(H\text{-}XXXVIII)(CO)_2](PF_6)_2$. The

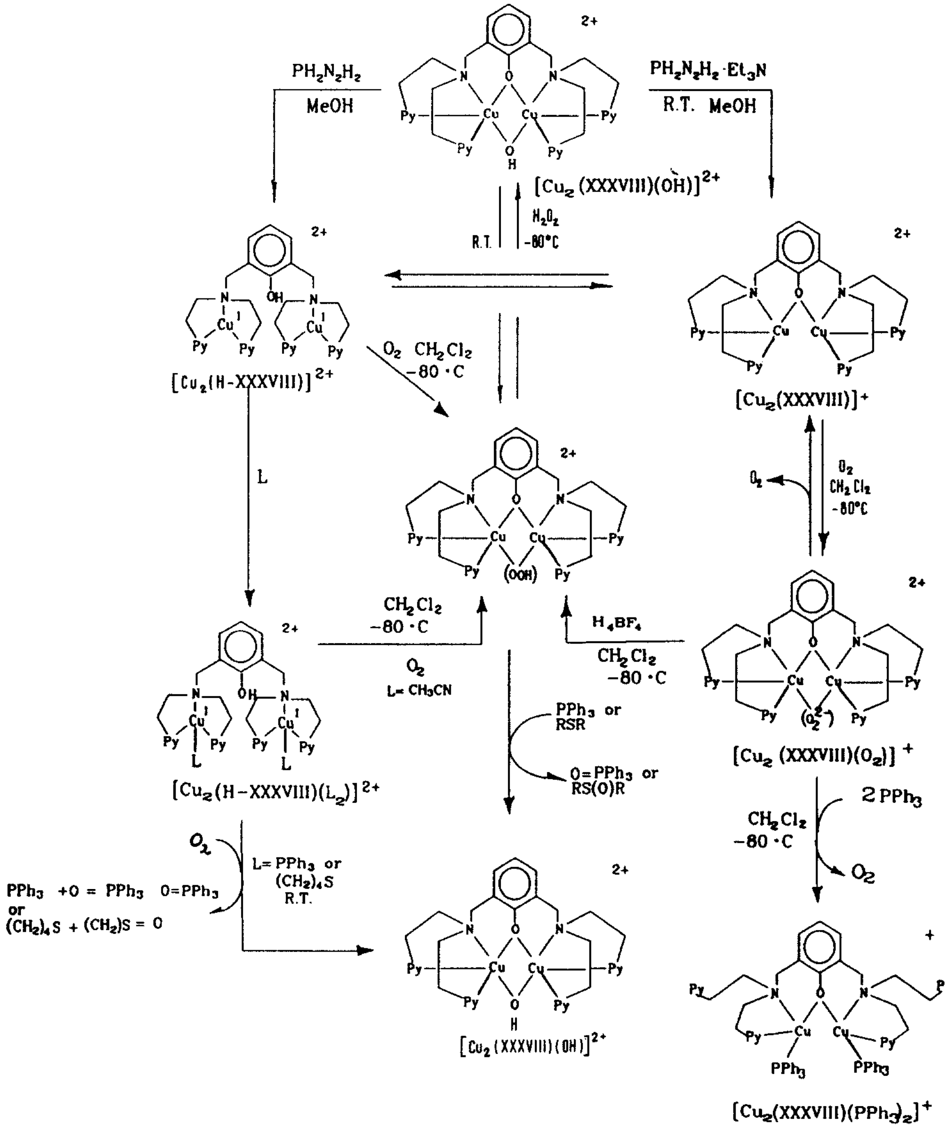

Scheme 22. Preparation and reactivity of [Cu(XXXVIII)(OOH)]$^{2+}$ (from ref. 164).

carbonyl groups can be removed from the dicarbonyl complex under reduced pressure at 0°C; then cooling the CH_2Cl_2 solution to $-80°C$, followed by exposure to O_2, results in rapid conversion into the hydroperoxo complex, as indicated by the UV–visible spectrum and the observed stoichiometry of dioxygen uptake (manometry at $-80°C$; $Cu{:}O_2 = 2{:}1$). Thus the phenol group serves as a stoichiometric source of H^+ and protonates a putative dioxygen adduct of $[Cu_2(\text{H-XXXVIII})]^{2+}$ to give $[Cu_2(\text{XXXVIII})(OOH)]^{2+}$.

A third method by which the hydroperoxo complex may be generated is the addition of an excess of aqueous hydrogen peroxide to a dichloromethane and/or DMF solution of $[Cu_2(\text{XXXVIII})(OH)]^{2+}$. This method of generating the hydroperoxo complex provides further support that it contains a peroxidic moiety.

As reported above, the addition of triphenylphosphine to $[Cu_2(\text{XXXVIII})(O_2)]^{+}$ results in the simple displacement of the peroxo ligand, and the quantitative liberation of O_2. By contrast, $[Cu_2(\text{XXXVIII})(OOH)]^{2+}$ reacts with 1 equivalent of either PPh_3 or tetrahydrothiophene to give essentially quantitative yields of $O=PPh_3$ or tetrahydrothiophene *S*-oxide; the copper product quantitatively produced in both cases is $[Cu_2(\text{XXXVIII})(OH)]^{2+}$. These results suggest that protonation of a dioxygen–Cu complex may result in activation via the formation of a hydroxoperoxo-like complex which is capable of transferring an oxygen atom to a substrate while leaving behind a stable hydroxo–$Cu(II)_n$ moiety.

The distances, obtained by EXAFS studies of the hydroperoxo complex, are consistent with a copper(II) ion in a tetragonal geometry; the Cu–Cu distance of 3.04 Å found in $[Cu_2(\text{XXXVIII})(OOH)](ClO_4)_2$ is 0.27 Å shorter than the Cu–Cu distance found in the related dioxygen complex, $[Cu_2(\text{XXXVIII})(O_2)]^{+}$ and is in the range expected for a μ-1,1-bridged complex.

Thus the data obtained suggest the formulation of $[Cu_2(\text{XXXVIII})(OOH)](ClO_4)_2$ as having one pyridine nitrogen, one amino nitrogen, one phenoxo oxygen and one oxygen atom from the hydroperoxo ligand as the four equatorial donors to copper(II), with a Cu···Cu distance of 3.04 Å. The EXAFS studies thus suggest considerable structural similarity between $[Cu_2(\text{XXXVIII})(OOH)]^{2+}$ and $[Cu_2(\text{XXXVIII})(OH)]^{2+}$ (Fig. 30).

$[Cu_2(\text{XXXVIII})(OOH)]^{2+}$ can be handled only at low temperatures, but an analogous stable and crystalline acylperoxo-bridged dicopper(II) complex has been prepared according to the reaction scheme given in Scheme 23 [166].

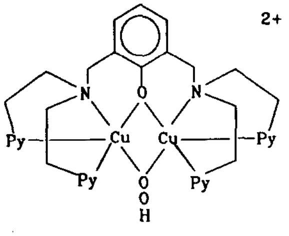

Fig. 30. Proposed structure of $[Cu_2(\text{XXXVIII})(OOH)]^{2+}$.

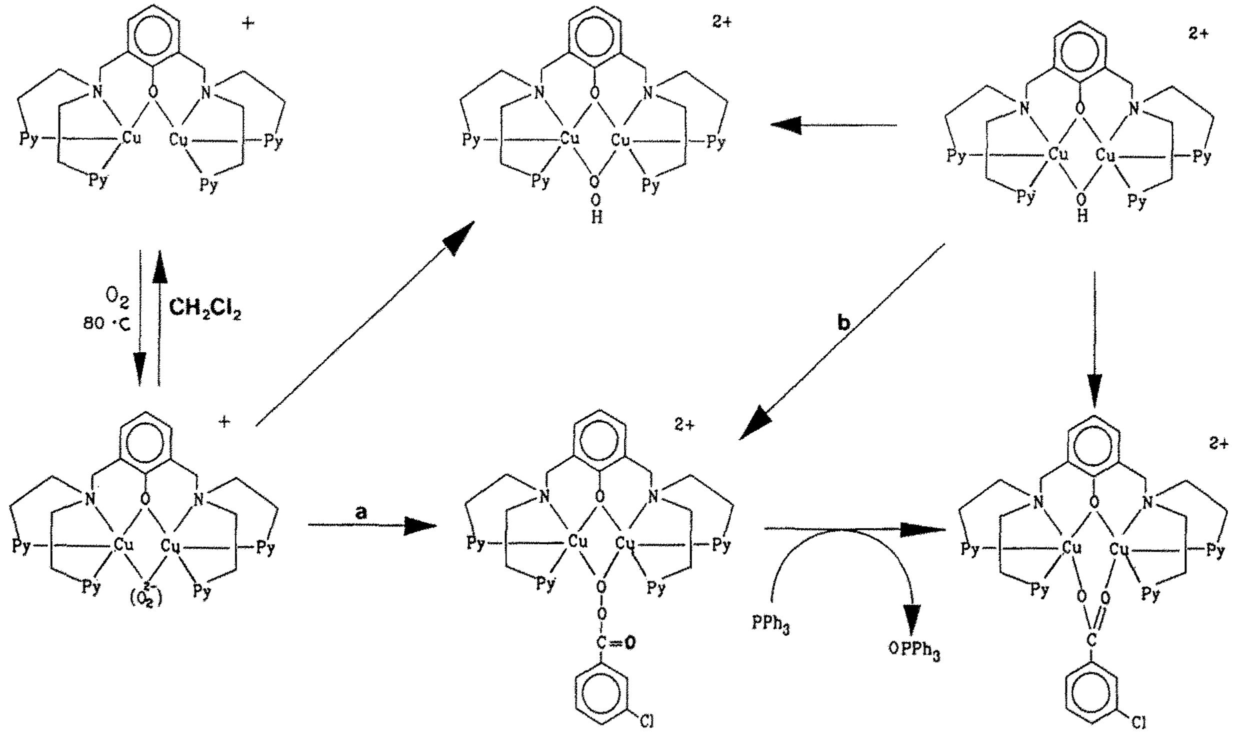

Scheme 23. Preparation and reactivity of the acylperoxo-bridged dicopper(II) $[Cu_2(\mathbf{XXXVIII})(m\text{-}ClC_6H_4C(O)O_2)]^{2+}$. (a): m-ClC_6H_4COCl, −80°C in CH_2Cl_2, $AgPF_6$ in CH_3CN; (b): m-$ClC_6H_4C(O)OOH$, −80°C in CH_2Cl_2 containing 2,2 dimethoxypropane (from ref. 166).

The structure of the peroxo complex $[Cu_2(XXXVIII)(m\text{-}ClC_6H_4)C(O)O_2](ClO_4)_2CH_3CN$ consists of a phenoxo and a peroxo oxygen doubly bridged to the dicopper(II) species. The acylperoxo group is coordinated through an oxygen in a μ-1,1 fashion. Three nitrogen atoms complete the coordination about the copper ions (Fig. 31).

The acylperoxo complex reacts with PPh_3 to produce quantitatively $Ph_3P=O$ and the carboxylato complex. The same carboxylato complex can be obtained by reaction of $[Cu_2(XXXVIII)(OH)]^{2+}$ with *m*-chlorobenzoic acid.

In the proposed mechanism of phenol oxygenation and oxidation by the tyrosinase-coupled dinuclear copper site (Fig. 2), an intramolecular two-electron-transfer reaction produces *o*-quinone and regenerates the copper(I) centre.

A dinuclear phenoxo-bridged copper(II) complex containing a catecholate bridging group has been obtained through the reduction and coordination of tetrachloro-*o*-benzoquinone to the copper(I) complex $[Cu_2(XXXVIII)]^{2+}$. The Cu(II)–tetrachloro-*o*-catecholate complex is stable in the presence of O_2 and has a magnetic moment of 1.5 BM. In this complex the coordination geometry around each copper(II) has been described as square-based pyramidal with the amine nitrogen atoms, one pyridyl nitrogen atom, the bridging phenoxo oxygen and one of the catecholate oxygen donors forming the basal plane. The second pyridyl nitrogen atom occupies the apical position

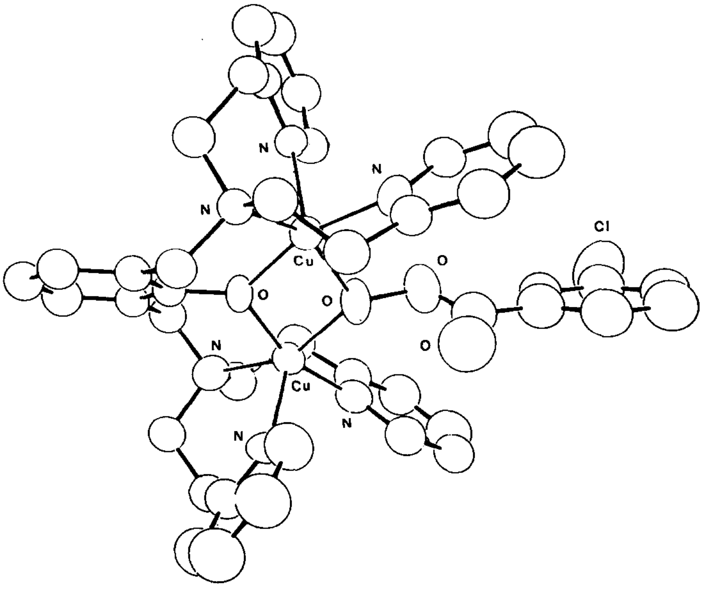

Fig. 31. Structure of $[Cu_2(XXXVIII)(m\text{-}ClC_6H_4C(O)O_2)]^{2+}$ (from ref. 166).

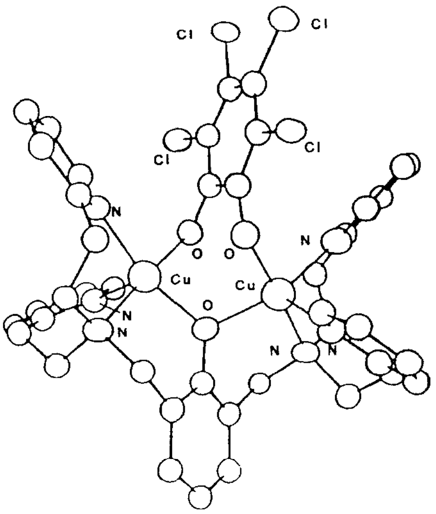

Fig. 32. Structure of Cu_2(**XXXVIII**)(tetrachloro-*o*-catecholate) complex (from ref. 158).

with a longer Cu–N distance. The Cu···Cu distance is 3.248 Å (Fig. 32) [158].

The dinuclear phenoxo and hydroxo complex $[Cu_2(\mathbf{XXXVIII})(OH)]^{2+}$ catalytically oxidizes 3,5-di-*t*-butylcatechol to the corresponding 3,5-di-*t*-butylquinone. The catecholate complex serves as a structural model for the probable intermediate in the catalytic oxidation of catechols by dicopper moieties [158].

The ligand H-**XLV** was synthesized by reaction of HCl with 1,3-bis-(hydroxymethyl)-*p*-cresol, followed by reaction of the chloromethyl product with 2-(2-methyl-aminoethyl)pyridine and triethylamine. The crude product was purified by chromatography on alumina (50% acetone–50% ethyl acetate). **XLV** was obtained following deprotonation of H-**XLV** with NaH in diethyl ether, and by reaction with two equivalents of $[Cu(CH_3CN)_4]PF_6$ in CO-saturated dichloromethane, which produced colourless crystals of $[Cu_2(\mathbf{XLV})(CO)_2](PF_6)$ after several days. The structure of the cation

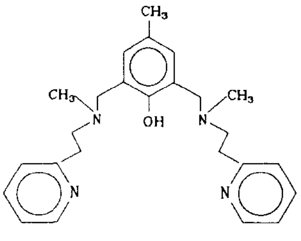

H–XLV

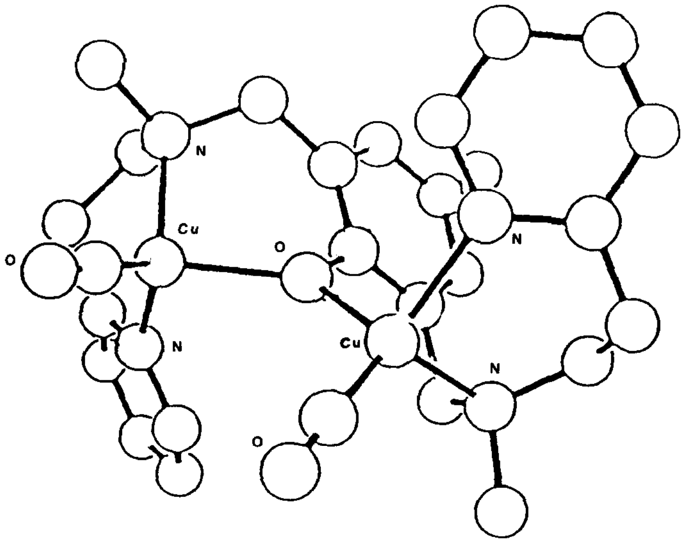

Fig. 33. Structure of $[Cu_2(XLV)(CO)_2]^+$ cation (from ref. 167).

(Fig. 33) shows there are two molecules in each asymmetric unit, each consisting of a phenoxo-bridged dicopper(I) moiety. Each copper(I) ion is coordinated in a distorted tetrahedral environment, by the tertiary amino and pyridyl nitrogen atoms, the carbonyl carbon atom and the bridging phenoxo donor. The Cu···Cu separation is 3.587 Å [167].

In the absence of CO, disproportionation occurs, even at low temperature, and metallic copper is deposited. Thus stabilization of a copper(I) derivative of **XLV** only seems possible by using CO.

Similar results have been obtained with 2,6-bis{[2-(1-pyrazolyl)ethyl]methylamino}-*p*-cresol (H-**XLVI**) and its 3-*t*-butylpyrazone derivative H-(*t*-bu-**XLVI**) [168].

Attempts to prepare dinuclear three-coordinated copper(I) complexes with the ligand H-**XLVI** produced only disproportionation products. However, stirring the potassium salt of H-**XLVI** or H-*t*-bu-**XLVI** with $[Cu(CH_3CN)_4CN)_4]BF_4$ in methanol under CO gives the very probably tetracoordinated copper(I) dimers $[Cu_2(XLVI)(CO)_2]BF_4$ and [Cu$_2$(*t*-bu-

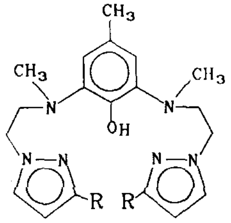

R		
	H	H-**XLVI**
	t-butyl	H-*t*-bu-**XLVI**

XLVI)(CO)$_2$]BF$_4$ which are stable indefinitely under either CO or N$_2$ in the solid state and show a strong CO stretch at 2075 cm^{-1} in their IR spectra.

Despite the presence of a cavity between the metal ions, which would result if CO groups were lost from the copper(I) complex, neither [Cu$_2$(**XLVI**)(CO)$_2$]BF$_4$ nor [Cu$_2$(*t*-bu-**XLVI**)(CO)$_2$]BF$_4$ forms a dioxygen adduct, even at low temperature. Reaction with O$_2$ in CH$_3$CN over the temperature range -40 to $+25$°C results in complete oxidation of the copper(I) ions to give greenish, probably oligomeric, μ-oxo products.

The low temperature absorption spectra for the reaction between [Cu$_2$(*t*-bu-**XLVI**)(CO)$_2$]BF$_4$ and O$_2$ show clean isosbestic behaviour during the first several minutes of the reaction. Moreover, the reaction stoichiometry, determined by manometric uptake of dioxygen at -35°C, is 2 molecules of [Cu$_2$(*t*-bu-**XLVI**)(CO)$_2$]BF$_4$ per molecule of O$_2$ (4Cu/O$_2$), signifying that a four-electron reduction of dioxygen occurs. The results for the oxygenation of [Cu$_2$(**XLVI**)(CO)$_2$]BF$_4$ are not as clean, and only about 28% of the theoretical amount of O$_2$ (assuming 1O$_2$/Cu dimer) is absorbed by an acetonitrile solution of [Cu$_2$(**XLVI**)(CO)$_2$]BF$_4$ even at low temperature (-35°C). It was suggested that [Cu$_2$(**XLVI**)(CO)$_2$]BF$_4$ must decompose in solution by another pathway, perhaps by dissociation of CO followed by disproportionation. The *t*-butylpyrazolyl group in [Cu$_2$(*t*-bu-**XLVI**)(CO)$_2$]BF$_4$ may stabilize the copper(I) complex so that the decarbonylated form is longer lived and can react with dioxygen before it disproportionates, resulting in a cleaner reaction [168].

Recently the dicopper(I) complex [Cu$_2$(OH-**XLVII**)(CH$_3$CN)$_2$](PF$_6$)$_2$ has been obtained by reaction of [Cu(CH$_3$CN)$_4$]PF$_6$ with the 5-hydroxy-substituted ligand OH-**XLVII** (synthesized by acetylation of 3,5-dimethylphenol and bromination of the methyl groups, followed by reaction with (C$_5$H$_4$N–C$_2$H$_4$–CH$_2$)$_2$NH and deprotection) in acetonitrile under argon followed by precipitation with diethyl ether [169].

The aim was that this compound with O$_2$ would provide the 2,5-dihydroxo copper(II) product which would collapse by an intramolecular redox process to a *p*-quinone dicopper(I) species. When the copper(I) complex is reacted with O$_2$ in dichloromethane an intense purple powder precipitates. This compound apparently contains chlorine and its general insolubility suggests that it is polymeric. However, a crystalline derivative

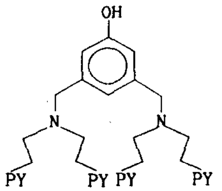

OH-XLVII

was obtained via a metathesis reaction of this purple powder with excess $NaBPh_4$ dissolved in DMF.

Crystals, grown from acetone–diethyl ether show that the ligand has been hydroxylated while the 5-hydroxyl group has also been arylated. The structure of the dication dicopper(II) complex (Fig. 34) consists of a phenoxo- and hydroxo-bridged dicopper unit where each copper(II) ion is in a square-based pyramidal coordination environment with a Cu···Cu separation of 3.108 Å.

The intense purple colour of the intermediate complex suggests that it may possess a quinoid moiety; this has not yet been proved unambiguously, since the organic compound obtained by stripping the copper from the intermediate is thermally unstable. Manometric dioxygen uptake experiments carried out on $[Cu_2(OH\text{-}\mathbf{XLVII})(CH_3CN)_2]^{2+}$ indicate that $Cu{:}O_2 = 4{:}1$, a stoichiometry which is inconsistent with the initial supposition that the design of OH-**XLVII** would provide a copper-mediated hydroxylation process (i.e. $Cu{:}O_2 = 2{:}1$) followed by an internal redox reaction to give dicopper(I) plus quinone. The participation of dichloromethane in the reaction is also apparent. Arylation of the intermediate purple complex was suggested to occur in the reaction with $NaBPh_4$.

Dinuclear copper(I) complexes with the bis imines derived from the condensation in dry methanol under an inert atmosphere of benzene-1,3-dicarboxaldehyde or benzene-1,4-dicarboxaldehyde and two molecules of histamine, L-histidine methyl ester, *N*′-methylhistamine and *N*-methyl-L-histidine, in the presence of an excess of $[Cu(CH_3CN)_4]ClO_4$ [170,171] have been synthesized and characterized. In the absence of such an excess,

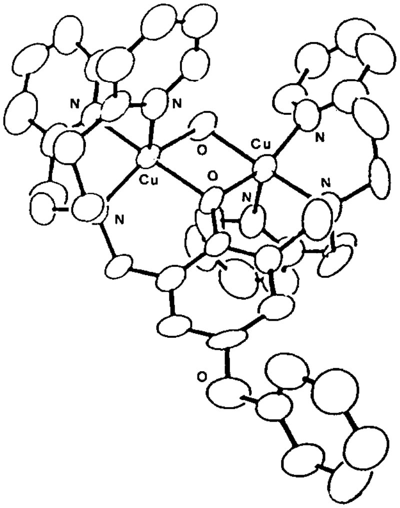

Fig. 34. Structure of $[Cu_2(5\text{-Ph-}\mathbf{XLVII})(OH)]^{2+}$ (from ref. 169).

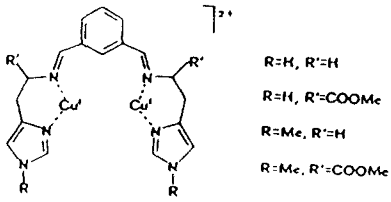

$[Cu_2(\underline{XLVIII - RR'})]^{2+}$

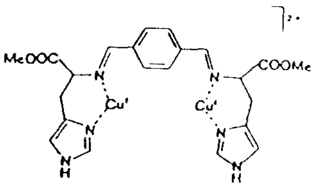

$[Cu_2(\underline{IL})]^{2+}$

the products may be contaminated by mononuclear complexes of the same ligands.

In the dinuclear complexes, the ligands provide two nitrogen donors, from an imine and an imidazole group to each copper(I) centre, but a molecule of solvent is additionally coordinated to the metal in solution.

The complexes $[Cu_2(\mathbf{XLVIII}\text{-}RR')]^{2+}$ ($R = CH_3$, $R' = H$; $R = CH_3$, $R' = COOMe$) in any solvent react with dioxygen to give the corresponding μ-phenoxo dinuclear complexes according to Scheme 24.

The copper(II) compounds have an additional μ-hydroxo bridge when the reaction is carried out in non-protic solvents, but this bridge may be replaced by a μ-alkoxo bridge when the reaction is performed in alcohol. The oxygenation reaction, to produce the hydroxylation of the aromatic ring, can be monitored by UV–visible spectroscopy while the stoichiometry of the reaction has been established by manometric measurements of

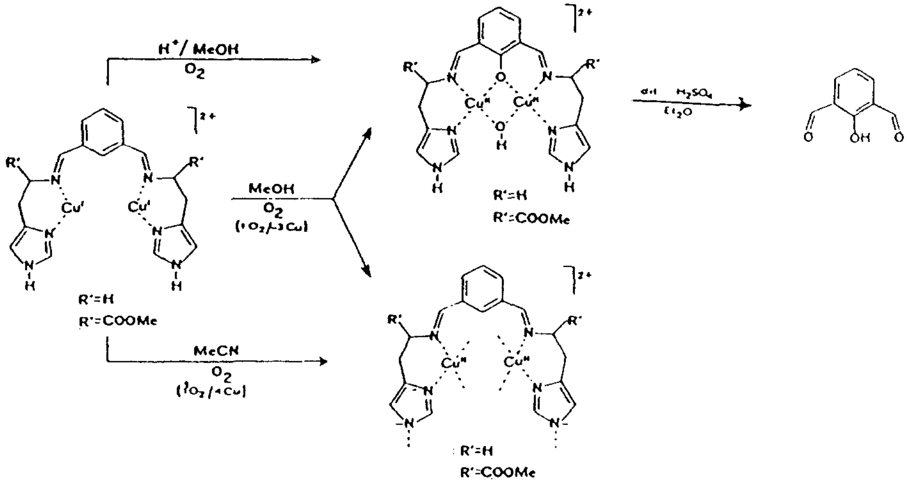

Scheme 24. Reaction of $[Cu_2(\mathbf{XLVIII}\text{-}RR')]^{2+}$ with O_2 in different solvents (from ref. 171).

dioxygen uptake; it corresponds to 1 mol O_2 per mole of dinuclear complex. The phenolic nature of the ligands in the copper(II) complexes has been probed by treating these products with mineral acid and extracting the dicarboxaldehyde with ether or chloroform. A labelling experiment with $^{18}O_2$ confirmed the incorporation of one ^{18}O atom into this product.

The reaction with O_2 of the complexes $[Cu_2(\mathbf{XLVIII}\text{-}RR')]^{2+}$ ($R = R' = H$ and $R = H$, $R' = COOMe$) is markedly affected by the medium. In dry non-protic solvents such as CH_3CN, a simple oxidation of copper(I) to copper(II) occurs with concomitant reduction of O_2 to H_2O.

The stoichiometry of the reaction, determined by the amount of O_2 absorbed by the solution, corresponds to 1 mmol of O_2 per 2 mol of dinuclear copper(I) complex. The protons necessary for the reduction of O_2 come from the imidazole NH groups of the ligand.

The reaction between O_2 and the complexes $[Cu_2(\mathbf{XLVIII}\text{-}RR')]^{2+}$ ($R = R' = H$ and $R = H$, $R' = COOMe$), carried out in protic solvents such as methanol, leads to a mixture of the hydroxylation products and oxidation products in an approximate ratio of 1:1, according to Scheme 24.

Owing to the solvent dependence of these reactions, it is possible to shift the ratio between the hydroxylation and the oxidation compounds in favour of the former product by increasing the proton donor ability of the medium. Acetic or perchloric acids in methanol markedly increase the formation of hydroxylation complexes (yields greater than 90%).

All the copper(I) complexes with the ligands **XLVIII-RR′** and **IL** react reversibly with CO in solution to form carbonyl adducts which lose CO by treatment of the solution under vacuum. The $\nu(CO)$, which occurs in the range 2088–2096 cm^{-1}, is indicative of terminally bound CO. The very similar position of $\nu(CO)$ for these complexes in the solid state and in solution was assumed to be indicative of a trigonal rather than a tetragonal coordination. Only the addition of an excess donor base to the solution of these dicopper(I) complexes promoted tetragonal carbonyl adducts. When an excess of imidazole is used, the $\nu(CO)$ lies at 2069–2073 cm^{-1} [173].

By reaction of THF solutions of 1,3-bis[*N*-(2-pyridylethyl)formidoyl]benzene (**L**), prepared from benzene-1,3-dicarbaldehyde and 2-(2-pyridyl)ethylamine, and $[Cu(CH_3CN)_4]BF_4$, followed by crystallization of the product from CH_2Cl_2–MeOH (10:1) the dinuclear copper(I) complex $[Cu_2(\mathbf{L})(CH_3CN)_2](BF_4)_2$ (Scheme 25) was obtained [172]. This complex is air stable for a few minutes in the crystalline state. X-Ray analysis revealed that each copper(I) is coordinated to three nitrogen donor atoms, two of which originate from the pyridylethylimine moiety and one from acetonitrile (Fig. 35).

In DMF or CH_3CN the complex becomes very sensitive to air oxidation. Manometric oxygen uptake experiments showed a stoichiometric reaction of

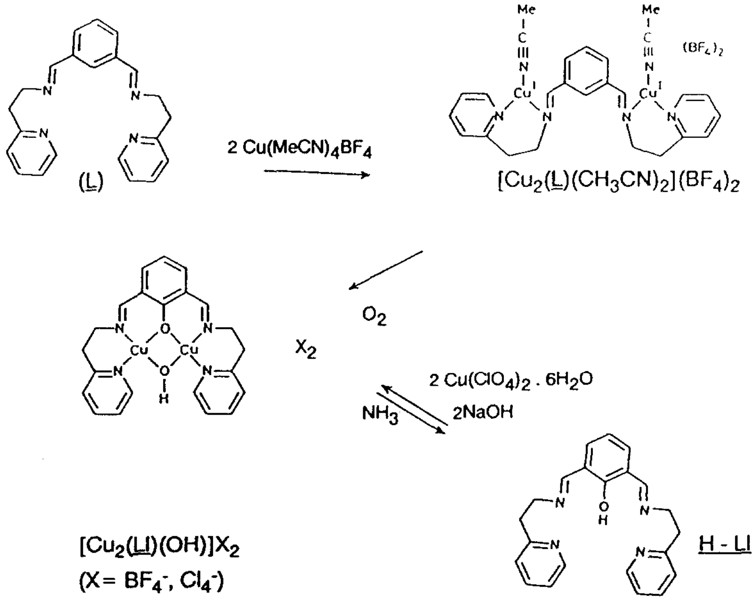

Scheme 25. Preparation of $[Cu_2(L)(CH_3CN)_2)](BF_4)_2$ and its reaction with O_2.

$[Cu_2(L)(CH_3CN)_2](BF_4)_2$ with molecular oxygen, resulting in the formation of the green complex $[Cu_2(LI)(OH)]^{2+}$ (identical with that obtained by the reaction of the preformed ligand H-LI with $Cu(ClO_4)_2 \cdot 6H_2O$ in a 1:2 molar ratio). The Schiff base H-LI, liberated from $[Cu_2(LI)(OH)](BF_4)_2$ with ammonia, is analogous to that obtained by condensation of 2,6-diformylphenol and 2-(2-pyridyl)ethylamine.

The X-ray structure of $[Cu_2(LI)(OH)](BF_4)_2$ (Fig. 36) confirms the formation of the phenolate and hydroxo group bridging two copper(II) ions. The geometry around each copper(II) ion is slightly distorted square planar with a Cu···Cu separation of 2.990 Å.

Cyclic voltammetric measurements on $[Cu(LI)(OH)](ClO_4)_2$ in acetoni-

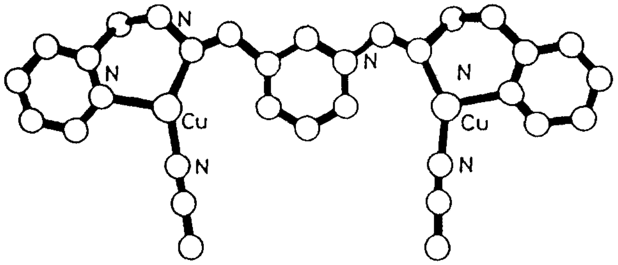

Fig. 35. Structure of $[Cu_2(L)(CH_3CN)_2]^{2+}$ (from ref. 172).

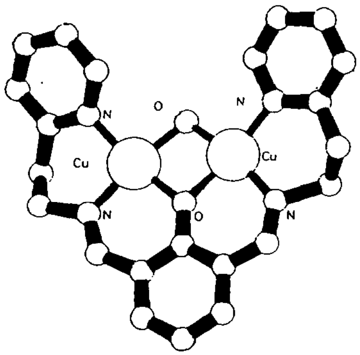

Fig. 36. Structure of $[Cu_2(LI)(OH)]^{2+}$ (from ref. 172).

trile under nitrogen showed no reversible oxidation–reduction sequence at the copper centres, presumably owing to reaction at the imine bond.

$[Cu(LI)(OH)]X_2$ ($X = BF_4^-$, ClO_4^-) complexes are able to act as catalysts in the oxidations of α-hydroxy ketones to diketones and hydroquinones to quinones with molecular oxygen. Thus benzoin was quantitatively oxidized in a few minutes with oxygen to benzil using 5 mol% of $[Cu_2(LI)(OH)](BF_4)_2$ in MeOH.

Reaction of $Li_2[C_6H_3(CH_2NMe_2)$-*o*,*o*$]_2$ with $CuBr[P(OMe)_3]$ afforded an arylcopper(I) complex which, on the basis of its ^1H NMR spectrum and its elemental analysis, was formulated as the copper bromide adduct $Cu[C_6H_3(CH_2NMe_2)_2$-*o*,*o*$]CuBr[P(OMe)_3]_2$ [173].

The molecular weight of $Cu[C_6H_3(CH_2NMe_2)_2$-*o*,*o*$]CuBr[P(OMe)_3]_2$, determined by cryoscopy in benzene, corresponds to the monomeric unit. The ^1H NMR spectrum in C_6D_6, shows singlets for the CH_2 and NMe_2 protons whose chemical shifts are consistent with the presence of uncoordinated CH_2NMe_2 substituents. During attempts to crystallize this compound, crystals of the phenoxocopper(I) compound $Cu[OC_6H_3(CH_2NMe_2)_2$-*o*,*o*$]CuBr[P(OMe)_3]_2$ originating from the reaction with oxygen (Scheme 26) were formed. An X-ray investigation confirms the structure proposed for the phenoxo–dicopper(I) compound; the Cu···Cu distance is 2.853 Å [174].

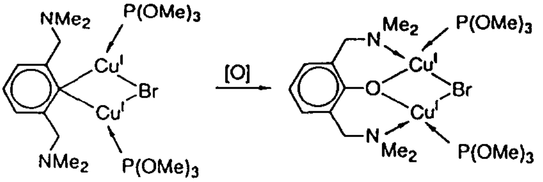

Scheme 26. Hydroxylation of $Cu[(C_6H_3(CH_2NMe_2)$-*o*,*o*$]CuBr[P(OCH_3)_3]_2$.

It was reported that the dinuclear copper(I) complexes of *N,N,N′,N′*-tetrakis[2-(4-Z-benzylideneamino)ethyl]-α,α′-diamino-*m*-xylene (**LII-Z**) are unreactive to dioxygen if handled in dried non-protic solvents, but form CO and imidazole adducts [175].

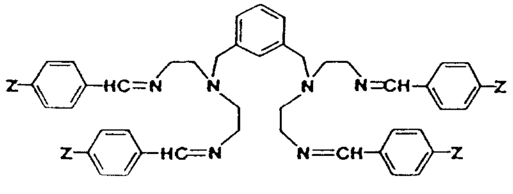

LII - Z (Z = H, -NO_2)

The carbonyl adducts can be formed upon exposure of methanol or dichloromethane solutions of the complexes to an atmosphere of CO. Their dissolution in acetonitrile results in the immediate and complete evolution of CO; they are stable to oxidation.

The solid state IR spectrum of the dicarbonyl complex with $Z = NO_2$ exhibits CO stretching bands at 2089 and 2104 cm^{-1} and two $\nu(C{=}N)$ bands at 1645 and 1633 cm^{-1}, while a single $\nu(C{=}O)$ at 2084 cm^{-1} and a single $\nu(C{=}N)$ at 1645 cm^{-1} were observed for the complex with Z = H. It was suggested that the two copper(I) centres of the complex with $Z = NO_2$ may have different environments, with one coordinated and one uncoordinated imine group. Both imine groups are suggested to be coordinated in the complex with Z = H.

The copper(I) complexes $[Cu_2(\mathbf{LII}\text{-}Z)](ClO_4)_2$ are sensitive to moisture; a hydrolysis of the imine linkage occurs when the complexes are dissolved in undried solvents.

A series of dinuclear copper(II) complexes with the ligands derived from the condensation of 1,3-bis[bis(3-aminopropyl)aminomethyl]benzene with salicylaldehyde, 2-pyrrolecarboxaldehyde, 2-pyridinecarboxaldehyde, or 1-phenyl-3-formyl-2(1*H*)-pyridinethione has been prepared [176] to suppress hydrolysis and to avoid rigid metal environments in the resulting complexes. The synthesis of the polyamine precursor 1,3-bis[bis(3-aminopropyl)aminomethyl]benzene, isolated as the hexahydrochloride salt, was carried out by reaction of diphthaloyldipropylenetriamine with α,α′-dibromo-*m*-xylene, followed by acid hydrolysis of the tetraphthaloyl intermediate, as indicated in Scheme 27.

The hexamine represents a useful precursor for dinucleating ligand systems H_4-**LIII**, where the flexibility of the propylenediamine bridges is expected to favour coordination of the tertiary nitrogen atoms of the

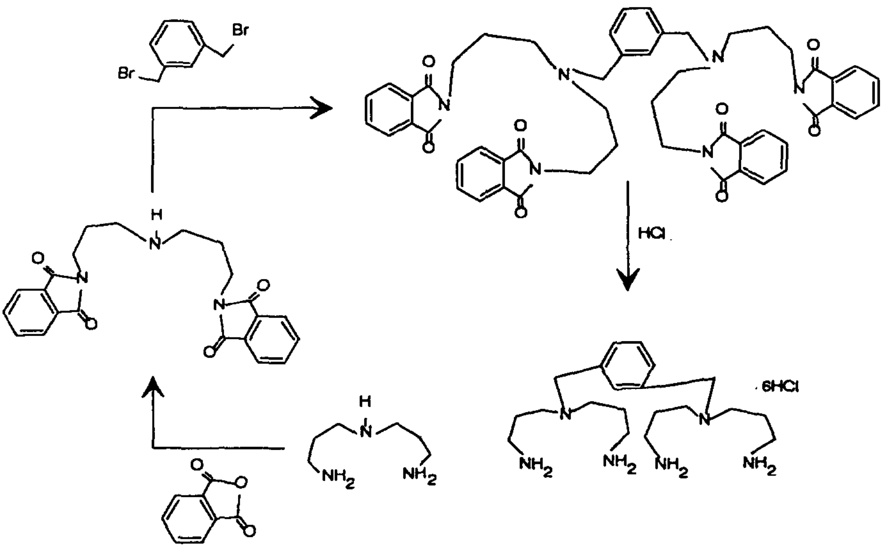

Scheme 27. Formation of a potentially hexadentate dinucleating polyamine.

diamino-*m*-xylene residue to the copper(II) centres, giving rise to five-coordinate structures of type [Cu_2(LIII)].

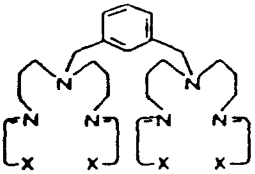

H_4-LIII

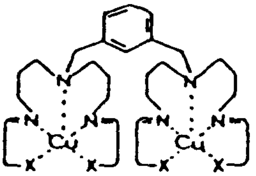

[Cu_2(LIII)]

In these complexes, obtained by reaction in MeOH of the appropriate ligand with copper(II) acetate or perchlorate in the presence of NaOH, the magnetic moment does not show any significant magnetic interaction between the metal centres while electronic and ESR spectra indicate that the copper(II) ions are five coordinate.

The catalytic activity of these complexes for the air oxidation of 3,5-di-*t*-butylcatechol and 4-methylcatechol to the corresponding quinones has been investigated and compared with that of the mononuclear complexes [Cu (LIV)] and [Cu(LV)].

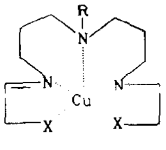

[Cu(LIV)] R = H

[Cu(LV)] R = $CH_2C_6H_5$

The most effective catalysts are the group of complexes derived from formylpyrrole, while the other complexes generally show rather low activity. The bulky substituents of the aromatic ring make difficult any further evolution of the quinone to more complex oxidation products.

Steric effects may thus explain the lower reactivity of the complexes of type [Cu_2(**LIII**)] and [Cu(**LV**)] with respect to that of type [Cu(**LIV**)] complexes. For the formylpyridinethione derivatives it is likely that the phenyl substituents at the pyridine nitrogen atoms completely hinder the approach of the catechol to the metal sites. In order to reduce the importance of steric effects in the oxidation reaction it is necessary to use less-substituted catechols, particularly those with no substituent adjacent to the hydroxyl groups; but the oxidation of these compounds leads invariably to complex mixtures of products.

A less-hindered substrate for the catalytic oxidation, 4-methylcatechol, was used, and the complexes derived from formylpyrrole are still found to be the most reactive. The reactivity sequence is opposite to that found for the oxidation of 3,5-di-*t*-butylcatechol (3,5-DTBC), since the dinuclear complexes are much more reactive than the mononuclear analogues. The derivatives of salicylaldehyde are practically unreactive under the reaction conditions. The catalytic activity of these copper(II) complexes for the oxidation of *N,N,N′,N′*-tetramethyl-*p*-phenylenediamine (TMPD) to $TMPD^+$ by dioxygen was also tested [176].

Only the formylpyridinethione and formylpyridine complexes are active and the higher reactivity of the dinuclear complexes over their mononuclear analogues is related to the need of coupling the one-electron oxidation of TMPD with the two-electron transfer to O_2; the order of reactivity in this case parallels the ease of reduction of the copper(II) centres in the complexes. The relatively high catalytic activity of the formylpyrrole complexes in the oxidation of catechols may thus be partially due to the small size of the five-membered pyrrole ring, compared with benzene or pyridine, but is quite certainly not related to the ease of reduction of copper(II) in the complexes. Interestingly, the formylpyrrole complexes of cobalt(II), [Co_2(**LIII**)], [Co(**LIV**)] and [Co(**LV**)], are also more reactive than their salicylaldehyde or formylpyridine analogues in the catalytic oxidations of catechols with O_2. Although these oxidations are actually due to the dioxygen adducts of the cobalt(II) complexes and may involve a completely different mechanism, it was suggested that a common and important factor in determining the reactivity of the copper(II) and cobalt(II) formylpyrrole complexes is the relatively high overall basicity of the ligands and the corresponding electron density accumulated at the metal centres.

In the presence of dioxygen the dinuclear cobalt(II) complex with the ligand 1,3-bis(2,5,8,11-tetraazaundecyl)benzene forms above pH 7 a di-

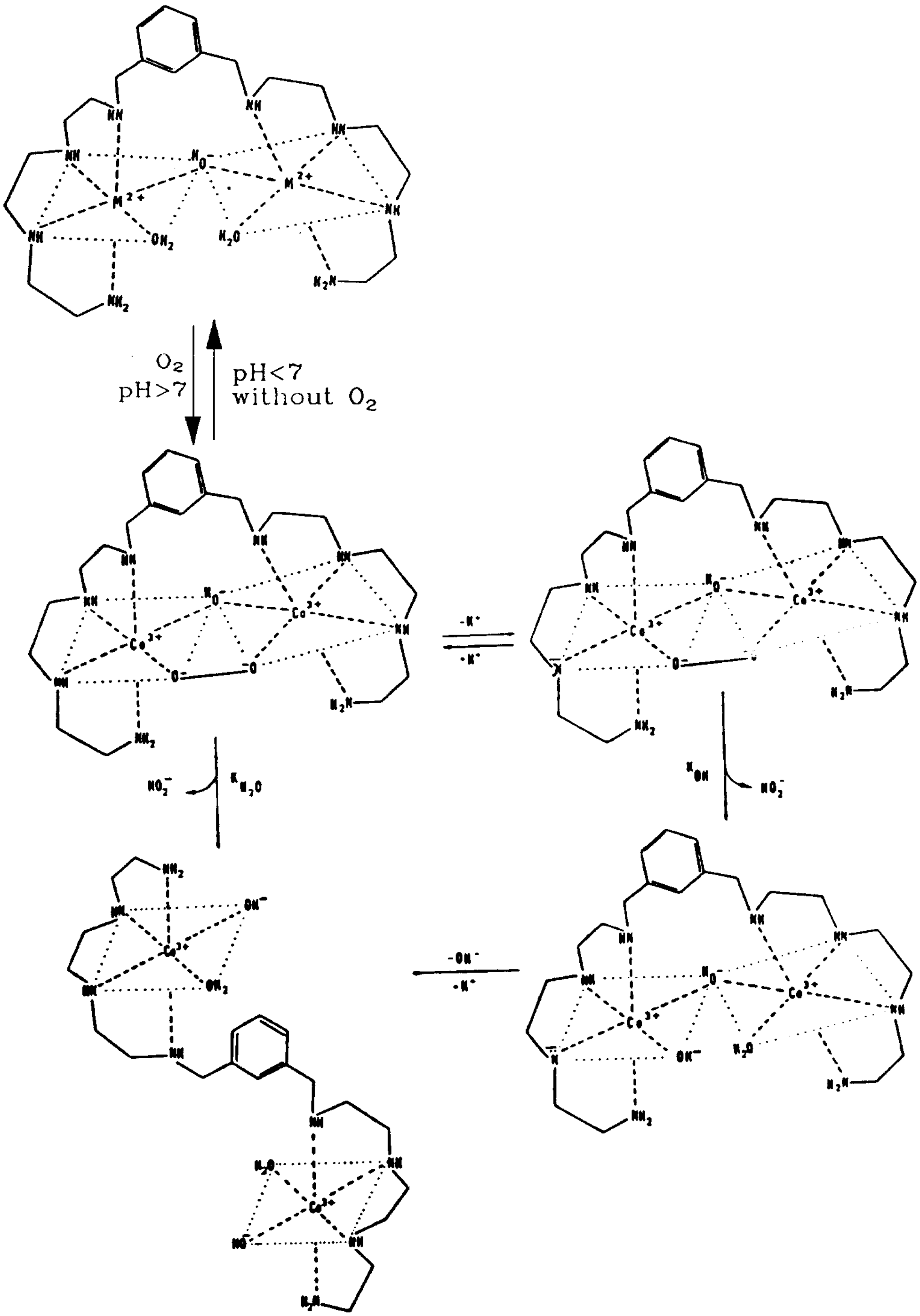

Scheme 28. Formation and degradation of the μ-hydroxo μ-peroxo dinuclear cobalt(III) complex with 1,3-bis(2,5,8,11-tetraazaundecyl)benzene (from ref. 177).

bridged μ-hydroxo-μ-peroxo dinuclear cobalt(III) complex [177]; this reaction is reversible at room temperature and the dinuclear cobalt(II) complex can be recovered by lowering the pH and excluding dioxygen from the solution. However, if the temperature is raised, the dioxygen is converted irreversibly to the dinuclear cobalt(III) complex, according to Scheme 28.

The autoxidation of the cobaltous complex through the formation of the dioxygen complex results in a metal-centred oxidation to form the dicobalt (III) chelate and hydrogen peroxide. The first step of the autoxidation reaction is first-order with respect to the concentration of both the dioxygen complex and hydroxide ion.

Recently, *N,N*-bis(3,5-dimethylpyrazol-1-ylmethyl)benzylamine and *N,N, N′,N′*-tetrakis(3,5-dimethylpyrazol-1-ylmethyl)-α,α'-di-amino-*m*-xylene have been prepared according to the reactions [178,179]

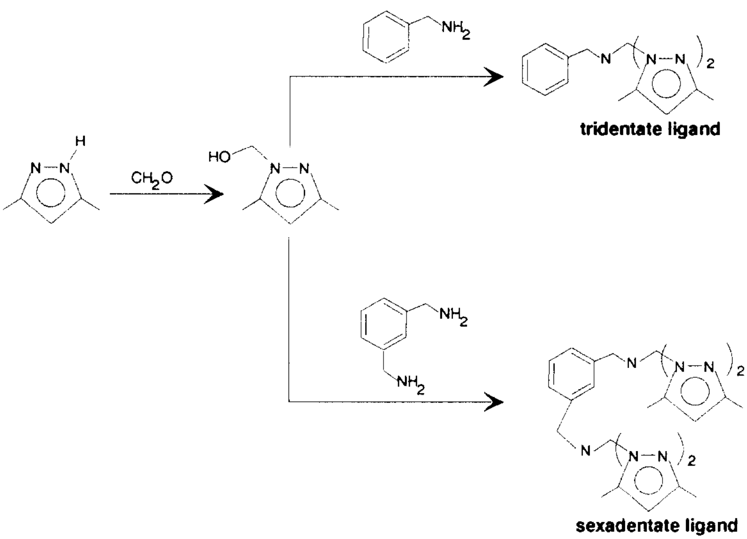

The condensation of 1-(hydroxymethyl)-3,5-dimethylpyrazole and the appropriate amine (benzylamine or α,α'-di-amino-*m*-xylene) resulted in ligands which can act as tridentate or sexadentate donors respectively.

The sexadentate ligand, by reaction with copper(II) salts, produces the dinuclear complexes [Cu_2(sexadentate ligand)$(X)_2$]Y_2 ($X = CH_3O^-$, Cl^-). The tridentate ligand, when treated with $CuCl_2$, gives a mononuclear complex of the form [Cu(*N,N*-bis(3,5-dimethylpyrazol-1-ylmethyl)benzylamine)$(Cl)_2$] with two terminal chloride atoms.

When $Cu(BF_4)6H_2O$ was the copper precursor, a dinuclear complex [Cu_2(*N,N*-bis(3,5-dimethylpyrazol-1-ylmethyl)benzylamine)$_2(OCH_3)_2$]$(BF_4)_2$ was formed, certainly due to the non-coordinating nature of the BF_4 anions.

The catecholase activity of these complexes was studied [178,179] and it was found that the complexes derived from the dinucleating ligand are the most active catalysts for the oxidation of catechol to quinone. However, even within complexes prepared from the same ligand, substantial changes in reactivity are found which depend on the nature of the bridging groups and the counter-ions present.

The complex $[Cu_2(\text{tridentate ligand})_2(OCH_3)_2](BF_4)_2$, although derived from a mononucleating ligand, was shown to be dinuclear in nature and was found to be intermediate in its reactivity towards catechol. It was suggested that in the oxidation of the catechol, dissociation of the bridging groups must occur prior to the complexation of the substrate. When this occurs, $[Cu_2(\text{tridentate ligand})_2(OCH_3)_2](BF_4)_2$ is transformed, in solution, into a mononuclear complex which would slow down its reactivity. This will not be the case for the complexes derived from the sexadentate dinucleating ligand.

The only true mononuclear complex $[Cu(\text{tridentate ligand})](ClO_4)_2$ is the least active of the complexes studied.

Many of the systems described above have been thought of as models for the hemocyanin and tyrosinase biosites. This stemmed from the early models of the site for which an endogenous bridge would be present throughout any reaction. Following the elucidation of the crystal structure of deoxyhemocyanin [32] there has been a necessary change of strategy as the endogenous bridge now appears unlikely to be present in the native protein (unless as a water molecule) until the oxygenation step, when, from EXAFS, it would appear to be formed.

The favoured candidate is now a hydroxide unit. This does not detract from the information retrieved in the preceding studies, without which we would be quite deficient in our knowledge of the chemistry available at dinuclear copper centres.

As we are concerned in this review with the general aspects of small-molecule activation by dinuclear centres, we have presented only the chemistry, leaving the reader to pass judgement on the role of the complexes as models for the biosites.

H. COMPLEXES DERIVED FROM MACROCYCLIC LIGANDS

Rigid and flexible monocycles have been used for metal complexation and for oxidative reactions, the extent of rigidity or flexibility being related to the nature of the lateral groups on **LVI**.

The catalytic behaviour and activity of the copper(II) complex, $[Cu_2(\mathbf{LVI})](ClO_4)_2$, synthesized by reaction of 2,6-diformyl-4-methylphenol and 1,3-diaminopropane in the presence of copper(II) perchlorate [180], in the air oxidation of substituted diphenols [113] is in between those observed with the "end-off" copper(II) complexes derived from the amino acids glycine and histidine, which have already been discussed in Section C.

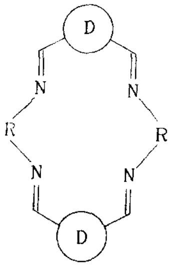

LVI

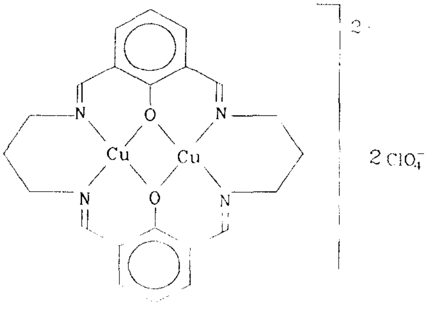

$[Cu_2(\mathbf{LVI})](ClO_4)_2$

The more flexible potentially decadentate Schiff bases **LVII** and **LVIII** have been isolated as dilead complexes [181,182]. Although it has yet proved impossible to isolate the free ligands the Pb^{2+} ions can be replaced by transmetallation reactions [182].

The reaction of O_2 with dinuclear copper(I) complexes of **LIX** obtained by BH_4^- reduction of $[Pb_2(\mathbf{LVIII})(SCN)_4]$, and **LX**, obtained by methylation of **LIX**, has been reported [183]. The complexes $[Cu_2(\mathbf{LIX})](ClO_4)_2$ and $[Cu(\mathbf{LX})](ClO_4)_2$ are bright yellow diamagnetic solids that turn green on exposure to O_2 in solution and, less rapidly, in the solid state.

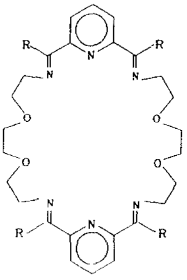

R = { CH_3 · LVII ; H · LVIII }

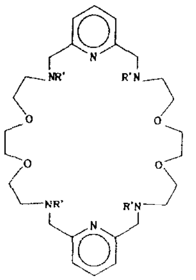

R' = { CH_3 . LIX ; H . LX }

$[Cu_2(\mathbf{LIX})](ClO_4)_2$ rapidly consumes 1 mol O_2 per mole of bi-copper(I) complex, this being followed by a much slower O_2 consumption, the final total uptake being in excess of 3 mol O_2 per 2 mol Cu(I).

The uptake of the first mole of O_2 is accompanied by the development of an absorption band characteristic of copper(II), which did not intensify on further oxygenation. No H_2O_2 was detected at any stage and no H_2O was detected immediately after absorption of the first mole of O_2 although it was found later in the reaction.

When the O_2 uptake was interrupted by replacement of the O_2 atmosphere by argon the green colour of the solutions changed to amber without gas evolution. The change was fairly rapid in the early stages, but became progressively slower. Re-admission of O_2 reversed the spectral changes with an isosbestic point at 15 900 cm^{-1}, whilst further O_2 was absorbed at an accelerated rate (Scheme 29).

On the basis of these observations and a kinetic analysis of the rates of O_2 uptake an interpretation in terms of a bi-Cu(I)/bi-Cu(II) redox cycle leading to dehydrogenated forms of the macrocycle has been proposed [184]. The results are consistent with the mechanism outlined in Scheme 29 (first redox cycle) in which the first rapid O_2 uptake generates a μ-peroxo-di-Cu(II) species. This is followed by proton transfer from the coordinated secondary amine groups to the coordinated peroxide. Elimination of H_2O regenerates a di-copper(I) species containing two C=N groups. The system is now set for further O_2 uptake leading to further oxidative dehydrogenation. Support for the mechanism was provided by the appearance of a ν(C=N) band at 1653 cm^{-1} and the disappearance of the ν(NH) bands in the IR spectra of the products and by the observation that when the secondary amine groups

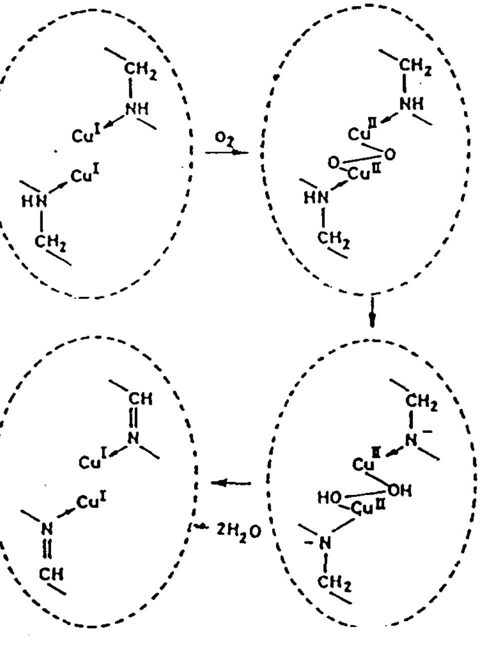

Scheme 29. Proposed mechanism for dinuclear copper(I)/copper(II) cycle in the oxidative dehydrogenation of $[Cu_2(LIX)](ClO_4)_2$ (from ref. 184).

are methylated, (as in **LX**) the rate of O_2 consumption after the first mole was suppressed about 100-fold. However, attempts to isolate an O_2 adduct at this stage were unsuccessful. Whatever the mechanistic details the results demonstrate a clear distinction between the initial coordination of the O_2 molecule and its subsequent (anaerobic) activation as well as the occurrence of a $Cu_2(I) \rightarrow Cu_2(II) \rightarrow Cu_2(I)$ redox cycle in the reduction of O_2 to H_2O with concomitant oxidation of organic functional groups.

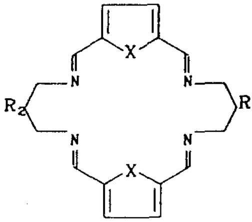

X=O, R=H LXII
X=O, R=Me LXIII
X=S, R=Me LXIV

The structures and properties of some dicopper(I) and dicopper(II) complexes of a macrocyclic ligand **LXII**, which function as catalysts for the oxidation of several organic substrates including catechols in the presence of oxygen, have been reported [185]. The macrocycle was synthesized as the complex Ba(**LXII**)$(ClO_4)_2 \cdot EtOH$ from 2,5-diformylfuran and 1,3-diaminopropane by use of Ba^{2+} ion as a template. Replacement of Ba^{2+} by Cu^{2+} led to a series of dicopper(II) complexes including $[Cu_2$(**LXII**)$(OH)_2$ $[(ClO_4)_2H_2O$, $[Cu_2$(**LXII**)$(OR)_2(MeCN)_2](BPh_4)_2$, and $[Cu_2$(**LXII**) $(OR)_2(NCS)_2]$ (R = Me, Et, *n*-Pr). In $[Cu_2$(**LXII**)$(OEt)_2(NCS)_2]$ (Fig. 37), each copper(II) ion is bonded to two imino nitrogen atoms of the macrocycle, the nitrogen of one terminally bound thiocyanate ion and to two bridging ethoxide groups in an approximate trigonal bipyramidal geometry. The two metal ions are displaced by 0.57 Å on opposite sides of the roughly planar macrocycle so that each bridging ethoxide occupies an axial site in the coordination sphere of one metal ion and an equatorial site of the other. The Cu···Cu separation is 3.003 Å. The furan oxygen atoms are not coordinated.

The complexes $[Cu_2$(**LXII**)$(OR)_2(MeCN)_2](BPh_4)_2$ have ligand field spectra nearly identical with those of $[Cu_2$(**LXII**)$(OR)_2(NCS)_2]$ and therefore undoubtedly have closely similar structures. The spectrum of $[Cu_2$(**LXII**) $(OH)_2](ClO_4)_2H_2O$ is different and suggests a tetragonal type of coordination. In the bis(μ-alkoxo) the pairs of copper(II) ions are strongly antiferromagnetically coupled ($2J = 600$–$700\ cm^{-1}$); the dihydroxo complex is less strongly coupled.

All the dicopper(II) complexes undergo reduction simply by heating their solutions in MeCN. For $[Cu_2$(**LXII**)$(OEt)_2(NCS)_2]$ the product is $[Cu_2$ (**LXII**)$(SCN)_2]$ whose structure is shown in Fig. 38 [186].

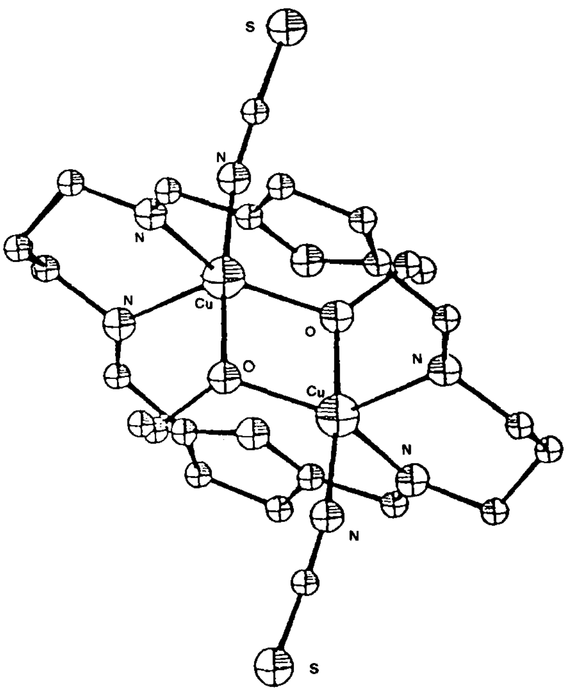

Fig. 37. Structure of $[Cu_2(LXII)(OEt)_2(NCS)_2]$ (from ref. 185).

The two copper atoms are each bonded to two nitrogen atoms of the macrocycle and to the two sulphur atoms of the bridging thiocyanate groups. The furan ring oxygen atoms are not bonded. The environment of the copper atoms is distorted tetrahedral. The macrocycle is approximately planar.

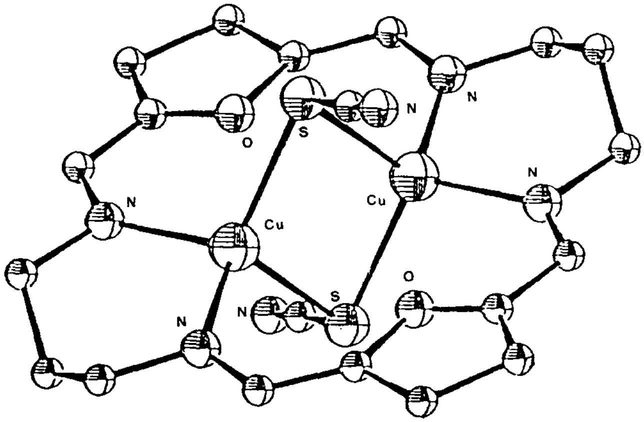

Fig. 38. Structure of $[Cu_2(LXII)(SCN)_2]$ (from ref. 186).

It seems likely that the unique thiocyanate bridging mode found in $[Cu_2(\mathbf{LXII})(SCN)_2]$ is a consequence of the nature of the macrocyclic ligand which, unlike other larger and more flexible dinucleating macrocycles, does not permit much variation in the metal···metal separation. In the present case the Cu···Cu separation (2.796 Å) is such as to preclude other than two single-atom bridges.

For $[Cu_2(\mathbf{LXII})(OH)_2](ClO_4)_2H_2O$ and $[Cu_2(\mathbf{LXII})(OR)_2(MeCN)_2](BPh_4)_2$ the reduction product is the diamagnetic complex $[Cu_2(\mathbf{LXII})(MeCN)_2]Y_2$ ($Y = ClO_4$ or BPh_4) in which each three-coordinate copper(I) ion is bonded to two macrocycle nitrogen donors and to the nitrogen of one MeCN molecule (Fig. 39). The stereochemistry is distorted trigonal planar with the copper(I) ions displaced 0.23 Å, on opposite sides, from the N_3 planes. The Cu···Cu separation is 3.35 Å [185].

In the presence of certain substrates the reduction of $[Cu_2(\mathbf{LXII})(OH)_2](ClO_4)_2H_2O$ or $[Cu_2(\mathbf{LXII})(OR)_2(MeCN)_2](BPh_4)_2$ is accompanied by substrate oxidation. Thus, PhSH, $PhC{\equiv}CH$, hydrazobenzene, catechols, hydroquinone and ascorbic acid afford respectively PhSSPh, $PhC{\equiv}CC{\equiv}Ph$, azobenzene, *o*-quinones, *p*-quinone and dehydroascorbic acid, together with $[Cu_2(\mathbf{LXII})(MeCN)_2]Y_2$ or other dicopper(I) complexes. When carried out in DMF solution in the presence of O_2, several of the oxidations proved to be catalytic in $[Cu_2(\mathbf{LXII})(OH)_2](ClO_4)_2H_2O$ or $[Cu_2(\mathbf{LXII})(OR)_2(MeCN)_2](BPh_4)_2$ but not in $[Cu_2(\mathbf{LXII})(OEt)_2(NCS)_2]$, with, as shown by O_2-uptake measurements, an O_2-to-substrate (H_2X_2 or 2HX) stoichiometry of 0.5 ± 0.02. No induction period was observed and the catalytic oxidation was equally successful whether the catalysts were the

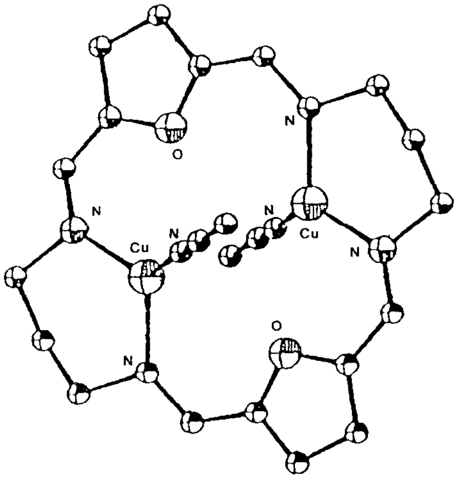

Fig. 39. Structure of $[Cu_2(\mathbf{LXII})(MeCN)_2]^{2+}$ CH_3 (from ref. 185).

dicopper(II) complexes $[Cu_2(\mathbf{LXII})(OH)_2](ClO_4)_2H_2O$ and $[Cu_2(\mathbf{LXII})(OR)_2(MeCN)_2](BPh_4)_2$ or the dicopper(I) $[Cu_2(\mathbf{LXII})(MeCN)_2]Y_2$. The inactivity of $[Cu_2(\mathbf{LXII})(OEt)_2(NCS)_2]$ reflects the need for coordinative unsaturation in the reduced state while the very poor activity of $Cu(ClO_4)_26H_2O$ indicates the importance of a "built-in" dicopper site.

The consumption by $[Cu_2(\mathbf{LXII})(MeCN)_2]Y_2$ is only 0.5 ± 0.03 mol O_2 per dicopper(I) unit in the absence of substrate. It was suggested that each O_2 molecule is associated, in its reduction, with four copper atoms rather than two. Such a situation could occur if the initial coordination of O_2 by $[Cu_2(\mathbf{LXII})(MeCN)_2]Y_2$ is followed, in the absence of substrate, by a fast bimolecular two-electron transfer with a second molecule of $[Cu_2(\mathbf{LXII})(MeCN)_2]Y_2$ to generate the μ-oxo species according to the reactions

$$Cu^I \cdots Cu^I + O_2 \rightarrow Cu^{II}\text{–}(O_2)^{2-}\text{–}Cu^{II} + Cu^I \cdots Cu^I \rightarrow [Cu^{II}\text{–}O\text{–}Cu^{II}]_2$$

For this oxo species an aggregate of two dimeric units was supposed. $[Cu_2(\mathbf{LXII})(OH)_2](ClO_4)_2H_2O$, whose μ-hydroxo–dicopper(II) structural unit was inferred from the antiferromagnetic behaviour ($\mu_{eff}/Cu = 1.37$ BM at 293 K and 0.70 BM at 93 K), by reaction with phenylacetylene in a MeCN–MeOH (2:1 v/v) solution at reflux for 15 min, gave orange crystals of $[Cu_4(\mathbf{LXII})_2(CCPh)][ClO_4]_30.5$dpda (dpda = diphenyldiacetylene) followed by white crystals which were shown by chemical analysis and mass and ^1H NMR spectra to be dpda. The total recovered yield of reacted phenylacetylene, i.e. $[CCPh]^- +$ dpda, was 0.95 mol per Cu atom.

The ^1H NMR spectrum of this tetranuclear copper(II) complex in MeCN showed the expected features of the coordinated macrocycle together with a pair of multiplets at δ 7.57 and 7.44 identical in position and contour with those occurring in a spectrum of dpda, and a multiplet at δ 7.10 attributable to the coordinated phenylacetylide group. In the structure of $[Cu_4(\mathbf{LXII})_2(CCPh)](ClO_4)_30.5$dpda (Fig. 40), each macrocycle is bonded to a pair of copper atoms via the four imino nitrogen atoms. The conformation of each "Cu_2N_4" moiety is such that the two metal atoms sit outside the approximate N_4 plane on the open face of the saddle-shaped macrocycle. The four nitrogen atoms of each macrocycle are almost planar. The two pairs of copper atoms are linked via the C–C bond of the phenylacetylide ion. The furan oxygen atoms are not coordinated. The bonding of the two pairs of copper atoms to the acetylide group is different [187].

The dicopper complex $[Cu_2(\mathbf{LXI})(RCN)_2](ClO_4)_2$ does not react with O_2 in acetonitrile; in DMF the action of O_2 with this dinuclear macrocyclic complex produces a tetranuclear species $[Cu_4(\mathbf{LXI})_2OH](ClO_4)_3H_2O$, the structure of which was also determined by X-ray diffraction [188].

Each asymmetric unit contains one $[Cu_4(\mathbf{LXI})_2OH]^{3+}$ cation, three perchlorate anions and two molecules of acetonitrile solvate. The cation

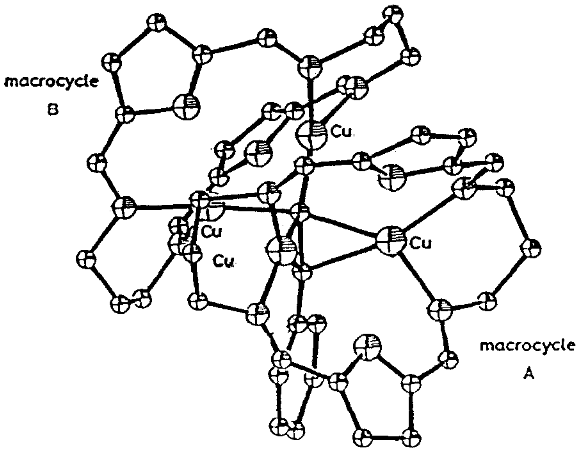

Fig. 40. Structure of $[Cu_4(\mathbf{LXII})_2(CCPh)]^{3+}$ (from ref. 187).

contains four coplanar copper(I) ions each coordinated to two imine nitrogen atoms, one from each of the two **LXI** macrocycles.

Within the square plane of the four copper atoms is a hydroxide ion disordered between two positions. Thus there is a planar Cu_4O assembly incorporated in a near-spherical complex ion.

The possible sequence of reactions

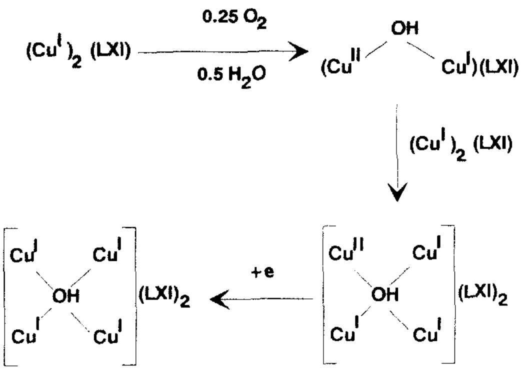

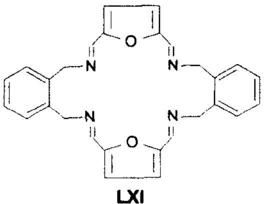

LXI

has been proposed [188].

A hexanuclear copper(I) structure **LXI** was found in the catalytic oxidation of PhSH to PhSSPh with $[Cu_2(\mathbf{LXII})(OH)_2](ClO_4)_2H_2O$ or $[Cu_2(\mathbf{LXII})(OR)_2(MeCN)_2](BPh_4)_2$ (Fig. 41). The cation $[Cu_6(\mathbf{LXII})_3(SPh)_2]^{2+}$ contains six three-coordinate copper(I) ions linked via two thiolate groups each tetrahedrally bound to three copper atoms and one phenyl carbon atom [184].

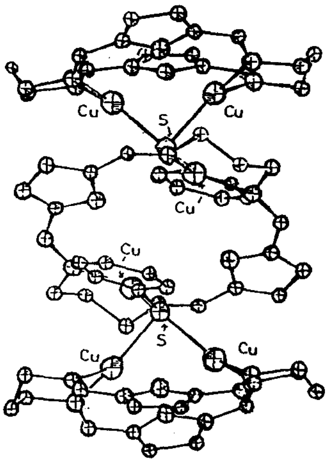

Fig. 41. Structure of $[Cu_6(\mathbf{LXII})_3(SPh)_2]^{2+}$.

By treatment of $Ba(\mathbf{LXII})(ClO_4)_2 \cdot EtOH$ and $Ca(\mathbf{LXIII})(ClO_4)_2 \cdot EtOH$ with a threefold excess of $[Cu(CH_3CN)_4]ClO_4$ in CH_3CN–EtOH (2:3) at 60°C and in the absence of air, the complexes $[Cu_2(\mathbf{LXII})(CH_3CN)_2](ClO_4)_2$ and $[Cu_2(\mathbf{LXIII})(CH_3CN)_2](ClO_4)_2$ have been obtained [189]. When the transmetallation was carried out at reflux temperature in "wet" solvent (1–2% H_2O) with access to air, the pentanuclear complexes $[Cu_5(\mathbf{LXIII})_2(dmt)_2](ClO_4)_3$ and $[Cu_5(\mathbf{LXIV})_2(dmt)_2](ClO_4)_3$ (dmt = 3,5-dimethyl-1,2,4-triazolate anion) were obtained in up to 55% yield. The same products were obtained starting from $[Cu_2(\mathbf{LXII})(MeCN)_2](ClO_4)_2$ and $[Cu_2(\mathbf{LXIII})(MeCN)_2](ClO_4)_2$. Separate experiments established the necessity of both H_2O and O_2 for the formation of the triazolate ring. Moreover, no triazolate was formed when $[Cu(MeCN)_4][ClO_4]$ was used in place of the dinuclear complexes $[Cu_2(\mathbf{LXII})(MeCN)_2](ClO_4)_2$ or $[Cu_2(\mathbf{LXIII})(MeCN)_2](ClO_4)_2$. The use of EtCN in the solvent mixture in place of MeCN afforded the corresponding pentanuclear complex of 3,5-diethyl-1,2,4-triazolate. The nature of the pentanuclear complexes was determined by their independent preparation in the absence of air and water via self-assembly from the dinuclear copper(I) complexes with the ligands **LXII–LXIV** (2 equivalents), pre-prepared Hdmt (2 equivalent), and $[Cu(MeCN)_4[ClO_4]$ (1 equivalent). The structure of $[Cu_5(\mathbf{LXIII})_2(dmt)_2](ClO_4)_3$ shows (Fig. 42) that the cation comprises five copper(I) atoms, two molecules of macrocycle and two triazole anions. Four of the copper(I) atoms have a three-coordinate distorted trigonal planar geometry while the central copper(I) atom, positioned at a centre of symmetry, is two coordinate with a linear arrangement. This central copper atom is linked to the two pairs of three-coordinate copper atoms by the two coplanar bridging triazolyl anions. The

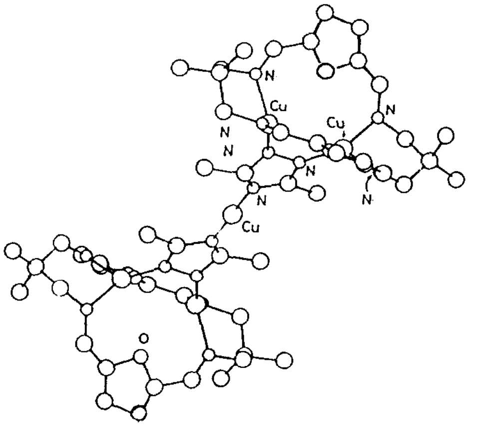

Fig. 42. Structure of $[Cu_5(\mathbf{LXIII})_2(dmt)_2]^{3+}$ (from ref. 189).

macrocycle molecules have a non-planar, saddle-shaped conformation. This is reflected in the ^1H NMR spectrum which shows the inequivalence of the CH_3 groups in each saturated segment of the macrocycle (at δ 0.8 and δ 1.15) and also in the two protons of the adjacent methylene groups (at δ 3.5 and δ 4.4).

The mechanism reported in Scheme 30 has been proposed [189] for the formation of the triazole from acetonitrile. The first step is an aerobic oxidation of the dicopper(I) complex to the di-μ-hydroxo–dicopper(II) species. This is followed by intramolecular nucleophilic attack by the bridging OH^- groups or intermolecular attack by H_2O at the nitrile carbon atoms. A concerted nitrile-to-Cu(II) electron transfer at both metal centres with accompanying coupling of the two adjacent nitrogen atoms leads to the species **3** of Scheme 30. The NH_3 needed for the final ring-closure step was supposed to come from a separate metal-promoted hydrolysis of acetonitrile, the intermediate hydrolysis product acetamide having been detected in the reaction mixture.

By reaction of $[Cu_2(\mathbf{LXII})(MeCN)_2](ClO_4)_2$ and $[Cu_2(\mathbf{LXIII})(MeCN)_2](ClO_4)_2$ with *cis*-azobenzene, the dark red crystalline compounds

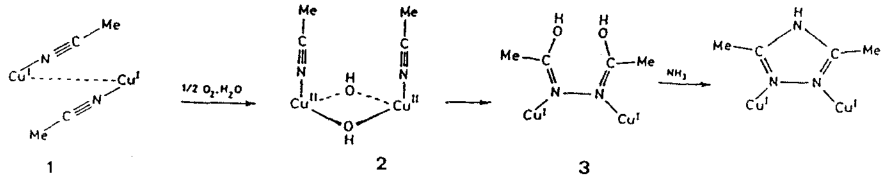

Scheme 30. Proposed mechanism for the copper-mediated hydrolysis/oxidation of acetonitrile to 3,5-dimethyl-1,2,4-triazole (from ref. 159).

$[Cu_2(\mathbf{LXII})(Ph_2N_2)_2](ClO_4)_2$ and $[Cu_2(\mathbf{LXIII})(Ph_2N_2)(MeCN)](ClO_4)_2$ were obtained. A four coordination for copper(I) was proposed for $[Cu_2(\mathbf{LXII})(Ph_2N_2)_2](ClO_4)_2$ while in $[Cu_2(\mathbf{LXIII})(Ph_2N_2)(MeCH)](ClO_4)_2$ one copper(I) is apparently three-coordinate. A basically planar macrocyclic conformation was suggested in the 4-azobenzene complex, with copper(I) occupying a tetrahedral site made up of two imino nitrogen atoms and two proximal azo nitrogen atoms from the pair of azobenzene bridges lying above and below the macrocyclic plane [161].

The efficacy of $[Cu_2(\mathbf{LXII})(MeCN)_2](ClO_4)_2$ and $[Cu_2(\mathbf{LXII})(OH)_2](ClO_4)_2$ as catalysts for the dehydrogenation of hydrazobenzene was examined [190]. The oxygen uptake in *N*,*N*-dimethylacetamide under an atmosphere of O_2 is in the range 0.49–0.60, depending somewhat on catalyst concentration.

It seems that at lower catalyst concentrations, side reactions take place, leading to products with oxidizable functions (e.g. aromatic amines, readily oxidized to nitroso compounds). Such side reactions seem more important when $Cu(ClO_4)_2$ or $[Cu(MeCN)_4]ClO_4$ is used as catalyst, as in these cases the stoichiometry observed is above 0.5 per mole of hydrazobenzene at all concentrations investigated. In the absence of catalyst, hydrazobenzene reacts slowly with O_2, taking up 0.80 mol O_2 per mole over a period of 30 h (though a very slow uptake continues after that time).

The rate of uptake of O_2 is faster with $Cu(ClO_4)_2$ or $[Cu(MeCN)_4]ClO_4$ than the macrocyclic complexes, with no advantage deriving from the ready-made dicopper site.

Indeed, as addition of a stoichiometric amount of base to $Cu(ClO_4)_2$ barely affects the rate of reaction, it seems that catalysis by "free" copper(II) in this system does not involve even a transient dicopper site.

The function of copper ions as oxidation catalysts involves redox processes where the metal cycles between 1+ and 2+ oxidation states. For catalysis of dehydrogenation by free copper ions, autoxidation of copper(I) plays a relatively indirect role, and the overall rate is determined by the slower of processes (1) or (2) (X_2H_2 represents a substrate containing labile hydrogen):

$$2Cu^{II} + X_2H_2 \rightarrow 2Cu^{I}X_2 + 2H^+ \tag{1}$$

$$2Cu^{I} + 2H^+ + 0.5O_2 \rightarrow 2Cu^{II} + H_2O \tag{2}$$

The effect of **LXII** coordination on copper is a relative stabilization of the 1+ state; thus it seems likely that process (2) is the one which has been affected in this case. Coordination of copper(I) by the macrocyclic ligand appears to have retarded this reaction significantly, perhaps even to the stage where an alternative dehydrogenation mechanism becomes favourable.

NMR data in CD_3CN show that when $[Cu_2(\mathbf{LXII})(OH)_2](ClO_4)_2$ is used as oxidant, a quantitative yield of *trans*-azobenzene is obtained. With $Cu(ClO_4)_2$, the only azobenzene obtained is again the trans isomer, but the oxidation is not quantitative and about 33% of another aromatic species (apparently an amine) is seen in the ^1H NMR spectrum. When a CD_3CN solution of hydrazobenzene is allowed to oxidize in air in the absence of catalyst over a period of about 6 days both cis and trans isomers are produced in comparable proportions [190].

When $[Cu(MeCN)_4]ClO_4$ is used under aerobic conditions, oxidation is somewhat faster than in the absence of copper(I) and results in the formation of a sizeable proportion of the cis isomer. On the other hand, when the experiment is carried out using $[Cu_2(\mathbf{LXII})(MeCN)_2][ClO_4]_2$ in the presence of O_2, a quantitative yield of the trans isomer is obtained within 24 h.

Electronic spectra in dimethylacetamide indicate complete *trans*-azobenzene formation when the macrocyclic dicopper catalyst $[Cu_2(\mathbf{LXII})(MeCN)_2]^{2+}$ is used, but somewhat more than 10% formation of the cis isomer with the mononuclear $[Cu(MeCN)_4]^+$ catalyst.

According to these data, a coordination of the substrate was suggested [161], which requires a mutual cis orientation of the N lone pairs, presumably accompanied by the anti arrangement of the phenyl groups.

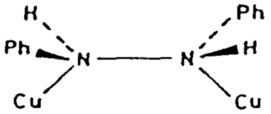

This geometry leads to the formation of *trans*-azobenzene, even in the limiting case of a one-step concerted dehydrogenation process.

Coordination of an N–N bridge is achieved only at the cost of some strain, as the X-ray structure has shown; steric problems are likely to be more severe with hydrazobenzene given the tetrahedral disposition of the phenyl rings.

Taken overall, these factors result in a slower rate of dehydrogenation for hydrazobenzene with $[Cu_2(\mathbf{LXII})(MeCN)_2]^{2+}$ than with free copper ions, in contrast with catechol dehydrogenation where the reverse is the case. This result, and particularly the implication that the *O,O'*-peroxo bridge may be sterically unfavourable in this macrocycle, provide some indirect evidences against the intermediacy of an *O,O'*-peroxo bridge in the transition state for $[Cu_2(\mathbf{LXII})(MeCN)_2]^{2+}$ catalysed oxidation [190].

Macrocycles of the type **LXV-*n*** may be useful for systematically investigating the properties of dicopper systems as a function of intermetal separations.

Advantages of the resulting monocyclic complexes over those of their

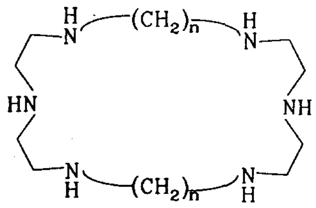

LXV-n

bicyclic counterparts [191] include more facile synthesis of the ligands, greater accessibility of the metal sites to substrates, and enhanced geometric flexibility. The greater flexibility could be important when considering geometrical requirements necessary for the activation of small molecules, that is, the monocyclic complexes would be able to adjust better to required intermetal distances and metal coordination geometries as a transformation progressed along the reaction coordinate. Structural studies of analogous macromonocyclic complexes do, in fact, demonstrate that these complexes can have intermetal separations from about 3–7 Å and can have either octahedral, square pyramidal, or trigonal bipyramidal coordination geometries, depending on the particular macrocycle used and the other ligands present.

The dinuclear copper(II) complexes [Cu$_2$(**LXV-*n***)](ClO$_4$)$_4$ or [Cu$_2$(**LXV-*n***) X$_n$](ClO$_4$)$_{4-n}$ (X = OCH$_3^-$, N$_3^-$, etc.) have been obtained by addition of 1 equivalent of **LXV-*n*** in MeOH to 2 equivalents of Cu(ClO$_4$)$_2$ in MeOH.

Crystallographic data on the dicopper(II) complex, which is supposed to have a bridging methoxide and a formulation [Cu$_2$(**LXV-3**)(OCH$_3$)](ClO$_4$)$_3$ when recrystallized from slow diffusion of benzene vapour into a nitromethane solution of the complex, showed the composition to be consistent with the formulation [Cu$_4$(**LXV-3**)$_2$(O$_2$)$_2$(H$_2$O)$_4$](ClO$_4$)$_6$2CH$_3$NO$_2$ [192]. In the cation (Fig. 43) the atoms are related by a crystallographic inversion centre, with the overall structure having approximately D_{2h} symmetry. The four

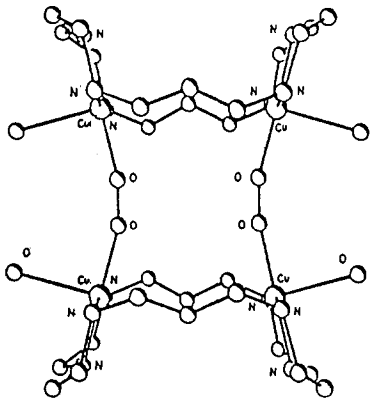

Fig. 43. Structure of [Cu$_4$(**LXV-3**)$_2$(O$_2$)(H$_2$O)$_4$]$^{6+}$ (from ref. 192).

copper atoms are in a nearly square planar arrangement, and disordered perchlorate anions and nitromethane of solvation are all separated from the cation and non-interacting. In the dimeric structure there are two dioxygen bridges between pairs of copper atoms in adjacent macrocycles. The Cu–O–O–Cu units are essentially planar with respect to the molecular plane defined by all four of the copper centres. The pentacoordinated copper centres have near-square-pyramidal geometries with an oxygen atom of the bridge and three nitrogen atoms of the macrocycle bound in the basal planes. A weakly bound water molecule occupies the axial site.

Dicopper(I) carbonyl complexes $[Cu_2(\mathbf{LXV}\text{-}\boldsymbol{n})(CO)_2](BPh_4)_2$ have been prepared by the addition of **LXV-*n*** to cuprous iodide in dry methanol under CO. They have been isolated after precipitation as the tetraphenylborate salts and are reasonably air stable when dry, but are rapidly oxidized in solution to uncharacterized copper(II). They do not lose CO under vacuum, but addition of excess triphenylphosphine in acetonitrile releases two equivalents of CO per dinuclear copper unit. EXAFS analysis gives a Cu–N distance of about 2.09 Å and a Cu···Cu distance of about 6.0 Å [192].

The dicopper(I) carbonyl complexes of **LXV-*n*** ($n = 3$ and 5) catalytically oxidize *o*-diphenols cleanly to *o*-benzoquinones in aprotic solvents at 25°C under an oxygen pressure of about 1 atm. The rates are enhanced by the addition of a base such as triethylamine, and the presence of a drying agent such as anhydrous calcium sulphate is required to scavenge water produced during the transformation. Negligible conversion of the *o*-diphenols is observed in the absence of the copper compounds. Under similar conditions, phenols are catalytically and selectively oxidized by molecular oxygen in the presence of the dicopper(I) complexes of **LXV-*n*** to the *o*-benzoquinones and *o*-diphenols.

The macrocyclic complex $[Cu_2(\mathbf{LXVII})](SO_3CF_3)_4$ and the related polypodal complexes $[Cu_2(\mathbf{XXXVII})](SO_3CF_3)_4$ and $[Cu_2(\mathbf{XL\text{-}4})](SO_3CF_3)_4$ [144,150] have been used in the epoxidation of olefins by iodosylbenzene, and a comparison of their catalytic activity with the mononuclear $[Cu(\mathbf{XXXIX})](SO_3CF_3)_2$ and $Cu(SO_3CF_3)_2$ has been carried out [193]. The mononuclear complex $[Cu(\mathbf{XXXIX})](SO_3CF_3)_2$ is not an effective catalyst under the same reaction conditions while the dinuclear complexes are also considerably better catalysts than cupric triflate $Cu(SO_3CF_3)_2$ [193].

Several internal olefins gave the corresponding epoxide as products, but the terminal olefins 1-hexane and 1-octene gave no epoxide products. (*E*)-stilbene was found to be more reactive than (*Z*)-stilbene and the products in both cases were the trans oxides and benzaldehyde.

Comparisons of the relative efficiencies of the above dinuclear and mononuclear complexes as catalysts for the epoxidation of cyclohexene were also carried out [193]. Significantly lower yields were obtained when the reactions were carried out in air, and different product distributions with much lower yields were seen in the presence of 2–5% H_2O. When the mononuclear cupric complex [Cu(**XXXIX**)](SO_3CF_3)$_4$ was substituted for [Cu_2(**XXXVII**)](SO_3CF_3)$_4$ in the reaction of cyclohexene, almost no reaction was observed. When a copper-deficient version of [Cu_2(**XXXVII**)](SO_3CF_3)$_4$ was used, small amounts of epoxide and 2-cyclohexen-1-one were formed. Thus the dinuclear nature of the complexes appears to play an important role in their reactivities as catalysts for this reaction. In this regard, it is important to note that cupric triflate, which was found to be an active catalyst when used at 20–40 mM concentrations, gave only small amounts of epoxide when used at 2 mM copper concentration.

The complexes [Cu_2(**XXXVII**)](SO_3CF_3)$_4$, [Cu_2(**XL-4**)](SO_3CF_3)$_4$, [Cu_2(**LXVII**)](SO_3CF_3)$_4$ and [Cu(**XXXIX**)](SO_3CF_3)$_2$ were reacted with iodosylbenzene (OIPh) in CH_3CN, in the absence of substrate, with the aim of identifying the reactive species. It was concluded that OIPh reacts with both mononuclear and dinuclear cupric complexes to form OIPh complexes or related species containing hypervalent iodine, but that the species formed from the dinuclear complexes are much more effective as epoxidation reagents than those formed from the mononuclear complexes. Moreover, it is clear that the intermediate formed in the reaction of OIPh with [Cu_2(**XXXVII**)](SO_3CF_3)$_4$ is different from that generated from the reaction of [Cu_2(**XXXVII**)]$^{2+}$ with hydrogen peroxide or from the reaction of the analogous cuprous complex with dioxygen, since the latter reactions give hydroxylation of the ligand.

It was not possible to distinguish between a reaction pathway in which the olefin reacts directly with an iodosylbenzene complex as opposed to one in which iodobenzene dissociates and the olefin traps a reactive high valent oxo intermediate. It was, however, observed that the dinuclear nature of complexes [Cu_2(**XXXVII**)](SO_3CF_3)$_4$, [Cu_2(**XL-4**)](SO_3CF_3)$_4$ and [Cu_2(**LXVII**)](SO_3CF_3)$_4$ plays an important role in determining the reactivity of the active species.

The reactivity of dicobalt(II) complexes with the ligands **LXVI**, **LXVII** and **LXVII-py** towards dioxygen has been tested [194–196].

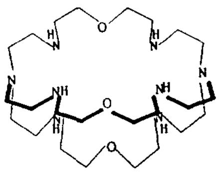

LXVI

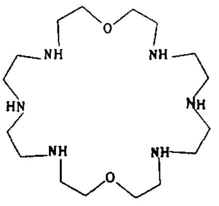

LXVII

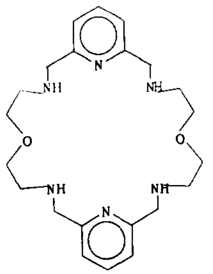

LXVII-py

The dibridged (μ-peroxo)(μ-hydroxo)-dinuclear cobalt(III) complex $[Co_2(\mathbf{LXVII})(OH)(O_2)]^{3+}$ shows relatively high stability in comparison with the corresponding dioxygen complex $[Co(\mathbf{LXVI})(OH)(O_2)]^{3+}$, which in solution is readily converted to the dihydroxo-dibridged complex so that it is never more than a minor species [194]. On the contrary $[Co_2(\mathbf{LXVII})(OH)(O_2)]^{3+}$ is formed as a major component in the solution [195]. The sixth position is probably occupied by H_2O, which by dissociation at higher pH easily forms a dihydroxo- and a trihydroxo-dioxygen complex. These additional OH groups have been assumed to be monodentate and not effective in excluding the peroxo bridge.

Solutions containing cobalt(II) and **LXVII**-py in a 2:1 molar ratio under an oxygen atmosphere indicate that dioxygen complexes are not very stable, though sufficiently so to prevent the precipitation of cobalt(II) hydroxide [198]. The dioxygen complex $[Co_2(\mathbf{LXVII})(OH)(O_2)]^{3+}$ is formed under basic conditions; it is less stable than the analogous complexes with the two ligands **LXVI**, and dioxygen complexes begin to form at pH values close to 7, but they are the predominant species only at pH 8.5 and above.

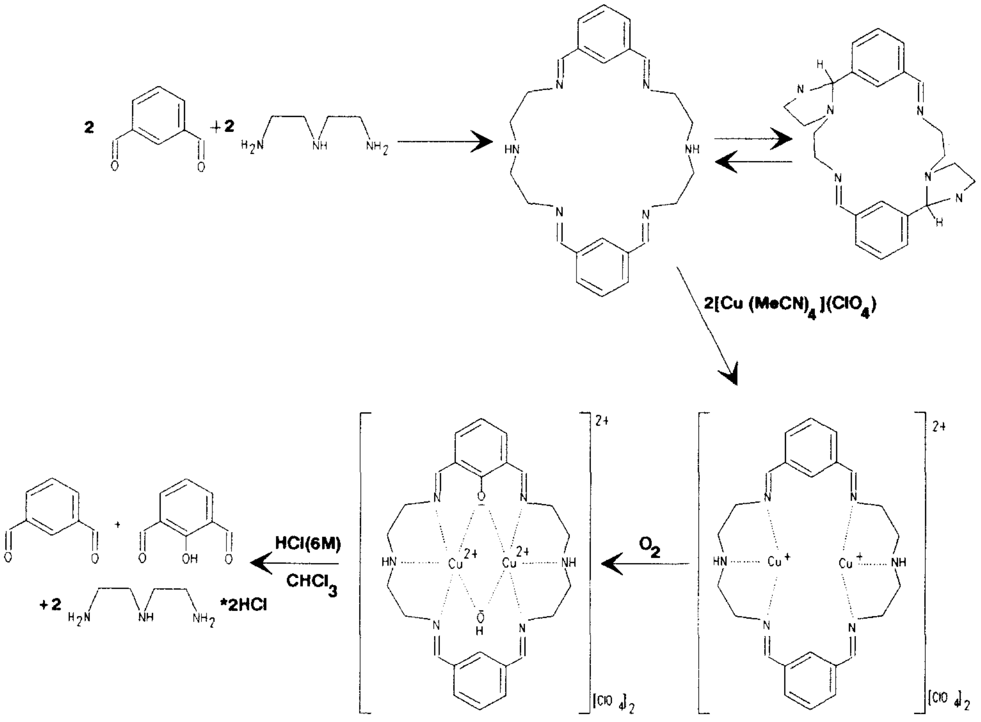

Scheme 31. Dinuclear copper(I) complex with the tetraimine Schiff base obtained from benzene-1,3-dialdehyde and diethylentriamine and its interaction with O_2.

The dibridged $[Co_2(LXVII\text{-}py)(OH)(O_2)]^{3+}$ complex is only a minor species because when it is formed in a significant amount the basic conditions favour its conversion to dihydroxo- and trihydroxo complexes as confirmed by electronic spectra of the 2:1 solutions under an oxygen atmosphere as a function of pH [196].

Very recently the first macrocyclic tyrosinase model has been achieved [197]. Benzene-1,3-dialdehyde and diethylenetriamine condense in good yield to give a tetraimine Schiff base macrocyclic complex which then reacts with copper(I) to give a dinuclear copper(I) macrocyclic complex. On exposure to dioxygen, hydroxylation is effected at the 2-position of one of the two *m*-xylyl head units. On dissolution in HCl the product breaks down and a mixture of benzene-1,3-dicarbaldehyde and 2-hydroxy-benzene-1,3-dicarbaldehyde are recovered (Scheme 31). The Schiff base macrocycle is believed to exist in solution as a mixture of isomers. An X-ray structure analysis of the crystals recovered on crystallization from CH_2Cl_2–CH_3CN showed that a double ring contraction process had occurred and that the bis(imidazolodine) macrocycle of Scheme 31 had been formed [198]. This requires that a ring opening must occur on dimetallation.

A series of macrocycles, named tropocoronands, which show a variety of stereochemical and electronic features, have been synthesized through the following reactions [199]:

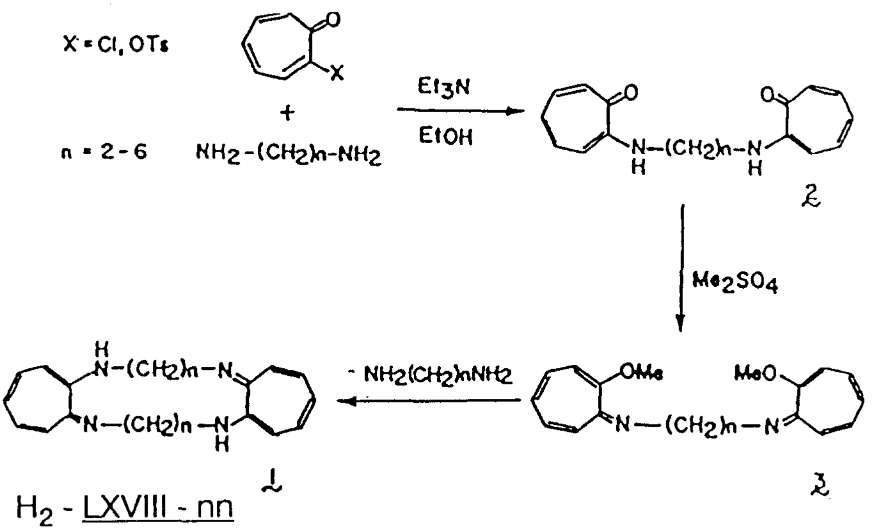

Thus it is possible to prepare a series of tropocoronands that comprise of two or more aminotropone imine moieties linked by methylene, ether, or thioether chains with high efficiency and good yield. Two tropone rings can be linked by reaction of an α-ω-diaminoalkane, or α-ω-diaminoethers or thioethers with 2-(tosyloxy)tropone or 2-chlorotropone to give the dimeric 2-aminotropones (**3**). The 2-aminotropone moiety can be converted to the corresponding 2-alkoxytropone imine by treatment with dimethyl sulphate in refluxing toluene or with triethyloxonium tetrafluoroborate in refluxing chloroform–hexamethylphosphonamide. The resulting alkoxy leaving group then undergoes facile amine displacement at 25°C in ethanol. Under high dilution conditions and with dropwise addition of an ethanolic solution of diamine to a solution of dimeric 2-alkoxytropone imine **3**, tropocoronands **1** can be obtained.

Complexes with tropocoronand ligands (H_2-**LXVIII-*n,n*** with $n,n = 3,3$, 4,4, 4,5, 5,5, 6,6) have been prepared and structurally characterized by X-ray crystallography [200–202]. For the copper(II) complexes Cu(**LXVIII-3,3**), Cu(**LXVIII-4,4**) and Cu(**LXVIII-5,5**) the geometry at the copper centre is smoothly distorted from planar towards tetrahedral along this series. The nickel(II) complexes Ni(**LXVIII-3,3**), Ni(**LXVIII-4,4**) and Ni(**LXVIII-4,5**) are also distorted planar molecules. Although molecular mechanical calculations reveal Ni(**LXVIII-4,5**) to be sterically strained, the strain energy is not sufficient to convert nickel(II) from the planar diamagnetic to the pseudotetrahedral paramagnetic form. With five or six atoms in both linker chains the electronic barrier is overcome and distorted tetrahedral structures occur for Ni(**LXVIII-5,5**), Ni(**LXVIII-6,6**) and Ni(**LXVIII-2,0,2**).

It was verified also that with copper(II), as the number of methylene groups in the linker chains connecting the two aminotropone imine poles of the macrocycle increases to six, the ligand becomes dinucleating [202]. Thus the attempt to prepare mononuclear Cu(**LXVIII-6,6**) resulted instead in the formation of the dinuclear [Cu_2(**LXVIII-6,6**)(OMe)(OAc)]. The X-ray structure (Fig. 44) shows that two copper(II) ions are coordinated to the two bidentate aminotropone iminate portions of the macrocycle and bridged by

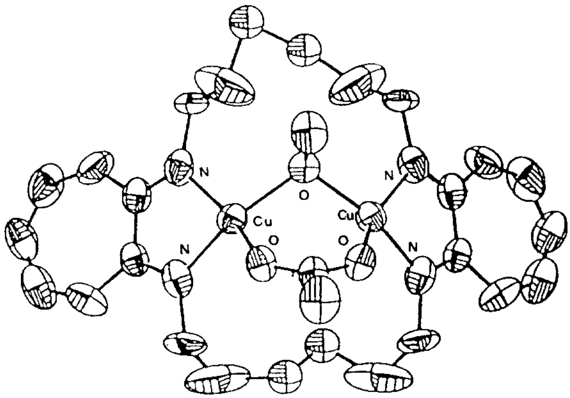

Fig. 44. View of the complex [Cu_2(**LXVIII-6,6**)(OCH_3)(OAc)] (from ref. 202).

both a methoxide and a bidentate acetate ligand. The resulting four-coordinate stereochemistry of copper is tetrahedrally distorted and the Cu···Cu distance is 3.100 Å.

The two metal ions are antiferromagnetically coupled ($J = -35.4\ \mathrm{cm}^{-1}$); an exchange coupling was found also in solution, showing that the dinuclear structure persists in solution.

This complex thus demonstrates the versatility of the tropocoronand ligand system and suggested the opportunity to explore new methods of chemical reactivity between metal centres held in close proximity. Thus homodinuclear carbonyl copper(I) complexes [Cu_2(**LXVIII-5,5**)$(CO)_2$] and [Cu_2(**LXVIII-6,6**)$(CO)_2$] [203,204] have been prepared by allowing suspensions of [$Cu(CH_3CN)_4$]BF_4 to react with either Li_2(**LXVIII-5,5**) or Li_2 (**LXVIII-6,6**) respectively in THF, under an atmosphere of CO at −78°C.

The dinuclear structure of these compounds was demonstrated by an X-ray diffraction study on [Cu_2(**LXVIII-5,5**)$(CO)_2$] [203] (Fig. 45).

Two nitrogen atoms of the aminotroponeiminate ligand and one terminal CO molecule are coordinated to each trigonal planar copper(I) centre. The two copper atoms are located on opposite faces of the macrocycle, separated by a distance of 4.132 Å. No evidence has been seen in the NMR spectra for the presence of a syn isomer while the IR spectra agree with terminally coordinated carbonyl groups ($\nu(CO) = 2071\ \mathrm{cm}^{-1}$).

[Cu_2(**LXVIII-5,5**)$(CO)_2$] decomposes readily in solution upon exposure to dioxygen or heat, producing the mononuclear Cu(**LXVIII-5,5**), metallic copper and an unidentified insoluble olive powder. The compound is, on the contrary, stable over long periods in the crystalline state. The thermal instability of this carbonyl compound limits its use as a catalyst for slow reactions such as the hydroformylation of alkenes.

[Cu_2(**LXVIII-5,5**)$(CO)_2$] and [Cu_2(**LXVIII-6,6**)$(CO)_2$] undergo smooth reactions with added alkynes to produce μ-alkyne complexes. $Cu_2(\mu$-

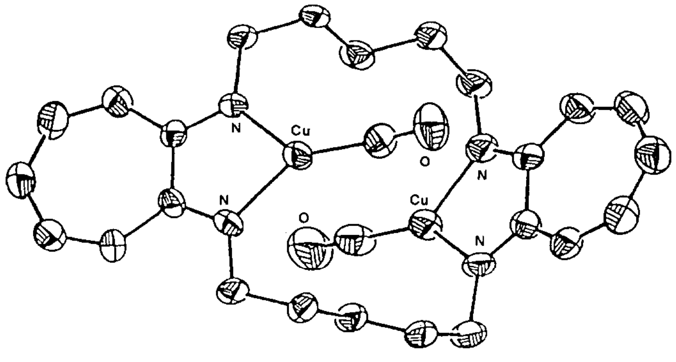

Fig. 45. Structure of [Cu_2(**LXVIII-5,5**)$(CO)_2$] (from ref. 203).

$\mathrm{RC{=}CR}$)(**LXVIII-6,6**) ($\mathrm{R = CO_2CH_2CH_3}$, $\mathrm{CO_2CH_3}$, $\mathrm{CH_3}$) have been alternatively prepared by addition of a THF solution of $\mathrm{Li_2}$(**LXVIII-6,6**) to a THF–$\mathrm{CH_3CN}$ solution of $\mathrm{[Cu(CH_3CN)_4]BF_4}$ at -78°C under nitrogen, followed by the addition of the appropriate alkyne.

The structure of $\mathrm{[Cu_2(\mu\text{-}CH_3CH_2O_2CC{\equiv}CCO_2CH_2CH_3)}$(**LXVIII-6,6**)] (Fig. 46) consists of two copper atoms bound to the tropocoronand ligand by the nitrogen donor atoms of the two aminotroponeiminate fragments and bridged by a molecule of diethylacetylenedicarboxylate oriented perpendicularly to the Cu–Cu vector. Each copper atom lies slightly above the plane defined by the centre of the C–C multiple bond and its two bonded nitrogen atoms. The alkyne moiety is able to bridge the short Cu···Cu distance of 2.806 Å, occupying the third coordination site for both copper atoms. A single alkyne molecule serves as a $4e^-$ donor. The bond order of the coordinated alkyne functionality is substantially diminished, as revealed by the C–C distance of 1.320 Å. The coordination of alkynes as $4e^-$-donor neutral bridging ligands in dicopper(I) tropocoronand complexes is a general one since both electron-withdrawing and electron-donating alkynes can be incorporated into the bridging position.

$\mathrm{[Cu_2}$(**LXVIII-5,5**)$\mathrm{(CO)_2]}$ is quite inert towards photochemical ejection of CO; when a 2-methyltetrahydrofuran solution of this complex was irradiated with a high pressure mercury lamp over a temperature range of -160 to -20°C, no product was obtained.

Addition of *n*-butyllithium to $\mathrm{[Cu_2}$(**LXVIII-5,5**)$\mathrm{(CO)_2]}$, followed by subsequent addition to the resulting solution of equimolar amounts of *n*-butyl magnesium chloride and 2-cyclohexen-1-one at -78°C, yielded the mixture of products reported in Scheme 32.

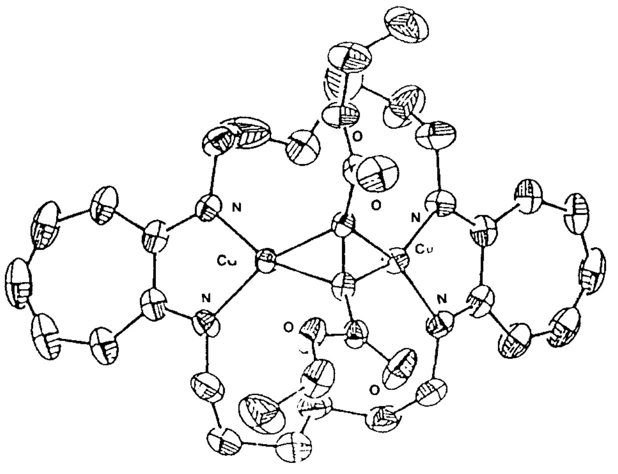

Fig. 46. Structure of $\mathrm{[Cu_2(\mu\text{-}CH_3CH_2O_2CC{\equiv}CCO_2CH_2CH_3)}$(**LXVIII-6,6**)] (from ref. 204).

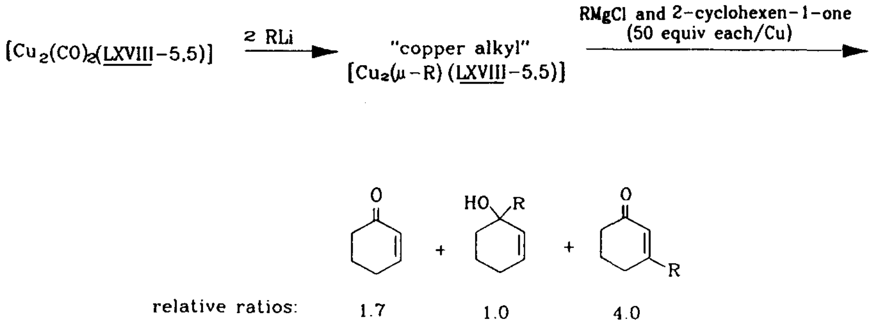

Scheme 32. Reactivity of $Cu_2(CO)_2$(**LXVIII-5,5**) with RLi.

The presence of greater than stoichiometric amounts of 3-butylcyclohexanone, arising from 1,4-addition of the *n*-butyl group to cyclohexanone, was assumed to be indicative of the intermediacy of a copper alkyl species that serves as catalyst for the 1,4-addition. The catalytic reaction is not very regiospecific, producing also tertiary alcohol. It was suggested that the copper alkyl species could be an anionic, alkyl-bridged dicopper(I) tropocoronand complex.

The reaction of $[Rh(CO)_2Cl]_2$ with Li_2(**LXVIII-5,5**) in THF under a CO atmosphere at low temperature produces an isomeric pair of compounds, *syn* and *anti*-$[Rh_2$(**LXVIII-5,5**)$(CO)_4]$.

In the two stereoisomers the $[Rh(CO)_2]$ moieties are situated on opposite sides of the mean plane through the tropocoronand macrocycle and on a common face of the ligand respectively. The rhodium atoms have four-coordinate square-planar stereochemistry with two nitrogen donor atoms from the aminotroponeiminate groups and two terminally bound molecules of CO comprising the coordination spheres. The metal···metal separation is 5.892 Å in the *anti* and 4.392 in the *syn* isomer [205] (Fig. 47).

The rhodium dicarbonyl tropocoronand complexes are thermally stable. Solid samples heated to 200°C showed only a small decrease in the intensity of the CO absorption band in the IR spectrum. This stability facilitated the high temperature NMR solution study, during which only a small amount of decomposition was observed. These studies showed that no isomerization occurs on the NMR scale up to a temperature of 130°C, from which a lower limit of $\Delta G^{\pm} > 20$ kcal mol^{-1} was estimated for the interconversion barrier between stereoisomers. However, thermal conversion of isomerically pure samples to a mixture of invertomers could be achieved by prolonged heating for several hours at 130°C.

The reaction of Li_2(**LXVIII-5,5**) with two equivalents of $CuBr \cdot Me_2S$ and excess of 12-crown-4 produces $[Li(12\text{-crown-}4)_2][Cu_2(\mu\text{-Br})$(**LXVIII-5,5**)$]$, which is air and temperature sensitive. The compound is stabilized by the

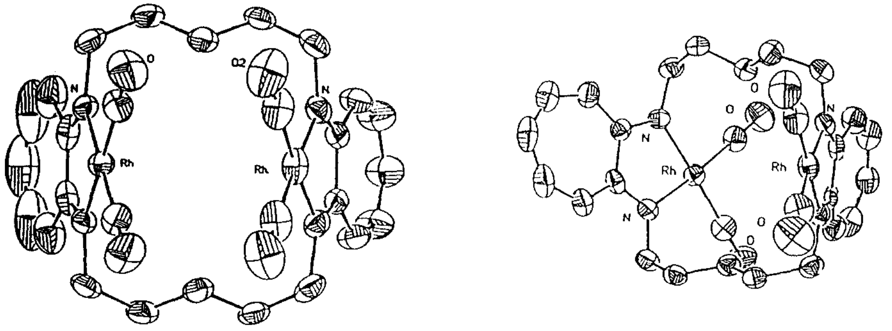

Structure of *syn*- Structure of *anti*-

Fig. 47. Structure of the *syn*- and *anti*-[Rh_2(**LXVIII-5,5**)$(CO)_4$] (from ref. 205).

crown ether, in the absence of which metallic copper and Cu(**LXVIII-5,5**) are obtained [206].

An X-ray diffraction study of this compound confirms the bridging bromine ligand in the anion and the complexation of the lithium cation by two 12-crown-4-macrocycles [206] (Fig. 48).

The copper(I) atoms are in a trigonal planar geometry while the tropocoronand ligand conformation is saddle shaped. The cation portion of this complex comprises an eight-coordinate lithium atom encapsulated by two 12-crown-4 molecules in approximate D_{4d} symmetry.

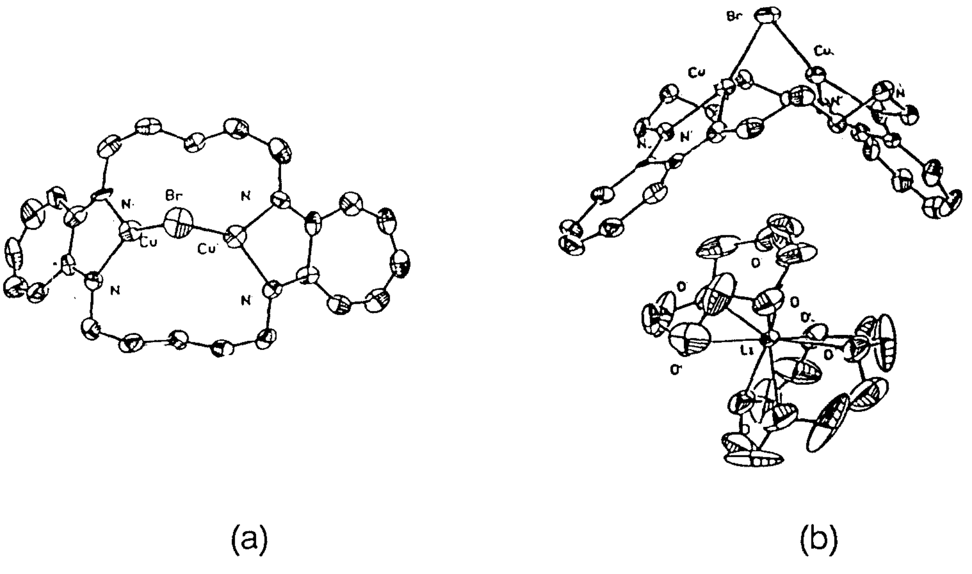

Fig. 48. Structure of (a) [Cu_2(μ-Br)(**LXVIII-5,5**)]$^-$ and (b) of the complex [Li(12-crown-4)$_2$][Cu_2(μ-Br)(**LXVIII-5,5**)] (from ref. 206).

A similar phenyl-bridged dicopper(I) tropocoronand, prepared according to the reactions

$$[\mathrm{Cu(NCCH_3)_4}](\mathrm{BF_4}) + \mathrm{PhLi} \xrightarrow[-78^\circ\mathrm{C}\ -\mathrm{r.t.}]{\mathrm{THF}} (\mathrm{CuPh})_n + \mathrm{LiBF_4}$$

$$\xrightarrow[\text{12-crown-4}]{\mathrm{Li_2}(\underline{\mathrm{LXVIII}}\text{-5,5})} [\mathrm{Li(12\text{-}crown\text{-}4)_2}][\mathrm{Cu_2}(\mu\text{-Ph})(\underline{\mathrm{LXVIII}}\text{-5,5})]$$

(red solid)

has a structure most probably analogous to the above μ-bromide complex. When a THF solution of $\mathrm{Li_2}$(**LXVIII-5,5**) and a suspension of $(\mathrm{CuR})_n$ in THF are combined at −78°C and allowed to warm up gradually, an air-sensitive burgundy solution of a tropocoronand dicopper(I) alkyl complex (TDAC) forms, which, when treated with cyclohexenone, produces no conjugate addition products. Only unreacted cyclohexenone and small amounts of products resulting from coupling of R fragments (e.g. biphenyl or octane) are detected according to the reactions

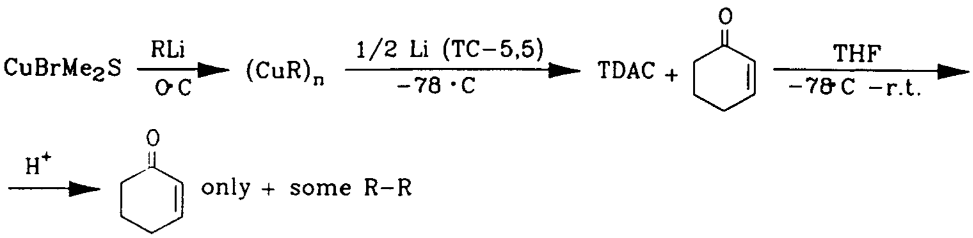

When TDAC is pretreated at −78°C with RLi, a reaction accompanied by a slight darkening of the burgundy solution, and then allowed to react with cyclohexenone at −78°C, 3-alkylcyclohexanone product is produced immediately after quenching of the reaction mixture. The intensity of the burgundy colour returns to its original shade after addition of the cycloalkenone, and no solids are observed over the course of the fast reaction. A small amount of coupled product, R–R, is still present according to the reaction

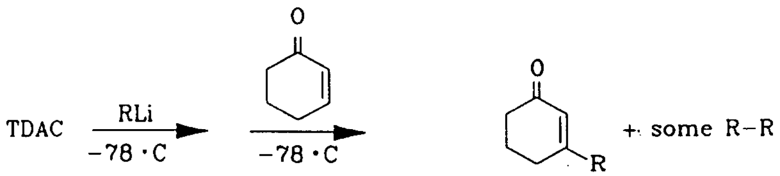

The persistence of the deep burgundy colour and the absence of any precipitate are taken as evidence that a TDAC is present throughout the course of the reaction and is responsible for the observed conjugate addition product in the presence of added alkyllithium or Grignard reagent.

The structure of TDAC produced in the reaction between CuR and Li$_2$(**XLVIII-5,5**) is probably also similar to that of Cu$_2$(μ-Br)(**LXVIII-5,5**) and hence the formulation Li[Cu$_2$(μ-Br)(**LXVIII-5,5**)] has been suggested. TDAC forms directly at the elevated temperatures (i.e. above −30°C) needed for complexation (characterized by a yellow-to-burgundy colour change) to take place. The alkyl-bridged dicopper(I) core may be sufficiently stable to account for its inertness towards cyclohexenone. In the presence of excess nucleophilic reagent at −78°C, however, a new species, containing perhaps two trigonal planar copper(I) atoms bearing terminal alkyl groups, forms that reacts readily with enone.

Solutions of the mononuclear complex, [Cu(**LXVIII-5,5**)], yield only 1,2-addition products under conditions that produce only 1,4-addition with TDAC. The RLi-pretreated TDACs, with R = Ph, Bu, and Me, undergo the "stoichiometric" reaction with cyclohexenone smoothly except that significant amounts (up to 20%) of the 1,2-addition product are obtained with R = Me. This result parallels the behaviour of the catalytic system.

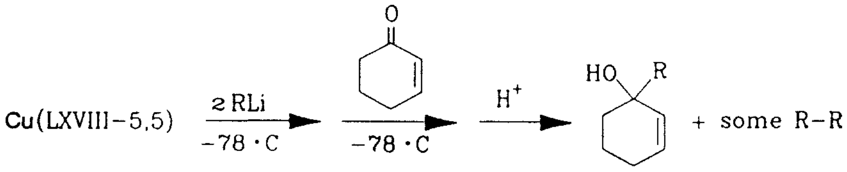

I. MACROPOLYCYCLES AND FACE-TO-FACE LIGANDS

Slow addition of 1,4-bis(1-oxa-4,10-dithia-7-azacyclododecan-7-ylmethyl)-benzene (**LXIX**) to a butan-2-one solution of [Cu(CH$_3$CN)$_4$]BF$_4$ under argon gave the white crystalline diamagnetic copper(I) complex [Cu$_2$(**LXIX**)](BF$_4$)$_2$·butan-2-one; the reaction of Cu(BF$_4$)$_2$, under argon, with **LXIX** in nitromethane followed by introduction of THF gave the green copper(II) complex [Cu$_2$(**LXIX**)]BF$_4$)$_4$·2THF [207].

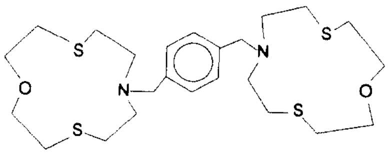

LXIX

The copper(I) complex [Cu$_2$(**LXIX**)](BF$_4$)$_2$, treated with CO in nitromethane gave the carbonyl adduct and reversibly lost CO on treating the solution with argon at 80°C. CO absorption occurs also in the solid state to give the same adduct. Similarly it reacts with O_2 at 80°C to give a pale green powder which on heating in vacuo at 110°C turns white with concomitant loss of the ESR signal, indicating the return to the copper(I) state. This oxygenation–deoxygenation sequence can be repeated several times with little noticeable decomposition in the starting material. In solution this oxygenation process is more complicated [207].

Treatment of $[Cu_2(\mathbf{LXIX})](BF_4)_2$ with NO yielded a dark green solution from which, on addition of THF, the dinuclear copper(II) complex $[Cu_2(\mathbf{LXIX})(NO_2)_2](BF_4)_2$ was obtained [208] (Fig. 49). Each copper(II) ion has a distorted octahedral environment consisting of the ONS_2 donor set of the ligand and an unexpected chelating NO_2^- group. The approximate symmetry of the cation is C_{2v}; the Cu(II)···Cu(II) intramolecular distance is 11.264 Å since **LXIX** is in an open configuration.

The copper(II) complex $[Cu_2(\mathbf{LXIX})(H_2O)_6](BF_4)_4$, prepared by addition of $Cu(BF_4)_2 \cdot 6H_2O$ to **LXIX** in propylene carbonate, when dissolved in water at pH 6, was transformed into the closely related copper(II) complex $[Cu_2(\mathbf{LXIX})(OH)](BF_4)_3$ [208].

The X-ray structure showed that the ligand **LXIX** is now in a closed conformation with the single bridging hydroxo group holding the two copper(II) atoms at a distance of 3.384 Å. The two copper atoms are in an approximately square pyramidal five-coordinate geometry, and are strongly antiferromagnetically coupled ($-2J = 820$ cm^{-1}). The dimer unit possesses a symmetry plane which is perpendicular to the phenyl ring and contains the oxygen atom of the bridge (Fig. 50).

These results lead to the important conclusion that the conformational flexibility of this type of ligand and the "face-to-face" approach of the two nucleating centres allow the observation of sensitive structural and physical changes at the dinuclear site, with the consequent ability to activate small molecules.

General synthetic methods for the construction of cylindrical macrotricycles which contain similar or different macrocyclic subunits have been

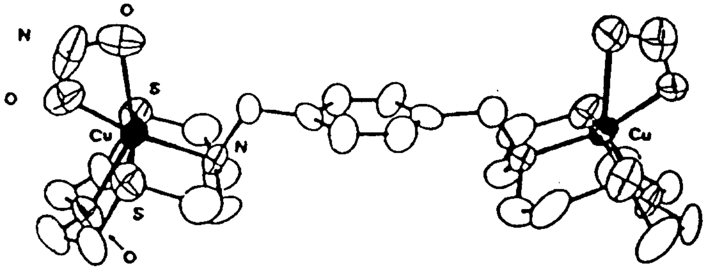

Fig. 49. Structure of $[Cu_2(\mathbf{LXIX})(NO_2)_2]^{2+}$ (from ref. 208).

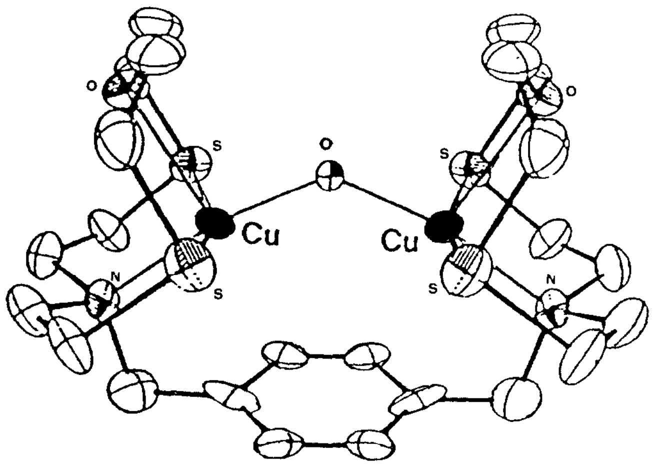

Fig. 50. Structure of $[Cu_2(\mathbf{LXIX})(OH)]^{3+}$ (from ref. 208).

reported [209]. These ligands can complex two different cations or stabilize different oxidation states.

In these macropolycycles each macrocyclic subunit may serve as a receptor site for a metal cation. Because of the difference in ring size and number of binding sites, macrotricycles may present different complexation properties. Complexation of a metal cation by each macrocyclic subunit of ligands yields dinuclear cylindrical macrotricyclic complexes, as represented schematically in Fig. 51. Based on crystal structure data, the intercationic distances may be grossly estimated to 5–7 Å for dinuclear macrotricyclic cryptates [209]. Thus there is space for inclusion between the cations of a substrate of compatible size and suitable binding properties, and insertion of a substrate molecule (O_2, N_2 etc.) between the two metal cations of dinuclear complexes leads to cascade complexes which may have interesting properties for fixation and dinuclear catalysis (such as the reduction of the included molecules).

Similar electronic spectra with absorption at 550–850 nm are obtained when adding KO_2 to $[Cu_2(\mathbf{LXX})]^{4+}$ or oxygen to $[Cu_2(\mathbf{LXX})]^{2+}$. Also, the intensity of the 355 nm band of the latter complex is strongly affected by O_2

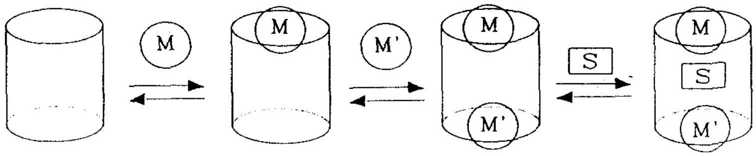

Fig. 51. Schematic representation of the formation of dinuclear cryptate complexes with cylindrical macrotricyclic ligands and of their activation of a substrate molecule S.

and CO. These changes might involve dinuclear reactions of superoxide and oxygen [209].

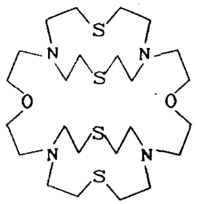
LXX

The chemistry of a group of dinuclear complexes, containing two identical or different metal ions and composed of two porphyrins covalently linked, at a variable distance, in a parallel configuration, has been developed [20]. As starting porphyrins to form face-to-face dimers, the monomeric porphyrin diesters were isolated in crystalline form and in good yield (Scheme 33(a)).

The *p*-nitrophenyl diesters offer stable, isolable, activated carboxylic acid derivatives.

The diamine porphyrins required for the amide-linked dimers were obtained via Curtis degradations of the diesters (Scheme 33(b)).

Equimolar amounts of the dinitrophenyl esters and diamines were heated at 50–40°C in dry pyridine to form the face-to-face dimers under high dilution conditions.

The products were readily isolated and purified by simple chromatography. By this method the four face-to-face dimers with linking groups of six, five (two isomers) and four atoms were obtained (Scheme 34(a)) [20].

Other 5,15-disubstituted porphyrins, principally amine $(CH_2)_nNHR$ ($n = 1$, 2, 3; R = H, CH_3) and acid chloride $[(CH_2)_nCOCl]_2$ ($n = 1$, 2) groups have been reacted together to produce new face-to-face ligands with an interporphyrin amide bridge of varying length (4–7 atoms) (Scheme 34(b)).

An amine-linked dimer has been produced by the reduction of an appropriate amide linkage (vide infra, Scheme 36) while purely hydrocarbon-linked dimers have been prepared by direct coupling of bis(dipyrrylmethanes) bridged by an aliphatic $(CH_2)_n$($n = 4$, 6) chain (Scheme 35).

Face-to-face dicobalt derivatives were prepared according to Scheme 34. The mixed-metal dimer [PdCo(**LXXI**-4-2CONH)] containing cobalt and palladium was prepared by coupling the palladium complex of the porphyrin diester and the free-base diamine; cobalt was then inserted in the dimer. The mild conditions of the coupling reaction should allow generalization of this approach to the preparation of a variety of mixed-metal complexes.

The Pd–Co dimer provides a test of the dinuclear catalyst concept. Since the ligand environments of this species and the related dicobalt dimer

[Co_2(**LXXI-4**-2CONH)] are identical, any unusual reactivity of the latter complex must be due solely to the presence of two cobalt centres. Palladium should be an "innocent" metal centre, as it shows no tendency to accept axial ligands, nor to participate in electron-transfer reactions [20].

As representative examples the crystal structures of some "face-to-face" complexes have been reported [20].

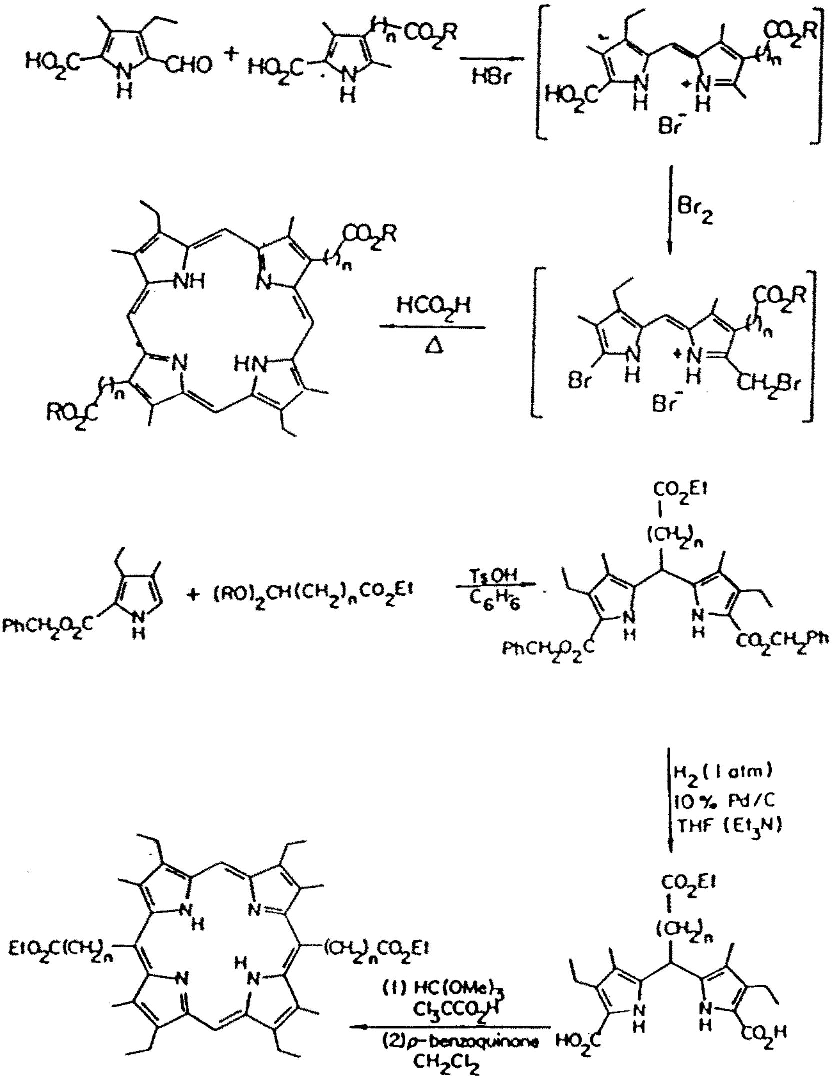

(a)

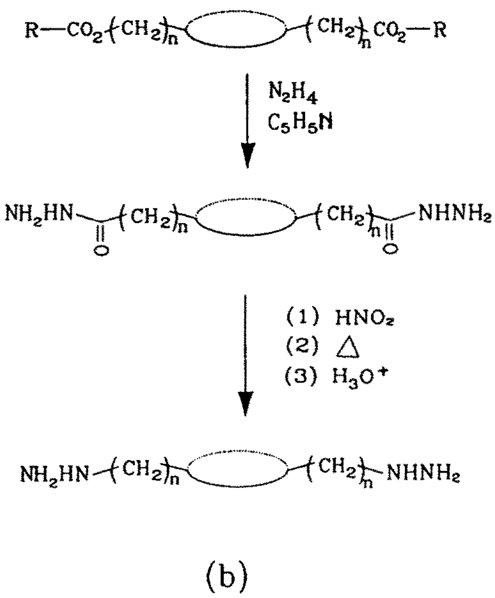

Scheme 33. Preparation of (a) monomeric porphyrins diesters and (b) monomeric diamine porphyrins (from ref. 20).

Although disordered, the dihydrate monotoluene solvate complex [Cu_2(**LXXI-6**-2CONH)] is indeed a porphyrin dimer linked at the 5,15 positions by amide linkages.

The crystal structure appears to be dominated by non-bonded aromatic-type interactions among porphyrin macrocyles and toluene solvate molecules. The two octaalkylporphyrin units are linked (Fig. 52) at the 10,20 (meso)-positions by two amide chains six atoms long. Rather than adopting

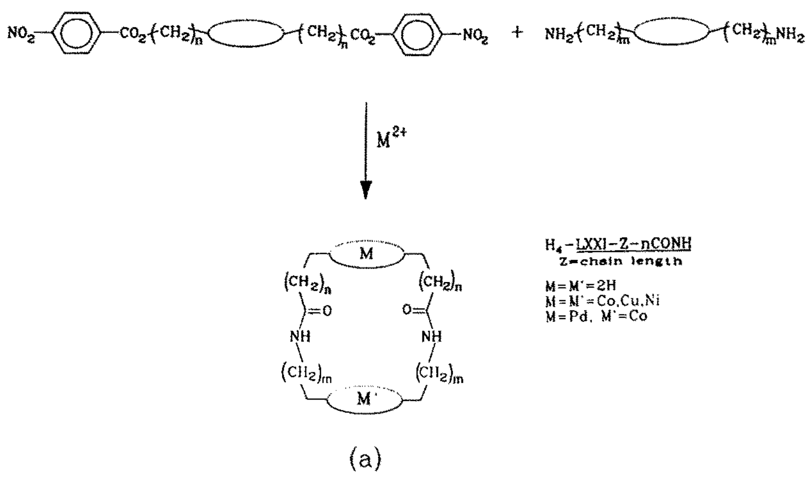

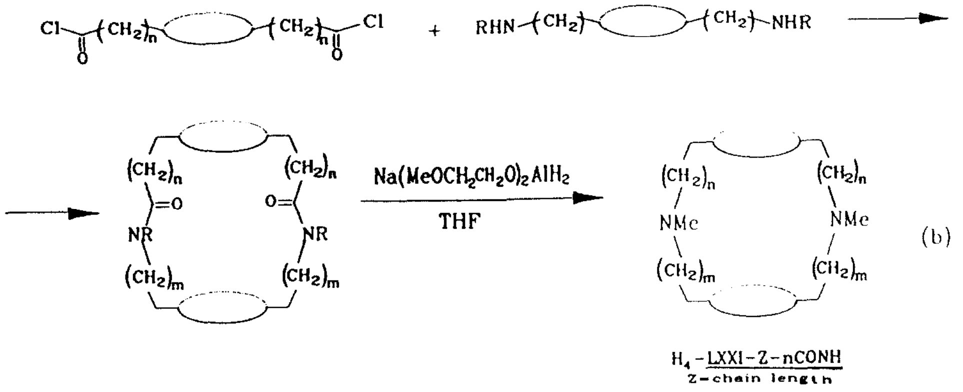

Examples of "face to face" ligands

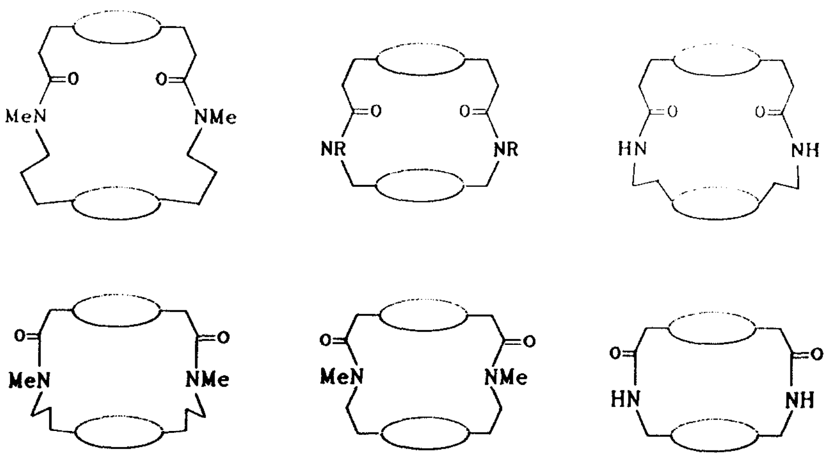

Scheme 34. Preparation of the "face-to-face" porphyrins (a) by dinitrophenol esters and diamines, (b) by secondary amines and acid chlorides (from ref. 20).

a "face-to-face" conformation with both copper ions lying on the normal to the porphyrinato skeleton and with a large empty space between the two macrocycles, there is a shear-like displacement of one porphyrinato unit with respect to the other, resulting in a close approach of the two macrocycles.

In this conformation, aromatic stacking is maximized. The intermolecular packing features partial stacking of porphyrin macrocycles with each other and with toluene solvate molecules. There is a water molecule hydrogen bonded to the carbonyl oxygen atom of each amide linkage. The crystal packing appears to be facilitated by a two-up two-down arrangement of the β-ethyl substituents. The closest intermolecular Cu–Cu separation is 8.760 Å.

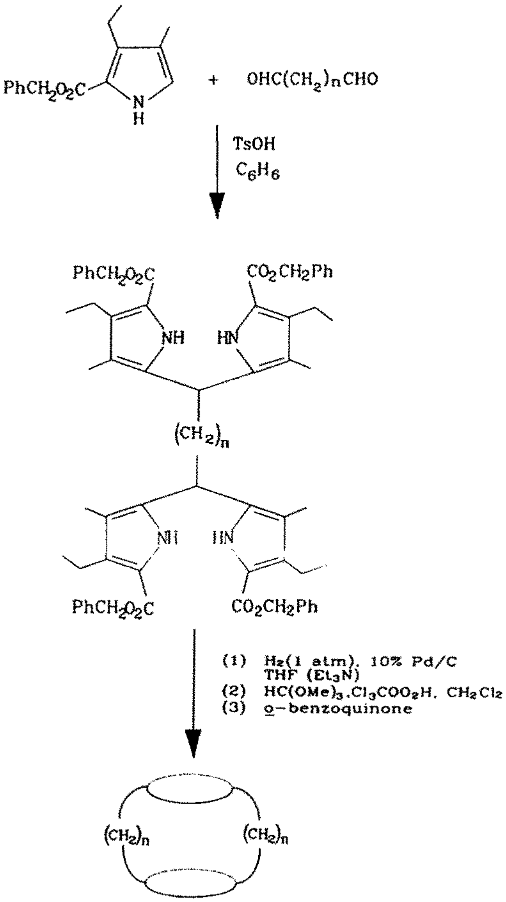

Scheme 35. Preparation of amine linked "face-to-face" porphyrins (from ref. 20).

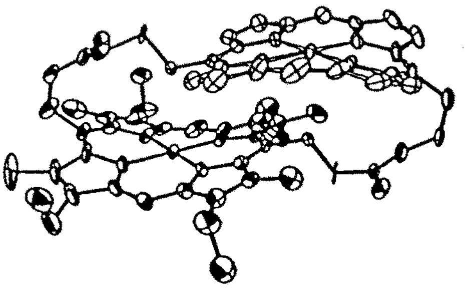

Fig. 52. Structure of [Cu$_2$(**LXXI-6**-2CONH)] (from ref. 20).

A striking feature of the structure is a shear-like displacement of one porphyrin unit with reference to the other by an average distance of 4.95 Å and the interplanar separation of the two porphyrin rings is 3.87 Å [20].

The cofacial dicopper hexyldiporphyrin-7 [Cu_2(**LXXI**-7–2CONH)] was prepared by coupling of the diacid chloride and the dibutylamine of 2,6-dihexyldeuteroporphyrin, followed by copper insertion using copper acetate in a chloroform–methanol mixture. This procedure statistically yields two diasteric isomers (designated as syn and anti) and each compound should consist of an enantiomeric pair because of the asymmetry in the carboxy-amine linkages [21].

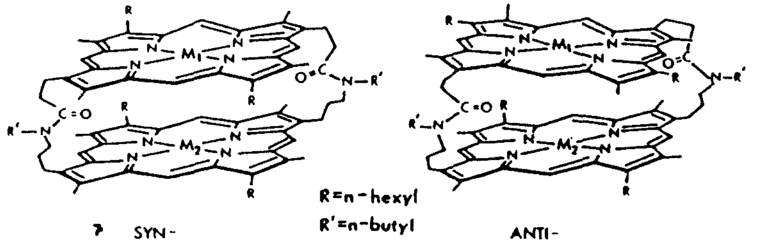

[Cu_2(LXXI-7 -2CoNH)]

It is notable that although the syn and anti forms have not been isolated, the crystals examined were apparently all in the syn configuration. The crystals, grown from toluene–DMSO, show that the porphyrin ring and the copper atom are planar. The two porphyrin rings are not stacked exactly over each other but have slipped, giving a Cu···Cu distance of 5.22 Å; the interplanar distance between rings is 3.52 Å. The geometry of the environment of the copper atom is square planar. Also the interplanar distance

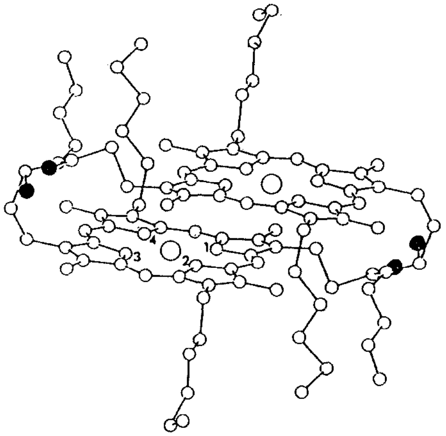

Fig. 53. Structure of [Cu_2(**LXXI**-7-2CONH)] (from ref. 21).

between dimer molecules is 3.47 Å, giving an intermolecular distance (4.60 Å) less than the intramolecular distance. This is due to a smaller intramolecular slip between adjacent rings of dimer molecules (Fig. 53).

Remarkable electrocatalytic effects for reducing molecular oxygen have been achieved when the above complexes are absorbed onto graphite electrodes. In most studies, dicobalt complexes have been used, but some work has been done with cobalt in one ring and another metal (such as iron, manganese, silver, aluminium) in the other. The influence of the length of the bridging chains and/or their locations at different positions around the periphery have also been studied. The only effective macrocyclic complex, capable of mediating the direct $4e^-$ path of dioxygen reduction is the dinuclear cobalt diporphyrin linked via two diametrically positioned four-atom amide chains [Co_2(**LXXI-4**-1CONH)], which can exist in two forms, syn and anti. Lengthening the bridges to five atoms causes a noticeable fall-off in activity; lengthening to six atoms or shortening to three causes even greater losses and a change in product from water to hydrogen peroxide. Unsymmetrical bridging, to produce a clamshell structure, also reduces catalytic facility sharply. Substitutions of one or both cobalt atoms lead almost exclusively to the production of peroxide.

Recently, efforts to grow single crystals of [Co_2(**LXXI-4**-1CONH)] were successful and the structure of [Co_2(**LXXI-4**-1CONH)]$\cdot CH_3OH \cdot$ $1.6CH_2Cl_2$ has been solved [210]. It exhibits crystallographically imposed twofold symmetry and has disordered bridges, the midpoints of which define the twofold axis. Although the starting powder sample contains about 10% of the minor isomer (syn), the crystal appears to be composed of only one enantiomorphic pair, d,l-anti.

One of the striking features of the structure is that the two porphyrin rings are stacked almost exactly over each other (Fig. 54). The $Co \cdots Co$ distance is 3.417 Å.

The cofacial porphyrin dimers show relatively short interplanar distances, presumably as a result of π–π interactions between the porphyrin rings. However, the very slight slippage between the two metal centres of Co_2(**LXXI-4**-1CONH) makes this structure different; as in the other structures, moderate to large slippage is found. In the present structure the two short rigid amide bridges at the transverse β-pyrrolic positions of the porphyrins apparently force the two rings to stack on top of each other.

The Co_2(**LXXI-4**-1CONH) structure represents one possible optimized diporphyrin geometry for $4e^-$ reduction of dioxygen.

The existence of a stable mixed-valence state, $CO^{III}Co^{II}$, was assumed to be a consequence of the very short distance that promotes a strong interaction between the two nearly equivalent Co centres. The mixed-valence complex exhibits a very high O_2 affinity and forms a stable O_2^-

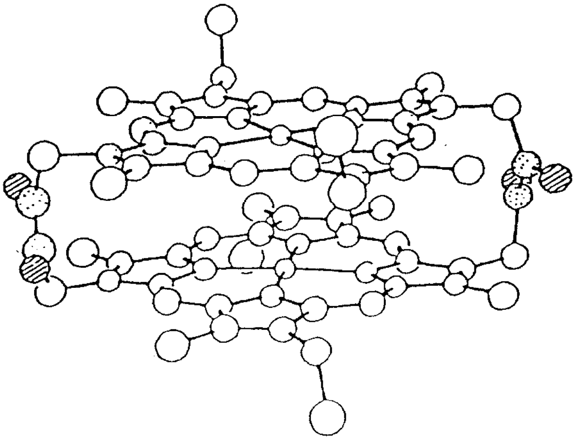

Fig. 54. Structure of [Co$_2$(**LXXI-4-1CONH**)] (from ref. 210).

(μ-superoxo) complex. On the basis of the shape of the EPR spectrum of the μ-superoxo complex, it was proposed that, in the four-atom-bridged dimer, dioxygen binds in a cis fashion (structure **A** in Fig. 55).

A theoretical study suggests that such a cis structure may exist if steric constraints allow it. However, the structure of Co$_2$(**LXXI-4-1CONH**) does not seem to support this hypothesis since enormous steric repulsion would result as the two porphyrin rings approach one another on one side to accommodate a cis-bound O$_2$ complex. Instead, it was suggested that dioxygen is bound between the Co centres parallel to the porphyrin rings either symmetrically (structure **B**) or asymmetrically (structure **C**). Structure **C** is attractive since it makes the coordinated O$_2$ molecule more susceptible to protonation.

The series of complexes capable of oxygen reduction was consequently enlarged by using 1,8-anthryldiporphyrin and 1,8-biphenylenediporphyrin.

The unique feature of this system is that the two porphyrin rings are anchored onto a rigid pillar such that the steric confines built into the system would prevent the two rings from rocking sideways to create a large lateral slippage. However, the two rings are still capable of bending back and forth along the ridge of the spacer groups. Such flexibility, presumably,

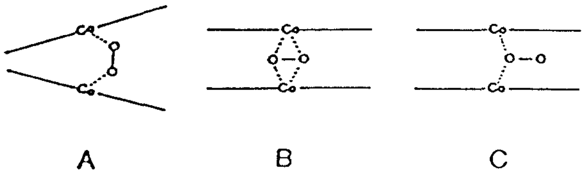

Fig. 55. The different modes of O$_2$ binding suggested for the μ-superoxo complex of a four-atom-bridged cofacial dimer (from ref. 210).

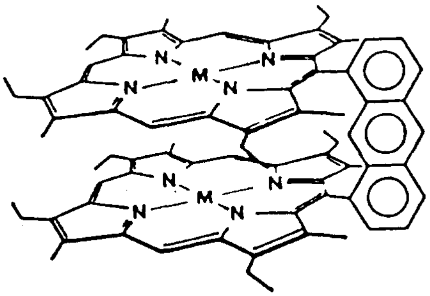

M_2(LXXII)

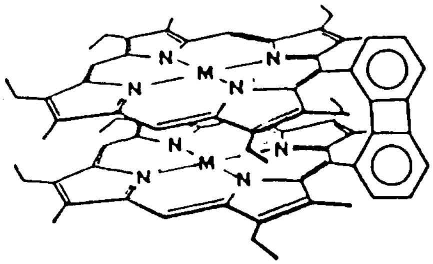

M_2(LXXIII)

M = $2H^+$, Co^{2+}

would make these two diporphyrins ideal dinuclear systems for trapping substrate between the metals. Indeed, the $Co^{II}Co^{II}$ dimers readily form the μ-peroxo species with dioxygen. A highly symmetric pattern in the EPR spectra of the μ-superoxo dimers was observed, in agreement with the suggestion of the correlation between the shape of the $Co–O_2–Co$ EPR signal and the electrocatalytical ability to mediate the $4e^-$ reduction of O_2 on a graphite surface; the well-resolved hyperfine lines would suggest these two dicobalt diporphyrins to be very good catalysts [22].

Rotating ring-disc voltammograms, obtained at a graphite electrode coated with these two complexes, in an oxygen-saturated 0.5 M aqueous trifluoroacetic acid solution, show that the O_2 reduction is comparable with [Co_2(**LXXI-4-1CONH**)]; these compounds distinguish themselves from the other porphyrins or diporphyrins in terms of $E_{1/2}$ for O_2 reduction as well as the ring current.

Thus there are many dicobalt diporphyrins, including [Co_2(**LXXI-5-1CONBu**)] and slipped [Co_2(**LXXI-4-1CONH**)], all capable of forming intercalated peroxo and superoxo complexes, but only [Co_2(**LXXI-4-1CONH**)], the anthracene and the biphenylene cobalt complexes are effective catalysts for the $4e^-$ reduction of O_2. Crystals have been obtained only for dinickel anthryldiporphyrin and dicopper diphenylene diporphyrin, and their X-ray structure has been solved in order to obtain information on the structural parameters which may be important for oxygen reduction [211].

In both complexes the porphyrin rings are not stacked over one another but rather have slipped with respect to each other giving an Ni–Ni distance of 4.566 Å and a Cu···Cu distance of 3.807 Å. The porphyrin rings of both complexes are markedly non-planar with the non-planarity being significantly less in the case of the copper(II) complex. The slip of the former leads to an average porphyrin plane-to-plane separation of 3.88 Å while that of the latter corresponds to about 3.45 Å.

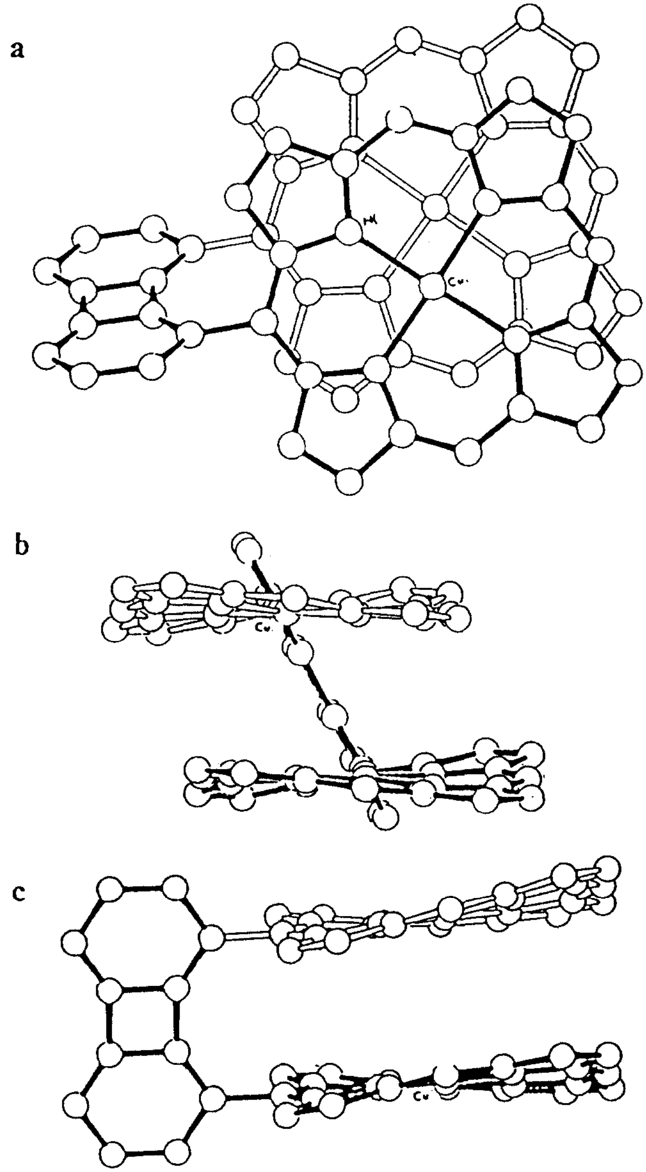

Fig. 56. Structure of dinickel anthryldiporphyrin complex excluding side groups. Views approximately mutually perpendicular: a, nearly perpendicular to porphyrin planes; b, parallel to *C*(*m*1)–*C*(*m*3) direction; c, parallel to *C*(*m*2)–*C*(*m*4) direction; ring 1 shaded (from ref. 211).

On the basis of these studies it was suggested that an exact metal–metal distance is not absolutely crucial for four-electron dioxygen reduction.

The metal separations in the two dimers differ by 0.76 Å yet do not seem to have much effect on their electrocatalytic performance. Although the use

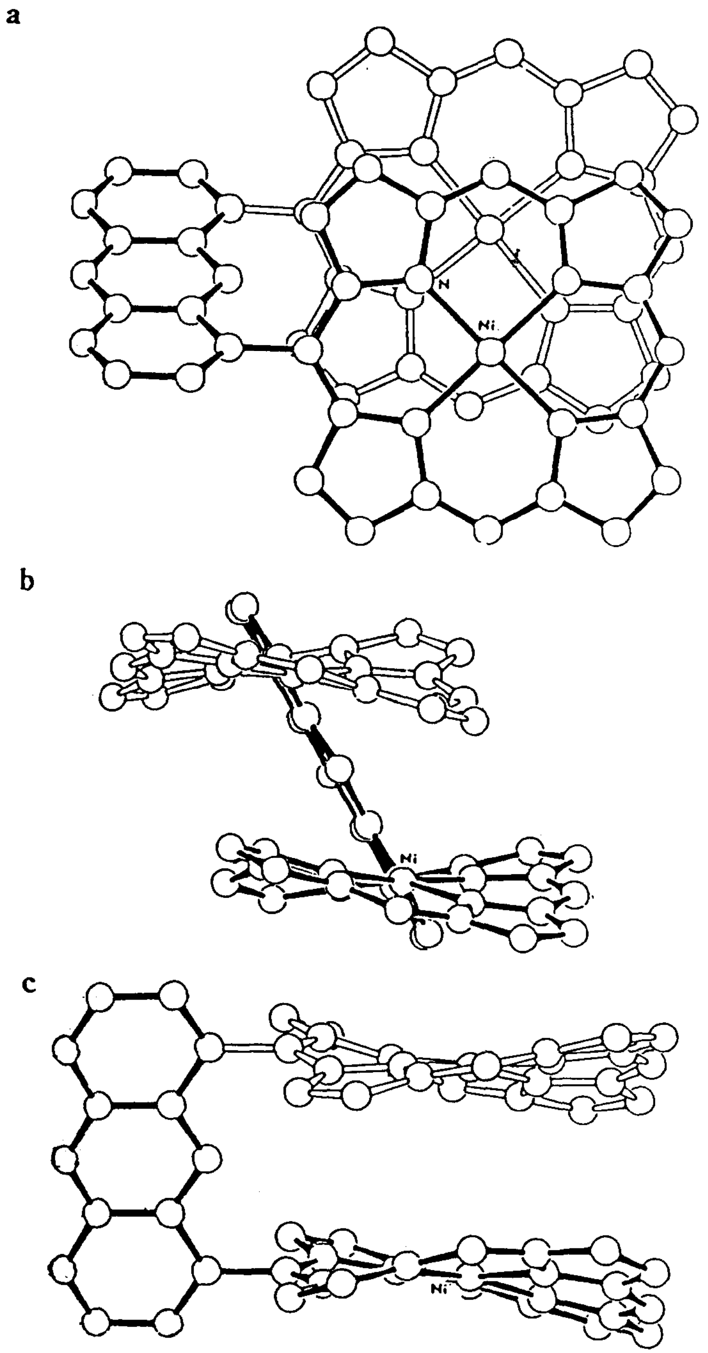

Fig. 57. Structure of dicopper diphenylene diporphyrin complex; details are as given in Fig. 56 (from ref. 211).

of such a distance obtained from non-cobalt complexes to discuss the behaviour of the cobalt catalyst on a graphite surface is admittedly not direct, there is, however, no evidence to prove that other metallodiporphyrins would adopt a grossly different structural configuration in another environment. In fact, an EPR spectroscopy study of six dicopper diporphyrin complexes in frozen solution showed that both the metal–metal separation and ring-to-ring distance obtained by the EPR method agree well with, although they are systematically higher than (but small compared with the above 0.76 Å difference), the reported crystallographic structures.

EPR spectroscopy was employed both in the characterization of the dicobalt dimers and as a means of monitoring their reaction with dioxygen. The dicobalt dimers exhibit spectra characteristic of exchange-coupled metal systems. For these species as well, the use of the EPR spectra to determine metal–metal distances was futile; estimates of D varied greatly for dicobalt and dicopper derivatives of the same dimeric ligand. It seems apparent that the use of EPR spectra to determine metal–metal separation in these systems may require more sophisticated analysis.

The EPR spectra of the oxygenated [CoPd(**LXXI-4**-1CONH)] and the more widely spaced [Co_2(**LXXI-6**-2CONH)] in the presence of an axial nitrogenous ligand are typical of 1:1 Co:O_2 adducts. The more tightly linked dicobalt dimers [Co_2(**LXXI-5**-1CONH)], [Co_2(**LXXI-5**-2CONH)] and [Co_2(**LXXI-4**-1CONH)], however, rapidly yielded EPR-silent samples upon exposure to limited amounts of oxygen, presumably owing to the formation of diamagnetic μ-peroxocobalt(III) species. Analogous results have been reported for Co_2(**LXXII**) and Co_2(**LXXIII**). In both series of complexes, these apparently diamagnetic complexes are readily oxidized by molecular iodine to give μ-superoxocobalt dimers, whose isotropic EPR spectra are consistent with the presence of a single unpaired electron, localized on the superoxo bridge, and interacting equally with the two $I = 7/2$ cobalt nuclei.

It should be noted that one dimer contains tertiary amide linkages, whereas others are linked with secondary amide groups. The rapid formation of the μ-peroxo species is thus not dependent upon the presence of an acidic NH proton, but rather upon the close proximity of the two cobalt centres. The marked contrast between the Pd–Co dimer [CoPd(**LXXI-4**-1CONH)] and the dicobalt species [Co_2(**LXXI-4**-1CONH)], which have identical ligands, illustrates this point.

The meso-linked dicobalt dimers [20] showed no tendency to form bridging peroxo complexes under comparable conditions. Even for dimers with linking groups as short as four atoms, only spectra typical of 1:1 Co:O_2 adducts were obtained.

On the basis of extensive experiments with modified electrodes carrying cyclic diporphyrin species the mechanism reported in Scheme 36 was

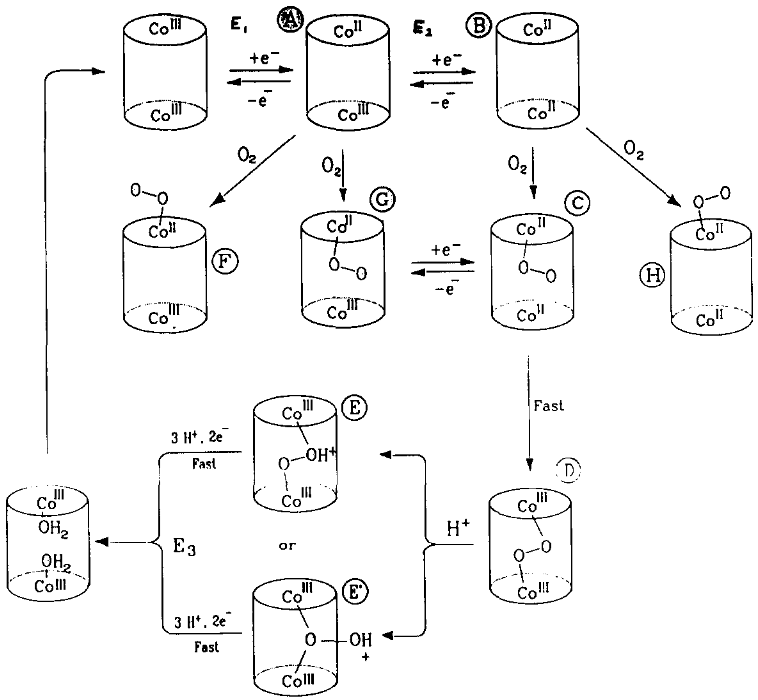

Scheme 36. Reaction mechanism of Co_2(LXXI-4-1CONH) with O_2 in aqueous acidic solution (from ref. 23).

proposed for acidic electrolytes. The cobalt centres cycle between the 2^+ and 3^+ oxidation states [23].

It was assumed for each molecule of Scheme 36 that the lower porphyrin ring is adsorbed on the graphite surface so that the axial ligand site on the corresponding cobalt centre is blocked. The first step in the catalytic sequence is depicted as the formation of an adduct between O_2 and a cobalt(II) centre in which the formal oxidation states of the reactants do not change.

The reduction of dioxygen is catalysed by Co_2(**LXXI-4**-1CONH) at potentials near the foot of the second reduction wave of the catalyst whose formal potential is labelled E_2 in Scheme 36. The first catalyst wave, at potential E_1, is not altered in position or magnitude by the presence of O_2. This insensitivity of the first wave to O_2 shows that the equilibrium constants for the formation of adducts such as Ⓕ and Ⓖ in Scheme 36 are not large. The same observation was made for the monomeric cobalt-porphyrin(I), whose single reduction wave precedes that for O_2 and is not affected by the presence of O_2.

The dioxygen complex that is catalytically active in the four-electron pathway is proposed to be Ⓒ, with the dioxygen molecule inside the cavity separating the two porphyrin rings, rather than Ⓕ or Ⓗ, because of the remarkable difference in behaviour between [Co$_2$(**LXXI-4**-1CONH)] and the analogous mononuclear cobalt porphyrin or [Co$_2$(**LXXI-5**-1CONH)], with only one additional atom in the bridging groups. Further support for this proposal is provided by the behaviour of [Co$_2$(**LXXI-3**-1CONH)] with only three atoms in the amide bridging groups. Coatings of [Co$_2$(**LXXI-3**-1CONH)] catalyse the reduction of O_2 to H_2O_2 but not to H_2O, a result to be expected according to Scheme 36 if the dioxygen molecule were unable to fit between the two porphyrin rings.

The formation of species Ⓔ, the (μ-hydroperoxo)dicobalt(III) complex, has been proposed in order to account for the unique ability of [Co$_2$(**LXXI-4**-1CONH)] to avoid the formation of H_2O_2. Scheme 36 includes the possibility that the hydroperoxide intermediate formed in the catalytic cycle leading to H_2O might be isomer Ⓔ' because analogous (μ-hydroperoxo)cobaltammine complexes are known, and in one case such a complex was shown to be a more reactive oxidant than the corresponding μ-peroxo isomer. The molecular geometric requirements for the formation of Ⓔ and Ⓔ' certainly differ, and evidence indicates that the catalytic effectiveness of the cofacial porphyrins is exceedingly sensitive to the relative configurations of the two cobalt centres. For example, although both Co$_2$(**LXXI-4**-1CONH) and Co(**LXXI − 4**-CONH$_2$), where the carbonyl groups of the amide linkages are directly bonded to the porphyrin ring, have been shown by ESR to form (μ-superoxo)dicobalt(III) complexes in non-aqueous media, they are not equally effective as dioxygen reduction catalysts: [Co$_2$(**LXXI-4**CONH)] catalyses the two-electron reduction instead of the four-electron reduction achieved by [Co$_2$(**LXXI-4**-1CONH)]. The ESR spectra of the two μ-superoxo complexes show dissimilarities that suggest less structural symmetry in the [Co$_2$(**LXXI-4**-1CONH)] complex. This apparent structural difference has major consequences in the catalytic behaviour of the two complexes.

In neutral and alkaline solutions the catalysed reduction of O_2 occurs at significantly more negative potentials and leads to H_2O_2 instead of H_2O. In highly alkaline solutions this change has been interpreted in the light of Scheme 36 as resulting from μ-hydroxo or μ-oxo groups competing successfully against O_2 molecules for the cavity in the catalyst, access to which is required for the four-electron reduction according to Scheme 36. The catalysed reaction may then be forced to proceed via species such as Ⓕ and Ⓗ in Scheme 36, which require more negative potentials for reduction of the coordinated O_2 and lead only to H_2O_2.

In neutral solutions, where the O_2 molecules may continue to be able to enter the cavity of the catalyst, the four-electron pathway may be blocked by the lack of protons necessary to convert the μ-peroxo intermediate Ⓓ into

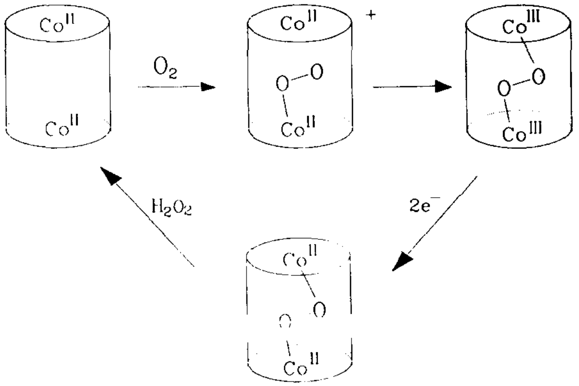

Scheme 37. Reaction mechanism of Co_2(LXXI-4-1CONH) with O_2 in aqueous neutral solution (from ref. 23).

species Ⓔ (or Ⓔ′), the only form of the intermediate that is reducible at the potential where it is generated. The coordinated peroxide is therefore released from the cavity as depicted in Scheme 37 instead of being further reduced. The resulting H_2O_2 accumulates in the solution because [Co_2(**LXXI-4**-1CONH)] is inert towards the reduction of H_2O_2 at any pH (Scheme 37).

Thus two factors have been reported to be most important in the catalytic cycle by which [Co_2(**LXXI-4**-1CONH)] reduces O_2 to H_2O without release of H_2O_2: (i) the two cobalt centres must be positioned so that the proposed μ-peroxo complex can be formed; (ii) protonation of the μ-peroxo bridge is required to render it reducible at the potential where it is formed. These two requirements are necessary but apparently not sufficient because the dicobalt cofacial porphyrin with four-atom bridges in the meso position of the porphyrin is not an effective catalyst for reduction of O_2 to H_2O. Furthermore, the electroreduction in acidic media of stable (μ-peroxo)dicobalt complexes of some other macrocyclic ligands produces cobalt(II) and H_2O_2, not H_2O. Thus the μ-peroxo group in the complex formed by Co_2(**LXXI-4**-1CONH) is apparently unusually reactive towards protonation and further reduction. The combination of steric and electronic constraints imposed simultaneously on the μ-peroxo group and the cobalt centres by the cofacial porphyrin ligand with four atoms in its amide bridges seems of crucial importance to its unique catalytic action.

On the basis of extensive experiments on dicobalt and mixed Co–metal cyclic diporphyrins, it was shown that as the response obtained in the oxygen reduction is quite sensitive to the nature of the second cation in the cofacial complexes, the interaction of both metal centres of the catalyst with the O_2 molecule is involved in the course of the catalysed reduction reaction.

The results obtained with the heterodinuclear cofacial porphyrins add support to the mechanism depicted in Scheme 36 in that the metal centre present in addition to cobalt is catalytically inert unless it is electroactive at potentials prior to that where species such as Ⓕ, Ⓖ, or Ⓗ are reduced to H_2O_2. For example, the [CoAg(**LXXI-4**-1CONH)] catalyst, with two electroactive metal centres, yielded currents well in excess of those corresponding to the two-electron reduction of O_2 and at potentials more positive than those for any catalyst except [Co_2(**LXXI-4**-1CONH)]. A reaction pathway leading to H_2O as the reduction product is apparently accessible with this catalyst, and it can be traversed in parallel with the pathway leading to H_2O_2 that is shared by all the catalysts. Since neither [Ag_2(**LXXI-4**-1CONH)] nor the analogous monomeric silver porphyrin show catalytic activity toward the reduction of O_2 or H_2O_2, the apparent activity of the reduced silver centre in [CoAg(**LXXI-4**-1CONH)] may reflect is ability to react with the unbound end of the O_2 molecule in the species corresponding to Ⓖ in Scheme 36 to produce a hydroperoxo intermediate that is reduced to H_2O at the electrode in the same potential range where the O_2 in the species corresponding to Ⓕ and Ⓗ are reduced to H_2O_2.

By contrast, the [CoFe(**LXXI-4**-1CONH)] complex, which also contains two electroactive metal centres, is no more active than the monomeric cobalt porphyrin because the electroactivity of the iron(III) centre lies at potentials well beyond those where the O_2 in the species corresponding to Ⓕ is reduced to H_2O_2.

Solutions of the cobalt porphyrin [Co_2(**LXXI-4**-1CONH)] in organic media have been studied in order to understand the role played by the catalyst and to characterize some of the intermediates (Scheme 38). The use of aprotic solvents permits separation of the redox, oxygen fixation and protonation steps [24]. A high oxygen affinity was found for the mixed-valence $Co^{II}Co^{III}$. The electrochemistry of the dicobalt(II) diporphyrin, [Co_2(**LXXI-4**-1CONH)], under a nitrogen atmosphere shows that the two cobalt(II) ions are oxidized separately.

A mixed-valence compound [$Co^{II}Co^{III}$(**LXXI-4**-1CONH)]$^+$ in which the cofacial porphyrin contains cobalt(II) and cobalt(III) is conveniently pro-

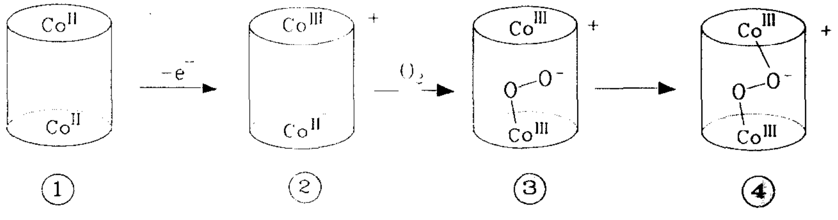

Scheme 38. Reaction mechanism of Co_2(**LXXI-4**-1CONH) with O_2 in organic solvents (from ref. 24).

duced by electrolysis. Although this mixed-valence dicobalt porphyrin seems to be very reactive, its solutions in benzonitrile or methylene chloride are chemically stable under an inert atmosphere and do not appreciably disproportionate.

In the absence of an axial ligand other than the solvent itself, $[Co_2$(**LXXI-4-1CONH**)] reacts slowly with oxygen, giving the putative μ-superoxo dicobalt(III) complex $[Co_2$(**LXXI-4-1CONH**)$(O_2)]^+$ (Scheme 38).

When a nitrogenous base was present the same oxygenated complex was obtained as soon as air or pure oxygen was bubbled through the solution, meaning that oxygen not only binds to the diporphyrin but also behaves as an oxidant.

The behaviour of the mixed-valence compound $[Co^{II}Co^{III}$(**LXXI-4-1CONH**)$]^+$ is different; in benzonitrile or methylene chloride solutions, in the absence of a potential axial ligand, it reacts instantaneously with oxygen. The UV–visible spectrum of a solution of $[Co^{II}Co^{III}$(**LXXI-4-1CONH**)$]^+$ prepared under a purified nitrogen atmosphere suffers a complete modification as soon as the solution is brought into contact with pure oxygen or air. When in contact with oxygen, the mixed-valence $[Co^{II}Co^{III}$(**LXXI-4-1CONH**)$]^+$, which is ESR silent at ambient temperature in methylene chloride, exhibited a spectrum typical of the μ-superoxo dicobalt complex $[Co_2$(**LXXI-4-1CONH**)$(O_2)]^+$, and was largely unchanged when a nitrogenous ligand (*N*-methylimidazole) was present in solution.

These results show that the coordination of oxygen by $[Co^{II}Co^{III}$(**LXXI-4-1CONH**)$]^+$ is fast and complete in the absence of an axial ligand other than the solvent itself.

The high reactivity of the mixed-valence cofacial porphyrin $[Co^{II}Co^{III}$ (**LXXI-4-1CONH**)$]^+$ was linked to the existence of the intermediate superoxo intermediate $[Co^{II}Co^{III}$(**LXXI-4-1CONH**)(O–O)] which spontaneously evolves to the μ-superoxo form $[Co^{II}Co^{III}$(**LXXI-4-1CONH**)$(O_2)]^+$ by interaction of the negative charge located on the O_2 moiety with the very close cobalt(III) centre.

Studies on the equilibrium affinity of this mixed-valence derivative for oxygen have shown that axial ligands have no measured effect on the magnitude of the O_2 binding constant, and water is a competitive inhibitor of O_2 binding [25].

A reversed reactivity was found with the planar dinuclear chelates bis(3,5-di-2-pyridyl-1,2,4-triazole)dicobalt dichloride $[Co_2$(**LXXIV**)$]Cl_2$ and 6,7,8,9,12,19,20,21,22,25-decahydro-8,8,10,21,23-hexamethyl-5,26,13,18-bis-(azo)-dibenz[1,2,6,7,12,13,17,18]oxaaza cyclodocosine, dicobalt(III)-μ-peroxotetranitrate $[Co_2$(**LXXV**)$O_2](NO_3)_4$ where reduction to water occurred in alkaline solution, whereas in acid solution only hydrogen peroxide was formed.

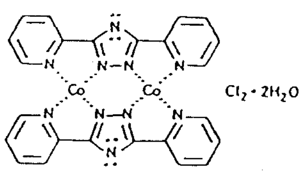

$Co_2(\underline{LXXIV})Cl_2.2H_2O$

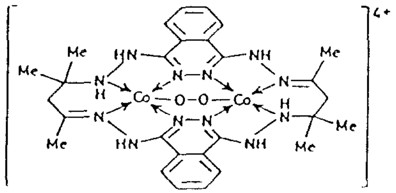

$[Co_2(\underline{LXXV})(O_2)](NO_3)_4$

It was proposed [26,27] that this phenomenon is related to the formal redox potentials of the cobalt centres; 4e$^-$ reduction seems to occur only if these potentials have values in the range 0.6–0.7 V vs. reference hydrogen electrode (RHE). The sandwich complexes fulfil this condition in acid solution. If it is assumed that the $Co^{(II)}$–$Co^{(III)}$ redox processes are pH independent, the potentials with respect to RHE in the same solution can shift 60 mV in the anodic direction per unit increase in pH. As a consequence, the potentials of the sandwich complexes will be too high in alkaline solution, leading to H_2O_2 production. Unfortunately, distinct redox peaks at the planar complexes in alkaline solution have not been detected but the experimental results indicate that these potentials have the appropriate values in this electrolyte. Likewise, these potentials will be too low in acid solution, leading, again, to H_2O_2 as end product. If this model is correct, it also implies that it is impossible to develop cobalt-containing catalysts that give 4e$^-$ reduction both in acid and in alkaline solution since the reduction of O_2 to H_2O can only occur in a limited pH range.

The observation that sandwich complexes produce virtually no H_2O_2, while the planar complexes yield considerable amounts, has been explained by the fact that the activity of the corresponding monomeric adducts differ in acid and alkaline solution. If O_2 is attached to one cobalt atom, the most probable rate-determining step is the formation of superoxide: $O_2 + e^- \rightarrow O_2^-$, leading to H_2O_2 as end product. This reduction to H_2O_2 is more reversible in alkaline solution because its rate-determining step is pH independent. At high pH the monomeric and dimeric pathways proceed at comparable rates, leading to mixed production of H_2O and H_2O_2. The dimeric pathway, however, seems to be pH dependent. The $E_{1/2}$ of this pathway with respect to the RHE therefore remains unchanged at different pH values. The $E_{1/2}$ of the monomeric pathway is pH independent and this $E_{1/2}$ vs. RHE shifts 60 mV in the anodic direction per unit increase in pH. In acid solution, the dimeric pathway is therefore much more favourable, so at low overpotential, there will be no competition between the two pathways, and only H_2O is formed. At potentials where the monomers also start to reduce oxygen, H_2O_2 can be formed. This is indeed observed experimentally.

It was also reported that the anthracene-linked diporphyrin, [Co(H_2-**LXXII**)] containing only one cobalt atom, was also able to reduce O_2 to H_2O, but at lower rates than the corresponding dicobalt complex. Although the second porphyrin ring does not contain a cobalt ion, the potential of the remaining cobalt has shifted to 0.6 V vs. RHE.

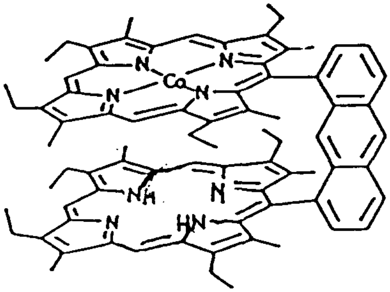

Co(H_2-**LXXII**)

For this complex the formation of an intramolecular adduct seems unlikely [28] since the molecule contains only one catalytic centre. Alternatively, an intermolecular μ-peroxo adduct was proposed. The lower activity of the monocobalt diporphyrin Co(H_2-**LXXII**) was explained by a lower number of active sites, since only relatively few dimeric species will be present on the surface. Such a decrease in the number of active sites shifts $E_{1/2}$ in the cathodic direction, but does not prevent the attainment of the limiting current. This hypothesis could be checked by repeating the experiment on "stress annealed" pyrolytic graphite. This approximates to a perfectly smooth surface. Assuming that the porphyrin rings of adsorbed molecules lie parallel to the surface, intermolecular Co–O–O–Co binding will be absent on this substrate, and consequently no $4e^-$ reduction should occur.

A different family of face-to-face bis(cyclidene) ligands have been synthesized and characterized as their nickel(II) complexes [212]. The ligands comprise pairs of 16-membered macrocylic ligating sites held in an approximate face-to-face orientation by various bridging moieties, including $(CH_2)_n$, where $n = 2$–8, *m*- and *p*-xylyl, and duryl. They are prepared by condensation reactions from monomeric macrocyclic precursor complexes. The same reactions also yield monomeric lacunar complexes in many cases. The dimeric bimetallic complexes were purified by fractional crystallization and/or chromatography (Scheme 39).

Dimers are the exclusive products of reactions utilizing relatively short linking chains, ethylene and trimethylene and relatively bulky aromatic

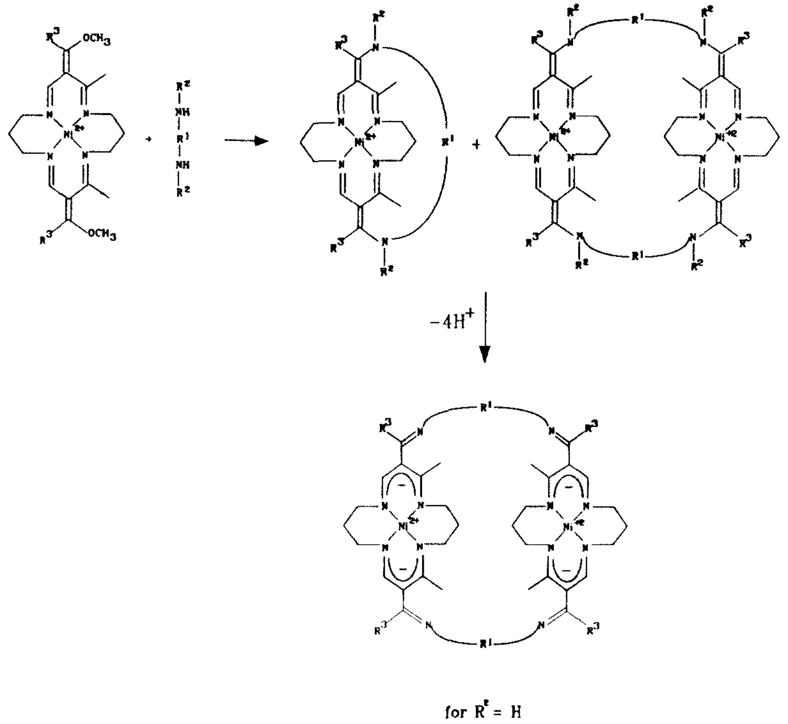

Scheme 39. Preparation of bis(cyclidene) complexes.

groups. The steric demands of the duryl group are sufficiently great to produce only dimers.

For these dimeric bimetallic complexes, four protons must be removed from the ligand to produce the neutral species. A simple procedure involving addition of 4 equivalents of $NaOCH_3$ in acetonitrile produces a deep red solution of the neutral complex. Evaporation and benzene extraction gives a clear red solution which on evaporation produces the desired neutral materials (Scheme 39).

On an NMR timescale the structure typically possesses two symmetry elements: a mirror plane and an inversion centre.

An X-ray determination of the *m*-xylene-bridged nickel(II) complex (Fig. 58) [212] shows that two macrocyclic moieties are linked by *m*-xylene bridges with the two halves of the molecule related by a crystallographic inversion centre. The xylyl groups are, by symmetry, parallel as are the macrocyclic N_4 planes. The square planar diamagnetic nickel(II) ions are 0.07 Å out of the N_4 planes. The six-membered rings containing the macrocyclic side-chain below the xylene groups are in boat conformations whereas the other six-membered rings are in the chair form. The metal ions

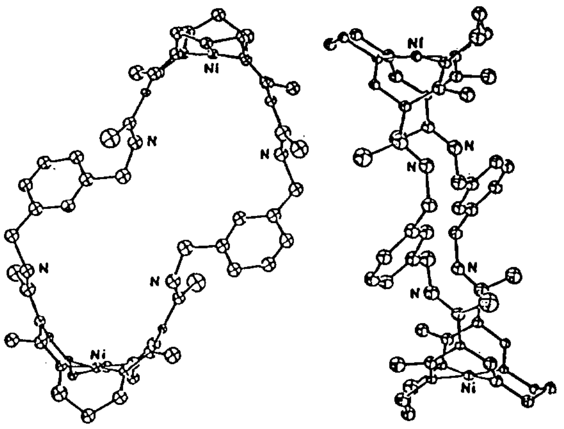

Fig. 58. Structure of the *m*-xylene-bridged dinickel(II) bis-(cylindrene) complex (from ref. 212).

are 13.6 Å apart, separated by an empty cavity that is from 3.87 to 6.18 Å wide.

Bis(cyclidene) dinuclear iron(II) [213] and cobalt(II) [214] complexes have been prepared by reaction of the analogous nickel(II) complexes with gaseous HCl or HBr, followed by addition of the appropriate iron(II) or cobalt(II) ion. For the cobalt(II) complexes, having chloride as counter-ion and *m*-xylene bridging groups, the X-ray structure [214] reveals a face-to-face configuration. The molecular unit (Fig. 59) is centrosymmetric and the two cyclidene centres and the two bridging *m*-xylene groups are constrained to be equivalent. The cyclidene groups are offset with respect to each other and the solvent methanol and the chloride ion form a pair of hydrogen-bonded bridges across the cavity, between NH groups of the ligand. Both cyclidene moieties adopt the chair conformation.

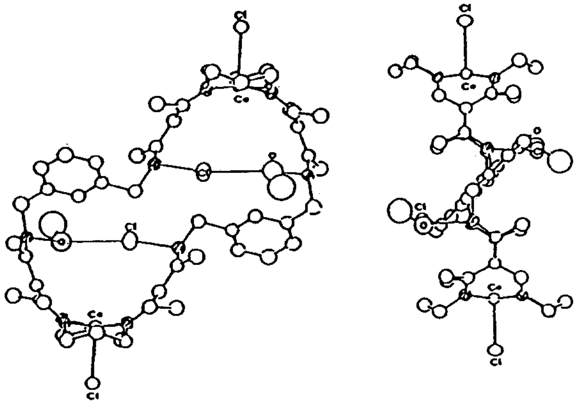

Fig. 59. Structure of the *m*-xylene-bridged dicobalt(II) bis-(cylindrene) complex (from ref. 214).

Although the vertical interplanar separation between the two cyclidene rings (N_4 plane) is only 10.70 Å, the large displacement (6.24 Å) of the two cyclidene units causes the two cobalt atoms to be separated by 12.38 Å.

Dicobalt(II) and diiron(II) complexes have flexible cavities that are large enough to preclude strong metal–metal interactions. This also eliminates the possibility that the two metal ions might simultaneously bind to the same O_2 molecule, favouring the binding of two O_2 molecules, one to each metal ion.

The diiron(II) complexes have been isolated as their $(PF_6)_4$ salts with a single neutral axial base per iron atom; the iron(II) centres are, however, six-coordinate and low spin in coordinating solvents [213]. These complexes interact with CO at room temperature, giving rise to $[Fe_2(CO)_2(B)_2(\text{cyclidene})]^{4+}$ (B = axial base). The CO is not sterically affected by the ligand framework as confirmed by the CO stretching frequencies of the adducts with a pyridine axial base (at about 1970 cm^{-1}) and is quite insensitive to the nature of the bridging groups linking the two macrocycles.

Exposure of these carbonyl complexes to very high vacuum for extended periods of time causes only slight CO loss while UV light accelerates this process.

Interaction of O_2 with iron(II) dinuclear cyclidenes has been explained according to the reaction

$$[Fe_2(L)_2(B)_2(S)_2]^{4+} + O_2 \xrightarrow{\text{slow}} \text{RP} \xrightarrow{\text{slow}} \text{FP}$$

The slow production of the reversibly formed products (RP) is followed by the still slower conversion of the RP into the final products (FP) by an irreversible process.

It was suggested that FP is most probably a μ-oxo oligomer of the RP formed in the basic medium. Since the EPR spectrum of this oxidized iron(III) species shows no absorption for either high or low spin iron(III), an antiferromagnetically coupled iron(III) oligomer of the μ-oxo dimer type was postulated.

The reversibly formed products (RP) in protic media (1:1 base–water) are the low spin solvated iron(II) complex and peroxide. It was also suggested that the two iron centres of the dinuclear species act totally independently of one another with superoxide as the logical reaction intermediate and peroxide as the eventual product of its disproportionation, in protic media.

Thus dinuclear iron(II) cyclidene complexes undergo a net two-electron reaction with dioxygen, generating superoxide or peroxide (depending on solvent) and the complex where the two ions are identical in the low spin trivalent state. This net redox reaction can be partially reversed by the removal of O_2, by N_2 flushing or dynamic vacuum, in mixed aqueous solvents at O°C. In this way alone the process resembles reversible dioxygen adduct formation. This behaviour is contrasted with true dioxygen adduct formation by a related mononuclear five-coordinate iron(II) complex.

The bis(cyclidene) dicobalt(II) complexes are rapidly autoxidized at room temperature, and no evidence is found for O_2 adducts. Studies at lower temperatures with the *m*-xylene-bridged dicobalt system, show that some 1:1 O_2 adduct does indeed form (Scheme 40), (eqns. (1) and (2)) and that the adduct is associated with the expected large oxygen affinity (since it saturates so readily at so low a partial pressure of O_2).

Further, the complex autoxidizes (Scheme 40, eqns. 3–5) to a diamagnetic species very rapidly, even at −40°C, since so much of the cobalt has become

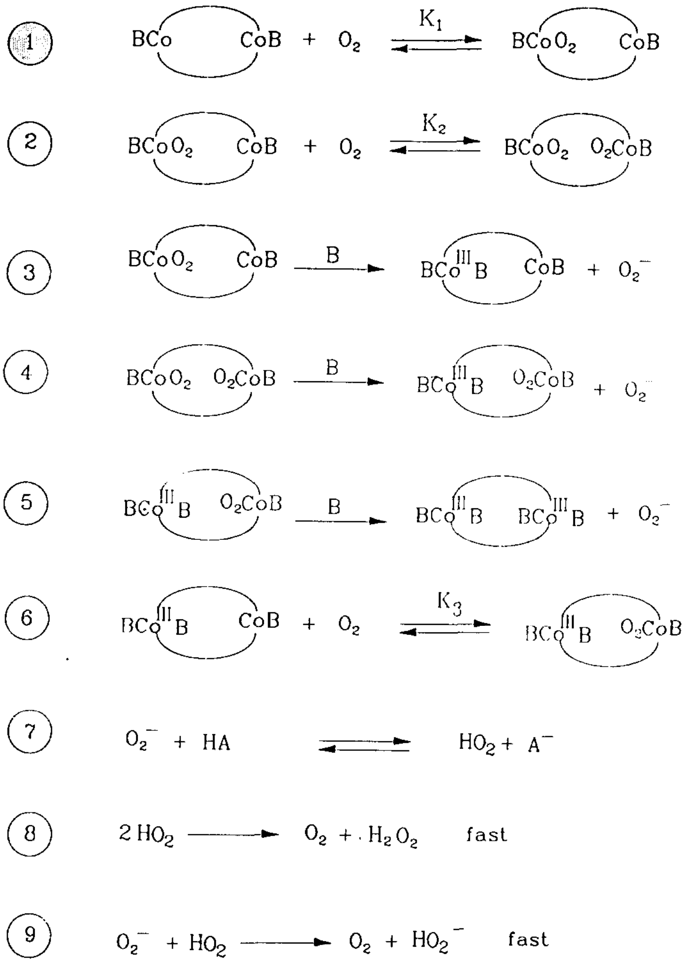

Scheme 40. Reaction mechanism of bis(cyclidene) cobalt(II) complexes with O_2 (from ref. 214).

ESR silent so quickly. The dicobalt(II) complex with relatively short dimethylene bridges behaves quite differently. In the absence of the *N*-methylimidazole axial ligand, the binding of O_2 is completely reversible at low temperatures and the oxygen affinity is modest, as would be expected. Only eqns. 1 and 2 of Scheme 40 are required to describe this behaviour. In contrast, in the presence of the axial base, irreversible oxidation of one of the cobalt(II) centres is extremely rapid and there is some evidence that the second centre persists in the form of its oxygen adduct. Thus, this system was described in terms of eqns. 1, 2, 4, and 6 of Scheme 40.

The variation in Co–Co distance is responsible for a number of observed differences in spectroscopic and chemical properties.

An unusual form of host–guest complexing has been demonstrated in which 4,4′-bipyridine is both enclosed in the cavity of the bis(cyclidene) complex $[Co_2(\mathbf{LXXVI})(4,4'\text{-bipyridine})]^{4+}$ and coordinated to the two metal atoms, serving as a bridging group and thereby greatly enhancing the metal–metal interaction between the two cobalt(II) atoms [214].

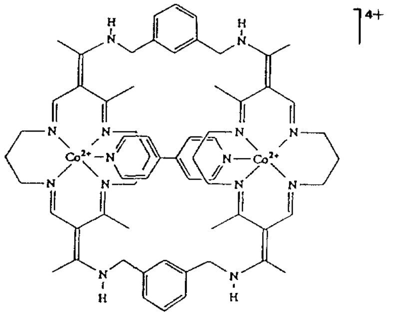

$[Co_2(\mathbf{LXXVI})(4,4'\text{-bipyridine})]^{4+}$

One-electron oxidation of this 4,4′-bipyridine-bridged dicobalt complex produces the $Co^{(II)}$–$Co^{(III)}$ mixed-valence species whose dioxygen reactions have been interpreted, on the basis of spectral and ESR data according to Scheme 41.

The gradual addition of O_2 to a solution of this complex in acetonitrile at $-38°C$ yields the spectral changes due to the formation of the oxygen adduct; the process is reversible under these conditions. However, two distinct isosbestic points, at 482 nm for $P_{O2} = 0$–37.1 Torr and 485 nm for higher pressures (up to 742.3 Torr) have been detected. ESR spectra show that the complex cobalt(II) forms a diamagnetic, ESR-silent 2:1 adduct at low O_2 partial pressures (P_{O2} range, 0–19 Torr), while at an O_2 pressure above 37 Torr substantial amounts of the 1:1 Co/O_2 adduct are formed.

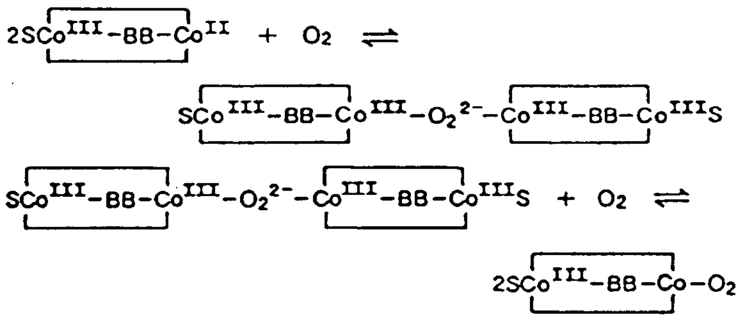

Scheme 41. Reaction of $Co_{II}Co_{III}$(LXXXVI)(4,4'-bipyridine) with O_2 (from ref. 214).

The behaviour of the mixed-valence guest-bridged complex as a fairly stable oxygen carrier is in marked contrast with that of the parent dinuclear host–guest complex itself; the dicobalt(II) species rapidly suffers autoxidation of one of its two cobalt centres. The marked resistance toward autoxidation of the mixed-valence product can be rationalized in terms of the low electron density at cobalt(II) due to the electron withdrawal by the cobalt(III) centre via the bridging base. That is, the effect is due to the presence of a very special axial base.

J. BIFUNCTIONAL COMPLEXES FOR CO_2 ACTIVATION

Reversible coordination of CO_2 at dinuclear complexes has been studied [215,216]. The precursor dinuclear complexes have been obtained by reaction of a suspension of Co(salen) with alkali metals (Li, Na) to give deep green THF solutions from which crystals of [Co(salen)M(THF)$_n$] have been isolated [216]. The degree of solvation of these dinuclear complexes depends on the nature of the alkali cation, the solvents used, and the crystallization rate. The M/Co ratio must be carefully controlled, since cobalt, over a much longer time and with a higher M/Co ratio, can be further reduced, while a M/Co ratio lower than unity gives mixed-valence Co^ICo^{II} polynuclear complexes. Their very low solubility, however, prevents a possible contamination of the final cobalt(I) complexes [215,216].

The structure of [Co(salen)Na(THF)] consists of Na^+ ions at special positions on twofold axes surrounded by six oxygen atoms provided by Co(salen) and THF molecules. These distorted octahedra share opposite faces to form infinite chains running along the *a* direction (Fig. 60). In the repetitive unit, $[Co_2(salen)_2Na(THF)_2]$ of this polymeric structure, both Co(salen) and THF molecules bridge contiguous Na^+ ions. The overall structure can be described in terms of Co(salen) layers, with Na^+ cations

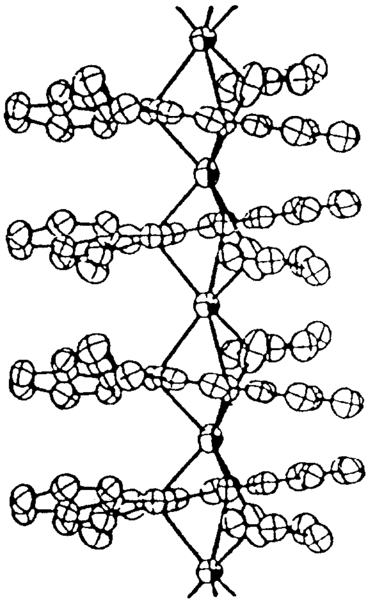

Fig. 60. Polymeric structure of [(Co(salen)Na(THF)]$_n$ (from ref. 216).

interposed between the layers. The coordination of salen around cobalt(I) is nearly planar.

In the structure of [Co(salen)Li(THF)$_{1.5}$] there are two different molecular complexes [Co(salen)Li(THF)$_2$] (Fig. 61) and [Co(salen)$_2$Li$_2$(THF)$_2$] (Fig. 62).

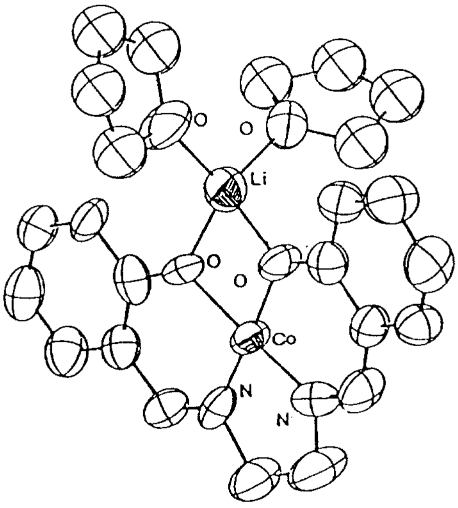

Fig. 61. View of the bimetallic unit [(Co(salen)Li(THF)$_2$] present in Co(salen)Li(THF)$_{1.5}$ (from ref. 216).

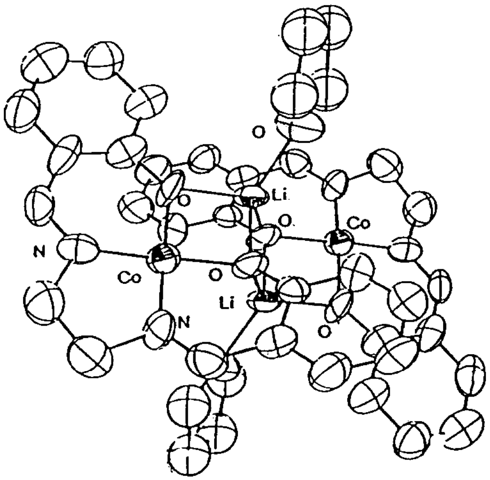

Fig. 62. View of the tetranuclear unit $(Co_2(salen)_2Li_2(THF)_2$ present in $Co(salen)Li(THF)_{1.5}$ (from ref. 216).

In the first complex the Li^+ coordinates four oxygen atoms provided by a Co(salen) group and two THF molecules, while the second complex is a dimer of the Co–Li bimetallic unit, where Li^+ coordinates the oxygen atom of one THF molecule and two oxygen atoms from Co(salen), while the fourth oxygen provided by the Co(salen) group is related to the first one through an inversion centre.

Less constraint in the structures of both lithium complexes gives rise to better square planar arrangements of the salen ligand around cobalt. The coordination sphere around lithium is nearly tetrahedral [216].

These complexes and the similar [Co(pr-salen)M(THF)] (H_2-pr-salen is the Schiff base derived by condensation of *o*-hydroxyphenyl-*n*-propyl ketone and ethylenediamine) react in THF with CO_2 at room temperature to produce [Co(salen)M(CO_2)]. These complexes release CO_2 in vacuo, giving back the starting green solution; this absorption–desorption cycle can be repeated several times and has also been observed in the solid state [215,217].

Crystals of the potassium complex $[Co(pr\text{-}salen)K(CO_2)THF]_n$, which displays four sharp IR bands due to the bound CO_2 at 1650, 1280, 1215 and 745 cm^{-1}, have been isolated working in a CO_2 atmosphere. The structure consists of parallel chains running along the *c* direction (Fig. 63) [217].

The chains could be described as being generated by the octahedra around K(1) and K(2) sharing opposite verticals through one of the CO_2 oxygen atoms. The two independent potassium ions in the asymmetric unit are at special positions on the inversion centre and on twofold axes respectively. The six oxygen atoms around K(1) are provided by two CO_2

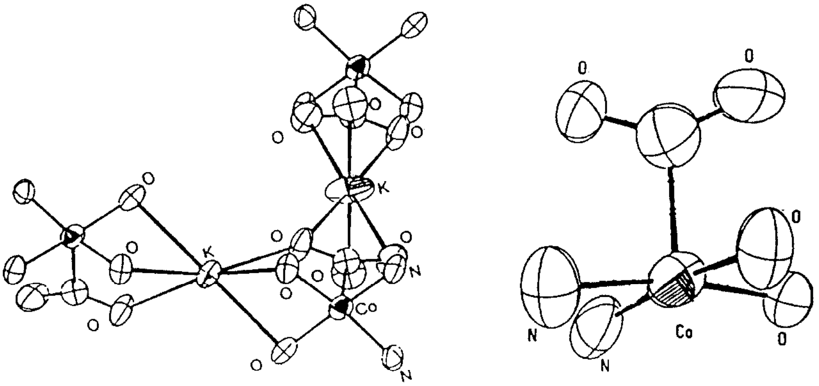

Fig. 63. A view showing the repetitive unit of (a) the polymeric $[Co(pr\text{-}salen)K(CO_2)THF]_n$ and (b) the coordination sphere around cobalt (from ref. 217).

and two THF molecules, while K(2) is bound to two bidentate pr-salen units and to two oxygen atoms of two CO_2 molecules. Each CO_2 molecule shares one oxygen between two K^+ ions. The structural determination confirms the bimetallic nature of the complex, where the Schiff base acts as a dinuclear ligand bringing cobalt and potassium ions close together; the geometry around cobalt is nearly square pyramidal. Carbon dioxide, which is C bonded to cobalt and O bonded to the two different K^+ ions, is bent, as expected from an approximated sp^2 geometry around carbon.

This structure proves both the presence and the special bonding mode of CO_2 interacting with three metal centres. This result strongly supports the hypothesis concerning the bifunctional activity of the starting Co(salen)-M-like systems; so, it was supposed that CO_2 fixation by complexes such as Co(salen)M involves concerted attack of the nucleophilic cobalt(I) on the electrophilic carbon of the CO_2, while the acid partner M^+ interacts with the basic oxygen atoms. Another interesting aspect of this chemistry is the very easy reversible formation and cleavage of a metal–carbon σ-bond.

Co(salen)Na reacts with CO_2 also in pyridine, with absorption of 1 mol CO_2 per cobalt atom, to give $[Cu(salen)Na(py)(CO_2)]$ which can be dried in vacuo without significant loss of CO_2; this indicates a stabilization of this complex by the axial ligand pyridine.

Reactions with different CO_2-like molecules, with electron-withdrawing substituents at the CO functionality, such as diethyl ketomalonate $(EtO_2C)_2CO$ and methyl pyruvate $(Me)(MeO_2C)_2CO$, have been carried out with the complex [Co(salen)Na(THF)] [218]. Diethyl ketomalonate has been used in organic synthesis as the equivalent of CO_2 [219].

[Co(salen)Na(THF)] reacts with diethyl ketomalonate and methyl pyruvate in THF at room temperature according to Scheme 42.

The bifunctional complex promotes the reductive coupling of methyl

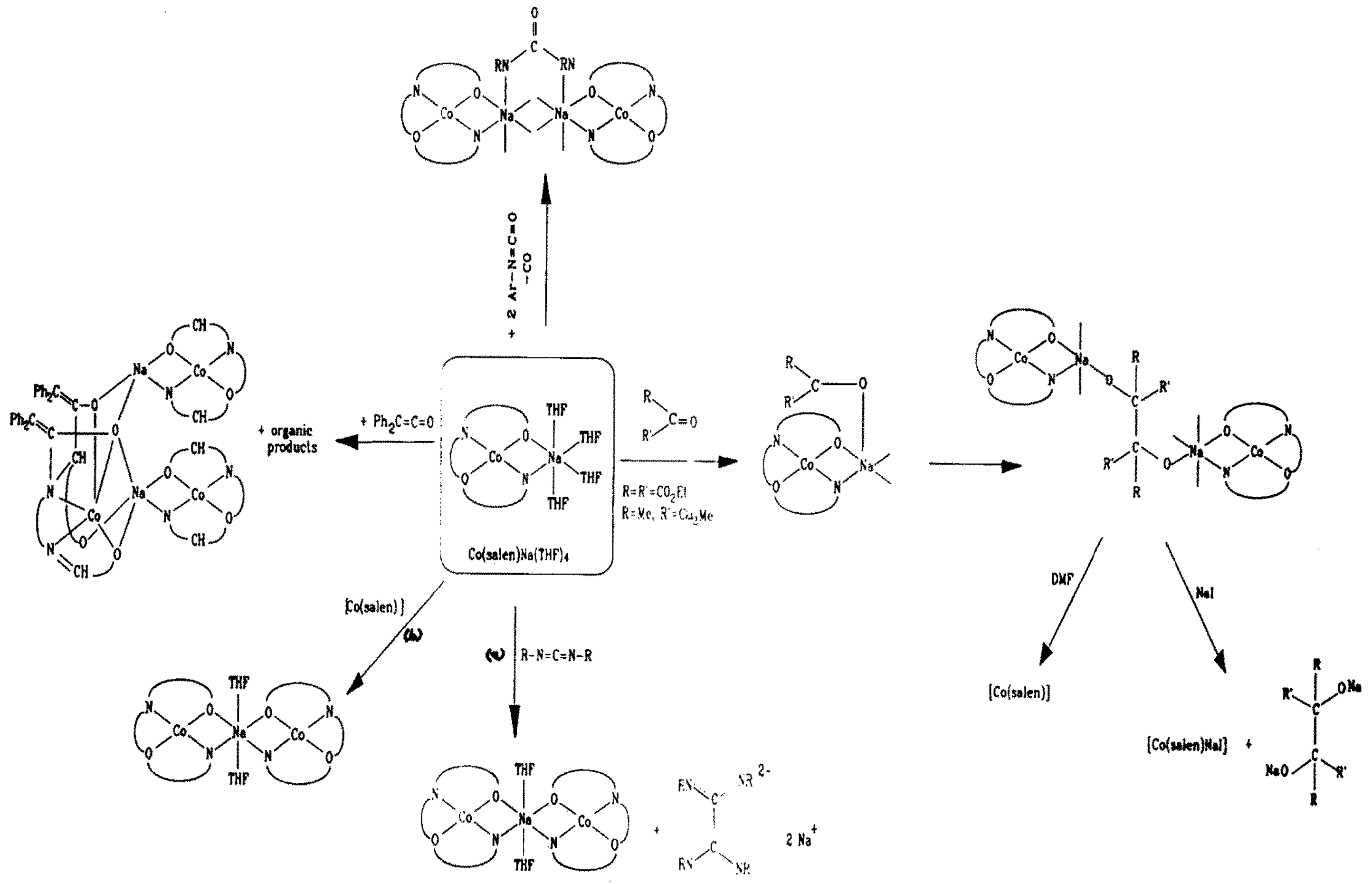

Scheme 42. Reactions of different CO_2-like molecules with Co(salen)Na(THF).

pyruvate, diethyl ketomalonate and *p*-tolylcarbodiimide via C–C formation. Methyl pyruvate is transformed in diastereoisomeric dimethyl dimethyltartrates and *p*-tolylcarbodiimide into tetra-*p*-tolyloxalamidine, while [Co(salen)Na(THF)] is oxidized to [Co(salen)]. A free radical pathway involving the homolytic cleavage of a Co–C σ-bond has been suggested.

It is known that diphenylketene (DPK) has in common with CO_2 the cumulene structure, which reacts with electron-rich oxophilic metals at the –C=O functionality adding to the metal site in an η^2-C,O form and being formally reduced by two electrons [220,221]. [Co(salen)Na(THF)] reacts with diphenylketene in a 1:1 molar ratio according to Scheme 42.

$\{[Co(salen)]_2Na_2[Co(salen(DPK)_2)]\}3THF$ is a trinuclear cobalt(II) complex containing two intact [Co(salen)] units bridged by two Na^+ ions to a third cobalt(II) unit, where the metal is surrounded by a hexadentate ligand resulting from the addition of two DPK molecules to the same imino group of the salen ligand. The X-ray analysis shows a rather close proximity between the carbon atoms belonging to the two DPK molecules as in a precoupling stage (Fig. 64).

Any C–C bond formation between those carbon atoms will restore the original imino functionality in the salen ligand. This has been suggested as another plausible pathway leading to a C–C bond between CO_2-like molecules. Processes involving reactive sites and electron transfers from an aromatic polydentate ligand surrounding a metal are very important in compounds driving reactions of small molecules.

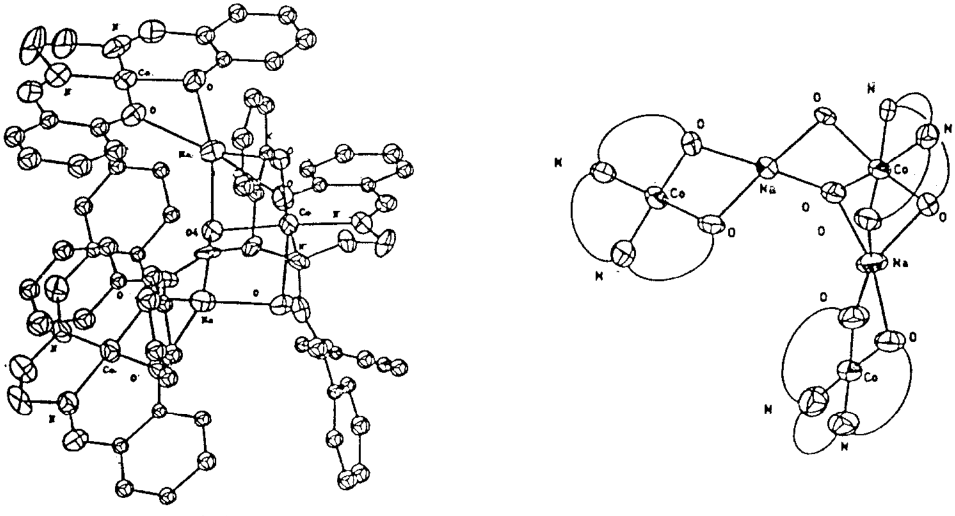

(a) (b)

Fig. 64. Structure of (a) $\{[Co(salen)]_2Na_2[Co(salen(DPK)_2)]\}_3 \cdot THF$ and (b) view of coordination polyhedra around cobalt and sodium ions (from ref. 218).

These results suggest how the polydentate ligand around the metal can drive reactions on CO_2-like molecules or on CO_2 itself, providing not only the assistance to the metal but also reactive sites on which the reaction can actually occur.

Organic isocyanates are among the most common cumulene structures used for mimicking CO_2, though they easily undergo, under various conditions, the reductive disproportionation according to the reaction [222,223]

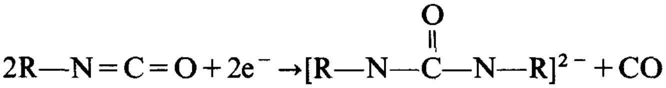

$$2R{-}N{=}C{=}O + 2e^- \rightarrow [R{-}N{-}\overset{O}{\overset{\|}{C}}{-}N{-}R]^{2-} + CO$$

This reaction was also observed when aryl isocyanates RNCO (R = 1-naphthyl, phenyl) were reacted with [Co(salen)(Na)(THF)] (Scheme 42).

Carbodiimides have a symmetric cumulene structure without oxygen atoms and very probably with different electron-acceptor properties. It was reported that carbodiimides undergo either the reductive disproportionation to dihydroguanidinium dianion and isocyanide in a process that seems to require the head-to-tail dimerization of the $>C{=}NR$ functionality or the reductive coupling to tetraalkyloxalamidinyl ligand [224–226]. Reaction of [Co(salen)Na(THF)] with *p*-tolylcarbodiimide (*p*-TCD) was carried out in refluxing THF and found to proceed with a 2:1 Co/*p*-TCD ratio.

The green crystalline solid [Co_2(salen)$_2$Na(THF)] and the tetra-*p*-tolyloxalamidinyl dianion was produced according to the reactions reported in Scheme 42.

The reductive coupling of *p*-TCD (pathway a) was promoted by cobalt(I) being oxidized to cobalt(II). [Co(salen)] was recovered, however, in the form of the mixed-valence $Co^{II}Co^{I}$ complex [(Co_2(salen))$_2$Na(THF)]. Pathway b leading to [Co_2(salen)$_2$Na(THF)$_2$] was proven by reacting an equimolar solution of Co(salen)Na(THF) and [Co(salen)] [227].

The structure of [Co_2(salen)$_2$Na(THF)$_2$] determined by X-ray analysis [227] (Fig. 65) shows that it is a neutral coordination compound of Na^+ having a pseudo-octahedral geometry, with two bidentate Co(salen) ligands trans to each other, while the trans axial positions are filled by two THF molecules. The neutrality of the complex requires one of the [Co(salen)] units to be formally mono anionic containing cobalt(I) and the other one neutral containing cobalt(II). The two [Co(salen)] units are, however, crystallographically identical, thus allowing [Co_2(salen)$_2$Na(THF)$_2$] to be defined as a mixed-valence $Co^{I}Co^{II}$ complex.

Even though the structure of [Co_2(salen)$_2$Na(THF)$_2$] shows a sterically accessible Co–Na unit, any of the reactivity associated with the same bifunctional unit in [Co(salen)Na(THF)$_4$] (e.g. with CO_2 and CO_2-like molecules) was observed.

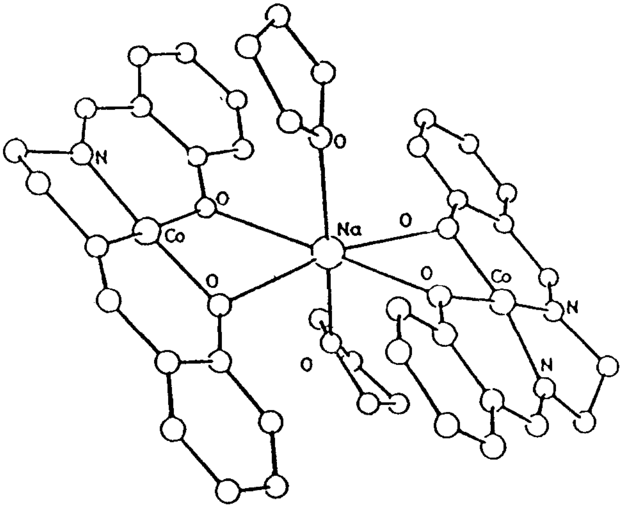

Fig. 65. Structure of $Co_2(salen)_2Na(THF)_2$ (from ref. 227).

K. CONCLUSIONS

Many dinuclear systems have been investigated in order to find useful systems for the activation of small molecules. In particular cobalt, iron and copper complexes have been studied both in reactions having industrial relevance (e.g. epoxidation) and having the potential to model the active sites in bimetalloproteins. The dinucleating ligands used have been modified as required, for example, from planar to tridimensional structures, by the introduction of fused multicycles, by the introduction of either rigid or flexible moieties, and so on. The range of complexes synthesized from these ligands has then given a broad spectrum of research opportunity. "Soft" donor atoms have been incorporated into the organic moieties in order to accommodate noble metal ions in close proximity and the importance of flexibility in the ligands has been demonstrated. The basic requirements for the catalysis of condensation processes at bimetallic centres may be summarized as:

(1) the site must be able to accommodate two separate reactants in close proximity;

(2) bond formation between the two reactants must occur; and

(3) the newly formed species must be released to permit a repetition of the cycle.

Using these procedures the catalytic hydration of nitriles to amides has been achieved.

In several systems it has been shown that activation/deactivation of small molecules such as oxygen or carbon monoxide occurs in cycles which may be repeated numerous times. It was possible to propose, for some systems, the formation of hydroperoxide intermediates. These propositions were confirmed by X-ray studies. The peroxy- and hydroperoxide complexes can be used to oxidize Ph_3P and RSR to the corresponding oxides.

As metal hydroperoxo species are important for oxidation of hydrocarbons it is necessary that studies of such systems be further developed. Information retrieved from such studies would also be of value in assisting in an understanding of the functioning of metalloenzymes.

The application of modified electrodes to electrocatalysis is an exciting area with so many possible avenues to success that one can predict that important scientific, technological and economic advances will come from this technique. The current stress on oxygen is appropriate and provides a practical focus, but important electrocatalytic processes can also be envisioned for the fixation of nitrogen or for the use of other small molecules, such as carbon dioxide, carbon monoxide or methane.

The efficacy of heterodinuclear complexes in the asymmetric activation of CO_2 and related molecules has been demonstrated. In these studies the concept of the use of non-innocent ligands surrounding the heterodinuclear entity was introduced wherein the ligand provides not only necessary support for the metal ions but also reactive sites on which the reactions can occur.

In conclusion it can be stated that excellent synthetic work leading to the preparation of dinuclear species which can offer a necessary basis for understanding the activation of small molecules has been achieved.

Of particular interest is the possibility offered to vary parameters such as the metal···metal distance, the intermetallic interaction, the type of metal centre and its geometry, and the flexibility of ligands in order to correlate them with any ability to initiate activation processes. In many cases quasi-reversible reactions have been demonstrated indicating the catalytic potential of the complexes. Results concerning the oxidation of phenols, the epoxidation of olefins, and the generation of sulphoxides and phosphine oxides have been published. It is certain that many efforts will be made in the future in order to gain further insight into the nature of such reactions and to apply this knowledge to the reproduction of reactions of biological and industrial significance.

REFERENCES

1 D.E. Fenton, in A.G. Sykes (Ed.), Advances in Inorganic and Bioinorganic Mechanisms, Vol. 2, Academic Press, London, 1983 p. 187.

2 K.D. Karlin and J. Zubieta, Copper Coordination Chemistry and Biochemistry: Biochemical and Inorganic Perspectives, Adenine Press, 1983.

3 K.D. Karlin and J. Zubieta, Biological and Inorganic Copper Chemistry, Vols. 1,2, Adenine Press, 1986.

4 D.E. Fenton, U. Casellato, P.A. Vigato and M. Vidali, Inorg. Chim. Acta, 95 (1984) 187.

5 D.E. Fenton, U. Casellato, P.A. Vigato and M. Vidali, Inorg. Chim. Acta, 62 (1982) 57.

6 R.D. Willet, D. Gatteschi and O. Kahn, Magneto-structural Correlations in Exchange Coupled Systems, Nato ASI Series, Reidel, Dordrecht, 1983.

7 U. Casellato, P.A. Vigato, D.E. Fenton and M. Vidali, Chem. Soc. Rev., 8 (1979) 199.

8 S.E. Groh, Isr. J. Chem., 15 (1976/1977) 277.

9 F.L. Urbach, in H. Sigel (Ed.), Metal Ions in Biological Systems, No. 13. Copper Proteins, Marcel Dekker, Basle, 1981, p. 73 and references cited therein.

10 E.I. Solomon, Dinuclear copper active site, in T.G. Spiro (Ed.), Copper Proteins, Wiley-Interscience, New York, 1981, Chapter 2.

11 D.M. Dooley, R.A. Scott, E. Ellinghaus, E.I. Solomon and H.B. Gray, Proc. Natl. Acad. Sci. U.S.A., 75 (1978) 3019.

12 D.J. Spira, M.E. Winkler and E.I. Solomon, Biochem. Biophys. Res. Commun., 107 (1982) 721.

13 C.D. LuBien, M.E. Winkler, T.J. Thamann, R.A. Scott, M.S.Co, K.O. Hodgson and E.I. Solomon, J. Am. Chem. Soc., 103 (1981) 7014.

14 M.E. Winkler, D.J. Spira, C.D. LuBien, T.J. Thamann and E.I. Solomon, Biochem, Biophys. Res. Commun., 107 (1982) 727.

15 J.A. Fee and R.G. Briggs, Biochim. Biophys. Acta, 400 (1975) 439.

16 J.A. Fee, J. Biol. Chem., 248 (1973) 4229.

17 (a) L. Calabrese, D. Cocco and A. Desideri, FEBS Lett., 106 (1979) 142.
(b) J.M. Latour, Bull. Chem. Soc. Fr., (1988) 508.

18 E.L. Mutterties, T.N. Rhodin, E. Band, G.F. Brucker and W.R. Pretzer, Chem. Rev., 79 (1979) 91.

19 E.C. Niederhoffer, J.H. Timmons and A.G. Martell, Chem. Rev., 84 (1984) 137.

20 J.P. Collman, A.O. Chong, G.B. Jameson, R.T. Oakley, E. Rose, E.R. Schmittou and J.A. Ibers, J. Am. Chem. Soc., 103 (1981) 516.

21 M.H. Hatada, A. Tulinski and C.K. Chang, J. Am. Chem. Soc., 102 (1980) 7115.

22 C.K. Chang, H.Y. Liu and I. Abdalmuhdi, J. Am. Chem. Soc., 106 (1984) 2725.

23 R.R. Durand, Jr., C.S. Bencosme, J.P. Collman and F.C. Anson, J. Am. Chem. Soc., 105 (1983) 2710.

24 Y. Le Mest, M. L'Her, J. Courtot-Coupez, J.P. Collman, E.R. Evitt and C.S. Bencosme, J. Chem. Soc. Chem. Commun., (1983) 1286.

25 Y. Le Mest, M. L'Her, J.P. Collman, N.H. Hendricks and L. McElwee-White, J. Am. Chem. Soc., 108 (1986) 533.

26 A. van der Putten, A. Elzing, W. Visscher and E. Barendrecht, J. Chem. Soc. Chem. Commun., (1986) 477.

27 E. Yeager, Electrochim. Acta, 29 (1984) 1527.

28 H.Y. Liu, I. Abdalmuhdi, C.K. Chang and F.C. Anson, J. Phys. Chem., 89 (1985) 665.

29 J.A. Fee, in H. Sigel (Ed.), Metal Ions in Biological Systems, No. 13. Copper Proteins, Marcel Dekker, Basle, 1981, p. 259.

30 H.M. Steinman, V.R. Naik. J.L. Abernethy and R. Hill, J. Biol. Chem., 249 (1974) 7326.

31 J.S. Richardson, K.A. Thomas, B.H. Rubin and D.C. Richardson, Proc. Natl. Acad. Sci. U.S.A., 72 (1975) 1349.

32 W.P.G. Gaykema, A. Volbeda and W.G.J. Hol, J. Mol. Biol., 187 (1985) 255.

33 (a) B.P. Gaber, R.D. Brown, S.H. Koenig and J.A. Fee, Biochim. Biophys. Acta, 271 (1972) 1.
(b) W. Boden, M.C. Holmes and P.F. Knowles, Biochem. Biophys. Res. Commun., 57 (1974) 845.

34 J.A. Fee and R.G. Briggs, in A.M. Michelson, J.M. McCord and I. Fridovic (Eds.), Superoxide and Superoxide Dismutase, Academic Press, London, 1977, p. 173.
35 R. Lontie and R. Witters, in H. Sigel (Ed.), Metal Ions in Biological Systems, No. 13. Copper Proteins, Marcel Dekker, Basle, 1981 p. 229.
36 E.I. Solomon, in T.G. Spiro (Ed.), Copper Proteins, Wiley Interscience, New York, 1981, Chapter 2.
37 R. Lontie and L. Vanquickenborne, in H. Sigel (Ed.), Metal Ions in Biological Systems, No. 3, Marcel Dekker, Basle, 1974, p. 183.
38 N.C. Eickman, R. S Himmelwright and E.I. Solomon, Proc. Natl. Acad. Sci. U.S.A., 76 (1979) 2094.
39 M. Sung Co, K.O. Hodgson, T.K. Eccles and R.J. Lontie, J. Am. Chem. Soc., 103 (1981) 984.
40 J.M. Brown, L. Powers, B. Kincaid, J.A. Larrabee and T.G. Spiro, J. Am. Chem. Soc., 102 (1980) 4210.
41 M.S. Co and K.O. Hodgson, J. Am. Chem. Soc., 103 (1981) 3200.
42 G.L. Woolery, L. Powers, M. Winkler, E.I. Solomon and T.G. Spiro, J. Am. Chem. Soc., 106 (1984) 86.
43 K.D. Karlin, R.W. Cruse, T. Gultneh, J.C. Hayes, J.W. McKown and J. Zubieta, in K.D. Karlin and J. Zubieta (Eds.), Biological and Inorganic Copper Chemistry, Vol. 2, Adenine Press, New York, 1985, p. 101.
44 M. Erecinska and D.F. Wilson, Arch. Biochem. Biophys., 188 (1978) 1.
45 D.C. Wharton, in G.L. Eichhorn (Ed.), Inorganic Biochemistry, Elsevier, Amsterdam, 1973, Chapter 27.
46 G. Palmer, G.T. Babcock and L.E. Vickery, Proc. Natl. Acad. Sci. U.S.A., 73 (1976) 2206.
47 C.H.A. Seiter, S.G. Angelos, Jr., and R.A. Perreault, Front. Biol. Energ., 2 (1978) 897.
48 C.A. Reed and J.T. Landrum, FEBS Lett., 106 (1979) 265.
49 P. Hemmerich, in J. Peisach, P. Aisen and W.E. Blumberg (Eds.), The Biochemistry of Copper, Academic Press, New York, 1966.
50 R.A. Scott, S.P. Cramer, R.W. Shaw, H. Bernert, and H.B. Gray, Proc. Natl. Acad. Sci. U.S.A., 78 (1981) 664.
51 T.D. Tullius, P. Frank and K.O. Hodgson, Proc. Natl. Acad. Sci. U.S.A., 75 (1978) 4069.
52 L. Powers, B. Chance, Y. Ching and P. Angiololło, Biophys. J., 34 (1981) 465.
53 J. Peisach, L. Powers, W.E. Blumberg and B. Chance, Biophys. J., 37 (1982) 396a.
54 S.J. Lippard, Angew. Chem. Int. Ed. Engl., 27 (1988) 344.
55 D.M. Kurtz, Jr., D.F. Shriver and I.M. Klotz, Coord. Chem. Rev., 24 (1977) 145.
56 R.E. Stenkamp and L.H. Jensen, in G.L. Eichhorn and L.G. Marzilli (Eds.), Advances in Inorganic Biochemistry, Vol. 1, North Holland, Amsterdam, 1979, Chapter 8.
57 J.S. Loehr and T.M. Loehr, in G.L. Eichhorn and L.G. Marzilli (Eds.), Advances in Inorganic Biochemistry, Vol. 1, Amsterdam, 1979, Chapter 9.
58 W.A. Hendrickson, in J.N. Lamy and J. Lamy (Eds.), Invertebrate O_2-binding Proteins, Marcel Dekker, Basle, 1981, p. 503.
59 W.A. Hendrickson, Nav. Res. Rev., 31 (1978) 1.
60 R.E. Stenkamp, L.C. Siecker and L.H. Jensen, Proc. Natl. Acad. Sci. U.S.A., 73 (1976) 349.
61 R.E. Stenkamp, L.C. Siecker, L.H. Jensen and J. Sanders-Loehr, Nature, 291 (1981) 263.
62 J.A. Ibers and R.H. Holm, Science, 209 (1980) 223.
63 C.L. Atkin, L. Thelander, P. Reichard and G. Long, J. Biol. Chem., 248 (1973) 7464.
64 L. Peterson, A. Graeslund, A. Ehrenberg, B.-M. Sjoeberg and P. Reichard, J. Biol. Chem., 255 (1980) 6706.
65 B.-M. Sjoeberg, T.M. Loehr and J. Sanders-Loehr, Biochemistry, 21 (1982) 96.
66 W.T. Elam, E.A. Stern, J.D. McCallum and J. Sanders-Loehr, J. Am. Chem. Soc., 104 (1982) 6369.
67 K. Lerch, in H. Sigel (Ed.), Metals in Biological Systems, No. 13. Copper Proteins, Marcel Dekker, Basle, 1981, p. 299.

68 K. Lerch, Proc. Natl. Acad. Sci. U.S.A., 75 (1978) 3635.

69 E. Pfiffner, C. Dietler and K. Lerch, in J.N. Lamy and J. Lamy (Eds.), Invertebrate O_2 binding Proteins, Marcel Dekker, Basle, 1981, p. 541

70 J.J. Villafranca, in T.G. Spiro (Ed.), Copper Proteins, Wiley-Interscience, New York, 1981 Chapter 7.

71 N.J. Blackburn, H.S. Mason and P.F. Knowels, Biochem. Biophys. Res. Commun., 595 (1980) 1275.

72 N.J. Blackburn and J. Sutton, Abstracts of 1st SUNYA Conversation in the Discipline; Inorganic and Biochemical Perspectives in Copper Coordination Chemistry, June 14, 1982.

73 A.K. Shiemke, T.M. Loehr and J. Sanders-Loehr, J. Am. Chem. Soc., 108 (1986) 2437.

74 R.E. Stenkamp, L.C. Siekes and L.H. Jensen, J. Am. Chem. Soc., 106 (1984) 618.

75 S. Sheriff, W.A. Hendricksm and J.L. Smith, J. Mol. Biol., 197 (1987) 273.

76 R.E. Stenkamp, L.C. Siekes, L.H. Jensen, J.D. McCallum and J. Sanders-Loehr, Proc. Natl. Acad. Sci. U.S.A., 82 (1985) 713.

77 W.T. Elam, E.A. Stern, J.D. McCallum and J. Sanders-Loehr, J. Am. Chem. Soc., 105 (1983) 1919.

78 J.M. Nocek, D.M. Kurtz, Jr., J.T. Sage, P.G. Debrunner, M.J. Maroney and L. Que, Jr., J. Am. Chem. Soc., 107 (1985) 3382.

79 M.J. Maroney, D.M. Kurtz, Jr., J.M. Nocek, L.L. Pearce and L. Que, Jr., J. Am. Chem. Soc., 108 (1986) 6871.

80 R.C. Reem and E.I. Solomon, J. Am. Chem. Soc., 109 (1987) 1216.

81 M.P. Woodward, D.S. Patil, R. Cannack, and H. Datton, Biochim. Biophys. Acta, 373, (1986) 273.

82 W.H. Armstrong, A. Spool, G.C. Papaefthymiou, R.B. Frankel and S.J. Lippard, J. Am. Chem. Soc., 106 (1984) 3653.

83 N. Kitajima, H. Fukui and Y. Moro-oka, J. Chem. Soc. Chem. Commun., (1988) 485.

84 J.B. Vincent, J.C. Huffman, G. Christom, Q. Li, M.A. Nanny, D.N. Hendrickson, R.H. Fong and R.H. Fish, J. Am. Chem. Soc., 110 (1988) 6898.

85 B. Reinhammer and B.G. Malmstroem, in T.G. Spiro (Ed.), Copper Proteins, Wiley-Interscience, New York, 1981, Chapter 3.

86 J.A. Fee, Struct. Bonding, 23 (1975) 1.

87 S.H. Laurie and E.S. Mohammed, Coord. Chem. Rev., 38 (1980) 279.

88 P.M. Colman, H.C. Freeman, J.M. Guss, M. Murata, V.A. Norris, J.A.M. Ramshaw and M.P. Venkatappa, Nature, 272 (1978) 319.

89 H.C. Freeman, in J.-P. Laurent (Ed.), Coordination Chemistry 21, Pergamon, New York, 1981.

90 E.T. Adman and L.H. Jensen, Isr. J. Chem., 21 (1981) 8.

91 A.E.G. Cass and H.A.O. Hill, CIBA Found. Symp. 79, Excerpta Medica, Amsterdam, 1980, p. 71.

92 C.D. Lu Bien, M.E. Winkler, T.J. Thamann, R.A. Scott, M.S. Co, K.O. Hodgson and E.I. Solomon, J. Am. Chem. Soc., 103 (1981) 7014.

93 J.A. Fee, Struct. Bonding, 23 (1975) 1.

94 A. Messerschmdt, A. Rossi, R. Ladenstein, R. Huber, M. Bolognesi, G. Gatti, A. Marchesini, R. Petruzzelli and A. Finazzi-Agrò, J. Mol. Biol., 206 (1989) 513.

95 R. Robson, Inorg. Nucl. Chem. Lett., 6 (1970) 125.

96 R. Robson, Aust. J. Chem., 23 (1970) 2217.

97 T.N. Sorrell, Tetrahedron, 45 (1989) 3.

98 M.G. Patch, V. McKee and C.A. Reed, Inorg. Chem., 26 (1987) 776.

99 R.L. Lintvedt, G. Ranger and C. Ceccarelli, Inorg. Chem., 24 (1985) 2359.

100 R.L. Lintvedt, G. Ranger and C. Ceccarelli, Inorg. Chem., 24 (1985) 456.

101 M.M. Rogic, M.D. Swerdloff and T.R. Demmin, in K.D. Karlin and J. Zubieta (Eds.), Copper Coordination Chemistry: Biochemical and Inorganic Perspectives, Adenine Press, New York, 1983, p. 259.

102 T.R. Demmin, M.D. Swerdloff and M.M. Rogic, J. Am. Chem. Soc., 103 (1981) 5795.

103 U. Casellato, S. Tamburini, P.A. Vigato, A. De Stefani, M. Vidali and D.E. Fenton, Inorg. Chim. Acta, 69 (1983) 45.

104 N. Oishi, Y. Nishida, K. Ida and S. Kida, Bull. Chem. Soc. Jpn., 53 (1980) 2847.
105 Y. Nishida, N. Oishi and S. Kida, Inorg. Chim. Acta, 46 (1980) L69.
106 Y. Nishida, N. Oishi, H. Kuramoto and S. Kida, Inorg. Chim. Acta, 57 (1982) 253.
107 S. Kida, H. Okawa and Y. Nishida, in K.D. Karlin and J. Zubieta (Eds.), Copper Coordination Chemistry: Biochemical Inorganic Perspectives, Adenine Press, New York, 1983, p. 425.
108 M. Vidali, U. Casellato, P.A. Vigato and R. Graziani, J. Inorg. Nucl. Chem., 38 (1976) 1455.
109 D.E. Fenton and S.E. Gayda, J. Chem. Soc. Dalton Trans., (1977) 2109.
110 D.E. Fenton, S.E. Gayda, U. Casellato, M. Vidali and P.A. Vigato, Inorg. Chim. Acta, 27 (1978) 9.
111 U. Casellato, D. Fregona, S. Sitran, S. Tamburini, P.A. Vigato and P. Zanello, Inorg. Chim. Acta, 95 (1984) 279.
112 K. Moore and G.S. Vigee, Inorg. Chim. Acta, 66 (1982) 125.
113 D. Bolus and G.S. Vigee, Inorg. Chim. Acta, 67 (1982) 19.
114 H. Okawa, S. Kida, Y. Muto and T. Tokii, Bull. Chem. Soc. Jpn., 45 (1972) 2480.
115 J. Grzybowski, P. Merrell and F.L. Urbach, Inorg. Chem., 17 (1978) 3078.
116 P. Sharma and G.S. Vigee, Inorg. Chim. Acta, 88 (1984) 29.
117 P. Sharma and G.S. Vigee, Inorg. Chim. Acta, 90 (1984) 73.
118 G. Hughes and R. Robson, Inorg. Chim. Acta, 35 (1979) 87.
119 T.E. Crossley, P. Davies, M. Louey, R. Robson and T.N. Huckerby, Inorg. Chim. Acta, 85 (1984) 199.
120 M. Lawey, P.D. Nichols and R. Robson, Inorg. Chim. Acta, 47 (1980) 87.
121 R. Robson, Inorg. Chim. Acta, 57 (1982) 71.
122 B.F. Hoskins and I.A.S. McDonald, Aust. J. Chem., 37 (1984) 725.
123 B.F. Hoskins and I.A.S. McDonald, Aust. J. Chem., 37 (1984) 1395.
124 T.E. Crossley, B.F. Hoskins, I.A.S. McDonald and R. Robson, Inorg. Chim. Acta, 111 (1986) 99.
125 M. Louey, C.J. McKenzie and R. Robson, Inorg. Chim. Acta, 111 (1986) 107.
126 C.J. McKenzie and R. Robson, Inorg. Chem., 26 (1987) 3615.
127 C.J. McKenzie and R. Robson, J. Chem. Soc. Chem. Commun., (1988) 112.
128 G. Schwarzenbach, G. Anderegg and S. Sallmann, Helv. Chim. Acta, 35 (1952) 1785.
129 B.P. Murch, P.D. Boyle and L. Que, Jr., J. Am. Chem. Soc., 107 (1985) 6728.
130 B.P. Murch, F.C. Bradley and L. Que, Jr., J. Am. Chem. Soc., 108 (1986) 5027.
131 U. Russo, M. Vidali, B. Zarli, R. Purrello and G. Maccarrone, Inorg. Chim. Acta, 120 (1986) L11.
132 R. Gagné, R.P. Kreh, J.A. Dodge, R.E. Marsh and M. McCool, Inorg. Chem., 21 (1982) 254.
133 Y. Nishida, M. Takeuchi, H. Shimo and S. Kida, Inorg. Chim. Acta, 96 (1984) 115.
134 Y. Nishida, K. Takahashi, H. Kuramoto and S. Kida, Inorg. Chim. Acta, 54 (1981) L103.
135 H.M.J. Hendriks, P.J.M.W.L. Birker, J. van Rijn, G.C. Verschoor and J. Reedijk, J. Am. Chem. Soc., 104 (1982) 3607.
136 N.C. Li, J.R. Tzou, S.W. Chen, S.M. Wang, Y.C. Chou, N.Y. Liang and H.J. Lin, Inorg. Chim. Acta, 138 (1987) 121.
137 J. van Rijn, J., Reedijk, M. Dartmann and B. Krebs, J. Chem. Soc. Dalton Trans., (1987) 2579.
138 M. Suzuki, H. Kanatomi and I. Murase, Chem. Lett. (1981) 1745.
139 A.S. Borovik and L. Que, Jr., J. Am. Chem. Soc., 110 (1988) 2345.
140 M. Suzuki, I. Ueda, H. Kanatomi and I. Murase, Chem. Lett., (1983) 185.
141 A. Avdeef and W.P. Schaefer, Inorg. Chem., 15 (1976) 1432.
142 M. Suzuki, H. Kanatomi and I. Murase, Bull. Chem. Soc. Jpn., 57 (1984) 36.
143 K.D. Karlin and Y. Gultneh, in J. Lippard (Ed.), Progress in Inorganic Chemistry, Vol. 35, Wiley, New York, 1987, p. 219.
144 K.D. Karlin, J.C. Hayes, Y. Gultneh, R.W. Cruse, J.W. McKown, J.P. Hutchinson and J. Zubieta, J. Am. Chem. Soc., 106 (1984) 2121.
145 K.D. Karlin, P.L. Dahlstrom, S.N. Cozzette, P.M. Scensney and J. Zubieta, J. Chem. Soc. Chem. Commun., (1981) 881.

146 K.D. Karlin, Y. Gultneh, J.P. Hutchinson and J. Zubieta, J. Am. Chem. Soc., 104 (1982) 5240.

147 K.D. Karlin, R.W. Cruse, Y. Gultneh, J.C. Hayes and J. Zubieta, J. Am. Chem. Soc., 106 (1984) 3372.

148 N.J. Blackburn, K.D. Karlin, M. Concannon, J.C. Hayes, Y. Gultneh and J. Zubieta, J. Chem. Soc. Chem. Commun., (1984) 939.

149 K.D. Karlin, Y. Gultneh, J.C. Hayes and J. Zubieta, Inorg. Chem., 23 (1984) 519.

150 K.D. Karlin, M.S. Haka, R.W. Cruse and Y. Gultneh, J. Am. Chem. Soc., 107 (1985) 5828.

151 K.D. Karlin, J. Shi, J.C. Hayes, J.W. McKown, J.P. Hutchinson and J. Zubieta, Inorg. Chim. Acta, 91 (1984) L3.

152 K.D. Karlin, M.S. Haka, R.W. Cruse, G.J. Meyer, A. Farooq, Y. Gultneh, J.C. Hayes and J. Zubieta, J. Am. Chem. Soc., 110 (1988) 1196.

153 K.D. Karlin, R.W. Cruse, M.S. Haka, Y. Gultneh and B.I. Cohen, Inorg. Chim. Acta, 125 (1986) L43.

154 K.D. Karlin, D.I. Cohen, R.R. Jacobson and J. Zubieta, J. Am. Chem. Soc., 109 (1987) 6194.

155 R.R. Jacobson, Z. Tyeklar, A. Farooq, K.D. Karlin, S. Liu and J. Zubieta, J. Am. Chem. Soc., 110 (1988) 3690.

156 N.J. Blackburn, R.W. Strange, A. Farooq, M.S. Haka and K.D. Karlin, J. Am. Chem. Soc., 110 (1988) 4263.

157 N. Kitajima, K. Fujisawa and Y. Moro-oka, J. Am. Chem. Soc., 111 (1989) 8975.

158 K.D. Karlin, Y. Gultneh, T. Nicholson and J. Zubieta, Inorg. Chem., 24 (1985) 3275.

159 K.D. Karlin, R.W. Cruse, Y. Gultneh, A. Farooq, J.C. Hayes and J. Zubieta, J. Am. Chem. Soc., 109 (1987) 2668.

160 J.E. Pate, R.W. Cruse, K.D. Karlin and E.I. Solomon, J. Am. Chem. Soc., 109 (1987) 2624.

161 N.J. Blackburn, R.W. Strange, R.W. Cruse and K.D. Karlin, J. Am. Chem. Soc., 109 (1987) 1235.

162 R.W. Cruse, S. Kaderli, C.J. Meyer, A.D. Zuberbühler and K.D. Karlin, J. Am. Chem. Soc., 110 (1988) 5020.

163 R.W. Cruse, S. Kaderli, K.D. Karlin and A.D. Zuberbühler, J. Am. Chem. Soc., 110 (1988) 6882.

164 K.D. Karlin, P. Ghosh, R.W. Cruse, A. Farooq, Y. Gultnech, R.R. Jacobson, N.J. Blackburn, R.W. Strange and J. Zubieta, J. Am. Chem. Soc., 110 (1988) 6769.

165 K.D. Karlin, R.W. Cruse and Y. Gultneh, J. Chem. Soc. Chem. Commun., (1987) 599.

166 P. Ghosh, Z. Tyeklar, K.D. Karlin, R.P. Jacobson and J. Zubieta, J. Am. Chem. Soc., 109 (1987) 6889.

167 K.D. Karlin, A. Farooq, Y. Gultnech, J.C. Hayes and J. Zubieta, Inorg. Chim. Acta, 153 (1988) 73.

168 T.N. Sorrell, C.C. Shen and C.J. O'Connor, Inorg. Chem., 26 (1987).

169 K.D. Karlin, B.I. Cohen, A. Farooq, S. Lin and J. Zubieta, Inorg. Chim. Acta, 153 (1988) 9.

170 L. Casella and L. Rigoni, J. Chem. Soc. Chem. Commun., (1985) 1668.

171 L. Casella, M. Gullotti, G. Pallanza and L. Rigoni, J. Am. Chem. Soc., 110 (1988) 4221.

172 O.J. Gelling, F. van Bolhuis, A. Meetsma and B.L. Feringa, J. Chem. Soc. Chem. Commun., (1988) 552.

173 E. Wehman, G. van Koten, C.J. Erkamp, D.M. Knotter, J.T.B.H. Jastrzebski and C.H. Stan, Organometallics, 8 (1989) 94.

174 E. Wehman, G. Van Koten, D.M. Knotter, C.J. Erkamp, A.N.S. Mak and C.H. Stam, Recl. Trav. Chim. Pays-Bas, 106 (1987) 370.

175 L. Casella and S. Ghelli, Inorg. Chem., 22 (1983) 2458.

176 L. Casella, M. Gullotti, C. Pessina and A. Pintar, Gazz. Chim. Ital., 116 (1986) 41.

177 R. Menif and A.E. Martell, Inorg. Chem., 28 (1989) 116.

178 M.R. Malachowski and M.G. Davidson, Inorg. Chim. Acta, 162 (1989) 194.

179 W.L. Driessen, Recl. Trav. Chim. Pays-Bas, 101 (1982) 441.

180 N. Pilkington and R. Robson, Aust. J. Chem., 23 (1970) 2225.

181 M.G.B. Drew, A. Rodgers, M. McCann and S.M. Nelson, J. Chem. Soc. Chem. Commun., (1978) 415.

182 M.G.B. Drew, M. McCann and S.M. Nelson, J. Chem. Soc. Chem. Commun., (1979) 481.

183 M.G. Burnett, V. McKee and S.M. Nelson, J. Chem. Soc. Chem. Commun., (1980) 829.

184 S.M. Nelson, J. Trocha-Grimshaw, A. Lavery, K.P. McKillop and M.G.B. Drew, in K.D. Karlin and J. Zubieta (Eds.), Biological & Inorganic Copper Chemistry, Vol. 2, Adenine Press, New York, 1986, p. 27.

185 S.M. Nelson, F. Esho, A. Lavery and M.G.B. Drew, J. Am. Chem. Soc., 105 (1983) 5693.

186 S.M. Nelson, F.S. Esho and M.G.B. Drew, J. Chem. Soc. Chem. Commun., (1981) 388.

187 M.G.B. Drew, F.S. Esho and S.M. Nelson, J. Chem. Soc. Chem. Commun., (1982) 1347.

188 K.P. McKillop, S.M. Nelson and V. Mckee, J. Chem. Soc. Chem. Commun., (1988) 387.

189 M.G.B. Drew, P.C. Yates, J. Trocha-Grimshaw, K.P. McKillop and S.M. Nelson, J. Chem. Soc. Chem. Commun., (1985) 262.

190 M.G.B. Drew, P.C. Yates, J. Trocha-Grinishaw, A. Lavery, K.P. McKillop, S.M. Nelson and J. Nelson, J. Chem. Soc. Dalton Trans., (1988) 347.

191 A.E. Martin and J.E. Bulkowski, J. Am. Chem. Soc., 104 (1982) 1434.

192 J.E. Bulkowski and W.E. Summers, in K.D. Karlin and J. Zubieta (Eds.), Copper Coordination Chemistry: Biochemical & Inorganic Perspectives, Adenine Press, New York, 1983, p. 445.

193 A. Fan Tai, L.D. Margerum and J.S. Valentine, J. Am. Chem. Soc., 108 (1986) 5006.

194 R.J. Motekaitis, A.E. Martell, J.-M. Lehn and E.-I. Watanabe, Inorg. Chem., 21 (1982) 4253.

195 R.J. Motekaitis, A.E. Martell, J.-P. Lecomte and J.-M. Lehn, Inorg. Chem., 22 (1983) 609.

196 M.G. Basallote and A.E. Martell, Inorg. Chem., 27 (1988) 4219.

197 R. Menif and A.E. Martell, J. Chem. Soc. Chem. Commun., (1989) 1521.

198 H. Adams, D.E. Fenton and G.P. Westwood, unpublished results.

199 A. Zask, N. Gonnella, K. Nakanishi, C.J. Turner, S. Imajo and T. Nozoe, Inorg. Chem., 25 (1986) 3401.

200 W.M. Davis, A. Zask, K. Nakanishi and S.J. Lippard, Inorg. Chem., 24 (1985) 3737.

201 W.M. Davis, M.M. Roberts, A. Zask, K. Nakanishi, T. Nozoe and S.J. Lippard, J. Am. Chem. Soc., 107 (1985) 3864.

202 W.M. Davis and S.J. Lippard, Inorg. Chem., 24 (1985) 3688.

203 G.M. Villacorta and S.J. Lippard, Inorg. Chem., 26 (1987) 3672.

204 G.M. Villacorta, D. Gibson, I.D. Williams and S.J. Lippard, J. Am. Chem. Soc., 107 (1985) 6732.

205 G.M. Villacorta and S.J. Lippard, Inorg. Chem., 27 (1988) 144.

206 G.M. Villacorta, Ch. P. Rao and S.J. Lippard, J. Am. Chem. Soc., 110 (1988) 3175.

207 J.E. Bulkowski, P.L. Burk, M.-F. Ludmann and J.A. Osborn, J. Chem. Soc. Chem. Commun., (1977) 498.

208 P.L. Burk, J.A. Osborn and M.-T. Youinou, J. Am. Chem. Soc., 103 (1981) 1273.

209 A.H. Alberts, R.A. Annunziata and J.-M. Lehn, J. Am. Chem. Soc., 99 (1977) 8502.

210 K. Kim, J.P. Collman and J.A. Ibers, J. Am. Chem. Soc., 110 (1988) 4242.

211 J.P. Fillers, K.G. Ravichandran, I. Abdalmuhdi, A. Tulinsky and C.K. Chang, J. Am. Chem. Soc., 108 (1986) 417.

212 D.H. Busch, G.C. Christoph, L.L. Zimmer, S.C. Jackels, J.J. Grzybowski, R.C. Callahan, M. Kojima, K.H. Holter, J. Mocak, N. Herron, M. Chavan and W.P. Schammel, J. Am. Chem. Soc., 103 (1981) 5107.

213 N. Herron, W.P. Schammel, S.C. Jackels, J.J. Grzybowski, L.L. Zimmer and D.H. Busch, Inorg. Chem., 22 (1983) 1433.

214 N. Hoshino, A. Jircitano and D.H. Busch, Inorg. Chem., 27 (1988) 2292.

215 C. Floriani and G. Fachinetti, J. Chem. Soc. Chem. Commun., (1974) 615.

216 G. Fachinetti, C. Floriani, P.F. Zanazzi and A.R. Zanzari, Inorg. Chem., 18 (1979) 3469.

217 G. Fachinetti, C. Floriani and P.F. Zanazzi, J. Am. Chem. Soc., 100 (1978) 7405.

218 F. Arena, C. Floriani, A. Chiesi-Villa and C. Guastini, Inorg. Chem., 25 (1986) 4589.

219 M.F. Salomon, S.N. Pardo and R.G. Salomon, J. Am. Chem. Soc., 106 (1984) 3797 and references cited therein.

220 M. Pasquali, S. Gambarotta, C. Floriani, A. Chiesi-Villa and C. Guastini, Inorg. Chem., 20 (1981) 165, 1173.

221 G. Facchinetti, C. Biran, C. Floriani, A. Chiesi-Villa and C. Guastini, Inorg. Chem., 17 (1978) 2995.

222 G. Facchinetti, C. Biran, C. Floriani, A. Chiesi-Villa and C. Guastini. J. Chem. Soc. Dalton. Trans., (1979) 792.

223 S. Cennini and G. LaMonica, Inorg. Chim. Acta, 18 (1976) 279.

224 N.J. Bremer, A.B. CutCliffe, M.F. Farona and W.G. Kofron, J. Chem. Soc. A. (1971) 3264.

225 J.D. Cotton and S.D. Zornig, Inorg. Chim. Acta, 25 (1977) L133.

226 D.M. Duggan, Inorg. Chem., 18 (1979) 903.

227 F. Arena, C. Floriani and P.F. Zanazzi, J. Chem. Soc. Chem. Commun., (1987) 183.